Astronomy Unit
Department of Physics and Astronomy
Queen Mary University of London

Gauss-Bonnet Theories of Gravity in Four Dimensions

Pedro Gonçalo da Silva Fernandes

October 2022

Supervised by David J. Mulryne and Timothy Clifton

Submitted in partial fulfillment of the requirements of the Degree of Doctor of Philosophy

Declaration

I, Pedro Gonçalo da Silva Fernandes, confirm that the research included within this thesis is my own work or that where it has been carried out in collaboration with, or supported by others, that this is duly acknowledged below and my contribution indicated. Previously published material is also acknowledged below.

I attest that I have exercised reasonable care to ensure that the work is original, and does not to the best of my knowledge break any UK law, infringe any third party's copyright or other Intellectual Property Right, or contain any confidential material.

I accept that the College has the right to use plagiarism detection software to check the electronic version of the thesis.

I confirm that this thesis has not been previously submitted for the award of a degree by this or any other university. The copyright of this thesis rests with the author and no quotation from it or information derived from it may be published without the prior written consent of the author.

Signature: Pedro Fernandes
Date: 07/10/2022

Publications

The research presented in this thesis was done throughout the course of my PhD studies, and is based largely on work published (or undergoing peer-review) in international refereed journals. These publications are as follows:

- *Charged black holes in AdS spaces in 4D Einstein Gauss- Bonnet gravity*
  P. G. S. Fernandes, Phys. Lett. B, vol. 805, p. 135468, 2020, 2003.05491. [1]

- *Derivation of Regularized Field Equations for the Einstein-Gauss-Bonnet Theory in Four Dimensions*
  P. G. S. Fernandes, P. Carrilho, T. Clifton, and D. J. Mulryne, Phys. Rev. D, vol. 102, no. 2, p. 024025, 2020, 2004.08362. [2]

- *Observational Constraints on the Regularized 4D Einstein-Gauss-Bonnet Theory of Gravity*
  T. Clifton, P. Carrilho, P. G. S. Fernandes, and D. J. Mulryne, Phys. Rev. D, vol. 102, no. 8, p. 084005, 2020, 2006.15017. [3]

- *Gravity with a generalized conformal scalar field: theory and solutions*
  P. G. S. Fernandes, Phys. Rev. D, vol. 103, no. 10, p. 104065, 2021, 2105.04687. [4]

- *Black holes in the scalar-tensor formulation of 4D Einstein-Gauss-Bonnet gravity: Uniqueness of solutions, and a new candidate for dark matter*
  P. G. S. Fernandes, P. Carrilho, T. Clifton, and D. J. Mulryne, Phys. Rev. D, vol. 104, no. 4, p. 044029, 2021, 2107.00046. [5]

- *The 4D Einstein–Gauss–Bonnet theory of gravity: a review*
  P. G. S. Fernandes, P. Carrilho, T. Clifton, and D. J. Mulryne, Class. Quant. Grav., vol. 39, no. 6, p. 063001, 2022, 2202.13908. [6]

- *Exploring the Small Mass Limit of Stationary Black Holes in Theories with Gauss-Bonnet Terms*

P. G. S. Fernandes, D. J. Mulryne, and J. F. M. Delgado, Class. Quant. Grav., vol. 39, no. 23, p. 235015, 2022, 2207.10692. [7]

- *A new approach and code for spinning black holes in modified gravity*
  P. G. S. Fernandes, and D. J. Mulryne, 12 2022, 2212.07293. [8]

Chapter 2 is based on Ref. [2]. Chapter 3 is based on Refs. [1,5]. Chapter 4 is based on Ref. [3]. Chapter 5 is based on Ref. [4]. Chapter 6 is based on (yet) unpublished work [8]. Chapter 7 is based on Ref. [7]. Most chapters contain material based on Ref. [6].
The aforementioned work was done partly in collaboration with David J. Mulryne, Timothy Clifton, Pedro Carrilho and Jorge Delgado. I have made a major contribution to the original research presented in this thesis. In particular, I led most aspects of the research done in the collaborative works presented in Refs. [2,5–8]. The work in Ref. [3] was led by Dr. Timothy Clifton, to which I contributed by studying some observational constraints on the discussed theory. I am the sole author of Refs. [1,4].

The research and results included in this thesis have been presented in talks given at the following meetings and conferences:

- COSMONATA, Faculty of Sciences University of Lisbon, Dec 2019
- Gravitational Geometry and Dynamics group seminar, University of Aveiro, May 2020
- Quantum Gravity group seminar, University of Groningen, May 2020
- XIII Black Holes Workshop, Instituto Superior Técnico, Speaker, Dec 2020
- 50^{th} BUSSTEPP School, Queen Mary University of London, Jan 2021 (award for best session talk)
- London Cosmology Discussion Meeting (LCDM), Dec 2021
- Center for Gravitation and Cosmology seminar, Yangzhou University, Aug 2022

Abstract

In this thesis, we discuss Gauss-Bonnet theories of gravity, with a focus on the topic of *4D Einstein-Gauss-Bonnet gravity*, which has been the subject of considerable interest over the past years. The thesis begins with a general introduction to gravitational physics, General Relativity, and its successes and shortcomings. We review Lovelock's theorem, and the subject of Gauss-Bonnet terms in the action for gravity. These areas are of fundamental importance for understanding modified theories of gravity, and inform our subsequent discussion of recent attempts to include the effects of a Gauss-Bonnet term in four spacetime dimensions by re-scaling the appropriate coupling parameter. We discuss the mathematical complexities involved in implementing this idea, and attempts at constructing well-defined, self-consistent theories that enact it. We then move on to consider the gravitational physics that results from these theories, in the context of black holes, cosmology, and weak-field gravity, showing that 4D Einstein-Gauss-Bonnet gravity exhibits a number of interesting phenomena in each of these areas. We follow up with the derivation of a generalized conformally coupled scalar field theory, which turns out to be intimately connected with the well-defined 4D Einstein Gauss-Bonnet gravity theories, and study its phenomenology. Adopting a more standard framework for Gauss-Bonnet theories in four dimensions, we also study the small mass limit of black holes and how it impacts on the self-consistency of these models. Finally, we study how spectral methods can be used to solve, with high accuracy, the systems of partial differential equations that result from the stationary and axisymmetric gravitational field equations in (generic) modified theories of gravity, obtaining with success spinning black holes in General Relativity, as a benchmark, and scalar-Gauss-Bonnet gravity. The estimated accuracy of the obtained solutions represent an improvement of several orders of magnitude with respect to other existing codes.

Acknowledgements

First and foremost, and I want to thank my supervisor David Mulryne for his constant support, guidance and for the freedom I had in researching. I deeply enjoyed my journey as a Ph.D. student, and you surely had a major influence on this outcome. You made me a better physicist.

I also want to take this opportunity thank my second supervisor, Timothy Clifton for his support, discussions and for embarking on my crazy ideas. A big acknowledgement goes to my collaborator and friend, Pedro Carrilho, who deeply helped me in many aspects of life and work during this journey. I am also indebted to all other members of the Astronomy Unit with whom I crossed paths and to Tony Padilla and Clare Burrage.

To my friends, I would like to thank you all, in particular Bernardo Sá, Catarina Monteiro, Daniel Alves, Diogo Sá, Fátima Pinto, Filipa Pintassilgo, Francisco Dias Pereira, Francisca Duarte, Gonçalo Figueiredo, Gonçalo Nogueira, Hugo Luzio, João Melo, João Pinheiro, João Tomázio, Júlia Silva, Luís Judícibus, Marisa Frade, Nelson Eiró, Paulo Pinto, Pedro Alves, Simão Escudeiro, Sofia Baeta, Sofia Freitas, Tiago França, Vítor Silva, my friends from JAGS, and *pessoal das cartas*.

To Bruno Valeixo Bento, for being the best friend one could ask for. És prigui!

To my late dog and companion, Winkie. I will always cherish our time together.

To my late grandmother Dores and grandfather Pedro. Thank you for everything.

A special acknowledgement goes to Bridie, Gervase, Sid and Sylvia Cox, for their hospitality in difficult times and their friendship. We had the best lockdown!

Finally, I thank my closest loved ones – my family. You are all completely deranged, but you are the best and this journey was only possibly thanks to you mom, dad, Diana and Matilde.

Words could never do justice to the gratitude and feelings I want to express here, so I will simply dedicate this thesis to my soulmate, Sofia Pinto.

This work was supported by the Royal Society grant RGF/EA/180022.

Notation and Conventions

The metric signature is chosen to be $(-,+,+,+)$, spacetime indices are denoted with Greek letters and spatial indices are denoted by Latin letters $(i,j,k,\ldots)$. We typically work in units such that $c = G = \hbar = k_B = 1$, although factors may occasionally be included for clarity.

$g_{\mu\nu}$	spacetime metric
g	determinant of the metric
$\Gamma^{\alpha}_{\mu\nu}$	Christoffel symbol of the metric $g_{\mu\nu}$
∇_{μ}	covariant derivative compatible with the metric $g_{\mu\nu}$
$R_{\mu\alpha\nu\beta}$	Riemann tensor
$C_{\mu\alpha\nu\beta}$	Weyl tensor
$P_{\mu\alpha\nu\beta}$	double-dual of the Riemann tensor
$R_{\mu\nu}$	Ricci tensor
R	Ricci scalar
$G_{\mu\nu}$	Einstein tensor
Λ	cosmological constant
$T_{\mu\nu}$	stress-energy tensor
$F_{\mu\nu}$	Maxwell tensor
T	trace of the stress-energy tensor
ds^2	line element
$\mathcal{G}$	Gauss-Bonnet term
G	Gravitational constant
c	speed of light
$\hbar$	Planck's constant
k_B	Boltzmann's constant
$\overline{M}_{\rm pl} = \sqrt{\frac{\hbar c}{G}}$	Planck mass
$M_{\rm pl} = \sqrt{\frac{\hbar c}{8\pi G}}$	reduced Planck mass
$l_{\rm pl} = \sqrt{\frac{\hbar G}{c^3}}$	Planck length
D	dimensionality of the spacetime
$\Box$	$\nabla_{\mu}\nabla^{\mu}$
$(\nabla\phi)^2$	$\nabla_{\mu}\phi\nabla^{\mu}\phi$
BH	Black Hole
GB	Gauss-Bonnet
GR	General Relativity
FLRW	Friedmann-Lemaître-Robertson-Walker
(A)dS	(Anti-)de Sitter
GW	Gravitational Wave
4DEGB	4D-Einstein-Gauss-Bonnet
EsGB	Einstein-scalar-Gauss-Bonnet

Contents

List of Figures

List of Tables

1 Introduction

1.1 How we got where we are

The year was 1687 when mathematician and physicist Isaac Newton published *Philosophiae Naturalis Principia Mathematica* (Mathematical Principles of Natural Philosophy) [9], in what turned out to be one of the most remarkable achievements of humankind. In it, the three laws of motion and the law of gravitation. With these rules in hand, the world around us finally made sense, from bouncing billiard balls to the motion of a falling apple or that of the heavenly bodies.

Newton's law of gravitation is as simple and elegant as can be, stating that the gravitational force between two objects of masses m_1 and m_2 at a distance r follows an inverse square law

$$F = G\frac{m_1 m_2}{r^2}, \tag{1.1}$$

where G is the gravitational constant. Since its inception, it has been able to explain and predict a plethora of physical phenomena. Indeed, Newton's law of gravitation would strongly reward those whose faith in its correctness was unshakeable.

1.1.1 The theory is correct

By the end of the 18th century there were signs that the orbit followed by the planet Uranus was anomalous. When confronted with observational data, the predictions that followed from Newton's gravitational law were simply inaccurate. Was the theory wrong?

It was not until 1846 that astronomer and mathematician Urbain Le Verrier came along to postulate the existence of a new celestial body, the culprit whose gravitational influence on Uranus, as described by Newton's law, was responsible for the mischievous deviation from theoretical predictions [10]. It would not be long until *Le Verrier's planet* was discovered at the predicted position. Le Verrier's planet is nowadays commonly known as *Neptune*. The world was excited by the find, for never before had mathematics predicted a natural object. Newton's law of gravita-

tion prevailed.

1.1.2 Or is it?

The sirens rang once again as observations dictated that Mercury's orbit was anomalous in light of Newton's theory. Indeed, its perihelion precessed with a discrepancy of about 43 arcseconds per century. For Le Verrier, the solution was obvious: some undetected mass, *Vulcan* [11], orbiting even closer to the Sun, was giving Mercury a regular gravitational push. Was another planet bound to be discovered at the tip of Le Verrier's pen? In the decades that followed, astronomers looked and searched, but the innermost planet was nowhere to be found. Mercury simply refused to obey the laws of gravity as formulated by Isaac Newton.

While discussions about the nature of Mercury's orbit were ongoing in the scientific community, James Clerk Maxwell formulated the laws of electromagnetism [12]. They were able to describe accurately electricity, magnetism and light as different manifestations of the same phenomenon. Maxwell's recently formulated theory was, however, at odds with Newton's laws of motion. Newtonian mechanics was built upon the Galilean Principle of Relativity, that assumes the existence a universal entity called *time* which is independent of the observer, and that the laws of motion are invariant under a Galilean transformation. Maxwell's theory was in conflict with such principle. In particular, Maxwell's equations predicted that the speed of light, c, is constant regardless of the state of motion of the reference frame in which it is measured in, clearly in contradiction to Newton's theory. Experimental facts such as the null result obtained by Michelson and Morley [13] demonstrated that the historically hypothesized luminiferous aether did not exist, supporting the constancy of the speed of light.

Aware of this incompatibility, Albert Einstein worked towards a solution, and was successful when in 1905 he formulated Special Relativity [14]. In Einstein's novel view of the world, the laws of physics are the same in all inertial frames, and the speed of light is the same for all observers, regardless of the motion of the light source or observer, and time and space are not absolute. The laws of motion had been rewritten, predicting and explaining with success a series of physical phenomena. These fundamental changes to the laws of physics were, nonetheless, ineffective in explaining Mercury's anomaly.

1.1.3 "Modified Gravity"

Soon after formulating special relativity, Albert Einstein started thinking about how to modify Newton's theory as to incorporate gravity into his new relativistic framework. It would take him another eight years and numerous detours and false starts before he finally presented in 1915 his theory of *General Relativity* (GR) described by the well-known field equations[1] [15]

$$R_{\mu\nu} - \frac{1}{2} g_{\mu\nu} R + \Lambda g_{\mu\nu} = \frac{8\pi G}{c^4} T_{\mu\nu}. \tag{1.2}$$

When asked what he would do if observations failed to match his theory of General Relativity, Einstein famously replied: "Then I would feel sorry for the good Lord. The theory is correct.". Fortunately for the good Lord, Einstein's modified theory completely overthrew Newtonian gravity. Besides being compatible with special relativity, the theory's prediction of Mercury's perihelion precession matched perfectly the observed value without the need of any unknown planet/mass, and predicted and explained with success other phenomena, such the gravitational deflection of light by massive objects, as measured in 1919 during a solar eclipse by Arthur Eddington [16]. Moreover, Einstein's theory reduces to Newtonian gravity in the appropriate limit, and is thus a generalization thereof.

1.2 Where we are

More than a hundred years have passed since the formulation of general relativity. With Einstein's theory at hand we were able to try and describe our cosmos and its evolution, predict and confirm the existence of black holes and gravitational waves. It is extremely well tested in the weak field regime, and solar system and pulsar binary scales. Consequently, it is not surprising that GR continues to reign as the most successful and well-accepted theory of gravity [17, 18]. However, this might be about to change.

Our current best cosmological model, Λ Cold Dark Matter (ΛCDM), is based on general relativity and posits the existence of a *dark sector* to fit observations. This dark sector is constituted by *dark matter*, needed to explain e.g. dynamics in galaxies and galaxy clusters (see e.g. [19–21]), and *dark energy* responsible for the late-time accelerated expansion of the Universe, first discovered in the late 90s [22, 23]. In

[1] Here we chose to include the cosmological term, even though it was absent from the original formulation.

the ΛCDM model, baryonic matter constitutes only about 5% of the mass-energy content of the universe, with dark matter and dark energy constituting about 26% and 69% respectively.

The ΛCDM model is not without shortcomings. First and foremost, the nature of the dark sector is unknown, indicating that about 95% of the energy content of the universe is unknown to us. So far, much like Le Verrier's Vulcan, the dark sector has been elusive, escaping all direct detection attempts. Although dark energy might be explained using merely a cosmological constant with a value $\rho_\Lambda = \frac{\Lambda c^2}{8\pi G} \sim (10^{-3}\,\mathrm{eV})^4$, there are strong theoretical and conceptual objections to this picture. The problem relates to the spectacular mismatch of about 120 (!) orders of magnitude between the observed value of the cosmological constant and theoretical expectation, based on naturalness and the standard description of quantum fields in a vacuum [24, 25]. This is known as the *cosmological constant problem* [24]. ΛCDM also faces many observational challenges [26], such as the H_0 tension that has become the most notorious tension in cosmology in recent years [27], and the σ_8 tension [28]. A good and fundamental understanding of the early Universe, namely of the inflationary epoch and subsequent reheating is also lacking.

To the best of our understanding, there are four fundamental interactions in Nature. These are the strong, weak, electromagnetic and gravitational interactions. The first three are quantum interactions successfully explained by standard model of particle physics, whereas gravity is classically described by GR. Power-counting arguments indicate that GR is not renormalizable in the standard quantum field theory sense, and a quantum description of gravity is currently unknown [29]. However, as we probe smaller and smaller length scales, quantum gravitational effects cannot be ignored. One simple example is that of a black hole with mass of the order of a Planck mass. In this setting, the Compton wavelength, which gives a lower bound on the length on which the mass can be localized, becomes comparable with the Schwarzschild radius of the black hole, and we need a quantum mechanical description of gravity. GR further seems to predict the existence of singularities, both inside black holes and at the beginning of the Universe, signaling a breakdown of the theory, and presumably a new quantum description is needed.

In addition to the questions raised concerning the validity of GR on cosmological and quantum scales, we have only just started to test gravity in the strong field regime, with the advent of gravitational wave astronomy and black hole imaging by the discoveries of the LIGO-Virgo [30] and Event Horizon Telescope [31, 32] collaborations, respectively, allowing us to probe previously inaccessible regimes with ever-increasing accuracy.

Much like physicists working with Newtonian gravity at the turn of the 19th century, we now have at hand many problems without satisfactory solutions given our current best theory of gravity, and it may well be that, as before, the solution to these problems is modified gravity. In this work we seek to explore alternatives to Einstein's theory.

1.3 A brief review of General Relativity

Before we delve into the realm of modified theories of gravity, let us review the basics of Einstein's theory and differential geometry following Refs. [33,34]. General Relativity is a metric theory of gravity, where spacetime is described by a 4-dimensional Lorentzian manifold, and whose fundamental dynamical variable is the symmetric and invertible rank-2 metric tensor, $g_{\mu\nu}$, which defines infinitesimal distances between events in spacetime

$$ds^2 = g_{\mu\nu}dx^\mu dx^\nu. \tag{1.3}$$

Defining the covariant derivative, ∇_μ, compatible with the metric and the Christoffel symbols

$$\Gamma^\mu_{\nu\lambda} = \frac{1}{2}g^{\mu\rho}\left(\partial_\nu g_{\rho\lambda} + \partial_\lambda g_{\nu\rho} - \partial_\rho g_{\nu\lambda}\right), \tag{1.4}$$

it is possible to define the Riemann curvature tensor

$$R^\mu{}_{\nu\lambda\rho} = \partial_\lambda\Gamma^\mu_{\nu\rho} - \partial_\rho\Gamma^\mu_{\nu\lambda} + \Gamma^\mu_{\lambda\sigma}\Gamma^\sigma_{\nu\rho} - \Gamma^\mu_{\rho\sigma}\Gamma^\sigma_{\nu\lambda}. \tag{1.5}$$

The Ricci tensor, $R_{\mu\nu}$, and Ricci scalar, R, are contractions of the Riemann curvature tensor

$$R_{\mu\nu} = R^\alpha{}_{\mu\alpha\nu}, \qquad R = g^{\mu\nu}R_{\mu\nu}. \tag{1.6}$$

A particularly important combination of these tensors is given by the divergence-free Einstein tensor

$$G_{\mu\nu} = R_{\mu\nu} - \frac{1}{2}g_{\mu\nu}R. \tag{1.7}$$

The left-hand-side of Einstein field equations, given in Eq. (1.2), is composed of a linear combination of the Einstein and metric tensors, as to ensure conservation of the stress-energy tensor, $T_{\mu\nu}$, on the right-hand-side, that describes the matter content of the theory.

The field equations for gravity also follow from an action principle, given by the

Einstein-Hilbert action

$$\begin{aligned} S &= \frac{c^4}{16\pi G}\int d^4x\sqrt{-g}\,(R-2\Lambda)+S_{matter}, \\ &\equiv \frac{M_{pl}^2}{2}\int d^4x\sqrt{-g}\,(R-2\Lambda)+S_{matter}, \end{aligned} \tag{1.8}$$

where g denotes the determinant of the metric tensor, and the variation of the matter action gives the stress energy-tensor

$$T_{\mu\nu} = -\frac{2}{\sqrt{-g}}\frac{\delta S_{matter}}{\delta g^{\mu\nu}}. \tag{1.9}$$

1.3.1 The basics of relativistic cosmology

Observations suggest that on cosmological scales the geometry of our Universe is well-described by the homogeneous and isotropic Friedmann-Lemaître-Robertson-Walker (FLRW) metric

$$ds^2 = -c^2dt^2 + a^2(t)\left[\frac{dr^2}{1-kr^2} + r^2\left(d\theta^2+\sin^2\theta d\varphi^2\right)\right], \tag{1.10}$$

where $k=\{0,-1,1\}$ for flat, negatively-curved, or positively curved spatial sections, respectively. Observations favor the flat case. Hereafter, an overdot denotes a derivative with respect to the temporal coordinate t.

The evolution of the Universe is then intimately connected to its matter content via the Einstein equations (1.2). Assuming the stress-energy tensor to be that of a perfect fluid[2]

$$T^{\mu}{}_{\nu} = \left(\rho+\frac{p}{c^2}\right)u^\mu u_\nu + p\,\delta^\mu{}_\nu, \tag{1.11}$$

where ρ is the energy density, p the pressure and u^μ is the four-velocity of the matter, the Einstein equations result in the well-known Friedmann equations

$$H^2 \equiv \left(\frac{\dot a}{a}\right)^2 = \frac{8\pi G}{3}\rho + \frac{\Lambda c^2}{3} - \frac{kc^2}{a^2}, \tag{1.12}$$

$$\dot H = -4\pi G\left(\rho+\frac{p}{c^2}\right) + \frac{kc^2}{a^2}, \tag{1.13}$$

where the first equality serves to define the Hubble rate H. Conservation of the

[2]See Ref. [35] for a discussion on the variational principle for a perfect fluid.

stress-energy tensor, $\nabla_\mu T^{\mu\nu} = 0$, further imposes

$$\dot{\rho} = -3H\left(\rho + \frac{p}{c^2}\right). \tag{1.14}$$

The pressure and energy density can be related through an equation of state $p/c^2 = \omega\rho$, where ω indicates the type of fluid considered, namely $\omega = \{1/3, 0, -1\}$ for radiation, dust and dark energy, respectively. Matter is typically modeled as dust. From the conservation of the stress-energy tensor one concludes that $\rho \propto a^{-3(1+\omega)}$.

1.3.2 The basics of black hole physics

The first non-trivial solution to the vacuum Einstein equations was discovered by Karl Schwarzschild in 1916 [36]. It describes the spherically symmetric black hole solution of general relativity, given by the line element[3]

$$ds^2 = -\left(1 - \frac{2GM}{rc^2}\right)c^2dt^2 + \frac{dr^2}{\left(1 - \frac{2GM}{rc^2}\right)} + r^2\left(d\theta^2 + \sin^2\theta d\varphi^2\right), \tag{1.15}$$

where M is the mass of the black hole. Note that as the mass vanishes, we recover flat spacetime and the metric is asymptotically flat. There is an event horizon located at $r = r_s$, where $r_s = \frac{2GM}{c^2}$ is called the *Schwarzschild radius*. A physical singularity exists at the centre of the black hole where the curvature diverges, as can be seen e.g. from the Kretschmann scalar

$$R_{\alpha\beta\gamma\rho}R^{\alpha\beta\gamma\rho} = \frac{12r_s^2}{r^6}.$$

The Schwarzschild black hole is not merely *a* solution, but rather *the* solution to the spherically symmetric vacuum Einstein equations, as asserted by Birkhoff's theorem [37][4]. Therefore, it represents the spherically symmetric spacetime surrounding a mass, such as the exterior of a static or collapsing non-spinning star.

The Schwarzschild black hole is described by only one parameter, its mass. However, in the standard picture black holes are capable of also having angular momentum and electric charge. In fact, in more realistic settings, black holes are expected to have a relevant non-vanishing angular momentum. For GR in the presence of an

[3] Here we ignored the cosmological term.

[4] Note however that the situation changes if the cosmological term is considered, where one can have the Nariai solution [38, 39] for example.

electromagnetic field, described by Eq. (1.8) with

$$S_{matter} = -\frac{1}{4}\int d^4x\sqrt{-g}F_{\mu\nu}F^{\mu\nu} \tag{1.16}$$

where $F_{\mu\nu} = \partial_\mu A_\nu - \partial_\nu A_\mu$ is the Maxwell tensor, the uniqueness theorems (see e.g. [40] for a review) state that the most general stationary, asymptotically flat, axially symmetric, regular on and outside the event horizon, black hole solution is given by the Kerr-Newman metric, which in Boyer-Lindquist coordinates reads [41]

$$\begin{aligned} ds^2 = &-\frac{\Delta - a^2\sin^2\theta}{\rho^2}dt^2 - \frac{2a\sin^2\theta\left(r^2+a^2-\Delta\right)}{\rho^2}dtd\varphi \\ &+\frac{\left(r^2+a^2\right)^2 - \Delta a^2\sin^2\theta}{\rho}\sin^2\theta d\varphi^2 + \frac{\rho^2}{\Delta}dr^2 + \rho^2 d\theta^2, \end{aligned} \tag{1.17}$$

where

$$\rho^2 = r^2 + a^2\cos^2\theta, \qquad \Delta = r^2 - r_s r + a^2 + r_Q^2,$$

$a \equiv J/Mc$ is the total angular momentum J per unit mass, $r_Q^2 = kQ^2G/c^4$, with k the Coulomb's force constant and Q the electric charge of the black hole. All other black hole solutions in electrovacuum are limiting cases of the Kerr-Newman black hole. Namely, when $Q = 0$ and $a \neq 0$ we recover the Kerr black hole, when $a = 0$ but $Q \neq 0$ we get the Reissner-Nordström black hole, and when $Q = a = 0$ we recover the Schwarzschild black hole presented before. Generalizations exist in the presence of a cosmological constant, namely the Kerr-Newman-(anti) de Sitter black hole. For completeness and later use, we present here the explicit form of the Reissner-Nordström geometry

$$ds^2 = -\left(1 - \frac{r_s}{r} + \frac{r_Q^2}{r^2}\right)dt^2 + \left(1 - \frac{r_s}{r} + \frac{r_Q^2}{r^2}\right)^{-1}dr^2 + r^2\left(d\theta^2 + \sin^2\theta d\varphi^2\right). \tag{1.18}$$

From now on we consider only the uncharged case, unless otherwise stated.

In GR, black holes are rather unique objects as they are described merely by three macroscopic quantities, their mass, angular momentum and electric charge, all of which can be measured asymptotically through a Gauss law. This fact has lead to the formulation of the well-known *no-hair conjecture* (see Ref. [42] for a review), stating that regardless of the stress-energy content one starts with, gravitational collapse will necessarily evolve dynamically towards a black hole whose end-state described only by its mass, electric charge and angular momentum, and no other quantities commonly denoted as *hair*.

In 1973 Stephen Hawking, Brandon Carter and James Bardeen published their seminal work [43] containing four laws of black hole mechanics which can be summarized as follows

- Zeroth law: The surface gravity, κ, is constant on the event horizon of a black hole.
- First law: The mass difference of any two neighbouring stationary axisymmetric black hole solutions is given by

$$c^2\delta M = \frac{c^2\kappa}{8\pi}\delta A + \Omega_H \delta J, \tag{1.19}$$

  where A is the area of the event horizon, J its angular momentum and Ω_H the angular velocity of the horizon.
- Second law: In any classical process, the area of the black hole event horizon, A, never decreases.
- Third law: In any physical process it is not possible to reduce the surface gravity to zero.

If we take the surface gravity and the horizon area to be analogous to the temperature and entropy of a thermodynamic system, then the resemblance to the four laws of thermodynamics is remarkable. In the following years a set of new ideas showed that, after all, this analogy was in fact a physical unification. Indeed, Hawking demonstrated that black holes behave as a thermodynamic system, radiating thermally with a temperature T proportional to their surface gravity [44]

$$T = \frac{\hbar c}{k_B}\frac{\kappa}{2\pi}, \tag{1.20}$$

from which follows that they should have an entropy given by

$$S = \frac{k_B A}{4l_{pl}^2}, \tag{1.21}$$

where we have defined the Planck length $l_{pl}^2 = \hbar G/c^3$ and where $\hbar$ and k_B are the Planck and the Boltzmann constants, respectively. The temperature of a black hole is typically referred to as *Hawking temperature* and the entropy as *Bekenstein-Hawking entropy* [45].

1.4 Lovelock's Theorem, Modified Theories of Gravity and the Gauss-Bonnet Term

1.4.1 Lovelock's Theorem

Modifying gravity is no easy task. Motivated by the idea of showing the uniqueness of Einstein's field equations, Lovelock asked which set of rank-2 tensors $A^{\mu\nu}$ could satisfy the following three conditions:

(i) $A^{\mu\nu} = A^{\mu\nu}(g_{\rho\sigma}, g_{\rho\sigma,\tau}, g_{\rho\sigma,\tau\chi})$

(ii) $\nabla_\nu A^{\mu\nu} = 0$

(iii) $A^{\mu\nu} = A^{\nu\mu}$.

Any such tensor would provide a plausible candidate for the left-hand side of the field equations of a geometric theory of gravity, and could be set as being proportional to the stress-energy tensor $T^{\mu\nu}$. Indeed, this seems to be a formalized version of the rationale that led Einstein to his formulation of the field equations in 1915, but here with the explicit aim of finding *all* possible field equations that would have consistent conservation and symmetry properties, as well as being free from Ostrogradski instabilities [46] and higher-derivatives.

The question Lovelock posed had been partially answered much earlier by Weyl [47] and Cartan [48], who showed that if $A^{\mu\nu}$ is required to be linear in $g_{\rho\sigma,\tau\chi}$ then the only possibility is that $A^{\mu\nu}$ is a linear combination of the Einstein tensor and a cosmological constant term. By dropping the requirement of linearity, Lovelock found that there was a considerably broader class of solutions to the problem, each of which could serve as a suitable left-hand side in a geometric theory of gravity, without introducing any extra fundamental degrees of freedom beyond those that exist in the metric [49, 50].

Lovelock's field equations can be derived from the following Lagrangian density:

$$\mathcal{L} = \sqrt{-g}\sum_{j=0}^{j_f} \alpha_j \mathcal{R}^j \,, \quad \text{where} \quad j_f = \begin{cases} \frac{D-2}{2}, & D \text{ is even} \\ \frac{D-1}{2}, & D \text{ is odd} \end{cases} \tag{1.22}$$

where

$$\mathcal{R}^j \equiv \frac{1}{2^j}\delta^{\mu_1\nu_1\ldots\mu_j\nu_j}_{\alpha_1\beta_1\ldots\alpha_j\beta_j}\prod_{i=1}^{j} R^{\alpha_i\beta_i}{}_{\mu_i\nu_i} \,, \tag{1.23}$$

and

$$\delta^{\mu_1\nu_1\ldots\mu_j\nu_j}_{\alpha_1\beta_1\ldots\alpha_j\beta_j} \equiv j!\delta^{\mu_1}_{[\alpha_1}\delta^{\nu_1}_{\beta_1}\ldots\delta^{\mu_j}_{\alpha_j}\delta^{\nu_j}_{\beta_j]}\,. \tag{1.24}$$

The α_j are a set of arbitrary constants, and the square brackets denote anti-symmetrization in the usual way.

The tensor $A_{\mu\nu}$ that satisfies properties (i)-(iii) above can be generated from the Lagrangian density in Eq. (1.22) by integrating it over a region of D-dimensional space-time Ω to construct an action S, and then by varying with respect to the inverse metric $g^{\mu\nu}$. This gives

$$\delta S = \delta\int_\Omega d^D x\,\mathcal{L} = \int_\Omega d^D x\,\sqrt{-g}A_{\mu\nu}\,\delta g^{\mu\nu} + \int_{\partial\Omega} d^{D-1}x\,\sqrt{h}B\,, \tag{1.25}$$

where h is the determinant of the induced metric on $\partial\Omega$, and where

$$A^\mu{}_\nu = -\sum_j \frac{\alpha_j}{2^{j+1}}\delta^{\mu\,\rho_1\sigma_1\ldots\rho_j\sigma_j}_{\nu\,\alpha_1\beta_1\ldots\alpha_j\beta_j}\prod_{i=1}^{j} R^{\alpha_i\beta_i}{}_{\rho_i\sigma_i}\,. \tag{1.26}$$

For further discussion of the derivation of this result, and an expression for the boundary term B, the reader is referred to the original literature [49, 50] and to the review [51].

One can immediately see that the sum in Eq. (1.26) will terminate as soon as $2j+1 > D$, where D is the dimensionality of space-time. This follows from the definition of $\delta^{\mu_1\nu_1\ldots\mu_j\nu_j}_{\alpha_1\beta_1\ldots\alpha_j\beta_j}$, as the number of possible values for each index must be greater than the number of lower indices in order for the quantity to be non-zero (otherwise at least two indices would have to take the same value, which would mean that it would vanish on anti-symmetrization). For even dimensional space-times we therefore have $D/2$ possible terms appearing in the tensor $A^\mu{}_\nu$, while for odd dimensional space-times we have $(D+1)/2$ possible terms.

This means that in dimensions $D = 1$ or 2 there is only one term possible in the Lovelock tensor $A^\mu{}_\nu$, and that this term will be of the functional form $\sim (Riemann)^0$ (i.e. a constant). In dimensions $D = 3$ and 4 there are two possible terms, corresponding to a constant and to a term of the form $\sim (Riemann)^1$. In fact, this latter term is exactly the Einstein tensor so that in $D = 4$

$$A^\mu{}_\nu = -\frac{1}{2}\alpha_0\delta^\mu_\nu + \alpha_1\left(R^\mu_\nu - \frac{1}{2}\delta^\mu_\nu R\right)\,. \tag{1.27}$$

This is clearly the left-hand side of Einstein's equations, with the constants expressed in a slightly less familiar form. As a corollary of Lovelock's approach to gravity, we

therefore have that Einstein's equations are the unique set of field equations that satisfy conditions (i)-(iii) above, which extends the result found by Weyl and Cartan to cases where $A^{\mu}{}_{\nu}$ is allowed to be non-linear in second derivatives of the metric.

While Lovelock's theorem demonstrates how unique GR is in four spacetime dimensions, it does provide direction for searching for modifications to GR in four dimensions and beyond. Thus, in order to construct gravitational theories whose field equations differ from those of GR one must relax one or more of the previous conditions. This leaves us with one of the following options, if we want to consider alternative theories of gravity: (i) Add extra fields that mediate the gravitational interaction, beyond just the metric tensor; (ii) Work in a spacetime with dimensionality different from four; (iii) Allow field equations with more than two derivatives of the metric; (iv) Give up on either rank-2 tensor field equations, symmetry of the field equations under exchange of indices, or divergence-free field equations; or (v) Give up on locality. Any of these options will in general introduce extra degrees of freedom in the theory.

1.4.2 Higher-curvature gravity and the Gauss-Bonnet term

The Einstein-Hilbert action in Eq. (1.8) is expected to be the only first in an infinite series of higher-curvature terms which become relevant at sufficiently high energy scales, and therefore should be viewed only as a consistent low-energy effective field theory (EFT) of some unknown UV-complete theory of gravity [52]. Non-renormalizability of GR is expected to be an artifact of its EFT nature, much like Fermi's theory of beta decay, which is able to explain observed phenomena at energies below the electroweak scale while being non-renormalizable. Of course, we now know that Fermi's interaction arises from the (UV-complete) electroweak interaction of the Standard Model of particle physics. Higher-curvature terms are then expected to be present on the gravitational action on general grounds.

Stelle showed long ago that if the classical gravitational action is supplemented with quadratic curvature terms

$$S = \int d^4x\sqrt{-g}\left[\frac{M_{pl}^2}{2}R + c_1R^2 + c_2R_{\mu\nu}R^{\mu\nu} + c_3R_{\mu\nu\alpha\beta}R^{\mu\nu\alpha\beta}\right], \tag{1.28}$$

then for suitably chosen coefficients c_1, c_2, and c_3, the theory is renormalizable [53]. Unfortunately, renormalizability comes at the price of introducing a ghost degree of freedom in the theory, rendering it non-unitary. This is a consequence of the presence of derivatives of order greater than two in the field equations (as asserted by

Lovelock's theorem), giving rise to instabilities. However, not all theories of gravity with higher-curvature terms are inconsistent and unhealthy, as we will discuss next.

Higher-curvature corrections are expected to modify gravitational dynamics in the strong field regime. One prominent example of such a regime concerns the very beginning of the Universe and the period of cosmic inflation. Indeed, there is observational evidence that higher-curvature corrections can induce with success this initial period of cosmic inflation e.g., within Starobinsky's model [54] where the gravitational action is supplemented by a R^2 term

$$S = \frac{M_{pl}^2}{2} \int d^4x\sqrt{-g}\left[R + \frac{1}{6M^2}R^2\right]. \tag{1.29}$$

Inflation is realized by the scalar degree of freedom introduced by the R^2 term, as can be seen more explicitly by performing a conformal transformation to the Einstein frame, where the above action becomes[5]

$$S = \int d^4x\sqrt{-\overline{g}}\left[\frac{M_{pl}^2}{2}\overline{R} - \frac{1}{2}\left(\nabla\phi\right)^2 - \frac{3}{4}M_{pl}^2M^2\left(e^{-\sqrt{\frac{2}{3}}\frac{\phi}{M_{pl}}} - 1\right)^2\right], \tag{1.30}$$

and describes Einstein's gravity minimally coupled to a scalar field with a (sufficiently) flat potential, ideal for an inflationary setting. Starobinsky-like models of inflation are favored by observations, with cosmic microwave background radiation observations fixing the mass scale $M/M_{pl} \sim \mathcal{O}\left(10^{-5}\right)$ [55]. The action in Eq. (1.29) is a subset of a broader class of models known as $f(R)$ theories, where f is a function of the Ricci scalar, which are healthy on general grounds. Another rather important example of a strong curvature regime concerns black holes, where higher-curvature terms are expected to affect the nature/existence of singularities, to change dynamics in the case of sufficiently small masses, and impact on the geometry in general, hopefully leading to observational consequences that differ from those predicted by GR. Indeed, later in Chapter 3 we will discuss a case where the influence of a higher-curvature term on Hawking evaporation of black holes cures the typical divergent behaviour observed in the late-time evaporation (e.g. as in the case of a Schwarzschild black hole), leading instead to small black hole relics that can act as dark matter.

[5]The overline denotes that quantities are those correspondent to the Einstein frame.

1.4.2.1 The Gauss-Bonnet term

Higher-curvature terms are also motivated from (more) fundamental principles. From Lovelock's theorem, we know that one possible way to modify Einstein's gravity is to consider higher-dimensions. Indeed, if $D > 4$, terms of quadratic and higher-orders in the curvature arise automatically. In particular, in the case $D = 5$ or 6 the tensor $A^{\mu}{}_{\nu}$ can contain *three* terms, with the last being order $\sim (Riemann)^2$ (i.e corresponding to $j = 2$ in the sum in Eqs. (1.22) and (1.26)). This gives the Lagrangian density

$$\mathcal{L} = \sqrt{-g}\left[\alpha_0 + \alpha_1 R + \alpha_2 \mathcal{G}\right] , \tag{1.31}$$

where

$$\mathcal{G} = R^2 - 4R_{\mu\nu}R^{\mu\nu} + R_{\mu\nu\rho\sigma}R^{\mu\nu\rho\sigma} \tag{1.32}$$

is known as the *Gauss-Bonnet* (GB) term, which will be of central importance for this work. Extremization of the action associated with this Lagrangian gives the Lanczos tensor [56, 57]:

$$\begin{aligned} A^{\mu}{}_{\nu} = &-\frac{1}{2}\alpha_0\delta^{\mu}_{\nu} + \alpha_1\left(R^{\mu}_{\nu} - \frac{1}{2}\delta^{\mu}_{\nu}R\right) \\ &+ \alpha_2\left(2R^{\mu\alpha\rho\sigma}R_{\nu\alpha\rho\sigma} - 4R^{\rho\sigma}R^{\mu}{}_{\rho\nu\sigma} - 4R^{\mu\rho}R_{\nu\rho} + 2R\,R^{\mu}_{\nu} - \frac{1}{2}\delta^{\mu}_{\nu}\mathcal{G}\right) . \end{aligned} \tag{1.33}$$

This tensor provides an alternative set of field equations from those of Einstein, which has no higher than second derivatives of the metric, and which obeys the required symmetry and conservation properties in order for it to be set as being proportional to the stress-energy tensor $T^{\mu}{}_{\nu}$.

The additional terms in the second line of Eq. (1.33) can be seen to vanish identically in $D = 4$ and lower. This follows from the discussion above, and can also be understood as resulting from applying dimensionally-dependent identities to $A^{\mu}{}_{\nu}$ [58]. However, the same result can also be seen to be a consequence of Chern's theorem [59] applied to the action that results from integrating Eq. (1.31) over the space-time manifold. In this latter case the integral of the Gauss-Bonnet term is equal to a constant with a value that depends on the Euler characteristic of the manifold χ,

$$\chi = \frac{1}{32\pi^2}\int d^4x\sqrt{-g}\mathcal{G}, \tag{1.34}$$

and which upon extremization contributes precisely zero to $A^{\mu}{}_{\nu}$. It is for this reason that the Gauss-Bonnet term in $D = 4$ is often referred to as a "topological term", and neglected. This is despite the fact that generically $\mathcal{G} \neq 0$ in $D = 4$.

In dimensions $D > 6$ there are further terms available in the Lovelock's theory, with the order of non-trivial new terms in powers of the Riemann tensor increasing consistently as the dimensionality of space-time increases. We will not consider these further possible terms here, but rather restrict ourselves to the Lagrangian that contains the Gauss-Bonnet term (1.31). Besides being the unique quadratic curvature combination appearing in the Lovelock Lagrangian, Gauss-Bonnet terms are of wide theoretical interest, as we will now describe.

The combination of Einstein-Hilbert and Gauss-Bonnet terms in the gravitational action result in theories that have come to be known as Einstein-Gauss-Bonnet gravity. Such theories are of interest partly because string theory predicts that at the classical level Einstein's equations are subject to next-to-leading-order corrections that are typically described by higher-order curvature terms in the action. As we have just seen, the Gauss-Bonnet term is the unique term that is quadratic in the curvature and that results in second-order field equations.

As an example of how Einstein-Gauss-Bonnet gravity arises, it can be shown that M-theory compactified on a Calabi-Yau three-fold down to $D = 5$ takes the effective form [60, 61]

$$S = \int d^5x\sqrt{-g}\left(R + \frac{1}{16}c_2^{(I)}V_I\,\mathcal{G}\right), \tag{1.35}$$

where $c_2^{(I)}V_I$ depends on the details of the Calabi-Yau manifold. This is nothing but the five-dimensional Lovelock theory presented in Eq. (1.31) (with suitably chosen α_i). Gauss-Bonnet terms also occur in heterotic string theory [62–66], where the 1-loop effective action in the Einstein frame displays couplings of the form[6]

$$S = \frac{M_{pl}^2}{2}\int d^4x\sqrt{-g}\left[R - (\nabla\phi)^2 + \frac{\alpha'}{8}e^{-\gamma\phi}\mathcal{G} + \ldots\right], \tag{1.36}$$

in the four-dimensional theory (where ϕ is a dynamical scalar field: the dilaton), α' is the (square) string length, and other higher-derivative terms are denoted by the ellipsis.

The mathematical foundations of theories containing both Einstein and Gauss-Bonnet terms have been extensively studied, with Choquet-Bruhat herself addressing the associated Cauchy problem [67], and the Hamiltonian problem being presented in Ref. [68]. Cosmological models have been particularly well studied in these theories, including during inflation, and in the context of "brane" cosmology (see Ref. [69] for a review). They have also found application in the study of black hole

[6] In particular, $\gamma = \frac{1}{\sqrt{2}}$ is motivated from heterotic string theory.

thermodynamics and in the emergent gravity paradigm (see Ref. [51] for a review). The reader will note, however, that the dimensionality of the manifold over which the integration is performed in the action in Eq. (1.35) must necessarily be $D > 4$, in order for there to be non-vanishing contributions to the field equations.

The appearance of Gauss-Bonnet terms in string-inspired theories of gravity, such as the one in Eq. (1.36), has also motivated the consideration of four-dimensional theories of the form

$$S = \frac{M_{pl}^2}{2} \int d^4x \sqrt{-g} \left[R - (\nabla\phi)^2 + \frac{\alpha}{8} f(\phi) \mathcal{G} \right] , \tag{1.37}$$

where α is a (generic) coupling constant with dimensions of $(length)^2$. In these theories it is possible to work in $D = 4$ space-time dimensions, and still have non-vanishing second-order contributions of the Gauss-Bonnet term to the field equations, due to the existence of the scalar field ϕ (and its non-minimal coupling). These scalar-tensor variants of Einstein-Gauss-Bonnet theory are also well studied, and have been found to exhibit a rich phenomenology [70–94]. In particular, they are expected to produce viable models of inflation in the early universe, display spontaneous scalarization in compact objects, and admit novel black hole solutions that evade the no-hair theorems.

1.4.2.2 Horndeski gravity

Scalar fields have been widely considered in recent years in modified theories of gravity for a variety of reasons. Indeed, they can, depending on the setting, be suitable dark matter and/or dark energy candidates, and are the simplest type of fields to consider. They are also motivated from fundamental arguments, e.g., they arise in four-dimensional effective theories of gravity from string theory, as we have seen above, or within the framework of non-commutative geometry quantum theories of gravity [95,96]. Quantum chromodynamics further predicts the existence of pseudoscalar fields that go by the name of *axions*. In particular, axions provide a solution to the strong CP problem [97] and are viable dark matter candidates, as their interaction with the other particles of the Standard Model of particle physics can be highly suppressed. Cosmological inflation is also typically modeled as a slowly-rolling scalar field on a potential, such as in Starobinsky's model presented in Eq. (1.30). Scalar fields further raise the possibility that modifications of gravity occur only in certain regimes, without altering predictions e.g. in solar system scales where GR is well-tested. This is achieved through *screening mechanisms* [98–102],

producing non-trivial effects in sparse cosmic environments, or through *spontaneous scalarization* [74–76, 103], altering only the strong field regime (e.g. near black holes or neutron stars). Spontaneously scalarized compact objects are endowed with *scalar charges*, which can leave imprints in gravitational wave observations.

The recently revived Horndeski class of theories [104] (see Ref. [105] for a review) defines the most general four-dimensional scalar-tensor theory with second-order equations of motion, and is described by the Lagrangian density

$$\begin{aligned}\frac{\mathcal{L}_H}{\sqrt{-g}} &= G_2(\phi,X) - G_3(\phi,X)\Box\phi + G_4(\phi,X)R + G_{4X}\left[(\Box\phi)^2 - (\nabla_\mu\nabla_\nu\phi)^2\right] \\ &\quad + G_5(\phi,X)G^{\mu\nu}\nabla_\mu\nabla_\nu\phi - \frac{G_{5X}}{6}\left[(\Box\phi)^3 - 3\Box\phi\,(\nabla_\mu\nabla_\nu\phi)^2 + 2\,(\nabla_\mu\nabla_\nu\phi)^3\right],\end{aligned}$$

where $X = -\frac{1}{2}(\nabla\phi)^2$ is the canonical kinetic term of the scalar ϕ, $G_{iX} \equiv \partial_X G_i$, and we have used the shorthanded forms $(\nabla_\mu\nabla_\nu\phi)^2 = \nabla_\mu\nabla_\nu\phi\nabla^\mu\nabla^\nu\phi$, and $(\nabla_\mu\nabla_\nu\phi)^3 = \nabla_\mu\nabla_\nu\phi\nabla^\nu\nabla^\lambda\phi\nabla_\lambda\nabla^\mu\phi$. The theory contains four arbitrary functions of ϕ and X, G_2, G_3, G_4, and G_5.

The scalar-tensor theories presented in Eq. (1.37) belong to the Horndeski class. In fact, it can be shown that the non-minimal coupling $f(\phi)\mathcal{G}$ in Eq. (1.37) can be reproduced in the Horndeski formalism by taking [106] (see also Refs. [107–109])

$$\begin{aligned}G_2 &= 8X^2(3-\log X)\partial_\phi^4 f, \\ G_3 &= 4X(7-3\log X)\partial_\phi^3 f, \\ G_4 &= 4X(2-\log X)\partial_\phi^2 f, \\ G_5 &= -4\,(\log X)\,\partial_\phi f.\end{aligned} \tag{1.38}$$

We remark that when it comes to purely geometric terms, only couplings of the scalar field to the Ricci scalar and the Gauss-Bonnet term are allowed by Horndeski's theory.

1.4.3 Novel Einstein-Gauss-Bonnet gravity in four dimensions

The ideas presented in this section are the subject of much research presented in this thesis.

In order to circumvent the stringent requirements of Lovelock's theory, and in an attempt to introduce the Gauss-Bonnet term in 4D gravity directly, Glavan & Lin

proposed rescaling the coupling constant α_2 such that [110]

$$\alpha_2 \to \frac{\alpha_2}{(D-4)}\,. \tag{1.39}$$

This quantity is clearly divergent in the limit $D \to 4$, but Glavan & Lin made the non-trivial suggestion that if this re-scaling were introduced into the Lanczos tensor (1.33) then the terms that contain this quantity as a factor might remain finite and non-zero. That is, they postulated that the divergence they introduced into α_2 might be sufficient to cancel out the fact that additional terms in Eq. (1.33) tend to zero as $D \to 4$. If this were the case, then the Gauss-Bonnet term would be allowed to have a direct effect in the 4D theory of gravity.

Motivation for this radical new approach came from the trace of the Lanczos tensor (1.33), which in D dimensions gives

$$A^{\mu}{}_{\mu} = -\frac{1}{2}D\alpha_0 - \frac{1}{2}(D-2)\alpha_1 R - \frac{1}{2}(D-4)\alpha_2\mathcal{G}\,. \tag{1.40}$$

The vanishing of the term from the Einstein tensor in $D = 2$ and the vanishing of the Gauss-Bonnet contribution in $D = 4$ are both made explicit here, and both can be seen to be due to a pre-factor of the form $(D - n)$ (recall that R and $\mathcal{G}$ can be non-zero only if $D > 1$ and $D > 3$, respectively). Using the re-scaling in Eq. (1.39) can then be seen to entirely remove the factor that usually results in the contribution from the Gauss-Bonnet term vanishing, and leaves a term that can in general be non-zero in the limit $D \to 4$.

The additional term that results in the trace of the field equations (1.40), after the re-scaling given in Eq. (1.39), are strongly motivated from studying quantum corrections to the stress-energy tensor in the presence of gravity. In this case the renormalized vacuum expectation value for the trace of $T_{\mu\nu}$ includes terms that are proportional to $\mathcal{G}$ [111], in just the same way that they are found in the trace of the left-hand side of the field equations in Eq. (1.40). This is known as the "conformal" or "trace" anomaly in the quantum field theory literature, and a natural interpretation of the Glavan & Lin re-scaling is that it is a way of accounting for the conformal anomaly in the gravitational sector of the theory. The reader may also note that a similar procedure to the re-scaling (1.39) has also been successfully applied to the Einstein term in the limit $D \to 2$ [112], in order to remove the factor of $(D-2)$ that would otherwise result from Einstein's equations being entirely absent. We will return to this particular point later on.

There has been a flurry of activity surrounding the idea of 4D-Einstein-Gauss-

Bonnet Gravity (4DEGB) in the years since it was published in *Physical Review Letters* back in 2020 [1–6, 112–279]. It is the re-scaling presented in Eq. (1.39), and the ideas, phenomenology and theories that have resulted from it, that are the subject of much research presented in this thesis. In particular, we aim to present a balanced guide to the ways in which the proposed re-scaling (1.39) can be considered a viable method of introducing the consequences of a Gauss-Bonnet term in 4D, as well as those in which it cannot, and its phenomenological consequences. We will draw on the work of many authors for this presentation, who will be referenced as we proceed, while focusing on the original contributions by the author of this thesis.

1.5 Outline

Having motivated the need for the study of modified theories of gravity, higher-curvature corrections (in particular, Gauss-Bonnet terms), and new scalar gravitational degrees of freedom, we now proceed to outline our structure. As previously mentioned, this thesis is based on the original works by the author in Refs. [1–8].

In chapter 2 we review and discuss in more detail the divergent rescaling in Eq. (1.39) proposed by Glavan & Lin, and discuss the concerns and criticisms that have been raised about this idea. Then, we propose a method to consistently regularize the 4D-Einstein-Gauss-Bonnet action by the introduction of counter-terms that remove the otherwise occurring divergences, resulting in a well-defined four-dimensional scalar-tensor theory that possesses many of the properties that the original proposal by Glavan & Lin possesses. We close with a discussion on other possible regularization procedures resulting in well-defined 4DEGB theories. This chapter is based on the ideas of Ref. [2].

Chapter 3 concerns the phenomenology of 4D-Einstein-Gauss-Bonnet theories, both in the Glavan & Lin proposal, and in the well-defined regularized theories discussed in chapter 2. In particular, we discuss the black hole solutions of the theory, including solutions with a cosmological constant and electric charge (based on the results of Ref. [1]), and their thermodynamics. Later, based on the results of Ref. [5], these black hole solutions are discussed in more detail for the well-defined regularized theories. A uniqueness theorem for solutions is obtained, and the possibility that Hawking evaporation remnants constitute dark matter is discussed. We finish with a discussion on the cosmologies allowed by the different versions of 4DEGB theories.

In chapter 4 we are interested in confronting the regularized 4DEGB theory ob-

tained in chapter 2 with observations, based on Ref. [3]. We obtain its weak-field limit, and later constraint the coupling constant of the theory taking into account many observations and experimental results in a wide variety of settings.

In chapter 5 the well-known theory of gravity with a conformally coupled scalar field is generalized while maintaining all its symmetries and equations of motion at second order. This is achieved by imposing conformal symmetry on the equation of motion for the scalar field. This generalization includes a Gauss-Bonnet sector which is shown to be intimately connected with the well-defined regularized 4DEGB theories discussed in the previous chapters. Black holes and the cosmologies of the generalized conformal scalar field theory are discussed. These results are based on Ref. [4].

Chapter 6 discusses a framework that is applicable to many modified theories of gravity, rather than exploring one specific modified gravity theory example. In particular, it discusses how pseudospectral methods can be used to solve the stationary and axisymmetric field equations of modified theories of gravity in order to obtain highly-accurate numerical solutions of spinning black holes. We start by introducing the framework of spectral methods and then move on to discuss their applications to black hole physics. We discuss on a particular code implementation of the described methods, benchmarking the code against the well-known Kerr solution, obtaining remarkable agreement and small numerical error. Finally, as an example to how these methods can be used outside GR, we use our machinery to obtain spinning black holes in a set of scalar-Gauss-Bonnet modified theories, obtaining highly-accurate solutions. These results are based on Ref. [8] which is yet to appear.

Then, in chapter 7 we address the issue of the small mass limit of black holes in more standard scalar-Gauss-Bonnet theories. In these theories, black holes cease to exist below a certain mass, with their endpoint in light of Hawking evaporation being uncertain. Our aim is to investigate self-consistency and observational constraints imposed in these theories and their coupling dependence. We use analytical and numerical techniques in both the static and spinning black hole cases to perform these studies. The results of this chapter are based on Ref. [7].

We conclude and point towards future research directions in chapter 8.

2 Einstein-Gauss-Bonnet Gravity in Four Dimensions

In this section we will discuss in more detail the proposal of Glavan & Lin to re-scale the coupling constant of the Gauss-Bonnet term [110], before discussing the concerns and criticisms that have been raised about this idea, and the theories that have resulted from it.

2.1 Glavan & Lin's theory and solutions

The presentation here closely follows that of Ref. [110]. Let us start by considering the typical Einstein-Gauss-Bonnet action, where for the moment we neglect any contributions from matter fields, focusing on the purely gravitational sector

$$S = \frac{1}{16\pi G}\int d^D x\sqrt{-g}\left(-2\Lambda + R + \hat{\alpha}\mathcal{G}\right) , \tag{2.1}$$

where $\hat{\alpha}$ is a constant. The reader will note that the number of space-time dimensions D is not yet specified. Varying and extremizing the action with respect to the metric results in the field equations of the theory, which read

$$G_{\mu\nu} + \Lambda\, g_{\mu\nu} = \hat{\alpha}\, H_{\mu\nu} , \tag{2.2}$$

where

$$\begin{aligned} H_{\mu\nu} &= 15\delta_{\mu[\nu}R^{\rho\sigma}{}_{\rho\sigma}R^{\alpha\beta}{}_{\alpha\beta]} \\ &= -2\left(RR_{\mu\nu} - 2R_{\mu\alpha\nu\beta}R^{\alpha\beta} + R_{\mu\alpha\beta\sigma}R_{\nu}{}^{\alpha\beta\sigma} - 2R_{\mu\alpha}R_{\nu}{}^{\alpha} - \frac{1}{4}g_{\mu\nu}\mathcal{G}\right) . \end{aligned} \tag{2.3}$$

The right-hand side of this equation is anti-symmetrized over five indices, and so must vanish in dimensions $D < 5$. Up until this point, the presentation has been that of the usual Einstein-Gauss-Bonnet theory. The novelty added in Ref. [110] is the possibility that the vanishing of $H_{\mu\nu}$ in four dimensions might be cancelled by

re-scaling the coupling constant of the Gauss-Bonnet term, such that

$$\hat{\alpha} = \frac{\alpha}{D-4}\,, \tag{2.4}$$

for some new *finite* coupling constant α as we take the limit $D \to 4$. That this might be a viable possibility is suggested by the trace of the field equations (2.2), which contains a contribution from the Gauss-Bonnet term that takes the form

$$g^{\mu\nu} H_{\mu\nu} = \frac{1}{2}(D-4)\,\mathcal{G}\,. \tag{2.5}$$

It is clear that in this case the multiplicative factor of $(D-4)$ would be precisely cancelled by the suggested re-scaling of $\hat{\alpha}$, which would leave a non-vanishing contribution to the trace of the field equations as $D \to 4$:

$$\hat{\alpha} g^{\mu\nu} H_{\mu\nu} = \frac{\alpha}{\cancel{(D-4)}} \frac{1}{2} \cancel{(D-4)} \mathcal{G} = \frac{\alpha}{2}\mathcal{G}. \tag{2.6}$$

The authors of Ref. [110] suggest that this non-vanishing contribution may not be exclusive to the trace of the field equations, but could be manifest in the full theory. To support this claim they note that one can observe that the field equations written in differential form are

$$\varepsilon_{a_D} = \sum_{p=0}^{D/2-1} \alpha_p \,(D-2p)\, \epsilon_{a_1 \ldots a_D} R^{a_1,a_2} \wedge \ldots \wedge R^{a_{2p-1},a_{2p}} \wedge e^{a_{2p+1}} \wedge \ldots \wedge e^{a_{D-1}} = 0, \tag{2.7}$$

where e^a is the *vielbein*. It may be noted here that the $(D-4)$ factor emerges in the field equations in this case, as $p = 2$ for the Gauss-Bonnet contribution. While this is an intriguing suggestion, it appears that the desired result does not follow quite so straightforwardly, as we will discuss below. Nevertheless, there do exist D-dimensional space-times, which in the limit $D \to 4$ are well-behaved under the proposed re-scaling.

Let us now focus on three important examples of physically interesting D-dimensional spacetimes: the maximally-symmetric, spherically-symmetric, and the homogeneous and isotropic FLRW spacetimes. Starting with the maximally-symmetric spacetime, we have

$$R_{\mu\alpha\nu\beta} = \frac{R}{D(D-1)} \left(g_{\mu\nu} g_{\alpha\beta} - g_{\mu\beta} g_{\alpha\nu}\right), \tag{2.8}$$

with the Ricci scalar R being constant. From this, one can prove that

$$H_{\mu\nu} = \frac{(D-4)(D-3)(D-2)}{2D^2(D-1)} g_{\mu\nu} R^2, \tag{2.9}$$

thus resulting in the following non-trivial contribution to the field equations under the singular re-scaling of Eq. (2.4):

$$\lim_{D\to 4} \hat{\alpha} H_{\mu\nu} = \lim_{D\to 4} \frac{\alpha}{\cancel{(D-4)}} \frac{\cancel{(D-4)}(D-3)(D-2)}{2D^2(D-1)} g_{\mu\nu} R^2 = \frac{\alpha}{48} g_{\mu\nu} R^2. \tag{2.10}$$

Under these conditions, there are two branches of solutions of the field equations (2.2) where the constant Ricci scalar acts as an effective cosmological constant, $\Lambda_{\rm eff}$, which obeys

$$\Lambda^{\pm}_{\rm eff} = -\frac{6}{\alpha}\left(1 \pm \sqrt{1 + \frac{4\alpha\Lambda}{3}}\right). \tag{2.11}$$

The existence of two branches of solutions is well-known in the higher-dimensional Einstein-Gauss-Bonnet theory (see e.g. [280]) and remains a feature of 4D EGB that will accompany us throughout this work.

The two branches found above are fundamentally different. Assuming the Gauss-Bonnet contribution is a small correction to the theory, such that $\alpha \ll 1$, one obtains from the positive branch that

$$\Lambda^{+}_{\rm eff}\alpha \approx -12 - 4\Lambda\alpha + \mathcal{O}\left(\alpha^2\right), \tag{2.12}$$

while the negative branch gives

$$\Lambda^{-}_{\rm eff}\alpha \approx 4\Lambda\alpha + \mathcal{O}\left(\alpha^2\right). \tag{2.13}$$

Clearly the positive branch does not possess a well-defined limit as α vanishes, whereas in the negative branch we recover the dynamics of GR. For this reason, the positive branch is dubbed the *Gauss-Bonnet branch*, and the negative one the *GR branch*.

At the level of perturbation theory, we perturb the metric as

$$g_{\mu\nu} = \overline{g}_{\mu\nu} + h_{\mu\nu}, \tag{2.14}$$

around the maximally symmetric space-time $\overline{g}_{\mu\nu}$. The linear perturbations in $D = 4$

are then described by (see e.g. [281] for details)

$$\left(1+\frac{4\alpha\Lambda}{3}\right)\Big[\nabla^\rho\nabla^\mu h_{\nu\rho}+\nabla_\nu\nabla_\rho h^{\mu\rho}-\Box h^\mu{}_\nu-\nabla^\mu\nabla_\nu h^\rho{}_\rho \\ +\delta^\mu_\nu\Big(\Box h^\rho{}_\rho-\nabla_\rho\nabla_\sigma h^{\rho\sigma}\Big)+\Lambda\Big(\delta^\mu_\nu h^\rho{}_\rho-2h^\mu{}_\nu\Big)\Big]=0\,, \tag{2.15}$$

where the correction from the Gauss-Bonnet term can be observed to amount to an overall factor in the equation of motion, while the term in brackets is the same as in GR. Thus, just as in GR, the graviton has two degrees of freedom and the Gauss-Bonnet contribution to the linearized dynamics is trivial.

The same procedure can be performed for an FLRW background

$$ds^2=-dt^2+a(t)^2\left(\frac{dr^2}{1-kr^2}+r^2d\Omega_{D-2}\right), \tag{2.16}$$

where $a(t)$ is the scale factor and $d\Omega_{D-2}$ the metric on the $D-2$-sphere. We define, again, the Hubble rate as $H=\dot{a}/a$ and supplement the 4D EGB theory with matter in the form of a perfect fluid with stress-energy tensor $T^\mu{}_\nu=\mathrm{diag}\{-\rho,p,p,p,\ldots\}$, where ρ and p are the energy density and pressure of the matter fields. Under these conditions, the following set of (modified) Friedmann equations can be obtained

$$H^2+\frac{k}{a^2}+\alpha\left(H^2+\frac{k}{a^2}\right)^2=\frac{8\pi G}{3}\rho+\frac{\Lambda}{3}, \\ \dot{H}=-\frac{4\pi G(\rho+p)}{1+2\alpha\left(H^2+\frac{k}{a^2}\right)}+\frac{k}{a^2}, \tag{2.17}$$

while the matter fields obey the standard continuity equation $\dot{\rho}+3H\left(\rho+p\right)=0$. Interestingly, these Friedmann equations have exactly the same form as the ones obtained in holographic cosmology [282, 283], from the generalized uncertainty principle [284], by considering quantum entropic corrections [285], and from gravity with a conformal anomaly [286]. Moreover, they are equivalent to the ones resulting from the following set of field equations

$$G_{\mu\nu}+\Lambda g_{\mu\nu}+\alpha\left(R_{\rho\mu\sigma\nu}R^{\rho\sigma}-\frac{1}{12}g_{\mu\nu}R^2\right)=8\pi G\,T_{\mu\nu}. \tag{2.18}$$

The tensor in brackets on the left-hand-side has long been known to be covariantly conserved in conformally flat spacetimes on its own (it is sometimes called *accidentally conserved*) [287–289], and appears naturally in the renormalized stress-energy tensor of matter fields in curved-spacetime [289]. In the next section we will provide

an explanation as to why the modified Friedmann equations of 4DEGB and those arising from the set of field equations presented in Eq. (2.18) are equivalent.

If we now consider transverse and traceless parts of the metric fluctuations, which describe gravitational waves, by perturbing as

$$g_{ij} = a^2(\delta_{ij} + \gamma_{ij}), \tag{2.19}$$

where $\partial_i \gamma_{ij} = 0$ and $\gamma_{ii} = 0$, then we obtain in the four-dimensional limit a well-defined equation of motion, as the $(D-4)$ factors once again cancel. This gives

$$\ddot{\gamma}_{ij} + \left(3 + \frac{4\alpha\dot{H}}{1+2\alpha H^2}\right) H\dot{\gamma}_{ij} - c_s^2 \frac{\partial^2 \gamma_{ij}}{a^2} = 0, \qquad \text{where} \qquad c_s^2 = 1 + \frac{4\alpha\dot{H}}{1+2\alpha H^2}\,. \tag{2.20}$$

We observe that the Gauss-Bonnet contribution alters the Hubble friction and the sound speed, potentially leading to some non-trivial observational effects, which should be expected to be especially relevant in the early Universe.

Employing a general static and spherically-symmetric line-element, of the form

$$ds^2 = -f(r)e^{-2\delta(r)}dt^2 + \frac{dr^2}{f(r)} + r^2 d\Omega_{D-2}\,, \tag{2.21}$$

where $d\Omega_{D-2}$ is the metric on the $D-2$ sphere, the field equations reveal, once again, an overall $(D-4)$ factor, leading to the following solution in the limit $D \to 4$:

$$f(r) = 1 + \frac{r^2}{2\alpha}\left(1 \pm \sqrt{1 + \frac{8GM\alpha}{r^3}}\right), \qquad \text{and} \qquad \delta(r) = 0\,. \tag{2.22}$$

This solution is interesting for several reasons. First, it is highly reminiscent of the Boulware-Deser black hole from the higher-dimensional Einstein-Gauss-Bonnet theory [280], which reads

$$f(r) = 1 + \frac{r^2}{2\alpha(D-3)(D-4)}\left(1 \pm \sqrt{1 + \frac{8GM\alpha(D-3)(D-4)}{r^{D-1}}}\right), \tag{2.23}$$

and which also has $\delta(r) = 0$. Second, these 4D EGB black hole solutions are exactly the same as solutions that appear in other contexts, namely by considering gravity with a conformal anomaly [290, 291], entropy corrections to the black hole entropy [292] and more interestingly as a solution to the proposed UV completion of gravity, Hořava-Lifshitz gravity [293], known as the Kehagias-Sfetsos spacetime [294]. We

will discuss this black hole solution in more detail in future sections.

2.1.1 Concerns and shortcomings

As alluded to above, the novel approach of Glavan & Lin has been met with a healthy amount of skeptical scrutiny [222–230]. Here we discuss these criticisms, and present the arguments they involve.

Let us begin with Refs. [222–225], which have shown that the tensor resulting from the variation of the Gauss-Bonnet term, $H_{\mu\nu}$ given in Eq. (2.3), can be written in D dimensions in terms of the Weyl tensor as

$$H_{\mu\nu} = 2\left(H^{(1)}_{\mu\nu} + H^{(2)}_{\mu\nu}\right) , \tag{2.24}$$

where

$$H^{(1)}_{\mu\nu} = C_{\mu\alpha\beta\sigma}C_{\nu}{}^{\alpha\beta\sigma} - \frac{1}{4}g_{\mu\nu}C_{\alpha\beta\sigma\rho}C^{\alpha\beta\sigma\rho} , \tag{2.25}$$

and

$$H^{(2)}_{\mu\nu} = \frac{(D-4)(D-3)}{(D-2)(D-1)}\Bigg[-\frac{2(D-1)}{(D-3)}C_{\mu\rho\nu\sigma}R^{\rho\sigma} - \frac{2(D-1)}{(D-2)}R_{\mu\rho}R^{\rho}_{\nu} + \frac{D}{(D-2)}R_{\mu\nu}R + \frac{1}{(D-2)}g_{\mu\nu}\left((D-1)R_{\rho\sigma}R^{\rho\sigma} - \frac{D+2}{4}R^2\right)\Bigg] , \tag{2.26}$$

and where here the D-dimensional expression for the Weyl tensor should be understood to be taken as

$$C_{\mu\alpha\nu\beta} = R_{\mu\alpha\nu\beta} - \frac{2}{D-2}\left(g_{\mu[\nu}R_{\beta]\alpha} - g_{\alpha[\nu}R_{\beta]\mu}\right) + \frac{2}{(D-1)(D-2)}Rg_{\mu[\nu}g_{\beta]\alpha} . \tag{2.27}$$

Now, while it is the case that in the limit $D \to 4$ the term $\hat{\alpha}H^{(2)}_{\mu\nu}$ is well-defined, such that

$$\begin{aligned}\lim_{D\to 4}\frac{H^{(2)}_{\mu\nu}}{(D-4)} &= -C_{\mu\rho\nu\sigma}R^{\rho\sigma} - \frac{1}{2}R_{\mu\rho}R^{\rho}_{\nu} + \frac{1}{3}R_{\mu\nu}R + \frac{1}{4}g_{\mu\nu}\left(R_{\rho\sigma}R^{\rho\sigma} - \frac{1}{2}R^2\right) \\ &= \frac{1}{2}\left(-3C_{\mu\rho\nu\sigma} + R_{\mu\rho\nu\sigma} - \frac{1}{12}g_{\mu\nu}g_{\rho\sigma}R\right)R^{\rho\sigma}\end{aligned} \tag{2.28}$$

the same limit of $\hat{\alpha}H^{(1)}_{\mu\nu}$ is not. That is because $H^{(1)}_{\mu\nu}$ vanishes identically in four dimensions, as the Riemann tensor loses independent components as one lowers the space-time dimension (a result analogous to $G_{\mu\nu} = 0$ in 2 dimensions). The poor behaviour of $\hat{\alpha}H^{(1)}_{\mu\nu}$ in the 4-dimensional limit is problematic, but if one were to simply

ignore the above contribution to the field equations, the finite part resulting from the Gauss-Bonnet term would not be covariantly conserved, which would clearly be unacceptable. Note however, that if we consider a conformally flat spacetime (such as the FLRW metric, for which the Weyl tensor vanishes identically), and neglect all the Weyl terms even in the 4D limit, then $H_{\mu\nu}$ is equivalent to the *accidentally conserved* tensor presented in Eq. (2.18).

Revisiting the arguments that employ the first-order formalism outlined in Eq. (2.7), Refs. [222–225] argue that one cannot simply re-scale the coupling constant and take the four-dimensional limit. To see why, one can re-cast Eq. (2.7) in terms of space-time indices and take the Hodge dual of the $(D-1)$-form obtaining (see Ref. [222] for details)

$$\varepsilon_{\nu\alpha} = 2\,(D-4)!H_{\nu\alpha} = 0, \tag{2.29}$$

where $H_{\nu\alpha}$ is the Gauss-Bonnet tensor defined in Eq. (2.3). The pre-factor here no longer vanishes when $D = 4$, and the result is therefore that this approach does not lead to a well-defined $(D-4)$ factor in front of the field equations in the metric formulation. Again, this is obviously problematic for the proposed re-scaling procedure.

At the level of perturbation theory the Glavan & Lin approach also seems ill-defined. Although at first-order there are no divergences, as observed in Eq. (2.15), the same cannot be said about second-order perturbations. Around a Minkowski background these obey [224, 225]

$$\begin{aligned}
0 = &\left[\text{GR terms of } \mathcal{O}\left(h^2\right)\right] \\
&+ \frac{\alpha}{(D-4)}\Big[- 2\nabla_\gamma\nabla_\alpha h_{\nu\beta}\nabla^\gamma\nabla^\beta h_\mu{}^\alpha + 2\nabla_\gamma\nabla_\beta h_{\nu\alpha}\nabla^\gamma\nabla^\beta h_\mu{}^\alpha \\
&+ 2\nabla^\gamma\nabla^\beta h_\nu{}^\alpha\nabla_\mu\nabla_\alpha h_{\beta\gamma} + 2\nabla^\gamma\nabla^\beta h_\mu{}^\alpha\nabla_\nu\nabla_\alpha h_{\beta\gamma} - 2\nabla^\gamma\nabla^\beta h_\mu{}^\alpha\nabla_\nu\nabla_\beta h_{\alpha\gamma} \\
&- 2\nabla^\gamma\nabla^\beta h_\nu{}^\alpha\nabla_\mu\nabla_\beta h_{\alpha\gamma} - 2\nabla_\mu\nabla^\gamma h^{\alpha\beta}\nabla_\nu\nabla_\beta h_{\alpha\gamma} + 2\nabla_\mu\nabla^\gamma h^{\alpha\beta}\nabla_\nu\nabla_\gamma h_{\alpha\beta} \\
&+ \eta_{\mu\nu}\left(2\nabla_\delta\nabla_\beta h_{\alpha\gamma}\nabla^\delta\nabla^\gamma h^{\alpha\beta} - \nabla_\delta\nabla_\gamma h_{\alpha\beta}\nabla^\delta\nabla^\gamma h^{\alpha\beta} - \nabla_\beta\nabla_\alpha h_{\gamma\delta}\nabla^\delta\nabla^\gamma h^{\alpha\beta}\right)\Big],
\end{aligned} \tag{2.30}$$

which can be seen to be ill-defined in the four-dimensional limit.

A hint that the original approach outlined by Glavan & Lin may be an incomplete description of a more complicated theory is given by an analysis of tree-level scattering amplitudes. These reveal that, albeit being different to those of GR, the ones obtained from the four-dimensional limit of the Glavan & Lin approach are not new. Instead, they all come from certain scalar-tensor theories, indicating the likely presence of a scalar degree of freedom, in addition to the two tensor degrees

of freedom in the graviton [226]. Moreover, the on-shell action can be observed to contain divergences [228], and the field equations cannot be variationally completed in $D = 4$, as the Lagrangian diverges [229].

Given the concerns discussed above, alternative regularizations have been sought for a well-defined version of the Einstein-Gauss-Bonnet theory in four-dimensions. These have resulted in novel scalar-tensor theories either via a counter-term regularization [2, 258] (first applied in Ref. [112] in two-dimensions), or via a regularized Kaluza-Klein reduction [256, 257]. Yet another regularization method focuses on temporal diffeomorphism breaking, instead of the inclusion of a scalar degree of freedom [259]. Here we will discuss in detail the counter-term regularization, first performed in Ref. [2], and briefly review each of the other approaches in the following sections. In all cases Lovelock's theorem is respected, contrary to the aim of Glavan & Lin.

2.2 Derivation of Regularized Field Equations for the Einstein-Gauss-Bonnet Theory in Four Dimensions

In this section, based on Ref. [2], we investigate a method of regularizing the 4DEGB theory, in order to produce an action and set of field equations which are well-defined in the limit $D \to 4$, and which can be written in closed form. Our method does not rely on the embedding or compactification of any higher-dimensional spaces, and results in a theory of gravity in which an extra scalar gravitational degree of freedom is made explicit. All solutions of the original 4DEGB theory published in [110] are also found to be solutions of our new formulation of the theory.

2.2.1 Regularization of the Ricci scalar in 2D

The regularization procedure we wish to employ has already been successfully applied in two space-time dimensions, in order to construct an action for Einstein's equations, and we will use this section of our chapter to outline its application in this case. We intend this to be an instructional demonstration of the methodology that will also be used in the four dimensional case in Section 2.2.2, to regularize the 4DEGB theory. This section closely follows the presentation used in Reference [112].

Two-dimensional theories of gravity are known to be simpler than their four-dimensional counterparts, but nevertheless have been shown to admit rich and in-

teresting structures (such as *e.g.* black holes and cosmologies). Their simplicity also makes them a useful tool for the study of quantum gravity, which can be realised in this case [295]. However, while it is possible to write down a consistent set of field equations, it is more problematic to write down an action from which the field equations can be derived. This is because in two dimensions the Einstein-Hilbert term has topological character, much like the Gauss-Bonnet term has in four dimensions, which has led to the construction of a number of gravitational theories (see, *e.g.*, [296] for a review on two-dimensional gravity).

A development in two-dimensional theories of gravity, which is useful for our present study, is the development of a regularization procedure that introduces a divergence in the gravitational coupling parameter when $D \to 2$, and then cancels it out by adding a counter term to the action [112]. In this case we start by considering the following action in D dimensions:

$$S = \frac{\alpha}{(D-2)} \int d^D x \sqrt{-g} R + S_M \,, \tag{2.31}$$

where a re-scaling of the coupling constant has been introduced in order to try and cancel the vanishing contribution that R gives to the field equations in $D = 2$. This causes the action to become divergent, and of course is highly reminiscent of the procedure introduced in the 4DEGB proposal. Now, if one were to insist on going down the Glavan & Lin route (i.e. varying the action, obtaining the equations of motion, and then taking the $2D$ limit), one would stumble upon similar problems as in the previously discussed four-dimensional case. This is because the Einstein-tensor is identically zero in two dimensions, and so the limit

$$\lim_{D\to 2} \left(\alpha \frac{G_{\mu\nu}}{(D-2)} - T_{\mu\nu} \right) \,, \tag{2.32}$$

is not well-defined. Note, however, that the trace of the field equations

$$\lim_{D\to 2} g^{\mu\nu} \left(\alpha \frac{G_{\mu\nu}}{(D-2)} - T_{\mu\nu} \right) = -\frac{1}{2} \left(\alpha R - 2T \right) = 0, \tag{2.33}$$

is well-defined, just as in the case of 4D EGB. One can attempt to solve this indeterminacy of the field equations by adding a counter-term to the action, in order to cancel the resulting ill-defined terms. This can be done in the present case by

adding to the action (2.31) the term [112]

$$-\frac{\alpha}{(D-2)}\int d^D x\sqrt{-\tilde{g}}\tilde{R}\,, \tag{2.34}$$

where the tilde denotes a quantity constructed from the conformal geometry defined by

$$\tilde{g}_{\mu\nu} = e^{2\phi} g_{\mu\nu}\,. \tag{2.35}$$

One may note that in D dimensions the square root of the determinant of the metric is related to its conformal counterpart by $\sqrt{-\tilde{g}} = e^{D\phi}\sqrt{-g}$, and that the Ricci scalar of the conformal metric can be specified as [297, 298]

$$\sqrt{-\tilde{g}}\tilde{R} = \sqrt{-g}e^{(D-2)\phi}\Big[R - 2(D-1)\Box\phi - (D-1)(D-2)\left(\nabla\phi\right)^2\Big]\,. \tag{2.36}$$

Substituting this all into the action produces the result

$$\begin{aligned} S &= \frac{\alpha}{(D-2)}\int d^D x\left[\sqrt{-g}R - \sqrt{-\tilde{g}}\tilde{R}\right] + S_M \\ &= \frac{\alpha}{(D-2)}\int d^D x\sqrt{-g}\Big[2\left(D-1\right)\Box\phi + \left(D-1\right)\left(D-2\right)\left(\nabla\phi\right)^2 \\ &\qquad\qquad - \left(D-2\right)\phi R + 2\left(D-2\right)\left(D-1\right)\phi\Box\phi\Big] + S_M\,, \end{aligned} \tag{2.37}$$

where we have expanded the exponential around $D = 2$ and discarded terms of order $\mathcal{O}((D-2)^2)$ or higher. After performing an integration by parts, and discarding boundary terms, we find that the divergent factor is canceled, allowing us to take the two-dimensional limit

$$\begin{aligned} S &= -\frac{\alpha}{\cancel{(D-2)}}\int d^D x\sqrt{-g}\cancel{(D-2)}\left(\phi R + \left(D-1\right)\left(\nabla\phi\right)^2\right) + S_M \\ &\to -\alpha\int d^2 x\sqrt{-g}\left(\phi R + \left(\nabla\phi\right)^2\right) + S_M\,. \end{aligned} \tag{2.38}$$

This action has field equations

$$\tilde{R} = 0, \tag{2.39}$$

which follows from varying with respect to the scalar field, and is equivalent to

$$R - 2\Box\phi = 0\,, \tag{2.40}$$

and from the metric variation

$$\nabla_\mu\phi\nabla_\nu\phi - \nabla_\mu\nabla_\nu\phi + g_{\mu\nu}\left(\Box\phi - \frac{1}{2}\left(\nabla\phi\right)^2\right) = \frac{1}{\alpha}T_{\mu\nu}\,, \tag{2.41}$$

where the stress-energy tensor obeys the conservation equation $\nabla^\mu T_{\mu\nu} = 0$. Of particularly interest in this case is that a suitable combination of the scalar field equation (2.40) and the trace of the field equations (2.41),

$$\Box\phi = \frac{1}{\alpha}T\,, \tag{2.42}$$

completely decouples from the scalar field resulting in

$$\alpha R = 2T\,, \tag{2.43}$$

where $T = T^\mu{}_\mu$, thus having the same trace equation as Eq. (2.33). Note that in two dimensions there is only a single degree of freedom in the geometry, which means that Eq. (2.43) contains all the information about the theory.

These field equations are particularly interesting as it can be seen that Equation (2.39) is equivalent to the vanishing of the Ricci curvature of the conformal geometry, and also that the classical evolution of the gravity-matter system is independent of ϕ (although the converse is not true).

The theory with field equation (2.43) is sometimes dubbed "$R = T$" gravity, and has been studied in much detail in the literature [299–303]. We remark that the regularized theory of [112] admits exactly the same solutions as $R = T$ gravity in $2D$ [135, 227, 304], but that it also admits a finite and well-defined action. In the next section we will deploy a similar procedure to regularize the 4DEGB theory, in which we will obtain similar results.

2.2.2 Regularization of the Gauss-Bonnet term in 4D

In this section we apply the ideas from the discussion above to the four-dimensional case with a Gauss-Bonnet term. We start by considering the (divergent) Einstein-Gauss-Bonnet action in D dimensions

$$S = \int d^D x\sqrt{-g}\left(R + \frac{\alpha}{(D-4)}\mathcal{G}\right), \tag{2.44}$$

to which we add the counter-term

$$-\frac{\alpha}{(D-4)}\int d^D x\sqrt{-\tilde{g}}\tilde{\mathcal{G}}\,, \tag{2.45}$$

where again the tilde denotes quantities constructed from a conformal geometry as in Eq. (2.35). Our reasoning to choose this particular counter-term to regularize the action was the following. First, an analogous procedure was applied with success in 2D as we have reviewed, suggesting that a regularized four-dimensional theory might be obtained with success as well. Now, if we take a look at Eq. (2.24), we observe that the problematic terms as we take the regularized four-dimensional limit are the ones composed only of the Weyl tensor, therefore possessing a conformally invariant character. By subtracting a conformal Gauss-Bonnet term, upon variation we are effectively canceling these conformally invariant problematic terms, leaving us only with terms proportional to a $(D-4)$ factor. This fact will be manifest even at the level of the action, as we will see next.

We can write the Gauss-Bonnet term of the conformal metric in terms of the original one as [297, 298]

$$\begin{aligned}\sqrt{-\tilde{g}}\tilde{\mathcal{G}} =&\sqrt{-g}e^{(D-4)\phi}\left[\mathcal{G}-8(D-3)R^{\mu\nu}\left(\nabla_\mu\phi\nabla_\nu\phi-\nabla_\mu\nabla_\nu\phi\right)-2(D-3)(D-4)R\left(\nabla\phi\right)^2\right.\\&+4(D-2)(D-3)^2\Box\phi\left(\nabla\phi\right)^2-4(D-2)(D-3)\left(\nabla_\mu\nabla_\nu\phi\right)\left(\nabla^\mu\nabla^\nu\phi\right)\\&+4(D-2)(D-3)\left(\Box\phi\right)^2+8(D-2)(D-3)\left(\nabla_\mu\phi\nabla_\nu\phi\right)\left(\nabla^\mu\nabla^\nu\phi\right)\\&\left.-4(D-3)R\Box\phi+(D-1)(D-2)(D-3)(D-4)(\nabla\phi)^4\right].\end{aligned} \tag{2.46}$$

Expanding the exponential around $D=4$, and neglecting terms of order $(D-4)^2$ or higher, we then obtain

$$\begin{aligned}&\sqrt{-\tilde{g}}\tilde{\mathcal{G}}=\sqrt{-g}\Big(\mathcal{G}-4(D-3)R\Box\phi+4(D-3)^2(D-2)\Box\phi\left(\nabla\phi\right)^2+4(D-3)(D-2)(\Box\phi)^2\\&-8(D-3)R^{\mu\nu}(\nabla_\mu\phi\nabla_\nu\phi-\nabla_\mu\nabla_\nu\phi)+8(D-3)(D-2)\nabla_\mu\phi\nabla_\nu\phi\nabla^\mu\nabla^\nu\phi\\&-4(D-3)(D-2)(\nabla_\mu\nabla_\nu\phi)(\nabla^\mu\nabla^\nu\phi)+(D-4)\Big[\phi\mathcal{G}-2(D-3)R\left(\nabla\phi\right)^2\\&+(D-3)(D-2)(D-1)(\nabla\phi)^4-4(D-3)\phi R\Box\phi+4(D-3)^2(D-2)\phi\Box\phi\left(\nabla\phi\right)^2\\&+4(D-3)(D-2)\phi(\Box\phi)^2-8(D-3)\phi R^{\mu\nu}(\nabla_\mu\phi\nabla_\nu\phi-\nabla_\mu\nabla_\nu\phi)\\&+8(D-3)(D-2)\phi(\nabla_\mu\phi\nabla_\nu\phi)(\nabla^\mu\nabla^\nu\phi)-4(D-3)(D-2)\phi(\nabla_\mu\nabla_\nu\phi)(\nabla^\mu\nabla^\nu\phi)\Big]\Big).\end{aligned} \tag{2.47}$$

Integrating by parts, and making use of the identity[7]

$$\nabla_\mu\left[\Box\phi\nabla^\mu\phi-\frac{1}{2}\nabla^\mu\left(\nabla\phi\right)^2\right]=\left(\Box\phi\right)^2-\left(\nabla_\mu\nabla_\nu\phi\right)^2-R^{\mu\nu}\nabla_\mu\phi\nabla_\nu\phi, \tag{2.48}$$

and the Bianchi identities, we can find that the action reads

$$\begin{aligned}S=\int_{\mathcal{M}}d^Dx\sqrt{-g}\Big[R+\frac{\alpha}{\cancel{(D-4)}}\cancel{(D-4)}\Big(&4(D-3)G^{\mu\nu}\nabla_\mu\phi\nabla_\nu\phi-\phi\mathcal{G}\\&-4(D-5)(D-3)\Box\phi\left(\nabla\phi\right)^2-(D-5)(D-3)(D-2)(\nabla\phi)^4\Big)\Big]+S_m\,.\end{aligned} \tag{2.49}$$

On taking the four-dimensional limit, this becomes

$$S=\int_{\mathcal{M}}d^4x\sqrt{-g}\Big[R+\alpha\Big(4G^{\mu\nu}\nabla_\mu\phi\nabla_\nu\phi-\phi\mathcal{G}+4\Box\phi(\nabla\phi)^2+2(\nabla\phi)^4\Big)\Big]+S_m\,, \tag{2.50}$$

which can be seen to be a four-dimensional action free of divergences. This action belongs to the Horndeski class of theories [104, 105], with functions

$$G_2=8\alpha X^2,\quad G_3=8\alpha X,\quad G_4=1+4\alpha X,\quad G_5=4\alpha\log X. \tag{2.51}$$

It can also be noted that the action has a shift symmetry in the scalar field, *i.e.*, invariance under the set of transformations $\phi\to\phi+C$, where C is an arbitrary constant, and therefore the theory possesses a conserved Noether current.

Given the four-dimensional action (2.50), the variational principle can be applied to get the field equations

$$G_{\mu\nu}+\alpha\mathcal{H}_{\mu\nu}=T_{\mu\nu}, \tag{2.52}$$

where

$$\begin{aligned}\mathcal{H}_{\mu\nu}=&2G_{\mu\nu}\left(\nabla\phi\right)^2+4P_{\mu\alpha\nu\beta}\left(\nabla^\alpha\phi\nabla^\beta\phi-\nabla^\beta\nabla^\alpha\phi\right)+4\left(\nabla_\mu\phi\nabla_\nu\phi-\nabla_\nu\nabla_\mu\phi\right)\Box\phi\\&+4\left(\nabla_\alpha\phi\nabla_\mu\phi-\nabla_\alpha\nabla_\mu\phi\right)\left(\nabla^\alpha\phi\nabla_\nu\phi-\nabla^\alpha\nabla_\nu\phi\right)\\&+g_{\mu\nu}\Big(2\left(\Box\phi\right)^2-\left(\nabla\phi\right)^4+2\nabla_\beta\nabla_\alpha\phi\left(2\nabla^\alpha\phi\nabla^\beta\phi-\nabla^\beta\nabla^\alpha\phi\right)\Big),\end{aligned} \tag{2.53}$$

with

$$P_{\alpha\beta\mu\nu}\equiv\frac{1}{4}\epsilon_{\alpha\beta\gamma\delta}R^{\rho\sigma\gamma\delta}\epsilon_{\rho\sigma\mu\nu}=2\,g_{\alpha[\mu}G_{\nu]\beta}+2\,g_{\beta[\nu}R_{\mu]\alpha}-R_{\alpha\beta\mu\nu}, \tag{2.54}$$

being the double dual of the Riemann tensor. The corresponding scalar field equa-

[7] The identity follows straightforwardly by commuting covariant derivatives after expanding the left-hand side.

tion is

$$\tilde{\mathcal{G}} = 0, \tag{2.55}$$

which is equivalent to

$$R^{\mu\nu}\nabla_\mu\phi\nabla_\nu\phi - G^{\mu\nu}\nabla_\mu\nabla_\nu\phi - \Box\phi\,(\nabla\phi)^2 + (\nabla_\mu\nabla_\nu\phi)^2 - (\Box\phi)^2 - 2\nabla_\mu\phi\nabla_\nu\phi\nabla^\mu\nabla^\nu\phi = \frac{1}{8}\mathcal{G}. \tag{2.56}$$

Interestingly, a suitable combination of the scalar field equation and the trace of the field equations results in the purely geometric condition,

$$R + \frac{\alpha}{2}\mathcal{G} = -T, \tag{2.57}$$

which is exactly the same form as the trace of the field equations of the original 4DEGB theory. Our theory therefore exactly reproduces the only known well-defined field equation of the 4DEGB theory, and suggests that there may have been a hidden scalar degree of freedom in the original theory, which may be one reason it has not yet been proven possible to write its full field equations in terms of curvature tensors only (see Section 2.1.1).

2.2.2.1 Regularization with the dimensional derivative

Before continuing, let us again consider the two-dimensional case, but where we employ the following regularization scheme for the Ricci scalar

$$\mathcal{L} = -\alpha \lim_{D\to 2} \frac{\sqrt{-\tilde{g}}\tilde{R} - \sqrt{-\tilde{g}}\tilde{R}\big|_{D=2}}{(D-2)}\,. \tag{2.58}$$

This looks very similar to the previously presented regularization, but differs as we add a counter-term whose numerator is already evaluated in two dimensions, where all quantities are tilded. A more careful reading reveals that the expression above is nothing but a dimensional derivative:

$$\mathcal{L} = -\alpha \frac{d}{dD}\left(\sqrt{-\tilde{g}}\tilde{R}\right)\Big|_{D=2}, \tag{2.59}$$

which one can immediately see to be free of divergences as there is no divergent factor. The dimensional derivative here plays the role of canceling the $(D-2)$ factors appearing in the equations of motion, much like the divergent factors introduced by

Glavan & Lin [110]. That is,

$$\frac{d}{dD}\left(D-N\right)\Big|_{D=N}=1 \qquad \text{instead of} \qquad \lim_{D\to N}\frac{1}{(D-N)}\left(D-N\right)=1. \tag{2.60}$$

To compute the Lagrangian (2.59) we proceed by going from the tilded frame to the non-tilded frame

$$\begin{aligned}\mathcal{L} =& -\alpha\frac{d}{dD}\left(\sqrt{-g}e^{(D-2)\phi}\Big[R-2(D-1)\Box\phi-(D-1)(D-2)\left(\nabla\phi\right)^2\Big]\right)\Big|_{D=2},\\ =& -\alpha\sqrt{-g}\Big(e^{(D-2)\phi}\phi\left[R-2(D-1)\Box\phi-(D-1)(D-2)\left(\nabla\phi\right)^2\right]\\ &-e^{(D-2)\phi}\left(2\Box\phi+((D-1)+(D-2))\left(\nabla\phi\right)^2\right)\Big)\Big|_{D=2},\end{aligned} \tag{2.61}$$

where we assumed that non-tilded quantities do not possess a dimensional dependence. Evaluating the two-dimensional limit, we observe no divergences and obtain

$$\mathcal{L}=-\alpha\sqrt{-g}\left(\phi R+\left(\nabla\phi\right)^2\right), \tag{2.62}$$

which is the same exact Lagrangian as we obtained in Eq. (2.38). The same dimensional derivative procedure can be applied in 4D to the Gauss-Bonnet invariant, resulting in the same action as the counter-term regularization of Eq. (2.50).

2.3 Other regularization procedures leading to well-defined Einstein-Gauss-Bonnet Theories in Four Dimensions

In this section we briefly review other regularization methods employed by other authors. In particular, we will review the procedure applied in Refs. [256, 257], which consists of performing a Kaluza-Klein compactification of $D-$dimensional Einstein-Gauss-Bonnet gravity on a maximally symmetric space-time of $(D-4)$ dimensions. Here the coupling factor α is taken to have the same singular scaling, and we keep only the breathing mode characterizing the size of the internal space. This regularization procedure will be of importance to the content presented in Chapter 5, for reasons that will become clearer later on.

We start the Kaluza-Klein regularization process by parametrizing the $D-$dimensional

metric as

$$ds_D^2 = ds_4^2 + e^{-2\phi} d\Sigma_{D-4,\lambda}^2 \,, \tag{2.63}$$

where the scalar field ϕ depends only on the 4-dimensional coordinates, ds_4^2 is the 4-dimensional line-element and $d\Sigma_{D-4,\lambda}^2$ is the line-element of an internal maximally symmetric space of $(D-4)$ dimensions whose curvature tensor is given by

$$R_{abcd} = \lambda(g_{ac}g_{bd} - g_{ad}g_{bc}), \tag{2.64}$$

with λ a constant representing the curvature of the internal space. Under these assumptions, the Einstein-Gauss-Bonnet action (2.1) reduces to

$$\begin{aligned} S =& \frac{1}{16\pi G}\int d^4x\sqrt{-g}e^{-(D-4)\phi}\Big\{ R + (D-4)(D-5)\big((\nabla\phi)^2 + \lambda e^{2\phi}\big) \\ &+ \alpha\Big(\mathcal{G} - 2(D-4)(D-5)\left[2G^{\mu\nu}\nabla_\mu\phi\nabla_\nu\phi - \lambda R e^{2\phi}\right] \\ &- (D-4)(D-5)(D-6)\Big[-2\left(\nabla\phi\right)^2\Box\phi + (D-5)(\nabla\phi)^4\Big] \\ &+ (D-4)(D-5)(D-6)(D-7)\left[2\lambda\left(\nabla\phi\right)^2 e^{2\phi} + \lambda^2 e^{4\phi}\right]\Big)\Big\}. \end{aligned} \tag{2.65}$$

As we are interested in taking the limit $D \to 4$ we employ a method similar to counter-term regularization, namely expand the exponential and discard terms of order $(D-4)^2$. Moreover, we can remove the bare Gauss-Bonnet term by introducing a counter-term and re-scaling the coupling constant as $\alpha \to \alpha/(D-4)$. In the end, the $D \to 4$ limit leaves

$$\begin{aligned} S = \int d^4x\sqrt{-g}\Big[R + \alpha\Big(&4G^{\mu\nu}\nabla_\mu\phi\nabla_\nu\phi - \phi\mathcal{G} + 4\Box\phi(\nabla\phi)^2 + 2(\nabla\phi)^4 \\ &- 2\lambda e^{2\phi}\left[R + 6\left(\nabla\phi\right)^2 + 3\lambda e^{2\phi}\right]\Big)\Big]. \end{aligned} \tag{2.66}$$

This regularized action can be seen to differ from the one obtained via the counter-term regularization by the terms proportional to λ, with $\lambda = 0$ (flat internal space) recovering the counter-term regularized theory in Eq. (2.50) precisely.

If one were to keep the λ-dependent terms, then the resulting field equations would take the form

$$G_{\mu\nu} + \alpha\left(\mathcal{H}_{\mu\nu} - 2\lambda e^{2\phi}\mathcal{A}_{\mu\nu} + 3\lambda^2 e^{4\phi} g_{\mu\nu}\right) = T_{\mu\nu}\,, \tag{2.67}$$

where

$$\mathcal{A}_{\mu\nu} := G_{\mu\nu} + 2\nabla_\mu\phi\nabla_\nu\phi - 2\nabla_\mu\nabla_\nu\phi + g_{\mu\nu}\left(2\Box\phi + (\nabla\phi)^2\right) , \tag{2.68}$$

and the scalar field equation takes the form

$$\begin{aligned} &4\lambda\left(6\lambda e^{4\phi} + e^{2\phi}\left(R - 6\Box\phi - 6\,(\nabla\phi)^2\right)\right) + 8R^{\mu\nu}\nabla_\mu\phi\nabla_\nu\phi - 8G^{\mu\nu}\nabla_\mu\nabla_\nu\phi \\ &- 8\Box\phi\,(\nabla\phi)^2 + 8(\nabla_\mu\nabla_\nu\phi)^2 - 8(\Box\phi)^2 - 16\nabla_\mu\phi\nabla_\nu\phi\nabla^\mu\nabla^\nu\phi - \mathcal{G} = 0\,. \end{aligned} \tag{2.69}$$

Again, the theory possesses the purely geometrical equation given in (2.57), and shares solutions with the original formulation of Ref. [110].

Finally, let us briefly discuss the alternative regularization of Ref. [259] in which temporal diffeomorphism symmetry is explicitly broken. This regularization procedure consists on performing a Arnowitt-Deser-Misner (ADM) decomposition and working with the Hamiltonian of the D dimensional Einstein-Gauss-Bonnet theory. The Hamiltonian is found to split into two parts, a regular part upon taking a 4D limit, and a Weyl part, much like the Lanczos tensor as we discussed above. The regularization of Ref. [259] consists on completely removing the Weyl part of the Hamiltonian (i.e., adding a counter-term which is the Weyl part of the Hamiltonian). The price to pay, is that the resulting is only invariant under spatial diffeomorphisms and therefore breaks the full 4D diffeomorphism invariance of GR. Furthermore, in order to fully determine the theory, a gauge-fixing condition must be added to the resulting Hamiltonian in order choose the constant time hypersurfaces that are preferred when breaking the temporal part of the diffeomorphisms. This gauge choice is part of the definition of the theory and one could therefore define many such theories with different gauges. This theory propagates the same number of degrees of freedom as GR, but breaks time diffeomorphisms and therefore is still in agreement with Lovelock's theorem. The phenomenology of the theory has some differences with respect to the original Glavan & Lin's theory [110], particularly regarding the propagation of gravitational waves [271, 272]. Nonetheless, the authors claim the black hole and FLRW solutions of the original theory are present in this framework [259].

3 Phenomenology of the Einstein Gauss-Bonnet Theory in Four Dimensions

In this chapter we will discuss the phenomenology of the 4D-Einstein-Gauss-Bonnet theories, with a focus on the well-defined theories derived in Chapter 2, in particular the one defined in Eq. (2.50). We will start by reviewing the black hole solutions and how they can be obtained within the original Glavan & Lin's approach [110]. These were briefly discussed in Chapter 2. Here we will analyse the black hole solutions in more detail, and discuss their charged (A)dS generalizations, based on the results of Ref. [1]. Later, we will move into the well-defined framework of the counter-term regularized theory, and discuss its black hole solutions, based on the results of Ref. [5]. In particular, we will demonstrate a Birkhoff-type theorem for the theory and argue that black hole remnants from Hawking evaporation can act as dark matter. Next, we will discuss the cosmologies of 4DEGB theories, partly based on the results of Ref. [6].

3.1 Black Holes, Uniqueness of Solutions and a New Dark Matter Candidate

3.1.1 Black holes in the original Glavan & Lin's approach

Consider now the Einstein-Maxwell Gauss-Bonnet theory in D dimensions with a cosmological constant Λ given by the action

$$S = \frac{1}{16\pi}\int d^D x\sqrt{-g}\left[R - 2\Lambda + \frac{\alpha}{D-4}\mathcal{G} - F_{\mu\nu}F^{\mu\nu}\right], \tag{3.1}$$

where $F_{\mu\nu} = \partial_\mu A_\nu - \partial_\nu A_\mu$ is the usual Maxwell tensor. We consider a static, spherically symmetric metric ansatz in D dimensions given by

$$ds^2 = -e^{2A(r)}dt^2 + e^{2B(r)}dr^2 + r^2 d\Omega_{D-2}, \tag{3.2}$$

and an electrostatic vector potential $A = V(r)dt$. All functions are radial dependent only and we shall omit this dependence henceforth. Substituting the metric ansatz (3.2) and the electrostatic potential in the action (3.1) (in a process also known as *symmetric criticality* [305]) we notice the existence of a first integral

$$V'(r) = -\frac{Q}{r^{D-2}} e^{A+B}, \tag{3.3}$$

with Q an integration constant interpreted as the electric charge measured at infinity, and the action reduces to the remarkably simple form

$$S = \frac{\Sigma_{D-2}}{16\pi} \int dt dr \left[r^{D-1}\psi\left(1+\alpha(D-3)\psi\right) - \frac{2\Lambda r^{D-1}}{(D-1)(D-2)} + \frac{2Q^2 r^{3-D}}{(D-3)(D-2)} \right]' \times e^{A+B}(D-2), \tag{3.4}$$

with the prime denoting a radial derivative, $\Sigma_{D-2} = \frac{2\pi^{\frac{D-1}{2}}}{\Gamma\left[\frac{D-1}{2}\right]}$ the surface area of the $(D-2)$-dimensional hypersurface $d\Omega_{D-2}$ and where we have defined

$$\psi = r^{-2}\left(1 - e^{-2B}\right). \tag{3.5}$$

From the action (3.4), upon variation with respect to the metric functions, one can find the solution

$$e^{A+B} = 1, \tag{3.6}$$

$$\psi\left(1+\alpha(D-3)\psi\right) - \frac{2\Lambda}{(D-1)(D-2)} + \frac{2Q^2 r^{4-2D}}{(D-3)(D-2)} = \frac{16\pi M}{(D-2)r^{D-1}\Sigma_{D-2}}, \tag{3.7}$$

with M the ADM mass, appearing as an integration constant. Taking the limit $D \to 4$, we obtain the exact solution in closed form

$$-g_{00} = e^{2A} = e^{-2B} = 1 + \frac{r^2}{2\alpha}\left(1 \pm \sqrt{1 + 4\alpha\left(\frac{2M}{r^3} - \frac{Q^2}{r^4} + \frac{\Lambda}{3}\right)}\right), \qquad A = \frac{Q}{r}dt, \tag{3.8}$$

As with maximally symmetric space-times, there are two branches: the Gauss-Bonnet branch with a plus sign, and the GR branch with the minus sign. The Gauss-Bonnet branch behaves asymptotically as

$$-g_{00} \sim 1 + \frac{2M}{r\sqrt{1+\frac{4\alpha\Lambda}{3}}} - \frac{Q^2}{r^2\sqrt{1+\frac{4\alpha\Lambda}{3}}} + \frac{r^2}{2\alpha}\left(1+\sqrt{1+\frac{4\alpha\Lambda}{3}}\right) + \mathcal{O}\left(\frac{1}{r^3}\right), \quad (3.9)$$

while the one with the minus sign behaves as

$$-g_{00} \sim 1 - \frac{2M}{r\sqrt{1+\frac{4\alpha\Lambda}{3}}} + \frac{Q^2}{r^2\sqrt{1+\frac{4\alpha\Lambda}{3}}} + \frac{r^2}{2\alpha}\left(1-\sqrt{1+\frac{4\alpha\Lambda}{3}}\right) + \mathcal{O}\left(\frac{1}{r^3}\right). \quad (3.10)$$

In the first case, in the limit of vanishing cosmological constant, we asymptotically obtain a Reissner-Nordström-AdS solution with negative gravitational mass and imaginary charge, while the latter reduces to the Reissner-Nordström solution with positive gravitational mass and real charge. The Gauss-Bonnet branch is typically disregarded as a physically-interesting solution, because it does not present a well-defined limit as α vanishes and because the mass term has the wrong sign. It is interesting to note that

$$1+\frac{r^2}{2\alpha}\left(1-\sqrt{1+4\alpha\left(\frac{2M}{r^3}-\frac{Q^2}{r^4}+\frac{\Lambda}{3}\right)}\right) = 1-\frac{\frac{2M}{r}-\frac{Q^2}{r^2}+\frac{\Lambda}{3}r^2}{\frac{1}{2}\left(1+\sqrt{1+\frac{4\alpha}{r^2}\left(\frac{2M}{r}-\frac{Q^2}{r^2}+\frac{\Lambda}{3}r^2\right)}\right)}, \quad (3.11)$$

where the GR limit ($\alpha \to 0$) is manifest.

The event horizon of the black holes r_+ is larger root of the following equation

$$1 - \frac{2M}{r} + \frac{Q^2+\alpha}{r^2} - \frac{\Lambda}{3}r^2 = 0, \quad (3.12)$$

which in the absence of a cosmological constant, has the simple solution

$$r_\pm = M \pm \sqrt{M^2 - Q^2 - \alpha}. \quad (3.13)$$

Note that Eq. (3.12) follow For a non-vanishing cosmological constant the expression for r_+ is complicated and not particularly elucidative, thus we do not present it here. The physical properties of this branch differ depending on whether the mass M is

larger or smaller than a critical mass given by

$$M_* = \sqrt{Q^2 + \alpha}. \tag{3.14}$$

To illustrate, in Fig. 3.1 we plot the radial dependence of the metric function $-g_{00}$ (for the branch with the negative sign) for three situations: one with $M < M_*$, other with $M > M_*$ and the extremal case $M = M_*$. If $M < M_*$ there are no

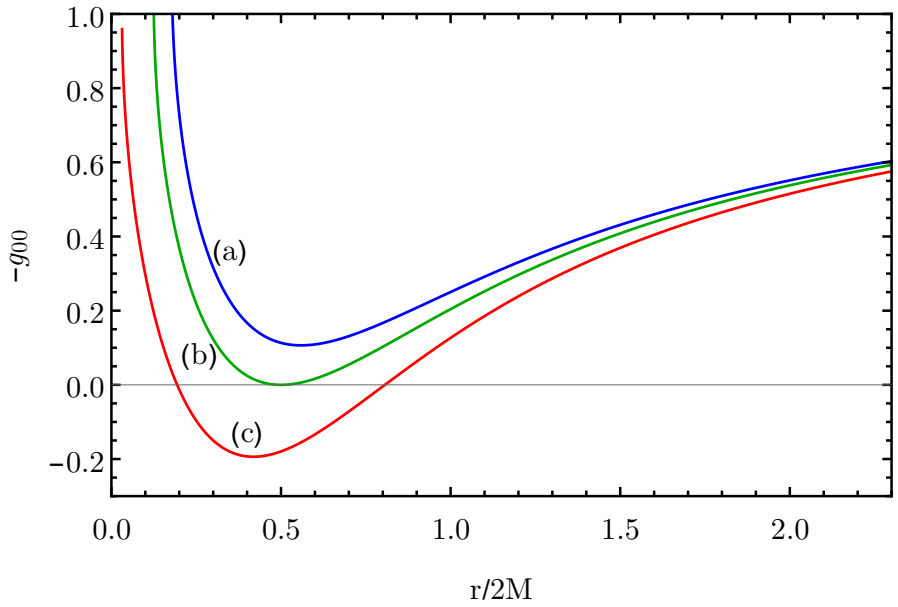

Figure 3.1: Metric function $-g_{00}$ as a function of the radial coordinate for several values of M_*/M for the minus sign branch, in the absence of a cosmological constant. (a, blue) $M < M_*$; (b, green) $M = M_*$; (c, red) $M > M_*$.

horizons, and thus no BH solutions, while for $M > M_*$ there are two horizons as given in (3.13), and for $M = M_*$ there is one degenerate horizon, corresponding to an extremal BH. In the limit $\alpha \to 0$ we recover, for the negative sign branch, the Reissner-Nordström-AdS metric from general relativity

$$-\lim_{\alpha\to 0} g_{00} = 1 - \frac{2M}{r} + \frac{Q^2}{r^2} + \frac{r^2}{l^2}. \tag{3.15}$$

Particularly important limits of the solution are:

1. In the case of vanishing charge Q and cosmological constant, we recover the solution in Eq. (2.22), first obtained in Ref. [110].

2. For a vanishing cosmological constant we obtain the electrically charged solution of the theory, analogous to the Reissner-Nordström BH from GR electro-

vacuum.

3. For both vanishing mass and charge we arrive at the (A)dS solutions of the model.

4. In the limit $\alpha \to 0$, we recover GR solutions.

Considering the simplest case (uncharged, without a cosmological constant), we find that the metric components are finite as $r \to 0$:

$$\lim_{r\to 0} f(r) = 1. \tag{3.16}$$

Even though the metric components are finite, the central singularity located at $r = 0$ still exists. The Ricci and Kretschmann scalars of the metric are

$$R = \frac{120\alpha^2 M^2 + 24\alpha M r^3 (3 - 2\mathcal{K}) + 6r^6 (1 - \mathcal{K})}{\alpha r^6 \mathcal{K}^3}, \tag{3.17}$$

$$R_{\mu\nu\alpha\beta}R^{\mu\nu\alpha\beta} = \frac{12\left(\frac{2\alpha M}{r^3} + 1\right)\left(4\alpha^2(37 - 20\mathcal{K})M^2 r^3 + 2\alpha(11 - 9\mathcal{K})M r^6 + (1 - \mathcal{K})r^9 + 216\alpha^3 M^3\right)}{\alpha^2 \mathcal{K}^6 r^9}. \tag{3.18}$$

where $\mathcal{K} = \sqrt{\frac{8\alpha M}{r^3} + 1}$. Near $r = 0$, assuming a non-vanishing value of α we have

$$R \approx \frac{15}{2}\sqrt{\frac{M}{2\alpha}} r^{-3/2}, \qquad \text{and} \qquad R_{\mu\nu\alpha\beta}R^{\mu\nu\alpha\beta} \approx \frac{81M}{8\alpha} r^{-3}, \tag{3.19}$$

Note that the Gauss-Bonnet term has weakened the singularity when compared to the Schwarzschild black hole from GR, where the Kretschmann scalar diverges as r^{-6} near the center. One should note that the expansion of the curvature invariants near $r = 0$ should be taken carefully, as in the limit of small α and r there are competing effects between the two. Another singularity exists if we were to consider a negative value of α, located at the radius for which the quantity inside the square root in the solution (2.22) vanishes:

$$r^3 = -8M\alpha. \tag{3.20}$$

The shadow, innermost stable circular orbit (ISCO) and the quasi-normal modes of these black holes have been studied in Refs. [113, 114].

3.1.1.1 Thermodynamics

In this section, we briefly explore the thermodynamics of these black holes. Henceforth, we shall restrict our discussion to the GR (negative) branch of solutions, as it should be considered the physical branch. The thermodynamics of charged Einstein Gauss-Bonnet black holes with a cosmological constant are discussed in detail in an arbitrary number of dimensions in Ref. [306].

We start by expressing the black hole mass M in terms of r_+ by solving $g_{00}|_{r=r_+} = 0$, resulting in

$$M = \frac{r_+}{2}\left(1 - \frac{\Lambda r_+^2}{3} + \frac{Q^2+\alpha}{r_+^2}\right). \tag{3.21}$$

The Hawking temperature, as discussed in the introduction, is given by

$$T = \frac{\kappa}{2\pi}, \tag{3.22}$$

where κ is the surface gravity given by $\kappa^2 = -\frac{1}{2}\nabla_\mu\xi_\nu\nabla^\mu\xi^\nu$, with ξ^μ a killing vector, which for a static, spherically symmetric case takes the form $\xi^\mu = \partial_t^\mu$. For our metric ansatz (3.2) the surface gravity is

$$\kappa = \frac{1}{2}\frac{d}{dr}(e^{2A})|_{r=r_+}, \tag{3.23}$$

resulting in a Hawking temperature given by

$$T = \frac{r_+^2 - \alpha - Q^2 - r_+^4\Lambda}{4\pi r_+(r_+^2+2\alpha)}. \tag{3.24}$$

For a null cosmological constant, the temperature vanishes if $M = M_*$ defined in Eq. (3.14). Thus, black holes whose mass is equal to the critical mass are extremal BHs.

In GR the entropy S of a black hole obeys the Hawking-Bekenstein formula $S = A/4$, where A is the area of the event horizon of the black hole. In general, when considering higher-order curvature terms, however, the black hole entropy does not satisfy the Hawking-Bekenstein relation. To compute the entropy we use the approach of Ref. [307], which is based on the fact that, as thermodynamic systems, black holes must obey the first law of thermodynamics

$$dM = TdS + \sum_i \mu_i dQ_i, \tag{3.25}$$

where μ_i are the chemical potentials corresponding to the conserved charges Q_i.

Using Eq. (3.25) one has

$$S = S_0 + \int \frac{1}{T} dM = S_0 + \int_0^{r_+} \frac{1}{T} \left(\frac{\partial M}{\partial r'_+} \right)_{Q_i} dr'_+, \tag{3.26}$$

where S_0 is an integration constant to be fixed later. The BH entropy is then given by

$$S = \pi r_+^2 + 2\pi\alpha \log r_+^2 + \tilde{S}_0 \equiv \frac{A}{4} + 2\pi\alpha \log \frac{A}{A_0}, \tag{3.27}$$

with A_0 a constant with units of area[8]. This expression coincides with the Hawking-Bekenstein formula plus a logarithmic correction term. According to statistical interpretations of the black hole entropy in some quantum theories of gravity such as loop quantum gravity and string theory, it can be argued that the leading term of statistical degrees of freedom yield the Hawking-Bekenstein area term, whereas the subleading term is logarithmic [290–292]. However, it is quite difficult to produce such a logarithmic term in the black hole entropy in some effective local theory of gravity even with higher-curvature terms. The 4DEGB theory then provides an example where a logarithmic correction to the black hole entropy is present. Remarkably, all explicit contributions from the charge Q and cosmological constant cancel out, resulting in a simple expression. As a remark, the branch with a positive sign, however, does not obey the Hawking-Bekenstein formula plus a simple logarithmic correction for the entropy, presenting a complicated lengthy expression which is not particularly elucidative.

3.1.2 Black holes in the counter-term regularized theory, uniqueness of solutions, and a new dark matter candidate

The results of this section are based of Ref. [5]. Now we turn to the scalar-tensor well-defined regularized theory that was presented in Eq. (2.50), to which we introduce a cosmological constant and an electromagnetic field in order to compare with the results from last section

$$S = \frac{1}{16\pi} \int d^4x \sqrt{-g} \Big[R - 2\Lambda - F_{\mu\nu}F^{\mu\nu} + \alpha \Big(4G^{\mu\nu}\nabla_\mu\phi\nabla_\nu\phi - \phi\mathcal{G} + 4\Box\phi(\nabla\phi)^2 + 2(\nabla\phi)^4 \Big) \Big] . \tag{3.28}$$

[8] Imposing that the entropy vanishes as the black hole tends to its minimum size (and its temperature vanishes), fixes $A_0 = 4\pi\alpha e^{1/2}$.

The field equations are

$$G_{\mu\nu} + \Lambda g_{\mu\nu} + \alpha \mathcal{H}_{\mu\nu} = 2\left(F_{\mu\sigma}F_{\nu}{}^{\sigma} - \frac{1}{4}g_{\mu\nu}F_{\rho\sigma}F^{\rho\sigma}\right), \tag{3.29}$$

where $\mathcal{H}_{\mu\nu}$ was defined in Eq. (2.53). The scalar field equation is the same as presented in Eq. (2.69), $\tilde{\mathcal{G}} = 0$. Because the electromagnetic stress-energy tensor is traceless, the usual trace equation holds

$$R - 4\Lambda + \frac{\alpha}{2}\mathcal{G} = 0. \tag{3.30}$$

We further note, again, that the action is shift-symmetric in the scalar field, i.e., it is invariant under the set of transformations $\phi \to \phi + \mathcal{C}$, for any constant $\mathcal{C}$. By virtue of this symmetry we acquire a Noether current with vanishing divergence [72]:

$$j^{\mu} = \frac{1}{\sqrt{-g}}\frac{\delta S}{\delta(\partial_{\mu}\phi)}, \qquad \text{such that} \qquad \nabla_{\mu}j^{\mu} = 0\,. \tag{3.31}$$

In fact, the vanishing divergence $\nabla_{\mu}j^{\mu} = 0$ implies $\partial_{\mu}\left(\sqrt{-g}j^{\mu}\right) = 0$, which also recovers the scalar field equation of motion. We will make use of this fact in what follows, where we will discuss the black hole solutions of this theory.

Solving the field equations for the following line element

$$ds^2 = -A(r)dt^2 + B(r)dr^2 + r^2\left(d\theta^2 + \sin^2\theta d\varphi^2\right), \tag{3.32}$$

one finds a solution equal to that presented in Eq. (3.8)

$$B(r)^{-1} = A(r) = 1 + \frac{r^2}{2\alpha}\left(1 \pm \sqrt{1 + 4\alpha\left(\frac{2M}{r^3} - \frac{Q^2}{r^4} + \frac{\Lambda}{3}\right)}\right), \tag{3.33}$$

and M is the associated mass and Q the electric charge. The corresponding scalar field profile for this solution is given up to a quadrature by

$$\phi'(r) = \frac{1 - \sqrt{A(r)}}{r\sqrt{A(r)}} = \frac{\sqrt{B} - 1}{r}, \tag{3.34}$$

where the prime here denotes a derivative with respect to r. A more in-depth analysis of the above geometry was already done in the previous section.

In what follows, we consider only the asymptotically flat, non-charged case, $Q = \Lambda = 0$, and therefore consider only the pure 4DEGB theory in Eq. (2.50). The

physical solution is then

$$B(r)^{-1} = A(r) = 1 + \frac{r^2}{2\alpha}\left(1 - \sqrt{1 + \frac{8M\alpha}{r^3}}\right), \tag{3.35}$$

with the same scalar field profile as before. We will show that this solution is one of only two static asymptotically-flat spherically-symmetric solutions to the regularized 4DEGB theory, and is the unique static and asymptotically flat black hole solution. We will follow this by demonstrating that the regularized 4DEGB theory admits no spherically-symmetric asymptotically-flat time-dependent perturbations to this solution, which indicates that there are no other spherically symmetric solutions (even time dependent ones) in the neighbourhood of this solution. Together, these results suggest that (3.35) is the unique asymptotically-flat spherically-symmetric vacuum black hole solution of this theory (without assuming staticity), a result analogous to Birkhoff's theorem of GR.

3.1.2.1 Uniqueness of Static Black Holes

The first step in demonstrating the uniqueness of (3.35) is to study the existence of solutions at spatial infinity under the assumption of asymptotic flatness. To do this we take Eq. (5.21) as an ansatz for the most general static spherically symmetric solution, and impose asymptotic flatness by assuming that in the limit $r \to \infty$, $A(r) \to 1$, $B(r) \to 1$ and $\phi(r) \to 0$[9], and expand the functions of interest as a power series in $1/r$:

$$A(r) = 1 + \sum_{n=1}^{\infty} \frac{A_n}{r^n}, \qquad B(r) = 1 + \sum_{n=1}^{\infty} \frac{B_n}{r^n}, \qquad \phi(r) = \sum_{n=1}^{\infty} \frac{q_n}{r^n}. \tag{3.36}$$

Substituting these expressions into the field equations, the (r-r) equation immediately tells us that $A_1 = -B_1$ and the scalar field equation that $q_1 = \pm B_1/2$. Selecting either the positive or negative branch, one finds that constants at higher order can all be fixed in terms of B_1 with no further choices, and therefore that there are two series solutions each of which can be written in terms of a single constant. We identify this constant as a mass setting $B_1 = 2M$, and at leading order one then finds the scalar charge, q_1, is given by $q_1 = \pm M$. Choosing $q_1 = -M$ and proceeding using the field equations to fix coefficients order by order, one finds a series solution which matches the Taylor expansion of the black hole solution (3.35) up to the order

[9] Here we can make use of the scalar field shift symmetry to impose $\lim_{r\to\infty} \phi(r) = 0$.

we have checked. On the other hand, choosing $q_1 = +M$ leads to a second solution with expansion

$$\begin{aligned} A(r) &= 1 - \frac{2M}{r} - \frac{4M^2\alpha}{r^4} + \mathcal{O}\left(\frac{1}{r^5}\right) , \\ B(r) &= 1 + \frac{2M}{r} + \frac{4M^2}{r^2} + \frac{8M^3}{r^3} + \frac{4M^2(4M^4 + 3M^2\alpha)}{r^4} + \mathcal{O}\left(\frac{1}{r^5}\right) , \\ \phi(r) &= \frac{M}{r} + \frac{M^2}{r^2} + \frac{4M^3}{3r^3} + \frac{2M^2(M^2+\alpha)}{r^4} + \mathcal{O}\left(\frac{1}{r^5}\right) . \end{aligned} \tag{3.37}$$

We note that for this solution the expansion tells us that $B^{-1} \neq A$, which we will comment on further below.

This analysis already indicates that there are only two static and spherically-symmetric asymptotically flat vacuum solutions in regularized 4DEGB, but relies on the validity of a perturbative expansion. Making use of the Noether current (3.31) we can go further: taking the ansatz (5.21) and utilizing the expressions in Ref. [72] we find that j^μ can be written as $j^\mu = (0, j^r, 0, 0)$, where

$$j^r = \frac{\left(A' + 2A\phi'\right)\left((r\phi' + 1)^2 - B\right)}{2r^2AB^2}. \tag{3.38}$$

Moreover, assuming the ansatz (5.21), Eq. (3.31) can be integrated to give

$$\sqrt{AB}r^2 j^r = \text{constant}. \tag{3.39}$$

Assuming asymptotic flatness, this constant can be seen to be zero by substituting the leading terms from either of the series solutions considered above into Eq. (3.38). The same result can also be demonstrated independently of perturbation theory by integrating Eq. (3.31) over a region of space-time that is external to the horizon, and which is bounded by the event horizon and two space-like surfaces that are identical to each other up to a translation along the Killing field ξ^μ, which is time-like in the black hole exterior.

To show this, we can begin by noting that Gauss' theorem means that the volume integral of $\nabla_\mu j^\mu$ can be converted to an integral of the normal component of $\vec{j}$ over the boundary. We can then see that the contribution to this integral from the integral over the event horizon will vanish. This is because the Killing vector ξ^μ is a generator of this horizon, and because the event horizon itself is a null surface. These two facts mean that ξ^μ must also be the normal to the horizon (as null vectors are normal to themselves), and therefore that the normal component of the current

$\vec{j}$ must vanish on this surface (assuming that $\vec{j}$ displays the same symmetries as the spacetime, and therefore that $j^\mu \xi_\mu = 0$). Now, the identical nature of the two space-like surfaces means that the integral of the normal component of $\vec{j}$ over them must sum to zero, and therefore they also contribute nothing to the integral over the boundary. We then conclude that the normal component of $\vec{j}$ must vanish at the remaining part of the boundary. This segment of the boundary is time-like, and as there is nothing special about its location, we must therefore conclude that $j^r = 0$ at all points exterior to the event horizon, which demonstrates that the constant in Eq. (3.39) must be equal to zero.

Now, Eq. (3.38) allows us to calculate the two possible scalar field profiles non-perturbatively, in terms of the functions A and B, as

$$\phi = -\frac{1}{2}\log(A) \qquad \text{or} \qquad \phi' = \frac{-1 \pm \sqrt{B}}{r}. \tag{3.40}$$

The second profile with the plus sign corresponds to the case of $q_1 = -M$. Substituting this into the field equations, the (t-t) equation and a suitable combination of the (t-t) and (r-r) equations give us[10]

$$\begin{aligned} &(B-1)B\left(-\alpha + B\left(\alpha - r^2\right)\right) - r(-2\alpha + B\left(2\alpha + r^2\right))B' = 0 \\ &\text{and} \\ &(-2\alpha + B\left(r^2 + \alpha\right))(AB' + A'B) = 0. \end{aligned} \tag{3.41}$$

The first equation admits a solution for B that coincides with B given by (3.35), while the second equation admits the solution $A = \mathcal{C}B^{-1}$ where $\mathcal{C}$ is a constant that can be absorbed into a redefinition of t in the metric. This scalar field profile therefore coincides with that of (3.35) and leads to the known black hole.

The first scalar field profile in Eq. (3.40) corresponds to the $q_1 = M$ case, and the Taylor expansion of this profile matches the expansion in Eq. (3.37). Recall that in this case the series solution indicates that the functions A and B^{-1} are not equal. Studying the field equations has not allowed us to find a closed-form solution for the metric functions A and B in this case, so in order to make progress in understanding this solution we instead integrate the field equations numerically in r from large r using the series solution to provide initial conditions. As seen in Fig. 3.2 (left), we observe that the functions A and B^{-1} coincide at large r, but differ drastically for

[10] Substitution of the second profile with the minus sign leads to the same exact field equations and solutions. In this case, however, the scalar field profile is not asymptotically flat (albeit $\phi' \to 0$, nonetheless).

small values of the radial coordinate, where the function B develops a kink outside any horizon (as indicated by the arrow in the figure). As this point is approached the curvature scalar diverges, as shown in Fig. 3.2 (right). This behaviour indicates the presence of a naked singularity. We also observe that the (t-t) component of the field's stress-energy tensor is negative, which may lead one to question whether this particular solution is of any direct physical significance at all.

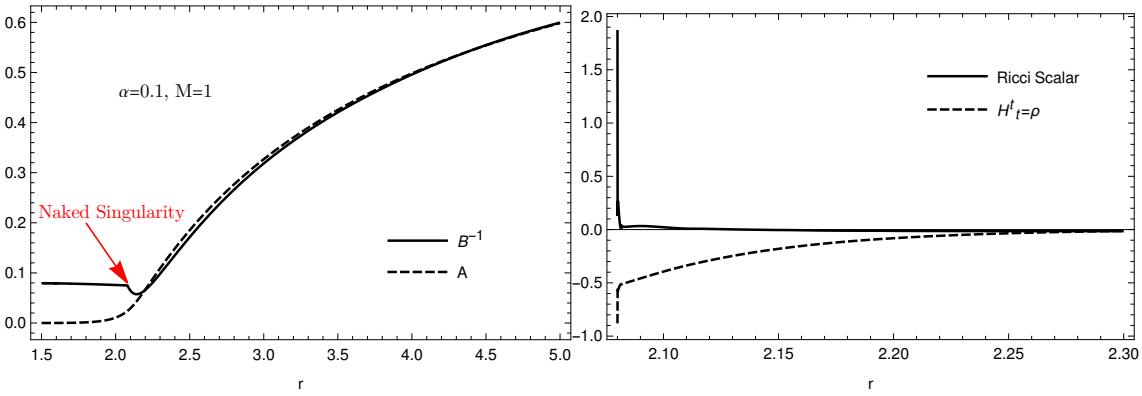

Figure 3.2: Left: Profiles for the metric functions that solve the field equations for the scalar field profile $\phi = -\frac{1}{2}\log(A)$, for the fiducial choice $\alpha = 0.1$ and $M = 1$. Right: Respective Ricci scalar and (t-t) component in the field's stress energy tensor. A similar behaviour is observed for other values of the coupling α.

Further evidence that demonstrates that these solutions do not represent a black hole can be obtained by expanding the metric functions in a power series around the position at which they would tend to zero, denoted r_+, if the solution was to describe a black hole. This gives

$$A = \sum_{n=1}^{\infty} a_n (r - r_+)^n, \qquad B^{-1} = \sum_{n=1}^{\infty} b_n (r - r_+)^n \,. \tag{3.42}$$

On substitution into the field equations, this immediately implies that $b_1 = 0$. A non-zero value of b_1 is required for this position to be the horizon of a non-extremal black hole, and hence this automatically indicates that if the solution describes a black hole, it has to be extremal. This can be seen by computing the black hole temperature T_+, which for the line-element of Eq. (5.21), assuming the near-horizon expansion of Eq. (3.42), reads

$$T_+ = \frac{\kappa}{2\pi} = \frac{1}{4\pi}\left[\frac{1}{\sqrt{-g_{tt}g_{rr}}}\frac{dg_{tt}}{dr}\right]_{r=r_+} = \frac{\sqrt{a_1 b_1}}{4\pi}, \tag{3.43}$$

where κ is the surface gravity of the black hole, and T_+ can be seen to vanish if $b_1 = 0$. Moreover, a more careful analysis reveals that the aforementioned power series is incompatible with the field equations, yielding no perturbative solutions.

To summarise, we have shown that (3.35) is the unique static spherically-symmetric and asymptotically-flat vacuum black hole solution to the regularized 4DEGB theory, and that there exists one other (likely unphysical) spherically-symmetric and asymptotically-flat solution which corresponds to a naked singularity.

3.1.2.2 Time-Dependent Perturbations

Let us now generalize our considerations to allow for time dependence. To do so we will return to the ansatz (5.21), but now allow A and B to be functions of t as well as r. We begin by considering spherically-symmetric time-dependent perturbations about (3.35). In GR such perturbations must of course be zero, by virtue of Birkhoff's theorem. We will now show that a similar result holds in regularized 4DEGB, provided we restrict our attention to spherically-symmetric, asymptotically-flat perturbations.

We denote quantities associated with the exact solution (3.35) using a subscript 0, and expand the metric functions as

$$\begin{aligned} A(t,r) &= A_0(r) + \sum_{n=1}^{\infty} \varepsilon^n A_n(t,r)\,, \qquad B(t,r) = B_0(r) + \sum_{n=1}^{\infty} \varepsilon^n B_n(t,r)\,, \\ \phi(t,r) &= \phi_0(r) + \sum_{n=1}^{\infty} \varepsilon^n \phi_n(t,r)\,, \end{aligned} \tag{3.44}$$

where ε is a small parameter. Substituting (3.44) into the field equations, and expanding to first order in ε, we find that the (t-r) field equation gives

$$\dot{B}_1 = 0\,, \tag{3.45}$$

where the dot indicates differentiation with respect to t. This implies that B_1 must be a function of r only, and by virtue of the results for the static case above we know any such function must be zero[11]. Therefore, setting $B_1 = 0$, we find that the (t-t) field equation is automatically satisfied to first order in ε. On the other hand,

[11] This is because $B_1(r)$ can be re-absorbed into $B_0(r)$. It can be explicitly verified that this is equivalent to considering a background solution with a slightly perturbed mass $M + \varepsilon\,\delta M$. New terms resultant from considering this new background solution are of $\mathcal{O}(\varepsilon)$, and can then in turn be reabsorbed into the perturbations A_1.

the (r-r) equation and trace equation give

$$\phi_1' = \frac{\left(2\alpha - 2\alpha A_0 + r^2\right)\left(A_0 A_1' - A_1 A_0'\right)}{4\alpha A_0\left(-rA_0' + 2A_0 - 2\sqrt{A_0}\right)}, \tag{3.46}$$

and

$$\begin{aligned} 0 =& A_1\left(A_0'\left(\left(2\alpha + 2\alpha A_0 + r^2\right)A_0' - 4rA_0\right) - 2A_0\left(2\alpha - 2\alpha A_0 + r^2\right)A_0''\right) \\ &+ A_0 A_1'\left(4rA_0 - \left(2\alpha + 2\alpha A_0 + r^2\right)A_0'\right) + 2{A_0}^2\left(2\alpha - 2\alpha A_0 + r^2\right)A_1'', \end{aligned} \tag{3.47}$$

respectively, where the dash again indicates a derivative with respect to r. Equation (3.47) has the general solution

$$A_1 = A_0\left(c_1(t) + c_2(t)\int^r \frac{1}{A_0^{3/2}\left(2\alpha - 2\alpha A_0 + r^2\right)}dr\right), \tag{3.48}$$

where $c_1(t)$ and $c_2(t)$ are free functions of time. Substituting Eq. (3.48) into Eq. (3.46), the term proportional to $c_1(t)$ drops out, and one finds

$$\phi_1 = c_3(t) + \int^r \frac{c_2(t)}{4\alpha\sqrt{A_0}\left(2A_0 - 2\sqrt{A_0} - rA_0'\right)}dr \sim c_3(t) - \frac{c_2(t)r^2}{32M\alpha} + \mathcal{O}(r), \tag{3.49}$$

where in the last step we have made an expansion in r near spatial infinity. If we now assume asymptotic flatness of the perturbations, we can set both c_2 and c_3 to zero. This implies $\phi_1 = 0$ and $A_1 = c_1(t)A_0$. Moreover, since c_1 is a function only of t, this can be absorbed into a re-definition of t in the line-element, such that we can effectively set $A_1 = 0$. With all linear perturbations set to zero, this further implies there are no source terms for higher-order perturbations.

We therefore conclude from this analysis that there exist no spherically-symmetric, asymptotically-flat perturbations to the solution (3.35), and therefore that the black hole solutions of Eq. (3.35) are perturbatively stable.

3.1.2.3 Evaporation remnants

In this section we reintroduce the constants c, G, $\hbar$ and k_B for clarity. Having argued for the uniqueness of the black hole solution (3.35), we now turn to its further consequences. First we observe that such a black hole has a minimum size, and that the evaporation process leads to a remnant[12].

[12] This is in contrast with other scalar-Gauss-Bonnet theories typically studied in the literature, where the evaporation never halts (see e.g. [7] and Chapter 7).

To see that black holes leave a remnant, we first note that the black hole solution (3.35) contains horizons located at

$$r_{\pm} = \frac{GM}{c^2} \pm \sqrt{\left(\frac{GM}{c^2}\right)^2 - \alpha}\,, \tag{3.50}$$

where we have reintroduced physical constants, and that r_+ has a minimum value of $r_{min} \equiv \sqrt{\alpha}$ (this happens when $M = c^2\sqrt{\alpha}/G$). The Hawking temperature of the black hole can be computed straightforwardly as before, giving

$$T_+ = \frac{\hbar c}{4\pi k_B} A'(r_+) = \frac{\hbar c}{4\pi k_B} \frac{r_+^2 - \alpha}{r_+\left(r_+^2 + 2\alpha\right)}\,, \tag{3.51}$$

where we observe that for $r_+ = r_{min}$ the Hawking temperature vanishes, as also seen in Fig. 3.3. A similar black hole temperature profile is found in other contexts commonly related to quantum gravity, such as non-commutative models [308–312] and asymptotically safe gravity [312–314].

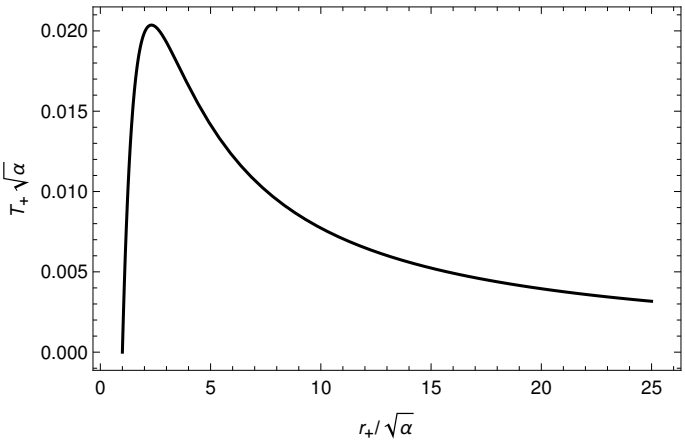

Figure 3.3: Temperature of the 4DEGB black hole as a function of the horizon radius. One observes that as $r_+/\sqrt{\alpha} \to \sqrt{\frac{1}{2}\left(5+\sqrt{33}\right)} \approx 2.31782$, the temperature hits a maximum, and rapidly falls as the horizon radius decreases. The temperature approaches zero as $r_+/\sqrt{\alpha} \to 1$.

Assuming a Stefan-Boltzmann law to estimate the mass and energy output as functions of time gives

$$-\frac{dE}{dt} = 4\pi r_+^2 \sigma T_+^4, \qquad \text{where} \qquad \sigma = \frac{\pi^2 k_B^4}{60\hbar^3 c^2} \tag{3.52}$$

which allows us to write the following dimensionless differential equation for our

black holes:

$$\frac{dm}{d\tau} = -\frac{1}{240\pi} \frac{\left[\beta^2 - m^2\left(1+\sqrt{1-\frac{\beta^2}{m^2}}\right)\right]^4}{\left(1+\sqrt{1-\frac{\beta^2}{m^2}}\right)^2 m^2 \left[\beta^2 + 2m^2\left(1+\sqrt{1-\frac{\beta^2}{m^2}}\right)\right]^4}, \tag{3.53}$$

where we have defined the dimensionless quantities

$$m := \frac{M}{M_{pl}}, \qquad \tau := \frac{t}{t_{pl}}, \qquad \beta := \frac{\sqrt{\alpha}}{\ell_{pl}}, \tag{3.54}$$

normalized with the Planck units[13]

$$M_{pl}^2 := \frac{\hbar c}{G}, \qquad \ell_{pl}^2 := \frac{\hbar G}{c^3}, \qquad t_{pl}^2 := \frac{\hbar G}{c^5}. \tag{3.55}$$

We see that the solutions to this equation will have a mass $m \to \beta$ as $\tau \to \infty$, as demonstrated by the numerical solutions displayed in Fig. 3.4. Observe that as $m \to \beta$, $dm/d\tau \to 0$ as indicated by Eq. (3.53). Furthermore, we note that the timescale over which a black hole with dimensionless mass $m = m_0$ evaporates to its final value $m = m_f$, $t_{\rm ev}$, is given by

$$\begin{aligned} t_{\rm ev} =& 20\pi t_{pl}\Bigg[128\left(m_0^3 - m_f^3 + m_0^2\sqrt{m_0^2-\beta^2}\right) + 960\beta^2(m_0 - m_f) + \\ & 486\beta^4\left(\frac{m_f}{m_f^2-\beta^2} - \frac{m_0}{m_0^2-\beta^2}\right) + 1024\beta^2\sqrt{m_0^2-\beta^2} - \frac{648\beta^2}{\sqrt{m_0^2-\beta^2}} \\ & + 729\beta^3 \log\left(\frac{(m_0-\beta)(m_f+\beta)}{(m_0+\beta)(m_f-\beta)}\right) - \frac{8\left(16m_f^4 + 112m_f^2\beta^2 - 209\beta^4\right)}{\sqrt{m_f^2-\beta^2}}\Bigg]. \end{aligned} \tag{3.56}$$

This means that evaporation of these black holes in regularized 4DEGB leads to a relic, which no longer radiates, and which has a size of $\sqrt{\alpha}$. This is a favorable feature from the point of view of cosmic censorship hypothesis.

3.1.2.4 Relic Primordial Black Holes and Dark Matter

An immediate consequence of the end state of evaporation identified above is that the relics of black holes formed in the early universe must survive until today. Such relics may therefore contribute to the dark matter that is observed in the late Universe.

[13] Our definition of $M_{\rm pl}$ here differs by a factor of 8π with respect to the one we have been using.

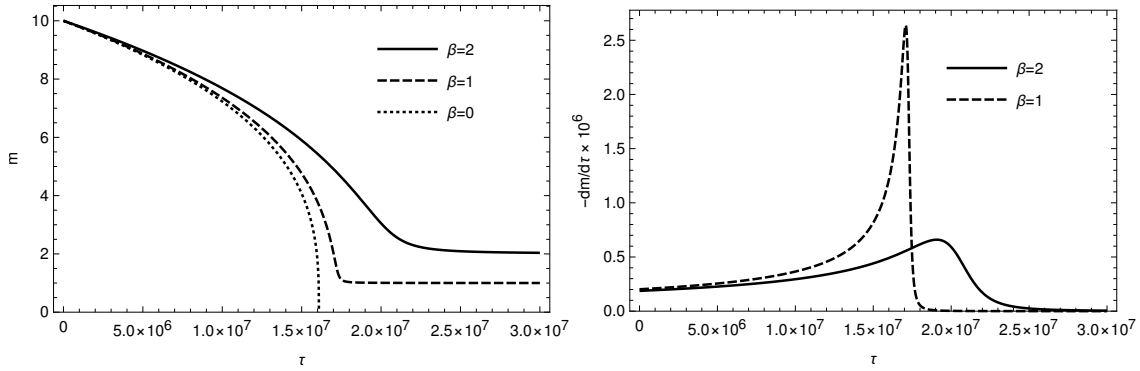

Figure 3.4: Time evolution of the dimensionless mass $m = M/M_{pl}$ (left) and its time derivative (right) due to Hawking evaporation, for black holes with initial mass $m_0 = 10$ for a sample of values of the dimensionless coupling β. If $\beta = 0$, black holes are described by the Schwarzschild solution of GR and evaporate completely, with $dm/d\tau \to \infty$ near the end of evaporation. 4DEGB black holes, on the other hand, approach a minimum size as $m \to \beta$ and evaporation comes to a halt.

The idea of primordial black holes (PBHs) contributing to the dark matter is not a new one [315,316], and the possibility of Planck-size black hole relics playing the role of dark matter was first pointed out by MacGibbon [317] and has been explored by many authors [311,312,318–330] (also see Ref. [331] for a review on black hole relics and their implications for the information loss paradox). In most of these studies the possible black hole relics are taken to be of Planck mass.

In the current setting there are several complications. First, the mass of the relic is now equal to $\beta M_{\rm pl} \propto \sqrt{\alpha}$. Secondly, the evaporation timescale is altered, being given by Eq. (3.56). And finally, the Friedmann equation for a flat universe in regularized 4DEGB gravity is given by[14]

$$H^2 + \frac{\alpha}{c^2} H^4 = \frac{8\pi G}{3}\rho\,. \tag{3.57}$$

The term proportional to α on the left-hand side of this equation may play a role in the early universe, as it scales like H^4.

In what follows, we will assume that a population of black holes can form when large perturbations re-enter the horizon during the period of radiation domination after inflation ends (in a qualitatively similar way to the process that occurs in standard general relativistic cosmology). We will further assume that all dark mat-

[14]For simplicity, here we ignored a dark-radiation-like term of the form K/a^4, where K is a free parameter. These type of terms are common in scalar-tensor theories. This equation is discussed in more detail in the next section.

ter today consists of black hole remnants, and that the black holes initially form with a single (dimensionless) mass, $m_{\rm PBH}$. On this basis, we will estimate the allowed parameter range of $m_{\rm PBH}$ and β. Of course, it would be interesting to study further the precise details of how structure collapses and black hole formation occurs within 4DEGB, though we note that it does *not* appear possible to construct Oppenheimer-Snyder collapse models in regularized 4DEGB, as the scalar field from the Friedmann interior cannot be made to match that of the black hole exterior[15]. Such considerations are left to future work.

When PBHs form, their mass is given by some sizable fraction, γ, of the mass of a horizon-sized region of the universe at the time of formation. Working in units such that $\hbar = c = 1$, this leads to the formula

$$m_{\rm PBH} = \gamma \frac{4\pi}{3H_*^3 M_{\rm pl}} \rho_* \tag{3.58}$$

where H_* is the Hubble rate at the time of re-entry, and

$$\rho_* = \frac{3M_{\rm pl}^2}{8\pi}\left(H_*^2 + \beta^2 \frac{H_*^4}{M_{\rm pl}^2}\right) \tag{3.59}$$

is the density. Typically, a value of $\gamma \sim 0.2$ is taken in the literature [332]. The number of horizon-sized patches of the universe in which a black hole forms is determined by the amplitude and statistical properties of the large-density perturbations, and hence the fraction of the universe's energy density that turns into PBHs can be taken as a free parameter.

There are then two main restrictions on the PBH remnant dark matter scenario. The first is that the mass of the black hole at the time of formation must be greater than β. The relations (3.58) and (3.59) given above imply

$$m_{\rm PBH} = \frac{\gamma}{2}\left(\frac{M_{\rm pl}}{H_*\beta} + \frac{H_*\beta}{M_{\rm pl}}\right)\beta \sim 0.1\left(\frac{M_{\rm pl}}{H_*\beta} + \frac{H_*\beta}{M_{\rm pl}}\right)\beta\,. \tag{3.60}$$

For $H_* \ll M_{\rm pl}/\beta$ this formula implies $m_{\rm PBH} \propto 1/H_*$, while for $H_* \gg M_{\rm pl}/\beta$ it gives $m_{\rm PBH} \propto H_*$. For a given β there is therefore a minimum mass of $m_{\rm PBH} \sim 0.2\beta$ that can form, which corresponds to $H_* = M_{\rm pl}/\beta$. Since the minimum mass allowed by Eq. (3.60) is just below the remnant mass, values of H_* close to $M_{\rm pl}/\beta$ are inconsistent with the outlined scenario. In fact, the consistency condition $m_{\rm PBH} \geq \beta$

[15] This is true despite the fact that the first and second fundamental forms on either side of the boundary can be made to match.

imposes $H_* \lesssim 0.1 M_{\rm pl}/\beta$ or $H_* \gtrsim 10 M_{\rm pl}/\beta$. The second main constraint is that by the time the Hubble rate reaches its value today, the density of dark matter and radiation must be in their correct ratio. For a given value of β, this places an upper bound on $m_{\rm PBH}$, for reasons we will explain in detail below. In turn this places an upper and lower bound on H_* due to the non-linear relationship between $m_{\rm PBH}$ and H_* given above. The region of parameter space that satisfies both constraints is illustrated in Fig. 3.5, where the further constraint that $H_* \lesssim 5 \times 10^{-6} M_{\rm pl}$ required by gravitational wave constraints [55] has also been imposed. The color of each point shows the time of decay of PBHs into relics in the form of the redshift $z_{\rm ev}$. We also apply the constraint $z_{\rm ev} > z_{\rm eq} \approx 3400$ [333] to avoid relic production occurring after matter-radiation equality.

Let us now attempt to understand the origin of the upper bound on $m_{\rm PBH}$. To do so we will assume that the evaporation of the black holes can be taken to occur instantly at some time $t_{\rm ev}$ after their formation. This time can be estimated using Eq. (3.56) taking $m_0 = m_{\rm PBH}$ and $m_f = 1.1\beta$. As $m_{\rm PBH}$ becomes larger the decay time of the black holes is pushed later into the universe's evolution. When PBHs evaporate, they produce radiation and this contribution to the total radiation, given by $\Delta\rho = (m_{\rm PBH}/\beta - 1)\rho_{\rm DM}^{\rm dec}$, must be smaller than the total radiation density, which includes it. Since we are assuming relics to form all the dark matter and the total radiation density is also well known, for sufficiently large masses, this consistency condition cannot be obeyed, otherwise the relative abundances of matter and radiation would not be correct at late time.

We can estimate the value of $m_{\rm PBH}$ at which this occurs by considering the universe today, and extrapolating into the past to see if a consistent evolution is possible. Doing so, the black hole remnants initially redshift like dust, and the ratio of remnant dark matter to radiation decreases towards the past. This behavior continues until the decay time is reached. At this time the dark matter density should jump by an amount given by $\Delta\rho$, and the radiation density, $\rho_{\rm rad}^{\rm dec}$ must drop by the same amount. This must occur at energy scales at least above those of matter-radiation equality for consistency with structure formation, and hence the universe is radiation dominated at this time. Consistency then demands that $\Delta\rho < \rho_{\rm rad}^{\rm dec}$. The radiation density at the time of decay can be estimated by using the expression $H^2 \approx t_{\rm ev}^{-2}/4$, valid during radiation domination once standard cosmology is recovered. This gives a good approximation of the density, except in the fine-tuned cases where $\Delta\rho \sim \rho_{\rm rad}$. If this inequality on $\Delta\rho$ cannot be satisfied it indicates there was no consistent evolution that lead to today's energy densities, and employing it gives the upper bound on the mass seen in Fig. 3.5. An analytic estimate for the upper limit on the

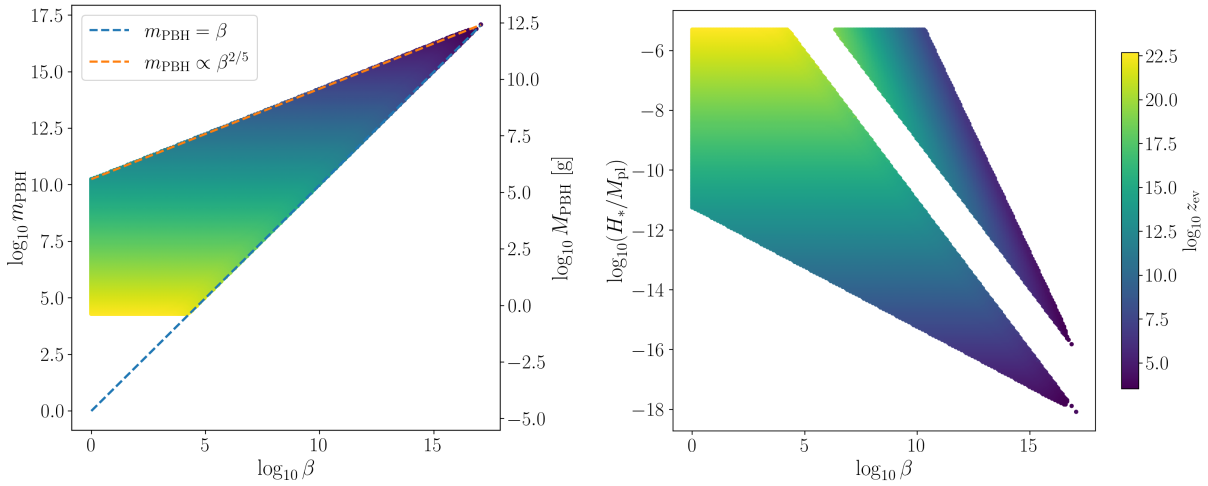

Figure 3.5: Bounds on the mass of the PBHs (left) and Hubble rate at formation (right) as a function of β in order that remnants make up all dark matter today. The scenario is allowed in the shaded region and color represents the evaporation redshift, $z_{\rm ev}$.

mass can be obtained by considering the GR limit of Eq. (3.56) for the evaporation time, resulting in

$$\tau_{\rm ev} \approx 5120\pi m_{\rm PBH}^3 \,. \tag{3.61}$$

In addition, for $m_{\rm PBH} \gg \beta$, we can use the approximation $\Delta\rho \approx \rho_{\rm DM}^{\rm dec} m_{\rm PBH}/\beta$. The ratio between the densities can be calculated by relating it to matter-radiation equality:

$$\frac{\rho_{\rm DM}^{\rm dec}}{\rho_{\rm rad}^{\rm dec}} = \frac{a_{\rm dec}}{a_{\rm eq}} \approx \sqrt{\frac{H_{\rm eq}}{H_{\rm dec}}} = \sqrt{2H_{\rm eq} t_{\rm ev}} \,. \tag{3.62}$$

This results in the consistency condition $\Delta\rho < \rho_{\rm rad}^{\rm dec}$ becoming

$$m_{\rm PBH} < (10240\pi H_{\rm eq}/M_{\rm pl})^{-1/5} \beta^{2/5} \,. \tag{3.63}$$

This approximate limit is shown in the left plot of Fig. 3.5, in which it is clear that it works very well, except for the largest values of β allowed in this scenario for which our approximation begins to fail, as all allowed masses are very similar to β.

In order to verify the bounds we also run more sophisticated simulations. These begin by fixing a value for β and for the Hubble rate, H_*, at which the primordial black holes form (and hence fixing the initial energy density and black hole mass at the time of formation). The simulation then picks a value for the fraction of energy density in black holes at this time, taking the rest of the energy density

to be radiation. Finally, the code solves the ordinary differential equations given by Eqs. (3.53) and (3.57), assuming the comoving number density of radiation and black holes to be conserved. A cosmological constant of the value observed today is also included. The simulation ends when the Hubble rate reaches its observed value today, at which time the ratio between dark matter and radiation is recorded. By trying different fractions for the initial energy density of black holes for the same β and H_* the simulation can then establish if any initial fraction gives the correct abundances today for this combination of β and H_*. The simulation then picks a new β and H_* and tries again. Our simulations also allow us to check other consistency requirements, such as the universe being radiation dominated at the time of nucleosynthesis. We find results that agree remarkably well with the simpler analytic estimate described above.

We conclude therefore that dark matter can be generated via the mechanism of PBH evaporation in 4DEGB. We also find that remnants with a mass larger than the Planck mass (which follow when $\beta > 1$) allow for the formation of PBHs at lower energy scales than in the standard scenario of Planck mass remnants. For a given energy scale, however, there is maximum value of β above which the scenario is no longer viable, and that $\beta \sim M_{\rm pl}/H_*$ is also not permitted. The situation considered here assumed all the dark matter to be composed of relics. Should their fraction be smaller, the upper limit on PBH mass would increase in proportion with that fraction, with the corresponding limits on H_* broadening too.

3.2 Cosmology

In order to be viable, any theory of gravity must give rise to a cosmology that is both internally consistent, and compatible with the myriad of modern cosmological observations across a huge range of energy, distance, and time scales. It is also interesting to see what new behaviour novel theories might allow, for example at very early times when observational constraints are less stringent. In this section, we turn to these considerations for the 4D Einstein-Gauss-Bonnet theory.

3.2.1 Cosmology in the original formulation of 4D Einstein-Gauss-Bonnet gravity

3.2.1.1 Background cosmology

We begin with the homogeneous and isotopic FLRW line-element in D dimensions

$$\mathrm{d}s^2 = -\mathrm{d}t^2 + a^2(t)\left[\mathrm{d}\chi^2 + S_k^2(\chi)\mathrm{d}\Omega^2\right] . \tag{3.64}$$

where $a(t)$ is the scale factor, $\mathrm{d}\Omega^2$ represents the line element for an $D-2$ sphere and S_k takes the form $S_k(\chi) = \sin(\chi)$ for a positively curved, $k = 1$, universe, $S_k(\chi) = \chi$ for a flat $k = 0$ universe, and $S_k(\chi) = \sinh(\chi)$ for a negatively curved $k = -1$ universe. As was previously described for the flat case, considering the original theory and following the steps discussed there, the space-time given in Eq. (3.64) with perfect fluid matter source, $T^\mu_\nu = \mathrm{diag}(-\rho, p, p, p, \ldots)$, gives rise to the following Friedmann equation in the limit $D \to 4$:

$$H^2 + \frac{k}{a^2} + \alpha\left(H^2 + \frac{k}{a^2}\right)^2 = \frac{8\pi G}{3}\rho\,, \tag{3.65}$$

where $H = \dot{a}/a$, and the density contains all fluids present, i.e. $\rho = \sum_m \rho_m$. We assume any cosmological constant is included in ρ, and note that since the stress-energy tensor is conserved that all the components of ρ are expected to obey the same conservation equations as in GR:

$$\dot{\rho}_m + 3H(\rho_m + p_m) = 0\,, \tag{3.66}$$

where p_m represents the pressure of the fluids (i.e. we will not consider interacting fluids here).

The scalar-tensor regularized theories lead to the same equations as (3.65)-(3.66) when particular forms for the scalar field solution are taken, and particular parameter choices are made. We will return to more general solutions, and possible restrictions on solutions in the context of regularized theories below, and for now focus on the behaviours prescribed by Eqs. (3.65)-(3.66).

Considering the Friedmann equation (3.65), we find that

$$H^2 + \frac{k}{a^2} = \frac{-1 \pm \sqrt{1 + \frac{32\pi G\alpha\rho}{3}}}{2\alpha} . \tag{3.67}$$

From this equation we see that the negative branch does not lead to a consistent

cosmology, but that selecting the positive branch leads us to an equation that agrees with the standard Friedmann equation as ρ tends to zero.

For negative α, H^2 becomes complex when $\rho > 3/(32\pi G|\alpha|)$, and hence our universe could not have existed at sufficiently high energies in our past for this case. This is problematic if this value of ρ is at or below the inflationary energy scale, placing a strong constraint on negative values of α [3] as will be discussed below. For positive α, there is no restriction on the energy scale at which Eq. (3.67) is valid, but one may note that the dynamics can be significantly altered at high energies, and hence early times, becoming closer and closer to standard cosmology as ρ decays. In this case when $\rho \gg 1/(\alpha G)$ one finds $H^2 + \frac{k}{a^2} \propto \sqrt{\rho}$, which can have interesting consequences particularly in the positively curved case.

Defining the equation of state w through the equation $\rho = wp$, the conservation equation (3.66) implies $\rho \propto a^{-3(1+w)}$. This in turn means that for large ρ the right-hand side Eq. (3.67) scales as $a^{-3(1+w)/2}$. For the positively curved case, this tells us that a collapsing universe will undergo a bounce if it is sourced by fluids with a combined equation of state that satisfies the condition $w < 1/3$ (recall that $w = 1/3$ is the equation of state for radiation). This follows because when this condition is met, the right-hand side of Eq. (3.67) grows more slowly than the curvature term as $a \to 0$. Taking the curvature term to the right-hand side of Eq. (3.67) we can see that it is negative for $k = 1$, and if it grows faster than the other, positive, term, there will come a value of a at which H^2 goes to zero. Before this point, in a collapsing universe, H is negative, and at this point it passes through zero and becomes positive and H^2 starts to grow again. Moreover, once the condition $\rho \ll 1/G\alpha$ is reached in the expansion phase, the term of the right-hand side Eq. (3.67) starts to decay more rapidly than the curvature term, and once again this will lead to H passing through zero, and the universe re-collapsing. The result is a cyclic universe. An example is shown in Fig. 3.6 for the case of a dust cosmology.

Given the appeal of bouncing universes, and the historical interest in them, it is intriguing that 4D Einstein-Gauss-Bonnet permits cyclic cosmologies. The exotic behaviour described is, however, unlikely to have physical consequences given that the phenomena is only apparent when $\rho\alpha G \gg 1$. As we will see below, for the values of α allowed by observational constraints, this condition would imply a value of ρ that corresponds to a time well into the radiation dominated era, when a bounce cannot occur.

More generally, however, we note that the modified Friedmann equation changes the relationship between energy density and the scale factor, changing the universe's expansion history. This change becomes significant as ρ approaches $1/(\alpha G)$ at early

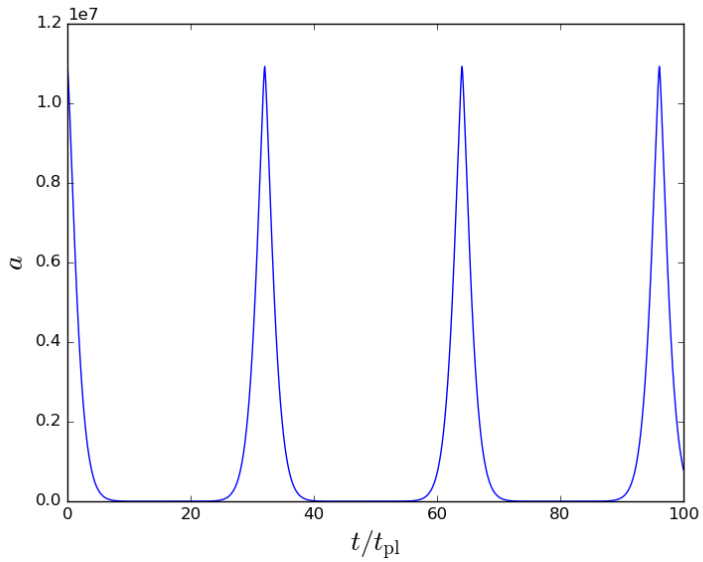

Figure 3.6: The results of numerically solving the equation of motion for $\ddot{a}$ (which follows from differentiating Eq. (3.65)) together with Eq. (3.67) for a dust cosmology with $w = 0$. We see that the universe undergoes repeating cycles. In this example $\alpha = 100 l_{\rm pl}^2$. The maximum value of a at which the simulation begins is found by fixing the initial density (which can be arbitrarily small), and finding the value of a which sets H^2 using Eq. (3.67) to be zero.

times, affecting for example the relation between time and temperature. This has consequences for the confrontation of the theory with observation, as we will see below.

3.2.1.2 Perturbed FLRW cosmology

In order to study the origin and evolution of structure in the universe, as well as the propagation of gravitational waves, it is necessary to introduce perturbations to the line-element (3.64), and to the stress-energy tensor. Specializing to the flat case and using Poisson gauge [334], we have

$$\mathrm{d}s^2 = -a^2(\tau)(1+2\varphi)\mathrm{d}\tau^2 + a^2(\tau)(1-2\psi\delta_{ij} + 2\partial_{(i}F_{j)} + \gamma_{ij})\mathrm{d}x_j^2 \,. \tag{3.68}$$

and

$$\delta T^0_0 = -\delta\rho \,, \quad \delta T^0_i = (1+w)\rho(\partial_i v + v_i) \,, \quad \delta T^i_j = \delta^i_j \delta P + \pi^i_j \,, \tag{3.69}$$

where τ is conformal time, φ, ψ, and v, $\delta\rho$ and δP are perturbative scalar quantities, F_i and v_i are transverse vector quantities and γ_{ij} is taken to be transverse and

trace-free, and represents gravitational waves. We use notation such that $\partial_i\partial^i \equiv \partial^2$, $\partial^2\partial^2 \equiv \partial^4$, and $\partial_i\gamma\partial^i\gamma \equiv (\partial\gamma)^2$. We have assumed a general fluid with anisotropic stress, π, whose scalar-vector-tensor decomposition is, at first order,

$$\pi_{ij} = (\partial_i\partial_j - \tfrac{1}{3}\delta_{ij}\partial^2)\Pi + \partial_{(i}\Pi_{j)} + \Pi_{ij}\,. \tag{3.70}$$

This line element leads to evolution equations for the perturbations which are modified from those of general relativity.

The propagation equation for gravitational waves [110, 213] is given by

$$\ddot{\gamma}_{ij} + \left(3 + \frac{4\alpha\dot{H}}{1+2\alpha H^2}\right) H\dot{\gamma}_{ij} - c_T^2\frac{\partial^2\gamma_{ij}}{a^2} = \frac{8\pi G}{1+2\alpha H^2}\Pi_{ij}\,, \tag{3.71}$$

where $c_T^2 = c^2(1 + \dot{\Gamma}/(H\Gamma))$ and $\Gamma \equiv 1 + 2\alpha H^2/c^2 = \sqrt{1 + 32\pi G\rho\alpha/3}$. Neglecting anisotropic stress, this equation also follows from the action

$$S_T = \frac{1}{2}\int \mathrm{d}^3x\mathrm{d}t\, a^3\Gamma\left(\dot{\gamma}^2 - c_T^2\frac{(\partial\gamma)^2}{a^2}\right)\,, \tag{3.72}$$

which will be useful below.

Defining $c_s^2 = \delta P/\delta\rho$ and $\delta = \delta\rho/\rho$, the scalar perturbations obey the equations [176, 213, 215]

$$\begin{aligned}
\delta' &= 3\mathcal{H}(w - c_s^2)\delta + (1+w)(3\psi' - \theta)\,,\\
\theta' + \left((1-3w)\mathcal{H} + \frac{w'}{1+w}\right)\theta + \partial^2\varphi + \frac{3\partial^2\delta P + 2\partial^4\Pi}{3(1+w)\rho} &= 0\,,\\
8\pi G a^4\rho\delta + 2\mathcal{A}(-\partial^2\psi + 3\mathcal{H}^2\varphi + 3\mathcal{H}\psi') &= 0\,,\\
\mathcal{A}\varphi + (\mathcal{B} - 4\alpha\mathcal{H}')\psi &= -8\pi G a^4\Pi\,,
\end{aligned} \tag{3.73}$$

where a dash indicates differentiation with respect to conformal time, $\theta = \nabla^2 v$, $\mathcal{A} = 2\alpha\mathcal{H}^2 + a^2$ and $\mathcal{B} = 2\alpha\mathcal{H}^2 - a^2$. The first two equations follow from the conservation of the stress-energy tensor and are identical to those of GR. The latter two follow from the 00- and ij-components of the field equations, respectively. For completeness, we include also the equations for vector modes. They are given by

$$\begin{aligned}
\mathcal{A}\partial^2 F_i' + 16\pi G(1+w)a^4\rho v_i &= 0\,,\\
v_i' + \left((1-3w)\mathcal{H} + \frac{w'}{1+w}\right)v_i + \frac{\partial^2\Pi_i}{2(1+w)\rho} &= 0\,.
\end{aligned} \tag{3.74}$$

As was the case for the background equations, the significance of deviations of

Eqs. (5.38)-(3.74) from those of GR are determined by the size of $\rho G\alpha$ (or equivalently αH^2) compared to unity, and hence tend to GR when this ratio is small.

3.2.2 Cosmology in the scalar-tensor version of 4D EGB

Let us now look at how the equations presented above arise within the scalar-tensor version of 4D Einstein-Gauss-Bonnet given by the action (2.50). Solving this theory with the line-element (3.64), one finds that the scalar field equation is given by

$$\alpha(k + a^2(H + \dot{\phi})^2)(\ddot{\phi} + \dot{H} + H(\dot{\phi} + H)) = 0\,, \tag{3.75}$$

which is solved by

$$\dot{\phi} = -H + \frac{K}{a}\,, \tag{3.76}$$

where K is a constant.

In this formulation of the theory, the Friedmann equation is

$$H^2 + \frac{k}{a^2} = \frac{8\pi G}{3}\rho + \alpha\dot{\phi}(2H + \dot{\phi})\left(2\left(H^2 + \frac{k}{a^2}\right) + 2H\dot{\phi} + \dot{\phi}^2\right)\,, \tag{3.77}$$

which, after substitution of the solution given in Eq. (3.76), results in

$$H^2 + \frac{k}{a^2} + \alpha\left(H^2 - \frac{K^2}{a^2}\right)\left(H^2 + \frac{K^2 + 2k}{a^2}\right) = \frac{8\pi G}{3}\rho\,. \tag{3.78}$$

It can clearly be seen that this only reduces to Eq. (3.65) when $K^2 = -k$. For the flat case, this requires $K = 0$, and for the positively curved case we need $K = \pm i$. Any other value, parametrized by $K^2 = -k + C$, where C is a free parameter, leads to an additional dark radiation term, such that the Friedmann equation can be written as

$$H^2 + \frac{k}{a^2} + \alpha\left(H^2 + \frac{k}{a^2}\right)^2 = \frac{8\pi G}{3}\rho + \frac{\alpha C^2}{a^4}\,. \tag{3.79}$$

It is interesting to note that in the positively-curved case a complex scalar field is required to set $C = 0$ and recover the Friedmann equation of the original theory, and the bouncing behaviour discussed above.

Finally, we note that for the perturbed line-element (3.68), taking Eq. (3.76) with $K = 0$ also recovers the perturbed equations (3.73) of the original theory. In more detail, the first-order equation of motion for the scalar field is

$$\alpha K^2\left(\partial^2(\delta\phi + \varphi) + 3(\psi'' - \delta\phi'') + 3K(\psi' + \varphi')\right) = 0\,, \tag{3.80}$$

which is automatically solved when $K = 0$ and thus does not constrain the field fluctuation, $\delta\phi$. The first-order field equations are modified by the presence of a non-zero C and become

$$\begin{aligned}
&8\pi G a^4\rho\delta + 2\mathcal{A}(-\partial^2\psi + 3\mathcal{H}^2\varphi + 3\mathcal{H}\psi') = 4\alpha K^2\left(3K^2\varphi + 3K(\psi' - \delta\phi') + \partial^2(\psi - \delta\phi)\right)\,,\\
&\mathcal{A}\varphi + (\mathcal{B} - 4\alpha\mathcal{H}')\psi = -8\pi G a^4\Pi + 2\alpha K^2(\varphi + \psi)\,,\\
&\mathcal{A}\partial^2 F_i' + 16\pi G(1+w)a^4\rho v_i = 2\alpha K^2\partial^2 F_i'\,,\\
&\mathcal{A}\gamma_{ij}'' + 2\mathcal{H}(a^2 + 2\alpha\mathcal{H}')\gamma_{ij}' + (\mathcal{B} - 4\alpha\mathcal{H}')\partial^2\gamma_{ij} = 8\pi G a^4\Pi_{ij} + 2\alpha K^2(\gamma_{ij}'' + \partial^2\gamma_{ij})\,,
\end{aligned} \tag{3.81}$$

where we have placed the K-dependent terms on the right-hand side, to clearly demonstrate that these equations reduce to those of the original theory when $K = 0$. Thus, the fact that, in that case, at the linear level, the field perturbation is undetermined is inconsequential, since it affects nothing else. In the general case, in which $K \neq 0$, the additional scalar degree of freedom is important and needs to be taken into account for a full description of the solutions, in addition to the extra terms depending on K. At the linear level, the additional field perturbations affect only the scalar equations, effectively sourcing the gravitational field. A clear effect of the K-dependent terms is on the propagation of gravitational waves, whose speed is now modified, since the parameter Γ is then given by $\Gamma \equiv 1 + 2\alpha(H^2 - K^2/a^2)$.

3.2.3 Cosmology in diffeomorphism breaking version of 4D EGB

The version of 4D Einstein-Gauss-Bonnet that breaks temporal diffeomorphisms differs from the original version by the introduction of a counter-term dependent on the Weyl tensor of the spatial sections, C_{ijkl}, and on the Weyl part of a combination of extrinsic curvature tensors, $K_{i[j}K_{k]l}$ [259, 271]. For that reason, if those Weyl components vanish, the solutions of this version of the theory are the same as those for the original version.

Due to it having conformally flat spatial sections, the flat FLRW space-time is a solution of this version of the theory obeying the same Friedmann equations as the original version of the theory (Eq. (3.64), with $k = 0$). Vector and tensor perturbations are expected to introduce a non-zero spatial Weyl tensor, and should obey different equations from those of the original theory. While vectors were not

studied yet, the evolution of tensor modes was derived in Ref. [271], and reads

$$\ddot{\gamma}_{ij} + \left(3 + \frac{4\alpha\dot{H}}{1+2\alpha H^2}\right) H\dot{\gamma}_{ij} - c_T^2 \frac{\partial^2 \gamma_{ij}}{a^2} + \frac{4\alpha}{\Gamma a^4}\partial^4 \gamma_{ij} = 0\,. \tag{3.82}$$

The additional term here has 4 spatial derivatives, and therefore modifies the dispersion relation of gravitational waves, adding a k^4 term (here k is the Fourier mode) and substantially modifying the predictions of the theory.

In addition to this, Ref. [272] has studied gravitational waves at second-order in perturbations, as applied to the calculation of the bispectrum of tensor modes from inflation. We do not go into detail here on that scenario, but it is clear from those results that at second-order there are also contributions with 4 spatial derivatives, which would not be present in the original or scalar-tensor versions of the theory.

In the next chapter we will return to cosmological discussions of 4DEGB as we discuss observational constraints on the theory from cosmology.

4 Observational Constraints on the Regularized 4D Einstein-Gauss-Bonnet Theory

As with any newly proposed theory of gravity, it is important to understand the weak-field behaviour of 4D Einstein-Gauss-Bonnet. It is the weak-field limit to which we have the most direct access, and in which the vast majority of experimental and observational tests of gravitational theories have so far been performed. Such a limit is sufficient to describe almost all astrophysical systems, with the notable exceptions of compact objects and cosmology, which have been discussed in the preceding sections of this thesis.

In order to explore the weak-field behaviour of 4D Einstein-Gauss-Bonnet we will deploy the standard framework; a post-Newtonian expansion of the field equations and equations of motion of the theory order-by-order in the typical velocity of bodies in the system as a fraction of the speed of light, v/c. Such an expansion is the bedrock of almost all weak-field gravity phenomenology, in the solar system as well as in extra-solar systems such as binary pulsars [335]. We will also restrict ourselves to the scalar-tensor version on this theory

$$S = \frac{1}{16\pi}\int d^4x\sqrt{-g}\Big[R+\alpha\Big(4G^{\mu\nu}\nabla_\mu\phi\nabla_\nu\phi-\phi\mathcal{G}+4\Box\phi(\nabla\phi)^2+2(\nabla\phi)^4\Big)\Big]+S_M\,. \quad (4.1)$$

The dynamical problem of two gravitationally interacting massive bodies is considered in Section 4.3, where constraints are imposed on α from observations made in relevant physical systems. In Section 4.4 we proceed to study the constraints that can be imposed from observations of the propagation of electromagnetic and gravitational radiation. Finally, in Section 4.5 we consider order-of-magnitude constraints that can be imposed on regularized 4DEGB from cosmology, black hole physics, and table-top experiments of gravity. Overall, we find that the LAGEOS satellites provide the tightest bounds on the coupling parameter α, but that observations based on early universe physics or gravitational waves from black hole mergers are

ultimately likely to give even tighter constraints.

4.1 Post-Newtonian Expansion

We want to investigate the behaviour of the theory given in (4.1) under a post-Newtonian expansion. This is an expansion of the metric about Minkowski space, where the gravitational field is assumed to be weak and the motion of matter is assumed to be slow compared to the speed of light.

We therefore consider a metric that can be written as

$$g_{\mu\nu} = \eta_{\mu\nu} + h_{\mu\nu} \,, \tag{4.2}$$

where $h_{\mu\nu}$ is a perturbation. We proceed by using an expansion parameter ϵ, which is taken to be of the typical order-of-magnitude of the 3-velocity v of a body in the system under consideration (in most cases of interest $\epsilon \sim v/c \sim 10^{-5}$ to 10^{-4}).

The different components of $h_{\mu\nu}$ can then be expanded as

$$\begin{aligned} h_{00} &= h_{00}^{(2)} + h_{00}^{(4)} + O\left(\epsilon^5\right) \\ h_{0i} &= h_{0i}^{(3)} + O\left(\epsilon^4\right) \\ h_{ij} &= h_{ij}^{(2)} + O\left(\epsilon^3\right) \,, \end{aligned}$$

where Latin indices run over the three spatial dimensions, and where numbers in brackets indicate the order of an object with respect to the parameter ϵ. Different components of the perturbation are expanded to different orders in ϵ due to the role each of them plays in the field equations and the equations of motion of particles and bodies. Here we have included the terms that are required to reproduce the leading-order Newtonian equations, and the next-to-leading-order post-Newtonian terms, for objects with time-like or null trajectories.

Matter fields in this approach are expanded such that

$$v = v^{(1)}, \qquad \rho = \rho^{(2)}, \qquad p = p^{(4)}, \qquad \Pi = \Pi^{(2)} \,,$$

where ρ is the density of mass, p is the isotropic pressure, and Π is the internal energy per unit mass (such that energy density is given by $\tilde{\mu} = \rho(1 + \Pi)$).

We also need to use the fact that time derivatives add an extra order of ϵ, compared

to spatial derivatives of the same quantity, such that

$$\frac{\partial/\partial t}{\partial/\partial x^i} \sim \epsilon \,. \tag{4.3}$$

This equation encodes the "slow motion" aspect of the expansion. We take this rule to apply to *all* fields, not just those directly associated with matter, which extends this notion from the motion of bodies themselves to the gravitational fields they generate.

The only remaining object that needs to be perturbed is the scalar field ϕ, which we now write as

$$\phi = \bar{\phi} + \delta\phi \tag{4.4}$$

where $\bar{\phi} \sim \epsilon^0 \sim 1$ is the constant background value of ϕ, and where $\delta\phi \sim \epsilon^2$ is a perturbation.

Everything described in this section is entirely standard in the post-Newtonian approach to weak-field gravity, and is explained in great detail in (for example) Ref. [336], to which the reader can refer for further explanation and justification. We will use this formalism in the following section to construct the slow-motion, weak-field metric for 4DEGB gravity.

4.2 Weak Field Gravity

The first task to perform in assessing the observational viability of 4DEGB in the weak field regime is to expand the field equations in the smallness parameter ϵ. The results can then be solved order-by-order, to build up a perturbative description of the gravitational field that can be used to compute observables.

4.2.1 Solving the Perturbed Field Equations

The leading-order part of the 00 field equation (5.16) occurs at order ϵ^2, and can be written

$$\nabla^2 h_{00}^{(2)} = -8\pi\,\rho\,, \tag{4.5}$$

which under asymptotically flat boundary conditions integrates to

$$h_{00}^{(2)} = 2\,U = 2\int \frac{\rho}{|\mathbf{x}-\mathbf{x}'|} d^3x'\,, \tag{4.6}$$

where the last equality serves to define the Newtonian gravitational potential $U = U(\mathbf{x})$, and where the mass density should be taken to be a function of the primed coordinate position (such that $\rho = \rho(\mathbf{x}')$). This metric perturbation is sufficient to describe all gravitational physics at the leading-order Newtonian level of approximation, for bodies following time-like geodesics.

To determine the trajectories of rays of light to Post-Newtonian order we require $h^{(2)}_{ij}$, as well as $h^{(2)}_{00}$. This can be determined from the leading-order part of the ij field equations (5.16), which are at order ϵ^2 and read

$$\nabla^2 h^{(2)}_{ij} = -8\pi\,\rho\,\delta_{ij}\,, \tag{4.7}$$

and which have the solution

$$h^{(2)}_{ij} = 2\,U\,\delta_{ij} = h^{(2)}_{00}\,\delta_{ij}\,. \tag{4.8}$$

Equation (4.7) is derived by choosing a gauge such that $2h^{\mu}{}_{i,\mu} - h^{\mu}{}_{\mu,i} = 0$, which can be retrospectively shown to be satisfied for the solutions we find.

The post-Newtonian equations of motion require knowledge of $h^{(3)}_{0i}$ and $h^{(4)}_{00}$, as well as $h^{(2)}_{00}$ and $h^{(2)}_{ij}$. The equation for $h^{(3)}_{0i}$ can be found by taking the leading-order contribution to the $0i$ field equations:

$$\nabla^2 h^{(3)}_{0i} + U_{,0i} = 16\pi\,\rho\,v_i\,, \tag{4.9}$$

where the gauge condition $2h^{\mu}{}_{0,\mu} - h^{\mu}{}_{\mu,0} = -h_{00,0}$ has been used, as well as the lower-order solutions above. Again, this gauge condition can be retrospectively verified by the solutions it generates. The asymptotically flat solution to Eq. (4.9) is

$$h^{(3)}_{0i} = -\frac{7}{2}V_i - \frac{1}{2}W_i \tag{4.10}$$

where the post-Newtonian gravitational potentials V_i and W_i are given by

$$V_i = \int \frac{\rho\,v_i}{|\mathbf{x}-\mathbf{x}'|}d^3x' \tag{4.11}$$

$$W_i = \int \frac{\rho\,[\mathbf{v}\cdot(\mathbf{x}-\mathbf{x}')](x_i - x'_i)}{|\mathbf{x}-\mathbf{x}'|^3}d^3x'\,, \tag{4.12}$$

and where various manipulations have been performed. The mass density ρ and the 3-velocity field $\mathbf{v}$ in these equations should be taken to be functions of the primed coordinate position $\mathbf{x}'$.

It now remains to determine $h_{00}^{(4)}$. In order to do this we use the scalar field propagation equation (2.56), which has its first non-trivial part at order ϵ^4:

$$\delta\phi_{,ij}\,\delta\phi_{,ij} - \left(\nabla^2\delta\phi\right)^2 = U_{,ij}\,U_{,ij} - \left(\nabla^2 U\right)^2 . \tag{4.13}$$

Imposing sensible boundary conditions, this equation admits the solutions

$$\delta\phi = \pm U . \tag{4.14}$$

This is remarkably simple, and gives the interesting interpretation that the value of the gravitational scalar ϕ at a point in space-time is simply equal to the value of the Newtonian gravitational potential (up to a sign).

Using Eq. (4.14), we can write the 00 field equation at order ϵ^4 as

$$\nabla^2\left(h_{00}^{(4)} + 2U^2 - 4\Phi_1 - 4\Phi_2 - 2\Phi_3 - 6\Phi_4\right) = \pm\alpha\,\mathcal{G}^{(4)} , \tag{4.15}$$

where

$$\Phi_1 = \int \frac{\rho\, v^2}{|\mathbf{x}-\mathbf{x}'|} d^3x' \tag{4.16}$$

$$\Phi_2 = \int \frac{\rho\, U}{|\mathbf{x}-\mathbf{x}'|} d^3x' \tag{4.17}$$

$$\Phi_3 = \int \frac{\rho\,\Pi}{|\mathbf{x}-\mathbf{x}'|} d^3x' \tag{4.18}$$

$$\Phi_4 = \int \frac{p}{|\mathbf{x}-\mathbf{x}'|} d^3x' \tag{4.19}$$

and where the order ϵ^4 part of the Gauss-Bonnet invariant is written as

$$\mathcal{G}^{(4)} = 8\left(U_{,ij}\,U_{,ij} - \left(\nabla^2 U\right)^2\right) .$$

Integrating Eq. (4.15) gives the solution

$$h_{00}^{(4)} = -2U^2 + 4\Phi_1 + 4\Phi_2 + 2\Phi_3 + 6\Phi_4 \mp \left(\frac{\alpha}{4\pi}\right)\Phi_{\mathcal{G}} , \tag{4.20}$$

where we have introduced the new potential

$$\Phi_{\mathcal{G}} = \int \frac{\mathcal{G}^{(4)}}{|\mathbf{x}-\mathbf{x}'|} d^3x' . \tag{4.21}$$

This equation represents a new type of gravitational potential that is sourced by

the Gauss-Bonnet invariant itself (in the same way that the mass density ρ sources the Newtonian potential U). The $\mp$ sign in Eq. (4.20) has its origin in the $\pm$ that occurs in Eq. (4.14).

Comparison of the results above with the PPN test metric gives the gravitational parameters of this theory as

$$\beta = \gamma = 1 \tag{4.22}$$

and

$$\xi = \alpha_1 = \alpha_2 = \alpha_3 = \zeta_1 = \zeta_2 = \zeta_3 = \zeta_4 = 0\,, \tag{4.23}$$

exactly as in GR [335]. The only difference is the appearance of the potential $\Phi_{\mathcal{G}}$ in Eq. (4.20), which has no counterpart in the standard PPN metric. In what follows we will determine the effects that this new post-Newtonian gravitational potential has on observables, and use these results to place observational constraints on the coupling parameter α.

4.2.2 The N-Body Problem

Let us now consider a collection of point sources, as the origin of the gravitational field. The energy density of such a group of sources can be written as

$$\tilde{\mu} = \sum_A m_A \frac{d\tau_A}{dt} \frac{\delta^3(\mathbf{r} - \mathbf{r}_A)}{\sqrt{-g}}\,, \tag{4.24}$$

where m_A is the rest mass of particle A, τ_A is the proper time along its world-line, and we have taken $p = 0$.

If we now recall that $\tilde{\mu} = \rho(1 + \Pi)$, we find that we can write

$$U = \sum_A \frac{m_A}{|\mathbf{x} - \mathbf{x}_A|}\,, \tag{4.25}$$

and

$$\Phi_1 = \sum_A \frac{m_A v_A^2}{|\mathbf{x} - \mathbf{x}_A|} \tag{4.26}$$

$$\Phi_2 = \sum_A \frac{m_A U_A}{|\mathbf{x} - \mathbf{x}_A|} \tag{4.27}$$

$$\Phi_3 = -\frac{1}{2}\Phi_1 - 3\Phi_2 \tag{4.28}$$

$$\Phi_4 = 0\,, \tag{4.29}$$

where U_A is the value of U at particle A, without including its own infinite contribution to this quantity.

The remaining vector post-Newtonian potentials are given by

$$V_i = \sum_A \frac{m_A v_{Ai}}{|\mathbf{x} - \mathbf{x}_A|} \tag{4.30}$$

$$W_i = \sum_A \frac{m_A \mathbf{v}_A \cdot (\mathbf{x} - \mathbf{x}_A)(x - x_A)_i}{|\mathbf{x} - \mathbf{x}_A|^3} \,. \tag{4.31}$$

It now only remains to calculate $\Phi_{\mathcal{G}}$, which is done in Appendix 4.A, and gives

$$\Phi_{\mathcal{G}} = -32\pi \left(\frac{1}{2} |\nabla U|^2 - \psi_1 \right) \,, \tag{4.32}$$

where

$$|\nabla U|^2 = \sum_{A,B} \frac{m_A m_B (\mathbf{x} - \mathbf{x}_A) \cdot (\mathbf{x} - \mathbf{x}_B)}{|\mathbf{x} - \mathbf{x}_A|^3 |\mathbf{x} - \mathbf{x}_B|^3} \tag{4.33}$$

$$\psi_1 = \sum_{A,\, B \neq A} \frac{m_A m_B (\mathbf{x} - \mathbf{x}_A) \cdot (\mathbf{x}_A - \mathbf{x}_B)}{|\mathbf{x} - \mathbf{x}_A|^3 |\mathbf{x}_A - \mathbf{x}_B|^3} \,, \tag{4.34}$$

and where infinite contributions have again been removed. The potentials listed in Eqs. (4.25)-(4.32) can be substituted back into the expressions derived in the previous section to find the relevant expressions for the components of the metric perturbation $h_{\mu\nu}$ at each order of interest.

4.3 2-Body Dynamics

We will find below that a promising route for constraining the 4DEGB theory with observations involves the bound orbits of two massive bodies. We will therefore begin this section by calculating the Lagrangian and Hamiltonian formulation of this problem.

4.3.1 Relativistic Lagrangian and Hamiltonian

To begin with, let us consider a single time-like particle, which we will label 1. The Lagrangian that can be used for investigating the motion of this particle can be written $L_1 = -m_1 d\tau_1/dt$, where m_1 is its mass and τ_1 is the proper time measured along its worldline. The Lagrangian L_1 gives the force on particle 1 by taking the partial derivative with respect to the field point: $\mathbf{F}_1 = (\partial L_1/\partial \mathbf{x})\,|_{\mathbf{x}=\mathbf{x}_1}$. If instead

we want a Lagrangian that will be valid for more than one particle then we can construct an L for which the force on the ith particle will be given by $\mathbf{F}_i = \partial L/\partial \mathbf{x}_i$.

For a two-body system this Lagrangian is given to the required order of accuracy by

$$\begin{aligned} L =& -(m_1+m_2) + \frac{1}{2}m_1 v_1^2 + \frac{1}{2}m_2 v_2^2 + \frac{m_1 m_2}{r_{12}} \\ &+ \frac{m_1 m_2}{2r_{12}}\left[3(v_1^2+v_2^2) - 7\mathbf{v}_1\cdot\mathbf{v}_2 - (\mathbf{v}_1\cdot\mathbf{n}_{12})(\mathbf{v}_2\cdot\mathbf{n}_{12})\right] \\ &+ \frac{1}{8}(m_1 v_1^4 + m_2 v_2^4) - \frac{m_1 m_2 (m_1+m_2)}{2r_{12}^2}\left(1 \pm \frac{4\alpha}{r_{12}^2}\right) , \end{aligned} \tag{4.35}$$

where $r_{12} = |\mathbf{x}_1 - \mathbf{x}_2|$ and $\mathbf{n}_{12} = (\mathbf{x}_1 - \mathbf{x}_2)/r_{12}$, and which can be seen to reduce to the usual expression from GR in the case $\alpha = 0$ [337].

This Lagrangian can be conveniently re-written by choosing a frame such that $m_1\mathbf{v}_1 + m_2\mathbf{v}_2 = 0$, which corresponds to the centre-of-momentum frame at Newtonian-level accuracy. If we also define the total and reduced masses by $M = m_1 + m_2$ and $\mu = m_1 m_2/M$, and the relative velocity by $\mathbf{v} = \mathbf{v}_1 - \mathbf{v}_2$ then we get

$$L = L^{(2)} + L^{(4)} \tag{4.36}$$

where $L^{(2)}$ (the Lagrangian at the Newtonian order of approximation) is given by

$$L^{(2)} = -M + \frac{1}{2}\mu v^2 + \frac{\mu M}{r} , \tag{4.37}$$

and $L^{(4)}$ (the first post-Newtonian correction) is

$$\begin{aligned} L^{(4)} =& \frac{\mu M}{2r}\left[\left(3 + \frac{\mu}{M}\right)v^2 + \frac{\mu}{M}\frac{(\mathbf{v}\cdot\mathbf{r})^2}{r^2}\right] \\ &+ \frac{\mu}{8}\left(1 - 3\frac{\mu}{M}\right)v^4 - \frac{\mu M^2}{2r^2}\left(1 \mp \frac{4\alpha}{r^2}\right) , \end{aligned} \tag{4.38}$$

where we have written $\mathbf{r} = \mathbf{x}_1 - \mathbf{x}_2$ and $r = |\mathbf{r}|$.

Using the expressions above for the two-body Lagrangian, we can construct the corresponding Hamiltonian and write it as

$$H = H^{(2)} + H^{(4)} , \tag{4.39}$$

where the Newtonian-level contribution is given by

$$H^{(2)} = M + \frac{p^2}{2\mu} - \frac{\mu M}{r} \tag{4.40}$$

and the first post-Newtonian contribution is given by

$$\begin{aligned} H^{(4)} = &- \frac{1}{2r}\left[3\frac{(M-2\mu)}{\mu}p^2 + 7p^2 + (\mathbf{p}\cdot\hat{\mathbf{r}})^2\right] \\ &- \frac{(M-3\mu)}{8M\mu^3}p^4 + \frac{M^2\mu}{2r^2}\left(1 \mp \frac{4\alpha}{r^2}\right), \end{aligned} \tag{4.41}$$

where the relative momentum is $\mathbf{p} = \mathbf{p}_1 = -\mathbf{p}_2$, with magnitude $p = |\mathbf{p}|$. We will now use this Hamiltonian to calculate the periapsis advance for two bodies in closed orbits.

4.3.2 Advance of Periapsis

We can calculate the advance of periapsis using the Hamilton-Jacobi approach, which has an action

$$\begin{aligned} S(r,\varphi,t) &= S_r(r) + S_\varphi(\varphi) + S_t(t) \\ &= S_r + J\varphi - Et\,, \end{aligned} \tag{4.42}$$

where J is angular momentum and E is energy. The radial momentum can be extracted from the radial part of this action using $p_r = \partial S_r/\partial r$ and the angular coordinate φ can be found using the equation for the generalized coordinate: $\varphi = -\partial S_r/\partial J + \text{constant}$. This gives the angle φ (up to a constant) as

$$\varphi = -\int \frac{\partial p_r}{\partial J} dr\,, \tag{4.43}$$

where p_r can be determined using the Hamiltonian (4.39).

Energy in this system is conserved, so $H = E = \text{constant}$. Solving Eq. (4.39) for p_r therefore gives

$$p_r^2 = -A + \frac{B}{r} - \frac{J^2}{r^2} + \frac{6M^2\mu^2}{r^2}\left(1 \pm \frac{2\alpha}{3r^2}\right), \tag{4.44}$$

where we have performed a gauge transformation so that $r \to r + \mu/2$, and where

$$A = -2(E - M)\mu + O(\epsilon^4)$$
$$B = 2M\mu^2 + O(\epsilon^4)\,.$$

The higher-order parts of these equations are not made explicit, as they are not required in the final result.

Using Eq. (4.44) in Eq. (4.43) gives, to Newtonian order, the usual result:

$$\varphi_{\rm N} = \cos^{-1}\left(\frac{2J^2/r - B}{\sqrt{B^2 - 4AJ^2}}\right)\,, \tag{4.45}$$

where the constant of integration has been chosen so that the moment of periapsis occurs at $\varphi = 0$, and where we have neglected the last term in Eq. (4.44), which is small compared to the first three.

The relativistic correction to φ can then be calculated using

$$\varphi_{\rm R} = -\int \frac{\partial p_r^{(4)}}{\partial J} dr \bigg|_{A=A^{(2)},\, B=B^{(2)}}\,. \tag{4.46}$$

Here there is no need to include the ϵ^4 parts of A and B, as the higher-order parts in the first two terms contribute in exactly the same way as the lower-order parts do to $\varphi_{\rm N}$, and the higher-order parts included in the last term would be of order ϵ^6.

We find that Eq. (4.46) evaluates to

$$\varphi_{\rm R} = \frac{3M^2\mu^2}{4J^6}\left[4J^4 \pm \alpha(5B^2 - 4AJ^2)\right]\varphi_{\rm N} \tag{4.47}$$
$$+ \text{ periodic terms}\,.$$

The constant of integration has been chosen here so that $\varphi_{\rm R} = 0$ at periapsis (i.e. when $\varphi_{\rm N} = 0$). The periodic terms in this expression are omitted as they do not produce a secular change that can accumulate.

To find the precession that occurs every orbit, we can put $\varphi_{\rm N} = 2\pi$ into Eq. (4.47), and neglect the periodic terms. This gives

$$\delta\varphi = \frac{6\pi M}{a(1-e^2)}\left[1 \pm \frac{\alpha(4+e^2)}{a^2(1-e^2)^2}\right]\,, \tag{4.48}$$

where a is the semi-major axis of the orbit and e is the eccentricity. In deriving this expression we have used the Newtonian results $J^2 = M\mu^2 a(1-e^2)$ and $E =$

$M - M\mu/2a$. This equation gives the contribution from the Gauss-Bonnet term to the advance of periapsis of a bound orbit, and can be seen to reduce to the usual expression from GR when $\alpha = 0$ (see e.g. [337]).

4.3.3 Observational Constraints

Let us now consider observational constraints that can be imposed on the coupling parameter α, using observations of closed orbits of time-like objects. We will first consider the classical test of Mercury's perihelion precession, before moving on to the orbits of satellites around the Earth, and the orbits of binary pulsars.

Perihelion Precession of Mercury: The detection of the anomalous perihelion precession of the orbit of Mercury pre-dates the discovery of relativistic gravity as discussed in the introduction, and was one of the original tests used to validate GR. It therefore has important pedagogical importance.

Contributions to the perihelion precession of Mercury come from the precession of the equinoxes of the coordinates' system ($\sim 5025''$ per century), from the gravitational influence of the other planets ($\sim 531''$ per century), and from the non-zero quadrupole moment of the Sun ($\sim 0.025''$ per century). A precise determination of these contributions, analyzed together with the ephemeris of Mercury, gives an anomalous deficit of $\sim 43''$ per century. This can be compared with the prediction from Eq. (4.48) to constrain our theory.

For definiteness, we use the anomalous perihelion precession determined by Pitjeva and Pitjev [338]:

$$\delta\varphi - \delta\varphi_{\rm GR} = (-0.0020 \pm 0.0030)'' \text{ per century}\,, \tag{4.49}$$

where $\delta\varphi_{\rm GR} = 42.98$ arcseconds per century is the famous prediction from GR. Other published values for this quantity exist in the literature, and can be found e.g. Ref. [339]. Taking the mass of the Sun to be $1.9884 \times 10^{30}\,\text{kg}$, the mass of Mercury to be $3.3011 \times 10^{23}\,\text{kg}$, and their orbit to have semi-major axis $a = 57,909,050\,\text{km}$ and eccentricity $e = 0.205\,630$, we find that Eq. (4.49) implies that the coupling parameter of 4DEGB is constrained to be

$$|\alpha| = |(-3.54 \pm 5.31)| \times 10^{16}\,\text{m}^2\,. \tag{4.50}$$

Alternate observations will of course give alternative bounds on α, but for errors on $\delta\varphi$ of the order of ~ 0.01 arcseconds per century we can see that the constraints are

going to be at the level of $|\alpha| \lesssim 10^{17}\,\mathrm{m}^2$.

LAGEOS Satellites: The LAGEOS satellites are two man-made satellites, which are spherical in shape with a diameter of 60 cm, and which orbit the Earth at an altitude of approximately 6 000 km. Lasers are reflected off the satellites from ground-based stations, which allow for precise tracking of their orbits. One of the many benefits of this is that the gravitational field of the Earth can be measured to very high accuracy.

Using 13 years of tracking data of the LAGEOS satellites, the precession of the periapsis of the LAGEOS II satellite was measured by Lucchesi and Peron to be [340]

$$\delta\varphi = \left[1 + (0.28 \pm 2.14) \times 10^{-3}\right] \delta\varphi_{\mathrm{GR}}\,,$$

where $\delta\varphi_{\mathrm{GR}}$ is the prediction from GR (i.e. Eq. (4.48) with $\alpha = 0$). Taking the mass of this satellite to be 405.38 kg, and taking its orbit to have a semi-major axis $a = 5.697 \times 10^6$m and eccentricity $e = 0.0135$, this corresponds to a bound on the 4DEGB coupling parameter of

$$|\alpha| = |(0.23 \pm 1.74)| \times 10^{10}\,\mathrm{m}^2\,, \tag{4.51}$$

where we have taken the mass of the Earth to be 5.9722×10^{24} kg. This is a much tighter bound than that obtained from the perihelion precession of Mercury, which we take to be due to the much smaller orbital radius of the LAGEOS satellites ($\sim 10^6$m, compared to $\sim 10^{10}$m for Mercury). This being the case, the $1/r^4$ form of the gravitational potential in Eq. (4.32) then suppresses the contribution of the new effects in 4DEGB by a much smaller amount.

Precession of S2 around Sgr A:* The motions of stars orbiting the central black hole of the Milky Way galaxy have now been observed for 27 years, which has enabled very accurate determinations of their orbital parameters. The GRAVITY collaboration has detected the precession of the star S2 to be [341]:

$$\delta\varphi = [1.10 \pm 0.19]\, \delta\varphi_{\mathrm{GR}}\,, \tag{4.52}$$

where $\delta\varphi_{\mathrm{GR}} = 12.1'$ per orbit is the prediction from GR. We find that this implies

$$|\alpha| = |(2.17 \pm 4.42)| \times 10^{25}\,\mathrm{m}^2\,, \tag{4.53}$$

where we have taken the mass of the central black hole to be $4.261 \times 10^6\, M_\odot$, the mass of S2 to be negligible, and its orbit to have eccentricity $e = 0.884649$ and semi-major axis $a = 1.54 \times 10^{14}\,\mathrm{m}$ (from an angular size of 125.058 mas and a distance of 8246.7 pc) [341].

This bound is weaker than that obtained from Mercury and LAGEOS, but is obtained in a very different environment. Further observations of S2, and other stars orbiting Sgr A*, may provide slightly better constraints in future, but should not be expected to improve to the level of those given by LAGEOS as the a^2 suppression in Eq. (4.48) is orders of magnitude larger in the present case. We note while canonical scalar-tensor theories (such as Brans-Dicke) have black hole solutions with a weak field that is identical to GR [342], this is not expected to be the case in 4DEGB. This is due to the form of the scalar field propagation equation (2.56), which is sourced by the Gauss-Bonnet curvature-invariant of the space-time, and not its energy-momentum content. The scalar field must therefore be non-constant, and satisfy Eq. (4.13) in the weak field limit, independent of whether the gravity is due to a black hole or matter.

Binary Pulsars: Binary pulsars are two-body systems that contain at least one pulsar (i.e. a rotating neutron star that emits regular pulses of radiation). These systems are excellent testing grounds for relativistic gravitational physics, as they allow precise data about orbits to be extracted from systems in which the bodies move at very high velocities.

The first and most famous, binary pulsar system to be found was PSR B1913+16 [343], also known as the *Hulse-Taylor binary* (after its discoverers). This system provided the first indirect evidence for the existence of gravitational waves, as the period of its orbit changed over time due to their emission. In general, binary pulsars provide the possibility to constrain relativistic gravity through five different *post-Keplerian* effects: the rate of advance of periapsis, the rate of change of orbital period, the gravitational redshift and two types of Shapiro time delay effect.

The most promising binary pulsar system for constraining 4DEGB is PSR J0737-3039A/B [344], also known as the *double pulsar*. In this system both bodies were (for a time) emitting pulses of radiation that were visible from Earth. In addition, the system was oriented edge-on, which meant that all five post-Keplerian parameters were visible, as well as the mass ratio of the pulsars being determinable.

As we will discuss later, the Shapiro time delay effects are unaltered in 4DEGB from their values in GR. The advance of periapsis, on the other hand, can be seen from (4.48) to be dependent on the coupling parameter α. We can therefore use the

mass ratio, together with observations of these two relativistic effects, to determine the masses of both pulsars together with the value of α (as there are three observables and three unknowns). Using the mass ratio and the periapsis advance to determine the masses, Kramer *et al.* find the time delay parameter r to be given by [345]

$$r = (1.009 \pm 0.055)\, r_{\rm GR}\,, \tag{4.54}$$

where $r_{\rm GR}$ is the value predicted in GR. Assuming this combination of observables leads to a similar constraint on the advance of periapsis of the system gives the following constraint on the coupling parameter:

$$|\alpha| = |(0.4 \pm 2.4)| \times 10^{15}\, \frac{\rm m^2}{\sin i}\,, \tag{4.55}$$

where i is the inclination angle of the system, where the mass ratio has been taken to be 1.0714 and the semi-major axis and ellipticity have been taken to be given by $a = 1.415032\,{\rm c\,s^{-1}}/\sin i$ and $e = 0.087777$. This gives a best estimate for the constraints available from these observations to be $|\alpha| \lesssim 10^{15}\,{\rm m^2}$, which is better than that available from Mercury, but worse than the constraints available from LAGEOS.

We note that while the structure of neutron stars in 4DEGB has not yet been studied, we still expect the analysis performed above to be applicable to the weak field of such bodies. This is despite non-perturbative effects, such as "spontaneous scalarization", being known to exist in some scalar-tensor theories [103]. This is because the only degree-of-freedom in our weak-field analysis that could be altered by such non-linear physics is the mass of the body, which is already treated as a nuisance parameter when extracting constraints from data. In particular, the coupling constant α cannot be dependent on environment, and so the cannot be affected by non-linearities in the same way as the coupling function $\omega(\phi)$ of canonical scalar-tensor theories.

4.4 Propagation of Radiation

As well as the motion of massive bodies, there are also a number of observational tests of gravity that rely on the propagation of radiation. In the case of isolated, weakly gravitating systems, two of the most widely used tests of this type are gravitational lensing and Shapiro time delay. More recently, there is also the direct detection of gravitational waves by LIGO/VIRGO.

4.4.1 Lensing and Time Delay

The first test of relativistic gravity to be performed after the publication of GR was the observation of the gravitational lensing of light by the Sun, which is predicted by Einstein's equations to be $1.75''$ for a null trajectory that grazes its edge. This effect was observed by Eddington in May of 1919, during his famous trip to Príncipe, and was of great importance in establishing the validity of GR. Today, this same effect is measured using Very Long Baseline Interferometry, with results from around 2500 days of observations taken over a period of 20 years giving the constraint [346]

$$\theta = (0.99992 \pm 0.00023)\, \theta_{\rm GR}\,, \tag{4.56}$$

where θ is the deflection angle, and $\theta_{\rm GR} = 1.75''$ is the prediction from GR. This is one of the highest precision results available on relativistic gravity, and is used to place constraints on the post-Newtonian parameter γ to around 1 part in 10^4 of its value in GR.

Even tighter constraints on γ are available from observations of the Shapiro time delay effect, which accounts for the deflection in time of a radio signal as it passes through a gravitational field. The most constraining observation of this effect in the Solar System to date was from radio signals sent to the Cassini spacecraft on its mission to Saturn. These give [347]

$$\Delta t = (1.00001 \pm 0.00001)\, \Delta t_{\rm GR}\,, \tag{4.57}$$

where $\Delta t_{\rm GR}$ is the expected size of the effect from GR. This gives a bound on γ of being within 1 part in 10^5 of its expected value, which is currently the best constraint available on this quantity (or on any post-Newtonian parameter associated with conservative theories of gravity).

We note that these observations, though extremely precise, provide no new constraints on the coupling parameter α. This can be seen from the results presented in Section 4.2, where the order ϵ^2 parts of both the 00 and ij components of the metric are identical to the form they take in GR. The equations of motion of null particles are only sensitive (at leading-order) to gravitational potentials that appear in these components of the metric at this order [335], so the lensing and time delay effects in 4DEGB should be expected to be exactly the same as they are in GR. This means that neither effect can be used to constrain α, and all that can be said is that the results quoted in Eqs. (4.56) and (4.57) are consistent with this theory.

4.4.2 Gravitational Waves

A further constraint on α comes from the propagation of gravitational waves from the double neutron star collision that resulted in the signal GW170817 [348].

As discussed in the last chapter, the spatially flat FLRW metric is a solution to the field equations, but results in an altered Friedmann equation:

$$H^2 + \alpha H^4 = \frac{8\pi}{3}\rho + \frac{C^4}{a^4}\,, \tag{4.58}$$

where $H = \dot{a}/a$ is the Hubble rate, ρ is the energy density, a is the scale factor, and C is a constant of integration.

For Horndeski theories we know that the propagation speed of gravitational waves is [105]

$$c_T^2 = \frac{G_4 - X\left(\ddot{\phi}G_{5,X} + G_{5,\phi}\right)}{G_4 - 2XG_{4,X} - X\left(H\dot{\phi}G_{5,X} - G_{5,\phi}\right)} \tag{4.59}$$

where $X = -\frac{1}{2}\partial_\mu\phi\partial^\mu\phi$. The reader may note that only G_4 and G_5 are required to calculate the gravitational wave speed.

Recalling that our theory is a subset of Horndeski with $G_2 = 8\alpha X^2$, $G_3 = 8\alpha X$, $G_4 = 1 + 4\alpha X$, $G_5 = 4\alpha \log X$, we can now calculate c_T in 4DEGB. We find this to be given by

$$c_T^2 = 1 + \frac{4\alpha\left(\dot{H} + \frac{C^2}{a^2}\right)}{1 + 2\alpha\left(H^2 - \frac{C^2}{a^2}\right)} = 1 + \frac{\dot{\Gamma}}{H\Gamma}\,, \tag{4.60}$$

where $\Gamma = 1 + 2\alpha(H^2 - C^2/a^2)$ and where we have used $X = \frac{1}{2}\dot{\phi}^2$ and $\dot{\phi} = -H + C/a$ in a Friedmann background. We note that the speed of propagation of gravitational waves in an FLRW cosmology in 4DEGB is not equal to the speed of light, but that it reduces to the speed of light in Minkowski space (i.e. when $H = C = 0$).

Now, the electromagnetic counterpart to GW170817 indicates that the deviation in the speed of gravitational waves from that of light must be less than one part in 10^{15} [349–353]. From Eq. (4.60) this leads to the rather weak constraint

$$\left|\frac{\dot{\Gamma}}{H\Gamma}\right| < 10^{-15}\,, \tag{4.61}$$

which, taking $C = 0$ for simplicity, implies

$$|\alpha| \lesssim 10^{36} m^2\,, \tag{4.62}$$

where we have taken $\dot{H} \approx H^2 \approx 5.8 \times 10^{-36}\,\mathrm{s}^{-2}$. Taking $C \neq 0$ will change this constraint, and will correspond to cosmologies that contain a period in which the free kinetic energy of the scalar field dominates over matter. This is an intriguing possibility, which often occurs in the cosmologies of scalar-tensor theories of gravity, but which we will not consider further here.

The result (4.62) agrees with similar estimates in Ref. [271], and can be seen to be considerably weaker than the constraints imposed from the trajectories of massive bodies studied in Section 4.3. It therefore appears to provide an exception to the rule that GW170817 tightly constrains Horndeski theories with non-trivial G_4 and G_5 [351–353].

4.5 Other tests

We have so far considered constraints that are available on the 4DEGB theory from bound orbits of massive bodies, and from the propagation of radiation. In this section we will discuss some other tests of gravity that are available, and what they may imply for 4DEGB.

4.5.1 Black Hole Shadows

The shadow of the super-massive black hole of M87 has recently been observed [354, 355], and can be used to constrain deviations from GR [77, 356–358]. Here we will recap what this implies for 4DEGB, following Refs. [113–115, 140].

Firstly, recall that the simplest static, spherically symmetric solution of 4DEGB has line-element

$$ds^2 = -f(r)dt^2 + f(r)^{-1}dr^2 + r^2 d\Omega_2\,, \tag{4.63}$$

where

$$f(r) = 1 + \frac{r^2}{2\alpha}\left(1 - \sqrt{1 + \frac{8M\alpha}{r^3}}\right)\,, \tag{4.64}$$

and where M is a constant mass parameter. The scalar field profile is given by

$$\phi' = \frac{1 - \sqrt{f(r)}}{r\sqrt{f(r)}}. \tag{4.65}$$

This is the same solution as given in chapter 3 in Eqs. (3.35) and (3.34), but reproduced here for the convenience of the reader.

The radius of the photon sphere, $r_{\rm ph}$, for an object described by (4.63), is given by

the appropriate solution of $rf'(r) = 2f(r)$, and the corresponding black hole shadow radius is well approximated by $R_{\rm Sh} = r_{\rm ph}/\sqrt{f(r_{\rm ph})}$. This all gives

$$\frac{R_{\rm Sh}}{M} = \frac{3+\delta^{\frac{2}{3}}}{\delta^{\frac{1}{3}}}\left(1+\frac{(3+\delta^{\frac{2}{3}})^2}{2\beta\delta^{\frac{2}{3}}}\left[1-\sqrt{1+\frac{8\beta\delta}{(3+\delta^{\frac{2}{3}})^3}}\right]\right)^{-\frac{1}{2}} \tag{4.66}$$

with $\delta = -4\beta + \sqrt{16\beta^2 - 27}$ and $\beta = \alpha/M^2$. It can be shown that the radius of the shadow monotonically decreases with α. Now, the black hole M87* has been measured by the Event Horizon Telescope to have a shadow of size $R_{\rm Sh} = (4.96 \pm 0.75) \times 10^{13}$ m. Using Eq. (4.66), this value, together with a value for the mass of the black hole, can be used to infer bounds on α.

Observations of stellar dynamics around M87* imply a mass of $M = 6.14^{+1.07}_{-0.62} \times 10^9 M_\odot$ [359], which in turn allows one to derive the constraint

$$\alpha = (-0.67 \pm 1.44) \times 10^{26}\,\mathrm{m}^2\,. \tag{4.67}$$

Alternatively, measurements of gas dynamics imply $M = 3.45^{+0.85}_{-0.26} \times 10^9 M_\odot$ [360], which gives[16]

$$\alpha = (-1.26 \pm 0.80) \times 10^{27}\,\mathrm{m}^2\,. \tag{4.68}$$

Both cases prefer negative values for the Gauss-Bonnet coupling, but clearly place much looser constraints than those obtained in Section 4.3.

In addition to the constraints above, further bounds can be placed on positive values of α by the requirement for the existence of an event horizon and a photon sphere. These require $\alpha < M^2$ and $\alpha < 3\sqrt{3}M^2/4$, respectively. Since we observe the shadow, this alone can be used to place the constraints $\alpha \leq 1.07 \times 10^{26}$ m^2 for the stellar dynamics case, and $\alpha \leq 3.37 \times 10^{25}$ m^2 for the gas dynamics mass measurement.

We note that the consequences of 4DEGB gravity for black holes depend greatly on the ratio α/M^2, which for M87* is not large enough to place competitive constraints on α. However, smaller black holes will result in larger effects, due to the existence of M in the denominator of this ratio. This means it may be possible to achieve $\alpha \lesssim 10^6$ m^2 from observations of a solar mass black hole, which could be possible through an analysis of gravitational wave emission from binaries.

A similar analysis could be performed for the recently observed shadow of the

[16] Note that the masses reported in Refs. [359, 360] are not those written here, as they assumed a distance to M87* of $D = 17.9$ Mpc. This does not agree with measurements made by the Event Horizon Telescope, and was corrected to the values presented above in Ref. [355].

SgrA* black hole in the center of the Milky Way, using the results from Ref. [32]. However, we expect constraints from this analysis to be on the order of $\alpha \lesssim 10^{20}$, and therefore not relevant when compared e.g. with the ones obtained from the LAGEOS satellites.

Finally, we note that an analysis of rotating solutions in 4DEGB should be performed in order to properly understand the shadows of realistic astrophysical black holes. Our intuition from GR is that the consequences of rotation should be small in this situation, but this should be verified to be true in 4DEGB too.

4.5.2 Black Hole Binaries

The gravitational waves events that have been observed by the LIGO/VIRGO collaborations, that resulted from the inspiral and merger of binary black holes, offer the possibility of imposing tight constraints on modified theories of gravity [361–364]. Here we will investigate the possible bounds that such observations could impose on the coupling constant α, using simple physical arguments (as in Ref. [364]). This is not intended as a replacement for more sophisticated studies of these events in 4DEGB, which will require complicated numerical implementation, but to gain some insight into the constraining power that they offer.

The black hole described by the metric function (4.64), with mass m_i, has an event horizon located at

$$r_H(m_i) = m_i + \sqrt{m_i^2 - \alpha}\,. \tag{4.69}$$

Let us consider the merger event that led to GW150914, using this radius as an approximate size for the black holes[17]. The frequency at which this waveform has maximum amplitude is around $f_{\rm GW} \sim 150Hz$, and the chirp mass of the black holes is inferred to be $M_c \sim 30M_\odot$ (assuming the two black holes are of equal mass, this corresponds to masses $m_1 \sim m_2 \sim 35\,M_\odot$) [361–364]. This value of $f_{\rm GW}$ is taken directly from the data, and does not require a particular theory of gravity in order to be determined. The value of M_c can be determined from the inspiral, and requires only weak gravity in order to be discovered. We therefore expect the orders of magnitude quoted here to be correct for both GR and 4DEGB.

Now, using a weak field analysis it can be shown that at the time of peak amplitude

[17] Rotation, and the perturbations due to the other black hole, will change this value, but we expect it be correct to an order of magnitude.

the two bodies have an orbital separation of

$$R = \left(\frac{m_1 + m_2}{\pi^2 f_{\rm GW}^2}\right)^{1/3} \sim 350km\,, \tag{4.70}$$

where the numerical value is obtained using the numbers above. In order to quantify the closeness of the two objects, relative to their natural gravitational radius, we introduce the compactness ratio:

$$\mathcal{R} = \frac{R}{r_H(m_1) + r_H(m_2)}. \tag{4.71}$$

Assuming both masses to be $m_i \sim 35 M_\odot$, and imposing $\mathcal{R} > 1$, so that the two black holes are not overlapping, we obtain a lower bound on negative values of the coupling parameter of $\alpha \gtrsim -10^{10}\,\mathrm{m}^2$. We can gain an upper bound on α by requiring that r_H is a real number. For this same black hole masses, this gives $\alpha \lesssim 10^9\,\mathrm{m}^2$. An order of magnitude estimate of the constraints that may be available from GW150914 is therefore

$$-10^{10}\,\mathrm{m}^2 \lesssim \alpha \lesssim 10^9\,\mathrm{m}^2\,. \tag{4.72}$$

This is among the tightest constraints we have found.

Of course, there are also many other gravitational wave events that could also be used for our current purpose, that have been detected since the discovery of GW150914. One of the more promising of these is GW170608 [365], which is the lowest mass binary black hole merger event that has been confirmed to date. Following through the same logic as above, this system could be expected to give the constraint $-10^{10}\,\mathrm{m}^2 \lesssim \alpha \lesssim 10^8\,\mathrm{m}^2$, which can be seen to be marginally tighter. If the sources of GW190814 are both confirmed to be black holes [366], this would give $\alpha \lesssim 10^7\,\mathrm{m}^2$. Combining constraints from multiple systems, or future events, may also improve on the constraining power of these observations.

We reiterate that this is only a rough estimate of the bounds that may be available from these systems, and that it may well be possible to gain significantly tighter constraints using a more thorough numerical relativity treatment. This will be a significant challenge to implement, however, and will be left for subsequent studies. In particular, as well as assuming the validity of weak-field treatments, we have neglected spin and assumed circular orbits. Such assumptions could be removed in proper numerical studies.

4.5.3 Table-Top Tests of Gravity

Due to the r^{-4} scaling of the extra terms that appear in the metric in 4DEGB, measurements of gravity on small scales offer the possibility of imposing tight constraints on the theory. Of particular interest in this regard are the so-called "tabletop" tests of gravity. These are gravitational physics experiments that seeks to directly measure gravitational effects in the laboratory, and which are the modern counterparts of the Cavendish experiment.

Tabletop tests of gravity most commonly test for deviations from the inverse square law by modelling extra gravitational forces as being due to an additional Yukawa-type potential. However, and of more relevance for our work, there have also been studies that look for additional power-law terms, of the form [367–369]

$$V = \frac{m_1 m_2}{r}\left(1 - \frac{A_n}{r^n}\right) , \tag{4.73}$$

where no sum is implied over n. Such a potential can be compared to Eq. (4.35), which gives

$$V \approx \frac{m_1 m_2}{r}\left[1 \mp \frac{2\,\alpha(m_1 + m_2)}{r^3}\right] , \tag{4.74}$$

where we have kept the additional term from 4DEGB and neglected all other post-Newtonian terms. It can be seen that Eqs. (4.73) and (4.74) give $A_3 = \pm 2\alpha\,(m_1 + m_2)$.

Now, the observational constraints from these experiments currently yield bounds of order $A_3 \lesssim 2.2 \times 10^{-14}\,\mathrm{m}^3$ [369], which from the above implies

$$|\alpha| \lesssim 10^{16}\,\mathrm{m}^2 , \tag{4.75}$$

where we have used a value of $\sim 1\mathrm{g}$ for the masses involved in the experiment.

This bound, while being one of the more promising we have found in this chapter, should be taken with a large pinch of salt. There are a number of reasons for this. Firstly, the experiments themselves do not involve two point-like masses, but are instead much more complicated set-ups. In particular, the study in Ref. [369] is based on a torsion balance in which one disk of metal with holes in is hung directly above two other disks with holes. The holes in these disks are the "masses", and the torque on the top disk is measured as the bottom disks rotate. A calculation involving multiple extended objects should therefore be performed to give more

precise results.

Secondly, the extra "potential" in Eq. (4.74) is a post-Newtonian term, rather than the Newtonian-level term. There is a gauge dependence on the 00 component of the metric at this level of accuracy, which introduces an extra degree of ambiguity, and which does not occur at the Newtonian level. This is not to say that this term does not affect the equations of motion of time-like objects in the same manner as a Newtonian potential (it does), but that one would need to make sure that the gauge choice that we used to calculate this metric corresponds to the coordinates used by the experimentalists in a sensible way, in order to make precise statements.

Giving thorough answers to the questions above would require a more detailed study of the experimental set-up that is used in Ref. [368, 369], which we leave for future work. Despite these issues, we nevertheless expect the bound in Eq. (4.75) to give a representative order of magnitude for what these experiments should be able to achieve. This is a bound that is competitive with those achievable from analyzing the orbit of Mercury, but is considerably weaker than those from the LAGEOS satellites and binary black hole systems.

4.5.4 Primordial Nucleosynthesis

If we take $C = 0$, then it can be seen from the Friedmann equation (4.58) that the size of corrections to the Hubble rate of standard cosmology is controlled by the combination αH^2, with the H^4 term in Eq. (4.58) becoming dominant if $\alpha H^2 \gg 1$. However, given that $H_0 \approx 2.4 \times 10^{-18}\,\mathrm{s}^{-1}$ at the present time, this suggests that a very large value of α would be required to make any noticable difference to the current rate of expansion of the Universe.

For example, for the correction term to be of order unity would require $\alpha \sim 10^{52}\,\mathrm{m}^2$. This means that any constraints from the recent expansion history of the universe, or from structure formation, are likely to be extremely weak. This is confirmed in Ref. [176], where structure formation in 4DEGB leads to the constraint $\alpha \lesssim 10^{50}\,\mathrm{m}^2$. To do better than this we must consider the evolution of the Universe at much earlier times.

An ideal environment for testing our theory is therefore the epoch of primordial nucleosynthesis, which occurred roughly between 10 seconds and 20 minutes after the big bang [370, 371]. The products of this period can be estimated by observing the abundance of the light elements in the Universe today, and can hence be used to constrain the rate of the Universe's expansion at energy levels of about 1 MeV, corresponding to $H^2 \approx 0.14\,\mathrm{s}^{-2}$.

A rough estimate of the constraints that can be imposed on the coupling parameter α can be achieved by requiring that the H^4 term in Eq. (4.58) does not dominate at the start of nucleosynthesis. This implies that

$$|\alpha| \lesssim 10^{18}\,\mathrm{m}^2\,. \tag{4.76}$$

To get a more precise result we can run the open source code PRIMAT[18] [372], with an appropriately modified expansion rate, to find the Helium mass fraction Y_P. Comparing the result of this to the observational bound $Y_P = 0.2449 \pm 0.0040$ [373] then gives $\alpha \lesssim 10^{17}\,\mathrm{m}^2$. Again, this bound is comparable to that which can be achieved using observations of the perihelion precession of Mercury, but is not as strong as those that can be found using LAGEOS.

4.5.5 Early Universe Inflation

At earlier times than primordial nucleosynthesis, and at higher energies, the physical processes that occurred in the Universe are less well understood. Nevertheless, the very early Universe is widely believed to have undergone a period of very rapid expansion, known as "inflation". It is during this epoch that the seeds of large-scale structure are believed to have been sown, and which therefore provides us with an opportunity to constrain α using processes that occurred at very early times, when the correction term in Eq. (4.58) may become more significant.

First, it is important to note that Eq. (4.58) in combination with the energy conservation equation, which is unchanged in this theory, indicates that $\dot{H}$ can become infinite at a finite value of the scale factor for negative values of α. This occurs when $\Gamma = 0$ and implies that there is an upper limit on H given by $H^2 = 1/(-2\alpha)$. If inflation takes place above the TeV scale, which is consistent with the lack of new physics at the LHC and also the need for Baryogenesis, we can turn this upper limit into the constraint $\alpha \gtrsim -10^{-6}\,\mathrm{m}^2$, which would be an extremely tight constraint. Now let us see if anything can be said concerning positive values of α.

Inflation occurs when $\epsilon \equiv -\dot{H}/H^2 < 1$. If we consider the matter content of the Universe during this period to be well modelled by a scalar field ϕ in a potential

[18] http://www2.iap.fr/users/pitrou/primat.htm

$V(\phi)$, then this translates to the condition[19]

$$\frac{2V'^2\alpha^2}{9m_{\rm pl}^2\Gamma_V(\Gamma_V-1)^2} \lesssim 1\,, \tag{4.77}$$

where $\Gamma_V = \sqrt{1+4V\alpha/(3m_{\rm pl}^2)}$, and where a dash indicates a derivative with respect to ϕ. This result implies that inflation is harder to achieve in 4DEGB than it is in GR, and that the slope of the potential (i.e. V'/V) must be shallower. However, we can always tailor the form of $V(\phi)$ in order to allow inflation to still proceed.

Let us now turn to the production of perturbations during inflation. The action for tensor perturbations in 4DEGB is given by

$$S_T = \frac{1}{2}\int d^3x\, dt\, a^3\,\Gamma\left(\dot{h}^2 - c_T^2\frac{(\partial h)^2}{a^2}\right)\,, \tag{4.78}$$

where h is the amplitude of either of the two gravitational wave polarizations, $c_T^2 = 1+\dot{\Gamma}/(H\Gamma)$ is the speed of propagation, and $\Gamma = 1+2\alpha H^2$ (i.e. we are again setting $C=0$, for convenience). The evolution of the uniform density curvature perturbation ζ follows from the action

$$S_\zeta = \frac{1}{2}\int d^3x\, dt\, a^3\Gamma\epsilon\left(\dot{\zeta}^2 - \frac{(\partial\zeta)^2}{a^2}\right)\,. \tag{4.79}$$

These equations imply that both the curvature and tensorial perturbations are conserved on super-horizon scales, when the wavenumber obeys $k > aH$.

Equations (4.78) and (4.79) allow the spectra of tensor and scalar perturbations to be calculated in the usual way, in terms of quantities at the time a given k crosses the apparent horizon, which results in

$$P_T = \frac{2}{\pi^2 m_{\rm pl}^2}\frac{H^2}{\Gamma}\bigg|_* \qquad \text{and} \qquad P_\zeta = \frac{1}{8\pi^2 m_{\rm pl}^2}\frac{H^2}{\epsilon\Gamma}\bigg|_*\,, \tag{4.80}$$

where the asterisk indicates quantities are to be evaluated at horizon crossing.

As already discussed in Ref. [151], these expressions imply that the tensor-to-scalar ratio takes its usual form $r = 16\epsilon$, while differentiating the power spectra with respect to horizon crossing scale $k = aH$ gives the spectral indices at leading-

[19] The reader will note that we have switched to Planck units here, as this is standard choice in this area of physics.

order in slow roll as

$$\frac{\partial \log P_\zeta}{\partial \log(aH)} = n_s - 1 = -2\epsilon - \dot{\epsilon}/(\epsilon H) - \dot{\Gamma}/(\Gamma H)\,,$$
$$\frac{\partial \log P_T}{\partial \log(aH)} = n_T = -2\epsilon - \dot{\Gamma}/(\Gamma H)\,. \tag{4.81}$$

It is clear that $n_T \neq -r/8$, meaning that the consistency equation of canonical single field inflation is violated. The form of n_s is also different from its canonical form, but even when $\alpha H^2 \gg 1$ it seems it should still be possible to choose a $V(\phi)$ that meets the tight observational constraints on this quantity [21].

We conclude that although both the background dynamics and the spectra of perturbations are different from their canonical form, there does not appear to be any compelling reason why inflation in 4DEGB should not be considered consistent with current observations for any positive value of α (assuming we are otherwise free to choose the shape of the inflationary potential). This may change in the future, when the spectrum of primordial gravitational waves is observed, and the consistency condition can be tested. It may also change when higher-order correlations are calculated, but we leave calculations of such quantities for future work.

Our results are summarized in Table 4.1.

Observation	Upper bound on $\lvert\alpha\rvert/\mathrm{m}^2$	Data source
GW observations	$\sim 10^8 *$	Ref. [362]
LAGEOS satellites	10^{10}	Ref. [340]
Double Pulsar	$\sim 10^{15}$	Ref. [345]
Tabletop experiment	$\sim 10^{16}$	Ref. [368]
Orbit of Mercury	10^{17}	Ref. [338]
Primordial nucleosynthesis	10^{18}	Ref. [373]
Orbits around Sgr A^*	10^{25}	Ref. [341]
Event Horizon Telescope	$\sim 10^{26} *$	Ref. [348]
Speed of GWs	10^{36}	Ref. [348]
Gravitational lensing	–	
Shapiro time delay	–	
Early Universe inflation	$- *$	

Table 4.1: A summary of the order-of-magnitude constraints available on $\lvert\alpha\rvert/\mathrm{m}^2$ for the various different observables considered in this chapter, ordered by stringency. A dash indicates no constraint, a $\sim$ indicates that constraints are indicative (due to simplifying assumptions), and a $*$ indicates that asymmetric bounds are available on positive and negative values of α (the weaker of the two are shown here).

Appendix

Appendix 4.A Calculating $\Phi_{\mathcal{G}}$

Here we wish to calculate the form of $\Phi_{\mathcal{G}}$ for a system of N bodies with energy density given by Eq. (4.24). We start by defining a general potential $\mathcal{V}$ sourced by a field X:

$$\mathcal{V}(X) = \int \frac{X'}{|\mathbf{x} - \mathbf{x}'|} d^3x' \,. \tag{4.82}$$

If we use the identity

$$U_{,ij}U_{,ij} = \frac{1}{2}\nabla^2|\nabla U|^2 + 4\pi\nabla\rho\cdot\nabla U \,,$$

then we can use $\Phi_{\mathcal{G}} = \mathcal{V}(\mathcal{G})$ to write

$$\begin{aligned}\Phi_{\mathcal{G}} =& 8\mathcal{V}(U_{,ij}U_{,ij}) - 8\mathcal{V}((\nabla^2 U)^2) \\ =& 4\mathcal{V}(\nabla^2|\nabla U|^2) + 32\pi\mathcal{V}(\nabla\rho\cdot\nabla U) - 8(4\pi)^2\mathcal{V}(\rho^2)\,.\end{aligned}$$

Now $\mathcal{V}(\nabla^2|\nabla U|^2) = -4\pi|\nabla U|^2$, and we can write

$$\mathcal{V}(\nabla\rho\cdot\nabla U) = 4\pi\mathcal{V}(\rho^2) + \psi_1 \,,$$

where we have discarded a surface term and where

$$\psi_1 = \int \frac{\rho'\rho''(\mathbf{x}-\mathbf{x}')\cdot(\mathbf{x}'-\mathbf{x}'')}{|\mathbf{x}-\mathbf{x}'|^3|\mathbf{x}'-\mathbf{x}''|^3} d^3x' d^3x'' \,. \tag{4.83}$$

This all gives

$$\Phi_{\mathcal{G}} = -32\pi\left(\frac{1}{2}|\nabla U|^2 - \psi_1\right) \,, \tag{4.84}$$

which on substituting for $\tilde{\mu}$ from (4.24) into the relevant expressions for U and ψ_1 gives Eqs. (4.33) and (4.34), once divergent terms are neglected.

5 A Generalized Conformally Coupled Scalar Field

Closed-form solutions of the gravitational field equations allow for a simple inspection of the spacetime and calculation of observable predictions. However, modified theories with new fundamental fields typically present field equations with increased complexity such that these calculations become analytically impossible. One is then typically forced to resort either to perturbation theory, which is not well-justified in the extreme gravity regime, or to challenging numerical techniques.

The structure of the regularized theories described above is highly non-trivial, comprising a representative of each one of the Horndeski terms, and yet they possess an extremely simple field equation (2.57) that completely decouples from the scalar field, and which therefore allows for simple closed-form solutions. One is then left to wonder about the relationship that connects these threads, and why it should be that a special combination of the field equations completely decouples from the scalar field. This problem was addressed in Ref. [4].

When a seemingly complicated problem has a simple solution, one typically suspects that there is a hidden symmetry in the problem. For example, the Einstein equations with a matter source possessing conformal invariance are greatly simplified since the theory has constant scalar curvature on-shell, restricting the possible spacetimes and allowing for closed-form solutions to be easily found. An example of a theory with conformally invariant matter sources leading to simple solutions is precisely electrovacuum (GR in the presence of an electromagnetic field), whose Reissner-Nordström (Kerr-Newman) solution was the first ever discovered static (spinning) black hole with a matter source. One more example is gravity with a conformally coupled scalar field, whose matter action enjoys conformal invariance and is of the well-known form

$$\int d^4x\sqrt{-g}\left(\frac{R}{6}\Phi^2+(\nabla\Phi)^2\right). \tag{5.1}$$

The first counter-example to the no-hair theorems (see e.g. Ref. [42] for a review)

was found precisely as a solution of this theory, the much-debated static BBMB black hole [374–376]. Due to its compelling properties, gravity with a conformal scalar field and its solutions have been extensively studied throughout the years (see e.g. Refs. [377–386] and references therein).

We note that in all the above examples the Einstein-Hilbert term explicitly breaks the conformal invariance of the full theory – a remnant of this symmetry is only observed in the matter field equations of motion, such as the Maxwell equations or the modified Klein-Gordon equation resulting from the action (5.1)

$$\Box\Phi - \frac{R}{6}\Phi = 0. \tag{5.2}$$

This suggests that the simplification of the equations of motion that was previously mentioned might in fact be related to the conformal symmetry of the matter field equations and not of the action. Then, extended theories with the same effective symmetries might exist if conformal invariance is required solely in the matter field equation and not necessarily in the matter action. As we show below resorting to the example of a scalar field, the conformally coupled theory presented in Eq. (5.1) can be extended in a natural way by incorporating a scalar-Gauss-Bonnet sector while preserving all of its effective symmetries. The extended theory presents field equations with a remarkable simplification that allows for simple closed-form black hole solutions and cosmologies, providing a framework to capture the essence of (scalar-)Gauss-Bonnet quadratic corrections to gravity in four-dimensions with analytical studies. This Gauss-Bonnet sector will be shown to be intimately tied to the scalar-tensor versions of regularized 4DEGB presented in the preceding sections.

5.1 Gravity with a generalized conformal scalar field

As before, we denote with a tilde quantities constructed from the conformal geometry

$$\tilde{g}_{\mu\nu} = e^{2\phi} g_{\mu\nu}, \tag{5.3}$$

which transforms as a metric under diffeomorphisms and is conformally invariant, with conformal transformations acting as[20]

$$g_{\mu\nu} \to e^{2\sigma} g_{\mu\nu}, \qquad \phi \to \phi - \sigma, \tag{5.4}$$

where $\sigma \equiv \sigma(x)$ depends on the spacetime point. For convenience, we work with exponential conformal factors.

A remarkable property holds for scalar-tensor theories with a conformally invariant scalar field equation. Consider the transformation of Eq. (5.4) in its infinitesimal form, such that $\delta_\sigma g_{\mu\nu} = 2\sigma g_{\mu\nu}$ and $\delta_\sigma \phi = -\sigma$, where δ_σ denotes the change under an infinitesimal conformal transformation. In this case, an action describing a theory that depends solely on the metric $g_{\mu\nu}$ and a scalar field ϕ, $S[\phi, g]$, varies by an amount

$$\begin{aligned} \delta_\sigma S &= \int d^4x \left(\frac{\delta S[\phi,g]}{\delta g_{\mu\nu}} \delta_\sigma g_{\mu\nu} + \frac{\delta S[\phi,g]}{\delta \phi} \delta_\sigma \phi \right) \\ &= -\int d^4x \left(-2 g_{\mu\nu} \frac{\delta S[\phi,g]}{\delta g_{\mu\nu}} + \frac{\delta S[\phi,g]}{\delta \phi} \right) \sigma, \end{aligned} \tag{5.5}$$

where we identify the first and second terms in brackets with the trace and the scalar field equations, respectively. The transformed action is then $S \to S + \delta_\sigma S$. Now, if the scalar field equation is conformally invariant, then $\delta_\sigma S$ should be independent of ϕ, such that the transformed action contains exactly the same scalar field content as the original one, resulting in the same scalar field equation. Thus, the quantity in brackets inside Eq. (5.5)

$$-2 g_{\mu\nu} \frac{\delta S[\phi,g]}{\delta g_{\mu\nu}} + \frac{\delta S[\phi,g]}{\delta \phi}, \tag{5.6}$$

should be a purely geometric quantity constructed only out of the metric $g_{\mu\nu}$. In short, a theory whose scalar field equation is conformally invariant, and not the scalar-field action necessarily, will possess a purely geometrical field equation given by the sum of the trace and scalar field equations. This equation can be, in principle, more general than a constant scalar curvature condition and, at the same time, restrict the allowed spacetimes possibly providing an easy path to find closed-form solutions.

[20] The transformation of Eq. (5.4) is in fact a Weyl transformation, but we refer to it as a conformal transformation to be consistent with typical terminology.

5.1.1 Deriving the theory

Our goal now is to derive the most general scalar-tensor theory with second-order equations of motion and a conformally invariant scalar field equation. To that end, we note that the derivatives of $\tilde{g}_{\mu\nu}$ are conformally invariant and so should the curvature scalars constructed from it. In fact, we remark that scalar quantities constructed solely from the tilded metric are the only conformally invariant scalar quantities that depend on only of the metric $g_{\mu\nu}$ and the scalar field ϕ. The proof is similar to the one used in Ref. [380] to construct the most general conformally invariant scalar-tensor action in four-dimensions, and is outlined next.

Let $\mathcal{I}[\phi, g]$ denote a scalar quantity that depends on the scalar field and the metric $g_{\mu\nu}$. Under a conformal transformation we obtain

$$\mathcal{I}[\phi, g] \to \mathcal{I}[\phi - \sigma, e^{2\sigma} g].$$

Imposing conformal invariance, and choosing $\sigma = \phi$, we obtain $\mathcal{I}[\phi, g] = \mathcal{I}[0, \tilde{g}]$. Thus, the only conformally invariant scalar quantities that depend only on the scalar field ϕ and the metric $g_{\mu\nu}$ are purely geometric scalar quantities built out of the tilded geometry given in Eq. (5.3), $\mathcal{I}[0, \tilde{g}]$. Therefore, in order for a theory to have a conformally invariant scalar field equation, the relation

$$\frac{\delta S[\phi, g]}{\delta \phi} = \sqrt{-\tilde{g}} \mathcal{I}[0, \tilde{g}], \tag{5.7}$$

should hold. This will be our starting point to derive the sought theory of gravity with a generalized conformal scalar field. The reader will note that $\mathcal{I}[0, \tilde{g}]$ is yet unspecified. We will come back to that in a minute.

We will integrate Eq. (5.7) to obtain an action functional whose scalar field variation leads to a conformally invariant equation. The procedure to do so is similar to the one to reconstruct a function of several variables from its partial derivatives and is outlined next, following Ref. [387, Section 9.7] closely. First, choose a configuration ϕ_c for the scalar field (typically taken to be zero) and a path $\phi(\eta)$ with $0 \leq \eta \leq 1$, that begins at the reference point $\phi(0) = \phi_c$ and leads to the desired final point $\phi(1) = \phi$. If an action $S[\phi, g]$ exists, then the construction will give the same result for any choice of the path. It is convenient to take a straight line path

$$\phi(\eta) = \eta\phi + (1 - \eta)\phi_c.$$

Consider now the action $S[\phi(\eta), g]$ evaluated along the path. We take its derivative

with respect to η obtaining

$$\frac{dS[\phi(\eta),g]}{d\eta} = \int d^4x \frac{\delta S[\phi(\eta),g]}{\delta\phi(\eta)} \frac{d\phi(\eta)}{d\eta}.$$

Integrating from $\eta = 0$ to $\eta = 1$ we can obtain the sought action up to an integration constant functional independent of the scalar $S_c[0,g]$, and taking $\phi_c = 0$, we obtain

$$S[\phi,g] = \int d^4x \int_0^1 d\eta \left.\frac{\delta S[\phi,g]}{\delta\phi}\right|_{\phi\to\eta\phi} \phi + S_c[0,g]. \tag{5.8}$$

Let us review our progress so far. Our goal is to derive the most general subset of the Horndeski family of theories whose scalar field equation of motion is conformally invariant. We have shown that such theory will necessarily contain a purely geometric field equation that may provide an easy path to obtain closed-form solutions. Next we demonstrated that a conformally invariant scalar field equation must obey Eq. (5.7). Finally, we outlined a procedure to obtain the action functional that describes the theory, starting from the conformally invariant scalar field equation (5.7). Obtaining the action that describes the sought theory then amounts to computing and simplifying Eq. (5.8).

To work out which quantities $\mathcal{I}[0,\tilde{g}]$ are suitable for Eq. (5.7), leading to an action made out only of ϕ and $g_{\mu\nu}$ whose equations of motion are second-order, we note the following. The quantity $\sqrt{-\tilde{g}}\mathcal{I}[0,\tilde{g}]$, once expressed in terms of $g_{\mu\nu}$ and ϕ inside Eq. (5.8), reveals that the action contains a term of the form

$$S[\phi,g] \supseteq \int d^4x\sqrt{-g}\int_0^1 d\eta\, e^{(4-2k)\eta\phi}\phi\mathcal{I}[0,g],$$

with k a constant related to the power of $\mathcal{I}[0,g]$ on the curvature (see e.g. Refs. [297, 298] for a review of useful conformal transformations). As a result, the theory will necessarily contain non-minimal couplings of the scalar field to the geometric quantity $\mathcal{I}[0,g]$. Then, making use of Horndeski's theorem [104, 105], the only scalar geometric quantity that can enter Eq. (5.7) without spoiling the requirement of second-order field equations is a linear combination of the form

$$\mathcal{I}[0,\tilde{g}] = -8\lambda - 2\beta\tilde{R} - \alpha\tilde{\mathcal{G}}, \tag{5.9}$$

where λ, β and α are constants and $\mathcal{G}$ is the Gauss-Bonnet term.

We will derive the effective action associated with each of the constituents of $\mathcal{I}[0,\tilde{g}]$ (i.e., the action whose scalar field variation leads to the respective constituent). To

that end, given the conformal geometry of Eq. (5.3), recall that we have the following useful relations in four dimensions [297, 298]

$$\begin{aligned}
&\sqrt{-\tilde{g}} = \sqrt{-g}e^{4\phi}, \\
&\tilde{R} = e^{-2\phi}\left(R - 6\Box\phi - 6\left(\nabla\phi\right)^2\right), \\
&\tilde{\mathcal{G}} = e^{-4\phi}\Big[\mathcal{G} - 8R^{\mu\nu}\nabla_\mu\phi\nabla_\nu\phi + 8G^{\mu\nu}\nabla_\mu\nabla_\nu\phi + 8\Box\phi\left(\nabla\phi\right)^2 - 8\left(\nabla_\mu\nabla_\nu\phi\right)^2 \\
&+ 8\left(\Box\phi\right)^2 + 16\left(\nabla_\mu\phi\nabla_\nu\phi\right)\left(\nabla^\mu\nabla^\nu\phi\right)\Big].
\end{aligned} \tag{5.10}$$

In what follows, we resort to integration by parts, discard boundary terms and in the last steps absorb purely geometric terms built out of $g_{\mu\nu}$ into $S_c[0,g]$, as they have no effect in the scalar field equation. Starting with the effective action associated with λ we use Eq. (5.8) obtaining,

$$S_\lambda[\phi,g] = -8\lambda\int d^4x\sqrt{-g}\int_0^1 d\eta\; e^{4\phi\eta}\phi + S_c[0,g] = -2\lambda\int d^4x\sqrt{-g}e^{4\phi}. \tag{5.11}$$

Following the same procedure for the part of the total action associated with the conformal Ricci scalar

$$\begin{aligned}
S_{\tilde{R}}[\phi,g] &= -2\beta\int d^4x\sqrt{-g}\int_0^1 d\eta\; e^{2\phi\eta}\left(R - 6\eta\Box\phi - 6\eta^2\left(\nabla\phi\right)^2\right)\phi + S_c[0,g] \\
&= -2\beta\int d^4x\sqrt{-g}\Bigg(\frac{e^{2\phi}R - R}{2} - 3\Box\phi\left(e^{2\phi} + \frac{1-e^{2\phi}}{2\phi}\right) \\
&- \frac{3\left(\nabla\phi\right)^2}{2\phi^2}\left(e^{2\phi} - 2\phi e^{2\phi} + 2\phi^2e^{2\phi} - 1\right)\Bigg) + S_c[0,g] \\
&= -\beta\int d^4x\sqrt{-g}e^{2\phi}\left(R + 6\left(\nabla\phi\right)^2\right).
\end{aligned} \tag{5.12}$$

The process to obtain the action associated with the Gauss-Bonnet term is similar, and the following relations might prove useful:

$$\nabla_\mu\left(\Box\phi\nabla^\mu\phi - \frac{1}{2}\nabla^\mu\left(\nabla\phi\right)^2\right) = \left(\Box\phi\right)^2 - \left(\nabla_\mu\nabla_\nu\phi\right)^2 - R^{\mu\nu}\nabla_\mu\phi\nabla_\nu\phi,$$

$$\int d^4x\sqrt{-g}\phi\nabla_\mu\phi\nabla_\nu\phi\nabla^\mu\nabla^\nu\phi = -\frac{1}{2}\int d^4x\sqrt{-g}\left(\left(\nabla\phi\right)^4 + \phi\Box\phi\left(\nabla\phi\right)^2\right) + \text{boundary terms}.$$

Then we obtain for the Gauss-Bonnet-related part of the action

$$\begin{aligned}
S_{\tilde{\mathcal{G}}}[\phi,g] &= -\alpha\int d^4x\sqrt{-g}\int_0^1 d\eta\Big[\mathcal{G}-8\eta^2R^{\mu\nu}\nabla_\mu\phi\nabla_\nu\phi+8\eta G^{\mu\nu}\nabla_\mu\nabla_\nu\phi\\
&\quad+8\eta^3\Box\phi\left(\nabla\phi\right)^2-8\eta^2\left(\nabla_\mu\nabla_\nu\phi\right)^2\\
&\quad+8\eta^2\left(\Box\phi\right)^2+16\eta^3\left(\nabla_\mu\phi\nabla_\nu\phi\right)\left(\nabla^\mu\nabla^\nu\phi\right)\Big]\phi+S_c[0,g]\\
&= -\alpha\int d^4x\sqrt{-g}\Big[\phi\mathcal{G}+4\phi G^{\mu\nu}\nabla_\mu\nabla_\nu\phi+2\phi\Box\phi\left(\nabla\phi\right)^2+4\phi\nabla_\mu\phi\nabla_\nu\phi\nabla^\mu\nabla^\nu\phi\\
&\quad+\frac{8}{3}\phi\big((\Box\phi)^2-(\nabla_\mu\nabla_\nu\phi)^2-R^{\mu\nu}\nabla_\mu\phi\nabla_\nu\phi\big)\Big]+S_c[0,g]\\
&= -\alpha\int d^4x\sqrt{-g}\Big[\phi\mathcal{G}-4G^{\mu\nu}\nabla_\mu\phi\nabla_\nu\phi-4\Box\phi\left(\nabla\phi\right)^2-2(\nabla\phi)^4\Big].
\end{aligned}\tag{5.13}$$

The final combined action can be obtained by summing all contributions, together with the Einstein-Hilbert term with a cosmological constant Λ that does not affect the scalar field equation

$$\begin{aligned}
S &= \frac{1}{16\pi G}\left[\int d^4x\sqrt{-g}\left(R-2\Lambda\right)+S_\lambda+S_{\tilde{R}}+S_{\tilde{\mathcal{G}}}\right]\\
&= \int\frac{d^4x\sqrt{-g}}{16\pi G}\Big[R-2\Lambda-\beta e^{2\phi}\left(R+6(\nabla\phi)^2\right)-2\lambda e^{4\phi}\\
&\quad-\alpha\Big(\phi\mathcal{G}-4G^{\mu\nu}\nabla_\mu\phi\nabla_\nu\phi-4\Box\phi(\nabla\phi)^2-2(\nabla\phi)^4\Big)\Big].
\end{aligned}\tag{5.14}$$

The action given above in Eq. (5.14) describes, up to field redefinitions, the most general scalar-tensor theory whose scalar field variation leads to a conformally invariant equation. It belongs to the Horndeski class with functions [21]

$$\begin{aligned}
&G_2=-2\Lambda-2\lambda e^{4\phi}+12\beta e^{2\phi}X+8\alpha X^2,\quad G_3=8\alpha X,\\
&G_4=1-\beta e^{2\phi}+4\alpha X,\quad G_5=4\alpha\log|X|,
\end{aligned}\tag{5.15}$$

where $X=-\frac{1}{2}\left(\nabla\phi\right)^2$. The field equations are obtained by varying with respect to the metric

$$G_{\mu\nu}+\Lambda g_{\mu\nu}=-\alpha\mathcal{H}_{\mu\nu}+\beta e^{2\phi}\mathcal{A}_{\mu\nu}-\lambda e^{4\phi}g_{\mu\nu},\tag{5.16}$$

where $\mathcal{H}_{\mu\nu}$ and $\mathcal{A}_{\mu\nu}$ have been defined previously in Eqs. (2.53) and (2.68), respectively. The scalar field equation resulting from the action (5.14) is equivalent to the

[21] Here we marginalized over the $1/16\pi G$ overall factor in the action.

vanishing of the quantity presented in Eq. (5.9)

$$\beta\tilde{R} + \frac{\alpha}{2}\tilde{\mathcal{G}} + 4\lambda = 0, \tag{5.17}$$

where the tilded quantities are defined in Eq. (5.10) in terms of $g_{\mu\nu}$ and ϕ. Interestingly, the purely geometric combination (5.6) results in the familiar condition

$$R + \frac{\alpha}{2}\mathcal{G} - 4\Lambda = 0. \tag{5.18}$$

The action described in Eq. (5.14) can be cast into a more familiar form via the field redefinition $\Phi = e^{\phi}$

$$\begin{aligned} S = \int \frac{d^4x\sqrt{-g}}{16\pi G}\Bigg[& R - 2\Lambda - 6\beta\left(\frac{R}{6}\Phi^2 + (\nabla\Phi)^2\right) - 2\lambda\Phi^4 \\ & - \alpha\left(\log(\Phi)\mathcal{G} - \frac{4G^{\mu\nu}\nabla_\mu\Phi\nabla_\nu\Phi}{\Phi^2} - \frac{4\Box\Phi(\nabla\Phi)^2}{\Phi^3} + \frac{2(\nabla\Phi)^4}{\Phi^4}\right)\Bigg], \end{aligned} \tag{5.19}$$

where we note the emergence of the usual conformally coupled scalar field action (5.1) with a conformally invariant quartic potential. Observe that the action is invariant under the $\mathbb{Z}_2$ symmetry $\Phi \to -\Phi$.

5.1.2 Connection with the regularized 4DEGB theories

By comparing the action in Eq. (5.14) with the Kaluza-Klein regularized theory presented in (2.66) (ignoring overall factors and the cosmological term), we observe that they are equivalent by taking

$$\beta = 2\lambda_{KK}\alpha, \qquad \lambda = 3\lambda_{KK}^2\alpha, \tag{5.20}$$

where we denoted the constant λ appearing in the Kaluza-Klein regularized theory (2.66) as λ_{KK} to avoid confusion with the λ appearing in Eq. (5.14). As a corollary, the counter-term regularized theory in Eq. (2.50) follows by taking $\beta = \lambda = 0$ in Eq. (5.14). Therefore, all the regularized 4DEGB scalar-tensor theories presented, and studied, in previous sections are subsets of a more general theory given in Eq. (5.14) (or in Eq. (5.19) upon a field redefinition). Note that Eq. (5.20) implies the relation $\lambda = \frac{3\beta^2}{4\alpha}$. This relation will recurrently appear when studying solutions to the theory.

5.2 Static black hole solutions

In this section we seek to obtain black hole solutions of the theory given in Eq. (5.19), where we employ the static and spherically symmetric line element

$$ds^2 = -f(r)\,dt^2 + \frac{dr^2}{f(r)} + r^2(d\theta^2 + \sin^2\theta\,d\varphi^2). \tag{5.21}$$

If $\alpha = 0$, the known solutions of the usual conformally coupled theory, such as the BBMB black hole, can be obtained. We are interested in the non-vanishing α case (furthermore, we assume $\beta \neq 0$). For the sake of completeness, we supplement the theory with the Maxwell action

$$S_{EM} = -\frac{1}{4}\int d^4x\sqrt{-g}F^{\mu\nu}F_{\mu\nu}, \tag{5.22}$$

where $F_{\mu\nu} = \partial_\mu A_\nu - \partial_\nu A_\mu$ is the Maxwell tensor and the subscript "EM" stands for *electromagnetic*. The associated (traceless) stress-energy tensor $T^{(EM)}_{\mu\nu}$ is

$$T^{(EM)}_{\mu\nu} = F_{\mu\sigma}F_{\nu}{}^{\sigma} - \frac{1}{4}g_{\mu\nu}F_{\rho\sigma}F^{\rho\sigma}, \tag{5.23}$$

while the Maxwell equations are

$$\nabla_\mu F^{\mu\nu} = 0. \tag{5.24}$$

Given the line element of Eq. (5.21), we assume a four-potential

$$A = V(r)\,dt - \frac{Q_m}{4\pi}\cos\theta\,d\varphi, \tag{5.25}$$

with Q_m the magnetic charge. The Maxwell equations imply

$$V(r) = -\frac{Q_e}{4\pi r} - \Psi_e,$$

with Q_e the electric charge and Ψ_e the electrostatic potential. For future convenience we define

$$\mathcal{Q}^2 = \frac{Q_e^2 + Q_m^2}{4\pi}. \tag{5.26}$$

Because any valid black hole solution must solve the geometric equation given in Eq. (2.57), that for the line element (5.21) takes the remarkably simple form

$$r^{-2}\left[(1-f)\left(r^2 + \alpha(1-f)\right)\right]'' - 4\Lambda = 0, \tag{5.27}$$

with the prime denoting a radial derivative, a solution is easily integrated to be of the type

$$f(r) = 1 + \frac{r^2}{2\alpha}\left[1 \pm \sqrt{1 + 4\alpha\left(\frac{2GM}{r^3} - \frac{q}{r^4} + \frac{\Lambda}{3}\right)}\right], \tag{5.28}$$

for any two integration constants M (interpreted as the ADM mass) and q. The metric function with the plus sign before the square-root does not present a well-defined limit as $\alpha \to 0$, and has a non-physical asymptotic behavior near spatial infinity, so we disregard it as the physical one. A black hole described by the line element (5.21) with $f(r)$ given in Eq. (5.28) has, in the absence of the cosmological constant, horizons located at

$$r_\pm = GM \pm \sqrt{G^2M^2 - \alpha - q}, \tag{5.29}$$

and is asymptotically flat.

Now, a suitable linear combination of the tt and rr Einstein equations factorizes into a condition equivalent to

$$\left(\frac{\Phi'}{\Phi^2}\right)'\left(f\Phi'\left(r^2\Phi\right)' + (f-1)\Phi^2 - \frac{\beta}{2\alpha}r^2\Phi^4\right) = 0. \tag{5.30}$$

That allows three distinct branches[22]

$$\begin{aligned}
&(1) \quad \Phi = \frac{c_1}{r + c_2}, \\
&(2) \quad \Phi = \frac{2\sqrt{2\alpha\kappa/\beta}}{r}\frac{\psi}{\psi^2 - \kappa}, \quad \text{where} \quad \psi \equiv \exp\left(\int^r \frac{1}{r\sqrt{f}}\right), \\
&(3) \quad \Phi = c_4,
\end{aligned} \tag{5.31}$$

where the c_i and κ are integration constants. We will analyze each situation in turn.

For the first scalar field profile, the remaining field equations allow a static black hole solution with $f(r)$ given by Eq. (5.28) with

$$q = G\mathcal{Q}^2 - 2\alpha, \quad c_1 = \sqrt{-2\alpha/\beta}, \quad c_2 = 0,$$

if $\lambda = \beta^2/4\alpha$, where $\mathcal{Q}$ is defined in Eq. (5.26).

Assuming the second scalar field profile, the remaining field equations are solved with the metric function of Eq. (5.28) provided that $q = G\mathcal{Q}^2$ as long as $\lambda = 3\beta^2/4\alpha$.

[22] Actually there are only two branches, as branches (1) and (3) belong to the same class $\Phi = \frac{1}{Ar+B}$, for suitably chosen constants A and B. However, we chose to discuss them separately.

We note that the scalar field has a free parameter, κ, that is not constrained by the field equations and so the scalar hair is, in a sense, primary. In all cases, the scalar field can be made regular on and outside the event horizon. In particular, if $\alpha/\beta > 0$, the scalar field is regular everywhere if $0 < \kappa < 1$, and if $\alpha/\beta < 0$, there are no divergences and the scalar field is real if $\kappa < 0$.[23]

We remark that, in the absence of the electromagnetic field, a close inspection of the field equations (5.16) reveals the existence of a *critical solution* with constant scalar field (third profile)

$$\Phi = c_4 = \sqrt{1/\beta},$$

as long as $\lambda = -\Lambda\beta^2$. In this extreme situation the Einstein equations (5.16) become an identity, and we have left to solve only the purely geometrical condition of Eq. (2.57), whose general solution is given by Eq. (5.28) with unconstrained q. We don't expect this solution to be physically relevant.

A feature of the black holes here discussed is that they present an entropy $\mathcal{S}$, equal to the well-known Bekenstein-Hawking area term with a logarithmic correction

$$\mathcal{S} = \frac{A_+}{4G} + \frac{2\pi\alpha}{G}\log\left(\frac{A_+}{A_0}\right), \tag{5.32}$$

as was the case in the scalar-tensor regularized 4DEGB theories.

5.3 FLRW Cosmology

In order to briefly study the cosmologies of the theory described by the action (5.19) we employ a FLRW background

$$ds^2 = -dt^2 + a(t)^2\left(\frac{dr^2}{1-kr^2} + r^2 d\theta^2 + r^2\sin^2\theta d\varphi^2\right), \tag{5.33}$$

and supplement the theory with matter content that has stress-energy tensor $T^{\mu}{}_{\nu} = \mathrm{diag}\,(-\rho, p, p, p)$, where ρ and p are the energy density and pressure of the matter fields, respectively. We assume all quantities are homogeneous and isotropic functions of cosmological time. The values $k = \{-1, 0, 1\}$ correspond respectively to a negatively, flat, and positively curved Universe.

For a flat ($k = 0$) FLRW metric, it can be shown that the scalar field equation of

[23] Note that $\psi \geq 1$ as the integrand inside the exponential is always positive.

motion (5.17) can be solved with a scalar field given by

$$\Phi = \frac{1}{a}\sqrt{\frac{3\beta}{2\lambda}\left(\pm\sqrt{1-\frac{4\alpha\lambda}{3\beta^2}}-1\right)}\left(\gamma+\int^t\frac{dt}{a}\right)^{-1}, \tag{5.34}$$

where γ is an arbitrary integration constant. This profile, when substituted in the Einstein equations (5.16), results in a set of modified Friedmann equations that take the form

$$\begin{aligned} H^2+\alpha H^4 &= \frac{8\pi G}{3}\rho+\frac{\Lambda}{3}, \\ \dot{H} &= -\frac{4\pi G(\rho+p)}{1+2\alpha H^2}, \end{aligned} \tag{5.35}$$

where $H = \dot{a}/a$ is again the Hubble rate (the dot denotes a temporal derivative) and the matter fields obey the continuity equation $\dot{\rho}+3H(\rho+p)=0$. These are the same Friedmann equations as the ones that result from the regularized 4DEGB theories, that we have studied in more detail in previous sections.

We now consider the curved ($k \neq 0$) FLRW cases. The scalar field equation is solved by the following profile

$$\Phi = \frac{1}{a}\sqrt{\frac{6\gamma\beta k}{\lambda}\left(\pm\sqrt{1-\frac{4\alpha\lambda}{3\beta^2}}-1\right)}\frac{\psi}{\psi^2+\gamma}, \quad \text{where} \quad \psi \equiv \exp\left(\sqrt{-k}\int^t\frac{dt}{a}\right) \tag{5.36}$$

with γ an arbitrary integration constant. This profile, when substituted in the Einstein equations (5.16), results in a set of modified Friedmann equations that are again equivalent to those of the regularized 4DEGB approaches

$$\begin{aligned} H^2+\frac{k}{a^2}+\alpha\left(H^2+\frac{k}{a^2}\right)^2 &= \frac{8\pi G}{3}\rho+\frac{\Lambda}{3}, \\ \dot{H} &= -\frac{4\pi G(\rho+p)}{1+2\alpha\left(H^2+\frac{k}{a^2}\right)}+\frac{k}{a^2}. \end{aligned} \tag{5.37}$$

Note however, that even though the modified Friedmann equations are the same here as they were in the regularized 4DEGB approaches, the theories are in general different. Indeed, if the condition in Eq. (5.20) does not hold, then the generalized conformal scalar field theory is question is different from the regularized 4DEGB ones we have discussed in previous chapters.

Recently, the neutron star merging event GW170817 [348] placed stringent constraints on the viable gravitational theories because the electromagnetic counterpart to GW170817 indicates that the deviation in the speed of gravitational waves, c_T,

from that of light must be less than one part in 10^{15} [351]. The propagation speed of gravitational waves in Horndeski theories with non-trivial G_4 and G_5 functions differ, in general, from unity and is given by [105]

$$c_T^2 = \frac{G_4 - X\left(\ddot{\phi}G_{5,X} + G_{5,\phi}\right)}{G_4 - 2XG_{4,X} - X\left(H\dot{\phi}G_{5,X} - G_{5,\phi}\right)}. \tag{5.38}$$

Consequently one might worry that the theory specified in Eq. (5.15) is severely constrained. As we have seen in previous sections, the counter-term regularized 4DEGB theory (which corresponds to $\beta = \lambda = 0$) easily evades these constraints. Remarkably, even in the presence of non-vanishing β and λ, something similar happens. If one considers a dark energy dominated universe where the scale factor is exponential $a \sim e^{\kappa t}$, using the scalar field profile of Eq. (5.34), then $c_T^2 = 1$, leaving the theory unconstrained. Adopting a more conservative approach where we take $H^2 \approx -\dot{H} \approx 5.8 \times 10^{-36}\,\mathrm{s}^{-2}$ and the fiducial value $\lambda = 3\beta^2/4\alpha$, we obtain the constraint

$$\left|c_T^2 - 1\right| = \left|\frac{4\alpha\dot{H}}{1 + 2\alpha H^2}\right| \lesssim 10^{-15} \Rightarrow \sqrt{|\alpha|} \lesssim 10^{15}\,\mathrm{km}, \tag{5.39}$$

which corresponds to the same weak upper bound on α as presented in Eq. (4.62).

6 Numerical Construction of Highly Accurate Spinning Black Hole Solutions in Modified Theories of Gravity

So far we have focused most of our research in 4D Einstein-Gauss-Bonnet theories motivated by the regularization introduced by Glavan & Lin [110]. The next two chapters (chapter 6 and 7) will diverge slightly from that line of research. In the present chapter we will investigate a method to numerically obtain stationary and axisymmetric black hole solutions in (generic) modified theories of gravity. We will, nonetheless, apply this method to more standard Gauss-Bonnet theories such as those presented in Eq. (1.37) as a suitable example. Chapter 7 will concern the study of black holes in theories of the form of Eq. (1.37) in more detail.

In the last decade with the observation of gravitational wave events [30, 388–392] by the LIGO/Virgo Collaboration, and with interferometry measurements of the center of the M87 [31] and Milky Way [32, 393] galaxies by the Event Horizon Telescope Collaboration, humankind has entered a new era of multi-messenger astronomy, opening up a new avenue to test the nature of black holes and Einstein's theory in the previously inaccessible strong field regime.

Mathematical theorems guarantee that in (electro-)vacuum the gravitational field of stationary black holes is described *uniquely* by the Kerr(-Newman) metric [40]. Supported by the uniqueness theorems, along with a set of other results dubbed *no-hair theorems* (see [42] for a review), the *Kerr hypothesis* paradigm asserts that the Kerr metric provides, as eloquently put by Subrahmanijan Chandrasekhar, *the absolute exact representation of untold numbers of massive black holes that populate the universe*. While all strong regime observations are, so far, compatible with the Kerr hypothesis, any eventual deviation would provide a much sought smoking-gun for new physics.

Once we delve onto the realm of modified theories of gravity, a large landscape of new possibilities emerges, with stationary vacuum spacetimes needing not to be described by the Kerr metric. Popular examples of black hole spacetimes defying the Kerr hypothesis include gravity coupled with new (complex) bosonic degrees of freedom [394–396], scalar-Gauss-Bonnet gravity [70, 71, 73–77, 79–83, 85], 4D-Einstein-Gauss-Bonnet gravity [2, 4–6, 110, 256–259], and dynamical Chern-Simons gravity [397–400].

With the modification of the field equations describing gravity, naturally comes an increase in their complexity, such that analytical analysis become intractable. One is then forced to either resort to perturbation theory or numerical methods. However, once we enter the strong field regime, perturbative approximations may not be well-justified, motivating a fully numerical study.

The need for accurate black hole solutions in modified theories of gravity comes from the ever-increasing precision of our observations and measurements, such that these models can effectively be tested against collected data, in order to get a better understanding of the true nature of gravity. In this chapter, much in the style of Refs. [401, 402], we will describe a numerical method capable of solving with high accuracy a system of non-linear elliptic partial differential equations (PDEs), such as those that appear when analyzing stationary and axially symmetric spacetimes. Our numerical implementation will then be validated against the Kerr black hole from GR and later applied to a class of modified theories of gravity, namely scalar-Gauss-Bonnet theories for several couplings.

A first version of our numerical implementation is available in the GitHub repository in Ref. [403], and can be run with ease by laptop-class computers. The code is written in the programming language Julia, being fast, memory efficient, and easy to manipulate such that implementing different models is not a difficult task. In this way, researchers can spend more time doing physics and less time coding.

The chapter is organized as follows. In section 6.1 we introduce the reader to pseudospectral methods and the technical machinery that will be necessary to apply them in the context of black hole physics. Next, in section 6.2 we will describe how we can use the aforementioned methods to solve the axisymmetric field equations for gravity, discussing the boundary conditions, coordinate compactifications, and numerical approach. We further discuss on many of the properties that can be extracted from a spinning black hole solution. Finally, in section 6.3 we start by validating our methods and code against the Kerr black hole, which is known in closed form, and later use our machinery to obtain stationary and axisymmetric black holes in Einstein-scalar-Gauss-Bonnet gravity for linear and exponential

couplings, discussing on their accuracy. We end by comparing our results to other existing codes.

6.1 Numerical Spectral Methods

The presentation in this section follows closely that of John P. Boyd's book on spectral methods [404]. Although we will try to summarize the most important points of spectral methods in application to the problem in question, readers that are new to the topic are nonetheless recommended to explore Ref. [404]. The idea behind spectral methods is to approximate the smooth solution $u(x)$ to a (system of) differential (or integral) equation(s) of the form[24]

$$\mathcal{R}\left(x, u\right) = 0, \tag{6.1}$$

where $\mathcal{R}$ is called *the residual* of the system, by a finite truncated series

$$u(x) \approx u_N(x) = \sum_{n=0}^{N-1} \alpha_n \phi_n(x), \tag{6.2}$$

where $\{\phi_n(x)\}_{n=0}^{\infty}$ is a set of *global* and *orthogonal* basis functions, $\{\alpha_n\}_{n=0}^{\infty}$ the set of *spectral coefficients*, and N the resolution. In this setup, $u_N(x)$ is said to be a numerical solution of the system (6.1) if its spectral coefficients are such that the residual is minimized to below a certain prescribed tolerance. The result is a global (rather than local) approximation method with an exponential (or spectral) convergence for problems with smooth solutions, using high-order polynomials or trigonometric functions that are infinitely differentiable. This is in contrast to the polynomial convergence rate of most other numerical methods, such as finite element/difference schemes that generically consist of low-order (local) polynomials, thus suffering from lower accuracy when compared to spectral methods. Furthermore, numerical solutions obtained via a spectral method provide a (high-accuracy) analytical approximation to the problem in question, rather than a set of values of the target solution at a discrete number of points.

Of importance is the concept of orthogonality, a condition the set of basis functions are required to obey. Typically, the word "orthogonal" is used when mentioning vectors and is defined with respect to the usual inner product of two vectors (the sum of the products of the corresponding components). The concept of the inner

[24] We consider only the one dimensional case for now

product can be generalized to deal with two arbitrary functions $f(x)$ and $g(x)$ with respect to the weight function $\omega(x) > 0$ on the interval $[a, b]$ as

$$(f, g) \equiv \int_a^b f(x)g(x)\omega(x)dx. \tag{6.3}$$

Two functions are then said to be orthogonal if their inner product vanishes. Therefore, a set of basis functions $\{\phi_n(x)\}_{n=0}^{\infty}$ is said to be orthogonal in the given interval $[a, b]$ if

$$(\phi_n, \phi_m) = c_n \delta_{mn}, \tag{6.4}$$

where δ_{mn} is the Kronecker delta and c_n are normalization constants. Orthogonality guarantees that a set of basis functions will be as different from one another as possible, in a sort of maximization of linear independence. Once a basis is found, all functions in that particular function space can be expanded with respect to the orthogonal functions.

The set of basis functions to use in a (numerical) spectral method should further have a number of properties – i) easy to compute (e.g. trigonometric functions or polynomials); ii) the approximations should converge rapidly to the true solution as the resolution is increased; iii) completeness, which means that any solution can be represented to arbitrarily high accuracy by taking the resolution to be sufficiently high. Two possible sets of basis functions that obey the above requirements are the basis of an ordinary Fourier series (sines and cosines) and a special class of polynomials dubbed Chebyshev polynomials.

6.1.1 Chebyshev Polynomials

For non-periodic problems, Chebyshev polynomials are the most natural choice as the spectral series is guaranteed to converge exponentially fast (provided our domain is restricted to the interval $x \in [-1, 1]$). The nth Chebyshev polynomial (of the first kind) is defined as

$$T_n(x) = \cos(n\theta), \qquad \theta = \arccos x \tag{6.5}$$

or equivalently by the three-term recurrence relation

$$\begin{aligned} &T_0(x) \equiv 1, \quad T_1(x) \equiv x \\ &T_n(x) = 2xT_{n-1}(x) - T_{n-2}(x), \quad n \geq 2. \end{aligned} \tag{6.6}$$

The first six Chebyshev polynomials are shown in Fig. 6.1.1 in the domain $x \in [-1, 1]$.

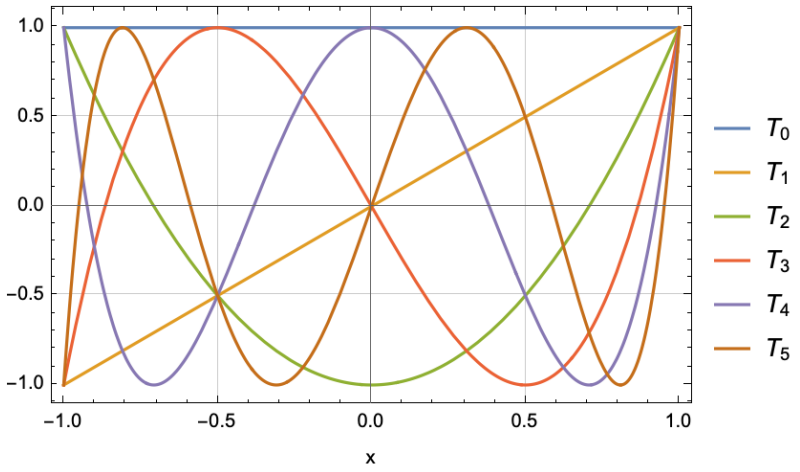

Figure 6.1.1: First six Chebyshev polynomials in the domain $x \in [-1, 1]$.

Importantly, it can be shown that Chebyshev polynomials obey the orthogonality relation in the domain $x \in [-1, 1]$

$$\int_{-1}^{1} \frac{T_m(x)T_n(x)}{\sqrt{1-x^2}} dx = \frac{\pi}{2}\left(1 + \delta_{0n}\right)\delta_{mn}, \tag{6.7}$$

and therefore they form an orthogonal basis. Their derivatives are given by

$$\frac{d}{dx}T_n(x) = nU_{n-1}(x), \tag{6.8}$$

where $U_n(x)$ denotes the nth Chebyshev polynomial of the second kind, defined by the recurrence relation

$$\begin{aligned} &U_0(x) \equiv 1, \quad U_1(x) \equiv 2x, \\ &U_n(x) = 2xU_{n-1}(x) - U_{n-2}(x), \quad n \geq 2, \end{aligned} \tag{6.9}$$

and with derivative

$$\frac{d}{dx}U_n(x) = \frac{(n+1)T_{n+1}(x) - xU_n(x)}{x^2 - 1}. \tag{6.10}$$

Note that some derivatives require special care at the boundaries $x = \pm 1$, and must be computed as a well-defined limit, namely

$$\left.\frac{d^2T_n}{dx^2}\right|_{x=-1} = (-1)^n \frac{n^4 - n^2}{3}, \qquad \left.\frac{d^2T_n}{dx^2}\right|_{x=1} = \frac{n^4 - n^2}{3}. \tag{6.11}$$

An important concept, intimately connected with Chebyshev polynomials, is in-

terpolation. Interpolation functions are typically ordinary or trigonometric polynomials, whose degrees of freedom are determined by the requirement that the interpolant agrees with the true function at the chosen set of interpolation (or collocation) points. The objective is that the interpolant provides a good approximation to the true function. By virtue of the minimal amplitude theorem [404], Chebyshev polynomials are widely used in interpolations. The reason is twofold. First, when using the so called Chebyshev nodes (or Gauss-Chebyshev points), given by

$$x_n = \cos\left(\frac{(2n+1)\,\pi}{2N}\right), \qquad n = 0, \ldots, N-1, \tag{6.12}$$

as collocation points, the effect of the Runge phenomenon (numerical instabilities near the boundaries in the form of uncontrolled oscillations) is minimized. Note that x_n are the roots of the Nth Chebyshev polynomial. Secondly, when Chebyshev polynomials are used as the basis for the interpolation, the interpolation error is distributed uniformly over the whole range.

The algorithm to interpolate a smooth function $u(x)$ using a truncated Chebyshev series[25]

$$u_N(x) = {\sum_{n=0}^{N-1}}' \alpha_n T_n(x), \tag{6.13}$$

relies on finding the optimal spectral coefficients $\{\alpha_n\}$ and uses the discrete orthogonality relation of Chebyshev polynomials

$$\sum_{j=0}^{N-1} T_n(x_j) T_m(x_j) = \frac{N}{2}\,(1+\delta_{0n})\,\delta_{mn}, \tag{6.14}$$

where the x_j are given in Eq. (6.12). To find the spectral coefficients we note that

$$\sum_{j=0}^{N-1} u_N(x_j) T_k(x_j) = {\sum_{i=0}^{N-1}}' \alpha_i \sum_{j=0}^{N-1} T_i(x_j) T_k(x_j),$$

and using the discrete orthogonality relations, we obtain

$$\alpha_n = \frac{2}{N} \sum_{j=0}^{N-1} u(x_j) T_n(x_j). \tag{6.15}$$

We present in Fig. 6.1.2 an illustrative example of a Chebyshev interpolation per-

[25] The prime in the sum denotes that the first coefficient is halved. We chose to halve the first coefficient in the sum in order to simplify some relations below, such as Eq. (6.15).

formed for several resolutions using the above expressions.

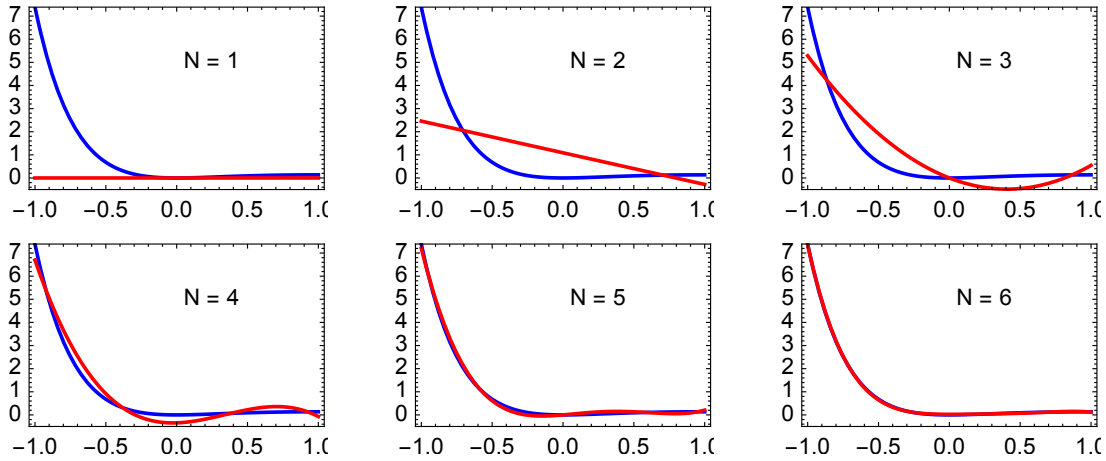

Figure 6.1.2: Interpolation of the function $u(x) = x^2 e^{-2x}$ on a Gauss-Chebyshev grid, for resolutions ranging from $N = 1$ to $N = 6$. Using Eqs. (6.13) and (6.15) we find that for $N = 6$ the spectral coefficients of the approximation $u_6(x)$ are $\alpha_0 \approx 1.48427$, $\alpha_1 \approx -2.49232$, $\alpha_2 \approx 1.85409$, $\alpha_3 \approx -1.01286$, $\alpha_4 \approx 0.395175$, and $\alpha_5 \approx -0.111169$.

6.1.2 Fourier Series

Fourier's theorem states that any (reasonably well-behaved) function can be written in terms of an infinite sum of trigonometric functions, a Fourier series. The Fourier series of a function $u(\theta)$ makes use of the orthogonality relationships of the sine and cosine functions

$$\begin{aligned} \int_0^{2\pi} \sin(n\theta)\cos(m\theta)d\theta &= 0, \\ \int_0^{2\pi} \sin(n\theta)\sin(m\theta)d\theta &= \pi\left(1-\delta_{0n}\right)\delta_{mn}, \\ \int_0^{2\pi} \cos(n\theta)\cos(m\theta)d\theta &= \pi\left(1+\delta_{0n}\right)\delta_{mn}, \end{aligned} \tag{6.16}$$

and is given by

$$u(\theta) = {\sum_{n=0}^{\infty}}' a_n \cos\left(n\theta\right) + \sum_{n=1}^{\infty} b_n \sin\left(n\theta\right), \tag{6.17}$$

where the expressions for the coefficients a_n and b_n are

$$a_n = \frac{1}{\pi}\int_{-\pi}^{\pi} u(\theta)\cos(n\theta)d\theta, \qquad b_n = \frac{1}{\pi}\int_{-\pi}^{\pi} u(\theta)\sin(n\theta)d\theta.$$

Taking into account the symmetries of the problem at hand, it is often unnecessary to use the full Fourier series, as the terms of a Fourier series not only possess definite parity with respect to $\theta = 0$, but also with respect to $\theta = \pi/2$. Table 6.1.1 summarizes the properties of the elements of a Fourier series of a function $u(\theta)$, depending on the parity symmetries, along with a scheme of its boundary values.

Fourier series	Parity w.r.t. $\theta = 0$	Parity w.r.t. $\theta = \pi/2$	$u(0)$	$u(\frac{\pi}{2})$	$\partial_\theta u(0)$	$\partial_\theta u(\frac{\pi}{2})$
$\cos([2n]\,\theta)$	Even	Even	$\neq 0$	$\neq 0$	$= 0$	$= 0$
$\cos([2n+1]\,\theta)$	Even	Odd	$\neq 0$	$= 0$	$= 0$	$\neq 0$
$\sin([2n]\,\theta)$	Odd	Odd	$= 0$	$= 0$	$\neq 0$	$\neq 0$
$\sin([2n+1]\,\theta)$	Odd	Even	$= 0$	$\neq 0$	$\neq 0$	$= 0$

Table 6.1.1: Properties of the elements of a Fourier series of a function $u(\theta)$, depending on the parity symmetries, along with a scheme of its boundary values. Here, $n \in \mathbb{N}^0$. The entries on this table for $\theta = \pi$ would be equivalent to those of $\theta = 0$.

Stationary and axisymmetric black holes are solutions to a system of two-dimensional elliptic PDEs that depend on the radial coordinate and the zenith angle $\theta \in [0, \pi]$. These solutions often possess definite parity with respect to $\theta = \pi/2$ (in most cases they are symmetric about $\theta = \pi/2$), and therefore we need only to consider the range $\theta \in [0, \pi/2]$. In this range, the following orthogonality relations hold

$$\begin{aligned}
&\int_0^{\pi/2} \cos(2n\theta)\cos(2m\theta)\,d\theta = \frac{\pi}{4}(1+\delta_{0n})\,\delta_{mn},\\
&\int_0^{\pi/2} \cos([2n+1]\,\theta)\cos([2m+1]\,\theta)d\theta = \frac{\pi}{4}\delta_{mn},\\
&\int_0^{\pi/2} \sin(2n\theta)\sin(2m\theta)\,d\theta = \frac{\pi}{4}(1-\delta_{0n})\,\delta_{mn},\\
&\int_0^{\pi/2} \sin([2n+1]\,\theta)\sin([2m+1]\,\theta)d\theta = \frac{\pi}{4}\delta_{mn},
\end{aligned} \tag{6.18}$$

and their discrete version

$$\begin{aligned}
\sum_{j=0}^{N-1} \cos\left(2n\theta_j\right) \cos\left(2m\theta_j\right) &= \frac{N}{2}\left(1+\delta_{0n}\right)\delta_{mn}, \\
\sum_{j=0}^{N-1} \cos\left(\left[2n+1\right]\theta_j\right) \cos\left(\left[2m+1\right]\theta_j\right) &= \frac{N}{2}\delta_{mn}, \\
\sum_{j=0}^{N-1} \sin\left(2n\theta_j\right) \sin\left(2m\theta_j\right) &= \frac{N}{2}\left(1-\delta_{0n}\right)\delta_{mn}, \\
\sum_{j=0}^{N-1} \sin\left(\left[2n+1\right]\theta_j\right) \sin\left(\left[2m+1\right]\theta_j\right) &= \frac{N}{2}\delta_{mn},
\end{aligned} \tag{6.19}$$

where

$$\theta_n = \frac{(2n+1)\,\pi}{4N}, \qquad n = 0, \ldots, N-1. \tag{6.20}$$

With the above relations, an expression similar to that of Eq. (6.15) can be obtained for trigonometric interpolation of function. For example, a function symmetric about $\theta = 0, \pi/2$ can be interpolated with even cosines by using the spectral coefficients

$$\alpha_n = \frac{2}{N}\sum_{j=0}^{N-1} u(\theta_j)\cos(2n\theta_j). \tag{6.21}$$

6.1.3 Solving an ODE with a spectral method – a first example

To get a better understanding on how to solve differential equations using a spectral method, we will first consider a simple ODE example. Namely, consider the one dimensional non-linear boundary value problem

$$\mathcal{R} = u_{xx} - u_x^2 = 0, \quad u(-1) - 2 = 0, \quad u(1) - 1 = 0, \tag{6.22}$$

with exact solution

$$u(x) = \log\left(\frac{2e^2}{(e-1)x + e + 1}\right). \tag{6.23}$$

We will approximate the solution to this boundary value problem using a Chebyshev spectral method, and later compare our results with the exact solution. To make calculations tractable analytically, we will consider a (very) low resolution of $N = 3$,

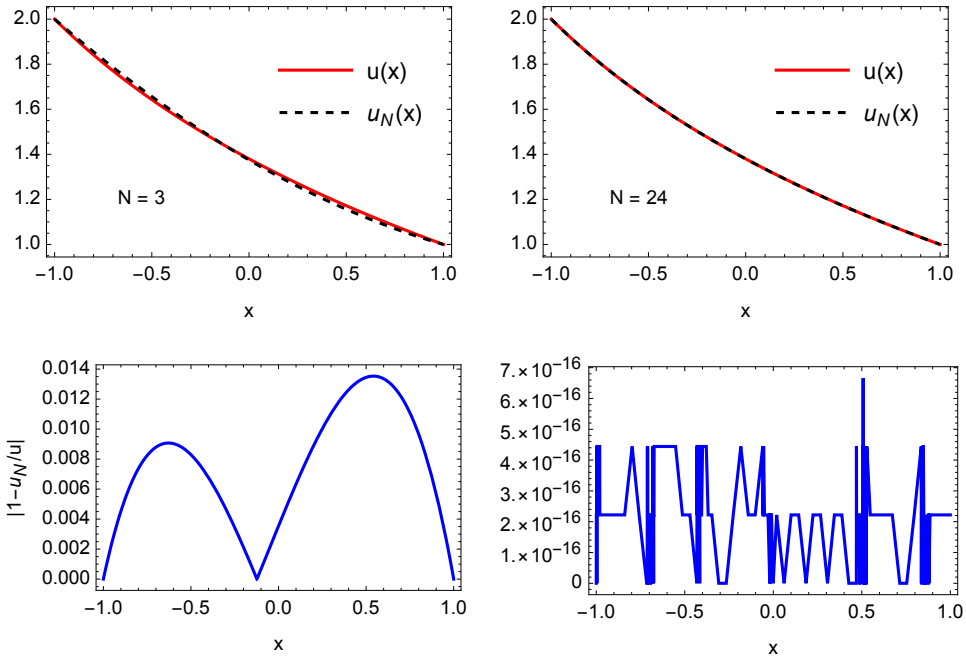

Figure 6.1.3: Approximations to the solution of the boundary value problem given in Eq. (6.22) (top) together with their absolute errors with respect to the exact solution (bottom) for resolutions $N = 3$ (left) and $N = 24$ (right).

i.e.,

$$u \approx u_3 = \frac{\alpha_0}{2} T_0(x) + \alpha_1 T_1(x) + \alpha_2 T_2(x) = \frac{\alpha_0}{2} + \alpha_1 x + \alpha_2 \left(2x^2 - 1\right), \tag{6.24}$$

where we have $N = 3$ degrees of freedom (α_0, α_1, and α_2). Note that we have a number of boundary conditions $N_{BC} = 2$. Once we substitute our ansätz of Eq. (6.24) onto the residual given in Eq. (6.22) we obtain

$$\mathcal{R} \approx 4\alpha_2 - (4\alpha_2 x + \alpha_1)^2 = 0, \tag{6.25}$$

together with the boundary conditions

$$\frac{\alpha_0}{2} - \alpha_1 + \alpha_2 - 2 = 0, \qquad \frac{\alpha_0}{2} + \alpha_1 + \alpha_2 - 1 = 0. \tag{6.26}$$

Given that we have only $N = 3$ degrees of freedom, and the two boundary conditions provide two constraints, to solve the system we have to evaluate the residual at only $N - N_{BC} = 1$ collocation point. The collocation point is chosen according to Eq.

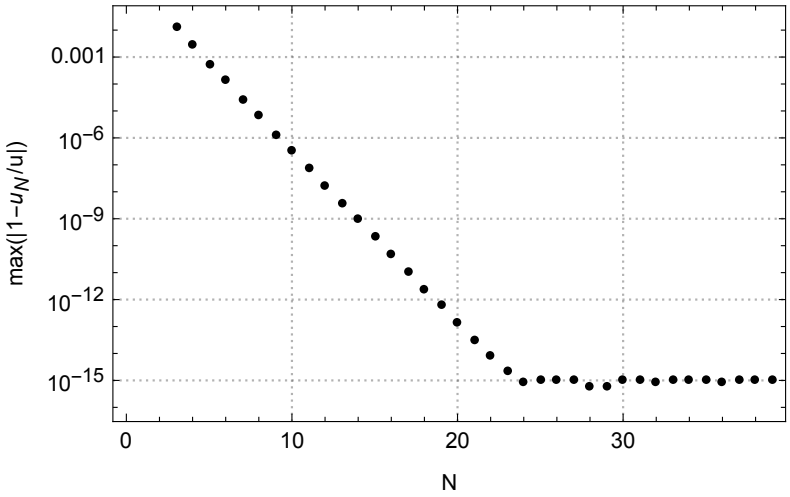

Figure 6.1.4: Logarithmic plot of the maximum absolute error in the approximation to the solution of the boundary value problem as a function of the resolution. Spectral convergence is observed, together with a roundoff plateau.

(6.12) with resolution $N - N_{BC} = 1$, which gives only the point $x = 0$.[26] In the end, with our resolution $N = 3$, finding an approximate solution to the boundary value problem reduces to solving $N = 3$ non-linear coupled algebraic equations for the spectral coefficients, given by the two boundary conditions of Eq. (6.26) together with the residual of Eq. (6.25) evaluated at $x = 0$. The solution to the system is

$$\alpha_0 = \frac{23}{8}, \quad \alpha_1 = -\frac{1}{2}, \quad \alpha_2 = \frac{1}{16}.$$

On Fig. 6.1.3 we plot the exact solution against the approximation obtained with $N = 3$, together with the absolute error, $|1 - u_N/u|$, whose maximum can be seen to be $\mathcal{O}(10^{-2})$ already for a very low resolution $N = 3$. Also on Fig. 6.1.3 we plot our approximation to the solution of the boundary value problem, but for a resolution $N = 24$, where we observe that errors of the order of machine precision ($\mathcal{O}(10^{-16})$) are attained. In Fig. 6.1.4 we plot the behaviour of the maximum absolute error as a function of the resolution, where exponential convergence is observed. As a rule of thumb, the truncation error is typically the same order-of-magnitude as the last coefficient retained in the truncation series.

An important point to make here is that even though for $N = 3$ the approximation system has a closed-form analytical solution for the spectral coefficients, once

[26] Had we chosen a resolution $N = 4$, the number of collocation points where we would have to evaluate the residual would be $N - N_{BC} = 2$, and the collocation points in that case, according to Eq. (6.12) would give the set $x = \pm \sin \pi/8 \approx \pm 0.382683$.

higher resolutions are considered, a numerical root-finding method (such as Newton-Raphson) has to be employed. To successfully employ a Newton-Raphson method, a good initial guess for the spectral coefficients is of the utmost importance. We will come back to this in the next section.

To conclude, spectral collocation methods are powerful tools that can be used to numerically solve differential equations, providing global analytical approximations for the solution, rather than obtaining a set of approximate values of the solution at a discrete grid. Mildly good results can be obtained with low resolutions, and highly accurate ones can be obtained by increasing the resolution as convergence is exponential. Furthermore, handling any kind of boundary conditions is straightforward. Spectral collocation methods are also known as pseudospectral methods.

6.1.4 Root-finding methods – Newton-Raphson

To numerically solve the system of algebraic equations for the spectral coefficients resulting from evaluating the residual at the collocation points, together with the boundary conditions, a root-finding method should (in general) be employed. In particular, we will focus on the Newton-Raphson method. Starting with the one-dimensional example, the main objective of the Newton-Raphson is to find a value x_* such that, starting from a value x_0, an equation of the form $f(x) = 0$ is solved to a certain prescribed tolerance. It follows from Taylor's theorem, and can be stated in an iterative form

$$x_{n+1} = x_n - \frac{f(x_n)}{f'(x_n)}. \tag{6.27}$$

Example: assume we want to find the root of the function $f(x) = x^3 + x - 1$, known to be $x_* \approx 0.6823278$ to eight decimal places. Starting with $x_0 = 1$ as our initial guess, using Eq. (6.27) we obtain

$$x_1 = 0.75, \quad x_2 = 0.68604651, \quad x_3 = 0.68233958, \quad x_4 = 0.6823278,$$

thus converging to x_* in four iterations to the prescribed tolerance of eight decimal places. In more complicated cases, an appropriate choice of starting point is extremely important and must be done carefully.

A generalization of the method given in Eq. (6.27) exists for systems of N variables with N equations (finding the root of a vector-valued function $F : \mathbb{R}^N \to \mathbb{R}^N$), and amounts to iteratively solve the linear system

$$\mathcal{J}(\mathbf{x}_n)\,(\mathbf{x}_{n+1} - \mathbf{x}_n) = -F(\mathbf{x}_n)\,, \tag{6.28}$$

for the unknown $\mathbf{x}_{n+1} - \mathbf{x}_n$, where $\mathcal{J}$ is the Jacobian matrix $(N \times N)$ of the system, defined as

$$\mathcal{J}_{ij} = \frac{\partial F_i}{\partial x_j}. \tag{6.29}$$

Constructing the Jacobian matrix of a given system is not always an easy task, and most existing packages will have methods to numerically approximate the Jacobian in an automatic way. However, these methods can be computationally expensive if the problem in question is rather large or complicated.

Of particular interest to this work, is how to compute the Jacobian matrix for a problem to be solved using a spectral method. In general, the system to be solved F, will be composed of the residual $\mathcal{R}$ evaluated at the Gauss-Chebyshev points (6.12), and the boundary conditions, depending on u, u_x, u_{xx}. Our unknowns are the spectral coefficients α_j. Thus, to facilitate the computation of the Jacobian, we may use the chain rule

$$\mathcal{J}_{ij} = \frac{\partial F_i}{\partial \alpha_j} = \frac{\partial F_i}{\partial u}\frac{\partial u}{\partial \alpha_j} + \frac{\partial F_i}{\partial u_x}\frac{\partial u_x}{\partial \alpha_j} + \frac{\partial F_i}{\partial u_{xx}}\frac{\partial u_{xx}}{\partial \alpha_j} \tag{6.30}$$

and only then substitute the spectral expansions for the function u. This process is easily generalizable to a system of ODEs/PDEs (rather than a single one)[27].

As previously stated, when using a Newton-Raphson method, the choice of initial guess to the spectral coefficients is extremely important, because non-appropriate choice of initial guess will likely result in non-convergence of the algorithm. A good initial guess can sometimes be difficult to obtain, especially when dealing with systems of PDEs, where the number of coefficients is large (for our specific black holes problem, typically of $\mathcal{O}(10^3)$ coefficients). A good way of tackling this issue stems from a good understanding of the problem in question. For example, from an effective field theory point of view, a Kerr black hole is probably a good approximation to a black hole solution in modified theories. Therefore, since we have a closed-form expression for a Kerr black hole, using the discussed interpolation techniques, the resultant spectral coefficients can be used as an initial guess to obtain a numerical solution of a black hole in modified theories.

[27] One must be careful when labeling the spectral coefficients of the different functions as it might be a source of errors.

6.2 Black Holes – Metric Ansätz, The Kerr Solution, Boundary Conditions, and Connection with the Numerical Approach

We will now apply the methods described in the previous sections to black hole physics, namely to obtain stationary solutions to the field equations of gravity (GR or modified theories), and study their properties.

Stationary black holes are solutions to a set of PDEs resulting from the field equations of a theory of gravity, and are described by a line-element. We will focus on a particular ansätz for the spacetime metric in quasi-isotropic coordinates, which is stationary, axisymmetric, and circular

$$ds^2 = -f\mathcal{N}^2 dt^2 + \frac{g}{f}\left[h\left(dr^2 + r^2 d\theta^2\right) + r^2 \sin^2\theta \left(d\varphi - \frac{W}{r}\left(1-\mathcal{N}\right)dt\right)^2\right], \quad (6.31)$$

where f, g, h and W are dimensionless functions of the radial and angular coordinates r and θ, and

$$\mathcal{N} \equiv \mathcal{N}(r) = 1 - \frac{r_H}{r},$$

where r_H is the (coordinate) location of the event horizon. The spatial coordinates range over the intervals

$$r \in [r_H, \infty[, \qquad \theta \in [0, \pi], \qquad \varphi \in [0, 2\pi]. \quad (6.32)$$

The spacetime possesses two Killing vector fields, $k = \partial_t$ and $\Phi = \partial_\varphi$, and the linear combination

$$\xi = \partial_t + \Omega_H \partial_\varphi, \quad (6.33)$$

where Ω_H is the angular velocity of the horizon (to be defined below), is orthogonal to and null on the event horizon. This Lewis-Papapetrou form for the metric is motivated by the discussion of Ref. [405], which asserts that the above metric ansätz is consistent for a generic theory of gravity provided that its solutions can be obtained perturbatively from a solution in the general relativity limit. Note that our form of the metric functions on the line element of Eq. (6.31) differ somewhat from the standard form used in other works (see e.g. [73, 77, 80, 81, 83, 84, 394–396]). The reasons for this will become clearer later on, once we make a connection to the numerical approach, and are related to numerical accuracy issues.

6.2.1 General Relativity – The Kerr Black Hole

For now let us focus on an analytical study of the known Kerr black hole, which is the solution to the stationary and axisymmetric field equations of GR in vacuum. For completeness, we present its charged generalization, the Kerr-Newman solution of electrovacuum in Appendix 6.A. The Kerr black hole solves the field equations

$$G_{\mu\nu} = 0, \tag{6.34}$$

where $G_{\mu\nu}$ is the Einstein tensor of the metric. The field equations can be obtained with the Einstein-Hilbert action principle

$$\mathcal{S} = \frac{1}{16\pi}\int d^4x\sqrt{-g}R, \tag{6.35}$$

where R and g are respectively the Ricci scalar of the determinant of the metric. With the ansätz of Eq. (6.31) the Kerr black hole solution reads

$$\begin{aligned} f &= \left(1+\frac{r_H}{r}\right)^2\frac{\mathcal{A}}{\mathcal{B}}, \\ g &= \left(1+\frac{r_H}{r}\right)^2, \\ h &= \frac{\mathcal{A}^2}{\mathcal{B}}, \\ W &= \frac{2M\left(Mr+r^2+r_H^2\right)}{r_H r^3\mathcal{B}}\sqrt{M^2-4r_H^2} \end{aligned} \tag{6.36}$$

where

$$\begin{aligned} \mathcal{A} &= \frac{2Mr\left(Mr+\left(r^2+r_H^2\right)\right)+\left(r^2-r_H^2\right)^2}{r^4} - \frac{\left(M^2-4r_H^2\right)}{r^2}\sin^2\theta, \\ \mathcal{B} &= \left(\mathcal{A}+\frac{\left(M^2-4r_H^2\right)}{r^2}\sin^2\theta\right)^2 - \frac{\left(r^2-r_H^2\right)^2\left(M^2-4r_H^2\right)}{r^6}\sin^2\theta, \end{aligned} \tag{6.37}$$

and M is the ADM mass of the black hole. The total angular momentum (per unit mass), a, of the solution is related to M and r_H via

$$r_H = \frac{\sqrt{M^2-a^2}}{2} \equiv \frac{M}{2}\sqrt{1-\chi^2}, \tag{6.38}$$

where we have defined the dimensionless spin

$$\chi \equiv a/M = J/M^2, \tag{6.39}$$

The mass M and total angular momentum J can be read of the decay off from the metric components as $r \to \infty$

$$\begin{aligned} g_{tt} &= -f\mathcal{N}^2 + \frac{g\left(1-\mathcal{N}\right)^2 W^2}{f}\sin^2\theta = -1 + \frac{2M}{r} + \mathcal{O}\left(r^{-2}\right), \\ g_{t\varphi} &= -\frac{gr\left(1-\mathcal{N}\right)W}{f}\sin^2\theta = -\frac{2J}{r}\sin^2\theta + \mathcal{O}\left(r^{-2}\right), \end{aligned} \tag{6.40}$$

which leads to

$$\begin{aligned} f &= 1 - \frac{2\left(M - r_H\right)}{r} + \mathcal{O}\left(r^{-2}\right), \\ W &= \frac{2J}{r_H r} + \mathcal{O}\left(r^{-2}\right). \end{aligned} \tag{6.41}$$

Note that the Kerr black hole in the quasi-isotropic coordinate system presented in Eq. (6.31) can be obtained from the standard textbook Boyer-Lindquist coordinates solution with the radial coordinate transformation

$$r_{BL} = r + M + \frac{M^2 - a^2}{4r} = r\left(1 + \frac{M}{r} + \frac{r_H^2}{r^2}\right). \tag{6.42}$$

The inverse transformation is given by

$$r = \frac{1}{2}\left(r_{BL} - M + \sqrt{\left(r_{BL} - M\right)^2 - 4r_H^2}\right). \tag{6.43}$$

6.2.2 Boundary Conditions

To solve the set of PDEs that result from the field equations, suitable boundary conditions should be imposed. These are obvious if an exact solution, such as the Kerr solution, is known by a trivial examination of the metric functions. However, in more intricate cases in modified gravity lacking an exact solution, the boundary conditions must be found with a careful examination of the field equations, by employing suitable expansions of the involved functions near the domain boundaries. With this process, we find that in all cases to be discussed in this work within modified gravity theories, the metric functions must obey the same boundary conditions as the Kerr solution does. These conditions are summarized next.

(i) Axis boundary conditions: Axial symmetry and regularity of the solutions on the symmetry axis $\theta = 0, \pi$, imply the following boundary conditions

$$\partial_\theta f = \partial_\theta g = \partial_\theta h = \partial_\theta W = 0, \qquad \text{for} \quad \theta = 0, \pi. \tag{6.44}$$

Moreover, the absence of conical singularities further imposes that on the symmetry

axis

$$h = 1, \qquad \text{for} \quad \theta = 0, \pi. \tag{6.45}$$

All solutions to be discussed in this work, much like the Kerr black hole, are symmetric with respect to a reflection on the equatorial plane $\theta = \pi/2$. Therefore, it is enough to consider the range $\theta \in [0, \pi/2]$ and one of the boundary conditions becomes

$$\partial_\theta f = \partial_\theta g = \partial_\theta h = \partial_\theta W = 0, \qquad \text{for} \quad \theta = \pi/2. \tag{6.46}$$

(ii) Event horizon boundary conditions: The black hole solutions here discussed do possess an event horizon located at a surface with constant radial variable $r = r_H$. The boundary conditions that the metric functions f, g and h obey are

$$\begin{aligned} f - r_H \partial_r f &= 0 \\ g + r_H \partial_r g &= 0, \\ \partial_r h &= 0, \end{aligned} \tag{6.47}$$

for $r = r_H$. The reason for the Robin type boundary conditions that the functions f and g obey comes from the inclusion of the $\mathcal{N}^2$ factor in front of f in the dt^2 coefficient of the metric ansätz (Eq. (6.31)). This factor is chosen such that these functions do not contain a double-zero in a near-horizon expansion, allowing for more accurate solutions in this region, and therefore, a more accurate extraction of horizon physical quantities such as the event horizon area and temperature. We find that there are (at least) two possibilities for the condition that the function W should obey at the horizon, one of which must be chosen appropriately such that the number of input parameters is kept at two (see discussion below in Sec. 6.2.3)

$$W = r_H \Omega_H \tag{6.48}$$

or

$$W - \frac{r_H}{2} \partial_r W = 0, \tag{6.49}$$

at $r = r_H$, where Ω_H is a constant interpreted as the angular velocity of the event horizon, which in the case of a Kerr black hole is given by

$$\Omega_H^{\text{Kerr}} = \frac{\sqrt{M^2 - 4r_H^2}}{2M\,(M + 2r_H)} = \frac{\chi^2 - 1 + \sqrt{1 - \chi^2}}{4 r_H \chi}. \tag{6.50}$$

(iii) Asymptotic boundary conditions: Requiring asymptotic flatness (i.e., that as $r \to \infty$, our solution approaches the Minkowski spacetime), the functions f,

g, and h obey

$$\lim_{r\to\infty} f = \lim_{r\to\infty} g = \lim_{r\to\infty} h = 1. \tag{6.51}$$

Similarly to the boundary conditions at the event horizon, we find (at least) two suitable conditions for the function W

$$\lim_{r\to\infty} W = 0, \tag{6.52}$$

or, from the asymptotic expansion of Eq. (6.41)

$$\lim_{r\to\infty} r_H r^2 \partial_r W + 2M^2\chi = 0 \Leftrightarrow \lim_{r\to\infty} \frac{r^2}{2r_H}\partial_r W + \left(1 + \frac{r^2}{2r_H}\partial_r f\right)^2 \chi = 0. \tag{6.53}$$

6.2.3 Connection with the numerical approach

The field equations of a gravitational theory once applied to the line element of Eq. (6.31) will result in a set of non-linear coupled elliptic PDEs in r and θ subject to the boundary conditions described above. Our objective is to solve this system of PDEs numerically using a spectral method. For this we introduce the compactified radial coordinate

$$x = 1 - \frac{2r_H}{r}, \tag{6.54}$$

mapping the range $r \in [r_H, \infty[$ to

$$x \in [-1, 1]. \tag{6.55}$$

With the compactified coordinate, the radial boundary conditions change as follows.
Event horizon boundary conditions: The boundary conditions that the metric functions f, g and h obey are

$$\begin{aligned} f - 2\partial_x f &= 0 \\ g + 2\partial_x g &= 0, \\ \partial_x h &= 0, \end{aligned} \tag{6.56}$$

for $x = -1$. For the function W, the first possibility (Eq. (6.48)) remains unchanged ($W|_{x=1} = r_H\Omega_H$), whereas the second becomes

$$W - \partial_x W = 0, \tag{6.57}$$

at $x = -1$.
Asymptotic boundary conditions: The asymptotic boundary conditions the

functions f, g, and h are now

$$f = g = h = 1, \qquad \text{for} \quad x = 1 \tag{6.58}$$

Asymptotically, function W now obeys either

$$W = 0, \tag{6.59}$$

or

$$\partial_x W + (1 + \partial_x f)^2 \chi = 0, \tag{6.60}$$

at $x = 1$.

With our compactified radial coordinate, and given the symmetries of our problem[28], a suitable spectral expansion for the black hole metric functions (collectively denoted by $\mathcal{F} = \{f, g, h, W\}$) is given by

$$\mathcal{F} = \sum_{i=0}^{N_x-1}{}' \sum_{j=0}^{N_\theta-1}{}' \alpha_{ij} T_i(x) \cos(2j\theta) \,, \tag{6.61}$$

where N_x and N_θ are the resolutions in the radial and angular coordinates. Note that the angular boundary conditions are automatically satisfied for all functions given our spectral expansion (c.f. Table 6.1.1). Of extreme importance to set up a good initial guess for our solver, is how to interpolate a generic function $u(x, \theta)$ (with the appropriate symmetries in the angular coordinate) given the above expansion.

As mentioned above, we will usually use the Kerr metric itself to set our initial guess when working with modified theories of gravity, and to do so we will need the expression for the spectral coefficients that follow from an interpolation of a two-dimensional function $u(x, \theta)$, which is given by

$$\alpha_{ij} = \frac{4}{N_x N_\theta} \sum_{k=0}^{N_x-1} \sum_{l=0}^{N_\theta-1} u(x_k, \theta_l) T_i(x_k) \cos(2j\theta_l) \,, \tag{6.62}$$

where x_k and θ_l are given in Eqs. (6.12) and (6.20) respectively.

Each Kerr black hole is uniquely described by two input parameters. For example, in the presentation given in Eq. (6.36), these are the location of the event horizon r_H and the ADM mass M. We have seen, however, in expressions (6.38) and (6.50) that they are related to the dimensionless spin χ and the horizon angular velocity Ω_H. Therefore, using the correct parametrization, the Kerr solution can be described by

[28] From now on we consider only the cases with even parity with respect to $\theta = \pi/2$.

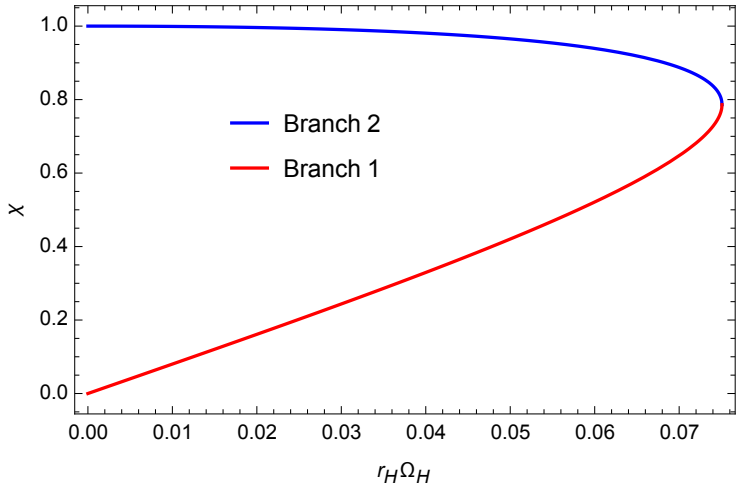

Figure 6.2.1: Choosing (r_H, Ω_H) as input parameters, for fixed r_H, two branches exist.

any input pair chosen from r_H, Ω_H, χ, and M. In the numerical approach, in a theory agnostic setting, one input parameter that must be used is r_H because it enters directly the metric ansätz and the definition of our compactified coordinate x. We have, however, freedom in the choice of the other input parameter in the numerics. To the best of our knowledge, so far in the literature for similar problems [73, 77, 80, 81, 83, 84, 394–396], the other input parameter has always been chosen as the event horizon angular velocity Ω_H. Using this input pair (r_H, Ω_H), we find compatibility with the boundary conditions for the function W if we choose Eqs. (6.48) and (6.59) at the horizon and infinity, respectively. Then, in the case of a Kerr black hole, one finds that for a fixed value of r_H, two branches of solutions exist as shown in Fig. 6.2.1. This follows from inverting the relation (6.50). The first branch of solutions starts at a vanishing value of Ω_H (for fixed r_H) and exists until

$$r_H\Omega_H = \frac{\sqrt{5\sqrt{5}-11}}{4\sqrt{2}} \approx 0.0750708, \tag{6.63}$$

at which point

$$\chi = \sqrt{\frac{\sqrt{5}-1}{2}} \approx 0.786151. \tag{6.64}$$

Then, a second branch appears, and Ω_H tends backwards towards zero. As $\Omega_H \to 0$ on this second branch, extremal solutions are approached. The existence of two branches of solutions is not unique to Kerr, and will be observed as well in the modified theories of gravity to be discussed in this work. We note that the numerical procedure gets rather difficult as near-extremal solutions are approached, as

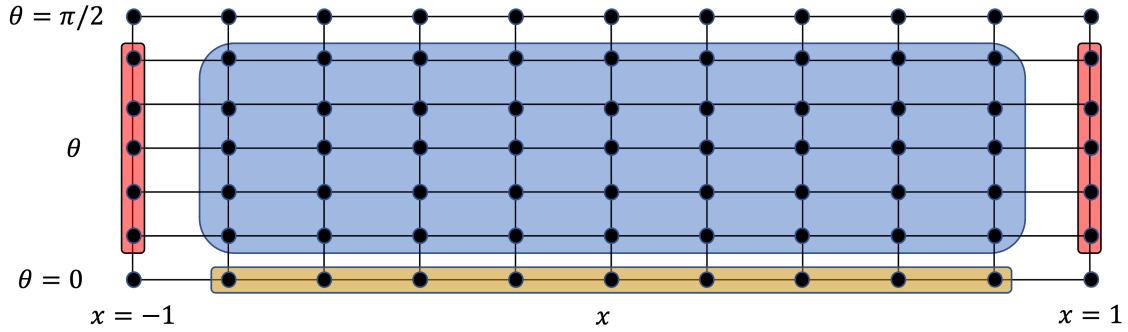

Figure 6.2.2: Fiducial grid with $N_x \times N_\theta = 11 \times 5$, highlighted in blue. The field equations (residuals) are evaluated in the blue region, with the boundary conditions imposed on the red one. The yellow highlight concerns the imposition of the condition of Eq. (6.45).

our metric ansätz with the described boundary conditions is not compatible with extremal solutions.

A novel approach that we can also adopt is to choose the pair (r_H, χ) as the input pair. This input pair is compatible with the W boundary conditions of Eqs. (6.57) and (6.60) while maintaining the number of input parameters at two. We find it very convenient to use the dimensionless spin as an input parameter when e.g. exploring domains of existence, or simply when working on a single solution where a certain χ is wanted. Our numerical spectral method is not only powerful because high accuracy solutions are produced, but also because highly non-linear boundary conditions can be handled with ease (which is the case of the boundary condition of Eq. (6.60)).

To solve the system of field equations subject to the discussed boundary conditions we must construct a suitable grid. This is done as follows, where we assume a resolution $N_x \times N_\theta$. The x points are chosen according to a Gauss-Chebyshev grid presented in Eq. (6.12), where we take $N = N_x - 2$, together with the boundary points $x = -1$ and $x = 1$, such that the total number of points in the x direction is N_x[29]. In θ, our points are chosen as in Eq. (6.20), where we take $N = N_\theta$. The x and θ points together form a grid, as schematically shown in Fig. (6.2.2), in blue. Assuming a total number of functions to solve for N_{funcs}, there are $N_{funcs} \times N_x \times N_\theta$ degrees of freedom (spectral coefficients), as seen from the spectral expansion of Eq. (6.61). Also from this expansion, we stress that the boundary conditions at the limiting values $\theta = 0$ and $\theta = \pi/2$ are automatically satisfied, which facilitates our numerical scheme a lot. For each value of θ in the grid at the x boundaries we impose for each function the horizon and asymptotic boundary conditions as

[29]This approach is also called *boundary-bordering* in the spectral methods' literature.

discussed before. This gives us a total of $N_{funcs} \times 2 \times N_\theta$ equations (Fig. 6.2.2, in red). The remaining $N_{funcs} \times (N_x - 2) \times N_\theta$ equations come from imposing the N_{funcs} residuals resulting from the field equations at each non-boundary x value, for each θ. The number of degrees of freedom is then equal to the number of equations to solve, as it should. A small caveat – the absence of conical singularities imposes that Eq. (6.45) must be obeyed (for our coordinate range, $h = 1$ at $\theta = 0$). While we could leave this condition outside the numerical scheme and use it as another test to the code, we find that imposing it allows obtaining solutions with (much) higher accuracy. In our particular implementation, we have swapped the evaluation of one of the residuals at $\theta = 0$ (for all interior values of x)[30] with the condition of Eq. (6.45), see Fig. 6.2.2 in yellow.

6.2.3.1 Numerical Approach: A summary

Here we summarize our numerical approach for clarity. To solve the field equations, some preliminary work must be done. First, we employ the metric ansätz of Eq. (6.31) which contains four unknown functions, f, g, h, and W. Plugging this metric ansätz onto the field equations of the theory, a set of non-linear coupled PDEs depending on the functions and their first and second derivatives $(\mathcal{F}, \partial_r\mathcal{F}, \partial_r^2\mathcal{F}, \partial_\theta\mathcal{F}, \partial_\theta^2\mathcal{F}, \partial_{x\theta}\mathcal{F})$ is obtained. The set of field equations is then expressed in terms of the compactified coordinate x defined in Eq. (6.54) and put in residual form (i.e., $\mathcal{R}\left(x, \theta, \partial^i\mathcal{F}\right) = 0$), and the same is done for the appropriate boundary conditions as discussed. This part of the process is usually done resorting to a computer algebra system such as *Mathematica*, *Maple* or *SageMath*[31]. The residuals (and appropriate Jacobian) are then exported to a coding file in order to solve the problem using the developed numerical infrastructure. Each function is expanded in a spectral series given by Eq. (6.61) and the input parameters are then specified (depending on the chosen boundary conditions for the function W). To successfully solve the field equations, a good initial guess must be provided. For this, we interpolate the functions of the known Kerr solution using Eq. (6.62), obtaining appropriate spectral coefficients to be provided as a good initial guess. If new fields are present, as is the case with modified theories, we typically take advantage of perturbative solutions and interpolate them as a guess.

To speed up the solver, the values of our basis functions and their first and second

[30] We empirically found that any of the field equations should equally valid to remove for this process, resulting in similar outcomes

[31] In this work we have used *Mathematica* along with the *OGRe* package [406] to obtain the explicit field equations of many theories.

derivatives are calculated at all the grid points and stored, such that no repeated evaluations are performed. Another optimization that we found particularly impactful was to store the values on the grid of the trigonometric functions that typically appear in the residuals, $\sin\theta$ and $\cos\theta$.

Once a solution is obtained, the appropriate physical quantities can be extracted, as discussed next, and the solution can be used for numerous investigations.

6.2.4 Physical Properties of Stationary and Axisymmetric Black Holes

Once we have obtained a stationary and axisymmetric black hole solution, we can extract important quantities of physical relevance. In this section, we review many of quantities that one can extract from the solutions, and how these can be used to test the accuracy of the code.

6.2.4.1 Quantities of interest

Starting with the asymptotic quantities, we have seen that the mass M and angular momentum J can be extracted from the asymptotic expansion of Eq. (6.40) or Eq. (6.41). In terms of the coordinate x these are given by

$$M = r_H \left(1 + \partial_x f\right)|_{x=1}, \qquad J = -r_H^2 \partial_x W|_{x=1}. \tag{6.65}$$

We remark that such simple expression for the extraction of J is the reason why we have defined the function W in this way – such that its decay is of the form $\sim 1/r$, allowing for more accurate results. In a circular spacetime, the zeroth law of black hole mechanics holds, which means that the surface gravity is constant on the horizon of the stationary black hole. The surface gravity is defined as $\kappa^2 = -1/2(\nabla_\mu \xi_\nu)(\nabla^\mu \xi^\nu)$, where ξ was defined in Eq. (6.33). The event horizon temperature can be obtained from the surface gravity as

$$T_H = \frac{\kappa}{2\pi} = \frac{1}{2\pi r_H} \frac{f}{\sqrt{gh}}\bigg|_{x=-1}. \tag{6.66}$$

The induced metric on the horizon is

$$d\Sigma^2 = \mathfrak{h}_{ij} dx^i dx^j = r_H^2 \, \frac{g}{f} \left[h d\theta^2 + \sin^2\theta d\varphi^2\right]\bigg|_{x=-1}. \tag{6.67}$$

From it we can compute several quantities of interest, the most important being the event horizon area

$$A_H = \int_H \sqrt{\mathfrak{h}} d\theta d\varphi = 2\pi r_H^2 \int_0^\pi d\theta \sin\theta \frac{g\sqrt{h}}{f}\bigg|_{x=-1}. \tag{6.68}$$

Also, of importance is the entropy which is given in the Iyer-Wald formalism by [407]

$$S = -2\pi \int_H \frac{\delta \mathcal{L}}{\delta R_{\mu\nu\alpha\beta}} \epsilon_{\mu\nu}\epsilon_{\alpha\beta} dA\bigg|_{\text{on-shell}} \tag{6.69}$$

where $\epsilon_{\mu\nu}$ is the binormal vector to the event horizon surface. In the case of a Kerr black hole the above expression reduces to the simple form $S = A_H/4$. The horizon and asymptotic quantities are connected via the Smarr type relation [407, 408]

$$M = 2T_H S + 2\Omega_H J - 2\int_\Sigma d^3x\sqrt{-g}\mathcal{L}\bigg|_{\text{on-shell}}. \tag{6.70}$$

The Smarr relation is extremely important when studying numerical solutions as it provides a test to the code that relates physical quantities obtained on the horizon and asymptotic regions, allowing us to estimate the accuracy of the numerical method. Also of interest is the perimetral radius $\mathfrak{R}$ which is a geometrically significant radial coordinate such that a circumference along the equatorial plane has perimeter $2\pi\mathfrak{R}$. It is related to the coordinate r by

$$\mathfrak{R} = \sqrt{g_{\phi\phi}}\big|_{\theta=\pi/2} = \sqrt{\frac{g}{f}} r\bigg|_{\theta=\pi/2}. \tag{6.71}$$

To explore the horizon geometry, it is useful to define the horizon circumference along the equator

$$L_e = 2\pi\mathfrak{R}_H, \tag{6.72}$$

and along the poles

$$L_p = 2\int_0^\pi \sqrt{g_{\theta\theta}}|_{x=-1} d\theta = 2r_H \int_0^\pi \sqrt{\frac{gh}{f}}\bigg|_{x=-1} d\theta. \tag{6.73}$$

With these two quantities, we can define the sphericity

$$s = \frac{L_e}{L_p}. \tag{6.74}$$

For a Kerr black hole $s \geq 1$, with s increasing with spin. That means that spin deforms the horizon towards oblateness. The linear velocity of the horizon quantifies how fast the null geodesics generators of the horizon spin relative to a static observer at infinity and is given by

$$v_H = \Omega_H \mathfrak{R}_H. \tag{6.75}$$

For a Kerr black hole we have in terms of M and r_H

$$\begin{aligned}
J &= M^2 \sqrt{1 - \left(\frac{2r_H}{M}\right)^2}, \\
T_H &= \frac{1}{4\pi M \left(1 + \frac{M}{2r_H}\right)}, \\
A_H &= 8\pi M^2 \left(1 + \frac{2r_H}{M}\right) \\
L_e &= 4\pi M, \\
L_p &= 4M \sqrt{2\left(1 + \frac{2r_H}{M}\right)} \text{EllipticE}\left(\frac{1}{2}\left[1 - \frac{2r_H}{M}\right]\right), \\
\mathfrak{R}_H &= 2M,
\end{aligned} \tag{6.76}$$

where EllipticE denotes the complete elliptic integral of the second kind, and also note that $2r_H/M = \sqrt{1-\chi^2}$. Also, the Kerr solution is Ricci flat, and thus the GR Lagrangian vanishes on-shell and therefore so does the last term in Eq. (6.70).

6.2.4.2 Ergoregion

The ergoregion, defined as the domain outside the event horizon wherein the norm of the asymptotically timelike Killing vector $k = \partial_t$ becomes positive, $g_{\mu\nu}k^\mu k^\nu > 0$. It is bounded by the event horizon and by the surface where

$$g_{tt} = -f\mathcal{N}^2 + \frac{g\left(1-\mathcal{N}\right)^2 W^2}{f}\sin^2\theta = 0. \tag{6.77}$$

Within the ergoregion, an object cannot appear stationary with respect to a distant observer due to the intense frame-dragging.[32] Furthermore, ergoregions raise the possibility of extracting energy from a black hole via the Penrose process, or superradiant scattering [409]. Starting from the well-known result for the ergosphere of

[32] This immediately follows from the fact that the 4-velocity of a massive particle must be timelike, $g_{\mu\nu}u^\mu u^\nu < 0$. Indeed, the worldline of an object standing still at a fixed point implies that $u = \partial_t$, and if $g_{tt} \geq 0$, then $g_{\mu\nu}u^\mu u^\nu \geq 0$.

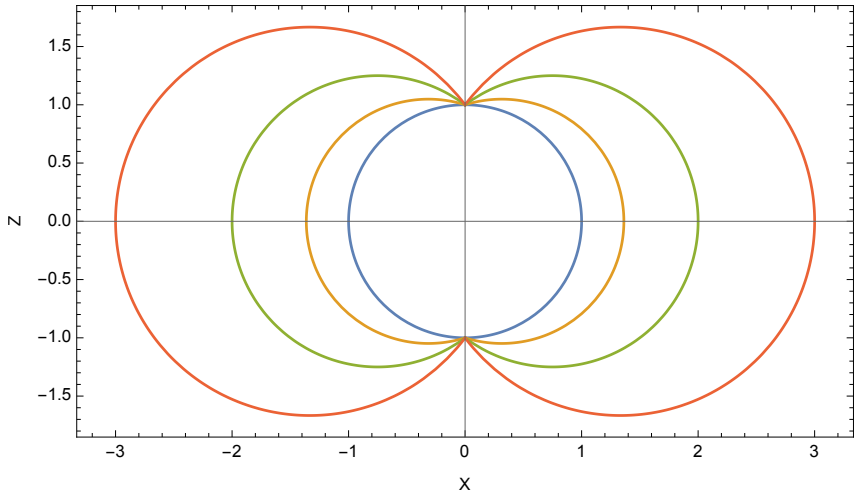

Figure 6.2.3: Ergoregion of a Kerr black hole with $\chi = 0.3$ (orange), $\chi = 0.6$ (green), and $\chi = 0.8$ (red) visualized on the $X - Z$ plane. The event horizon is shown in blue.

a Kerr black hole in Boyer-Lindquist coordinates and inverting the relation of Eq. (6.42) we obtain that in quasi-isotropic coordinates the ergosphere of a Kerr black hole is located at

$$r_E^{Kerr} = \frac{r_H}{\sqrt{1-\chi^2}} \left(\sqrt{1 - \chi^2 \cos^2\theta} + \chi \sin\theta \right), \tag{6.78}$$

where the subscript "E" refers to "ergoregion". Due to the symmetries of our problem, we need only consider the range $\theta \in [0, \pi/2]$. To visualize the ergoregion, we introduce the coordinates

$$X = \frac{r}{r_H} \sin\theta, \qquad Z = \frac{r}{r_H} \cos\theta. \tag{6.79}$$

In Fig. 6.2.3 we observe the ergoregion of a Kerr black holes in the $X - Z$ plane for several values of dimensionless spin.

6.2.4.3 Petrov type

The Petrov classification allows for a kinematic characterization of the gravitational field in a coordinate independent manner using algebraic properties of the Weyl tensor $C_{\mu\nu\alpha\beta}$, namely its number of distinct principal null directions. This classification is useful e.g. when searching for exact solutions, or for a Carter-like constant [410]. Using the Newman-Penrose formalism, the information is contained in five complex scalars, known as the Weyl scalars. With the null tetrad $\{l^\mu, n^\mu, m^\mu, \overline{m}^\mu\}$, where l^μ

Type	Conditions
O	$\psi_0 = \psi_1 = \psi_2 = \psi_3 = \psi_4 = 0$
I	$D \neq 0$
II	$D = 0, I \neq 0, J \neq 0, K \neq 0, N \neq 0$
III	$D = 0, I = J = 0, K \neq 0, L \neq 0$
N	$D = 0, I = J = K = L = 0$
D	$D = 0, I \neq 0, J \neq 0, K = N = 0$

Table 6.2.1: Summary of Petrov classification.

and n^μ are real, and $m^\mu, \overline{m}^\mu$ are complex conjugate satisfying the orthonormality conditions $l^\mu n_\mu = 1$, $m^\mu \overline{m}_\mu = -1$ and all other products zero, the Weyl scalars are defined as

$$\begin{aligned}
\psi_0 &= -C_{\mu\nu\alpha\beta} l^\mu m^\nu l^\alpha m^\beta, \\
\psi_1 &= -C_{\mu\nu\alpha\beta} l^\mu n^\nu l^\alpha m^\beta, \\
\psi_2 &= -C_{\mu\nu\alpha\beta} l^\mu m^\nu \overline{m}^\alpha n^\beta, \\
\psi_3 &= -C_{\mu\nu\alpha\beta} l^\mu n^\nu \overline{m}^\alpha n^\beta, \\
\psi_4 &= -C_{\mu\nu\alpha\beta} n^\mu \overline{m}^\nu n^\alpha \overline{m}^\beta.
\end{aligned} \tag{6.80}$$

With the above scalars, the following Lorentz invariant quantities can be constructed

$$\begin{aligned}
I &= \psi_0\psi_4 - 4\psi_1\psi_3 + 3\psi_2^2, \\
J &= -\psi_2^3 + \psi_0\psi_2\psi_4 + 2\psi_1\psi_2\psi_3 - \psi_4\psi_1^2 - \psi_0\psi_3^2, \\
D &= I^3 - 27J^2, \\
K &= \psi_4^2\psi_1 - 3\psi_4\psi_3\psi_2 + 2\psi_3^3, \\
L &= \psi_4\psi_2 - \psi_3^2, \\
N &= 12L^2 - \psi_4^2 I.
\end{aligned} \tag{6.81}$$

Given the above quantities, it is possible to determine the Petrov type of a given spacetime. The classification is summarized in Table 6.2.1 [411]. In particular, a spacetime is said to be *algebraically special* if $D = 0$. The Kerr(-Newman) spacetime is Petrov type D. In a numerical setup, we also find useful to introduce the *speciality index* defined as [412]

$$S = \frac{27J^2}{I^3}. \tag{6.82}$$

With an appropriate choice of tetrad, following Ref. [412], it is possible to gauge

away ψ_1 and ψ_3 to zero. Such a tetrad would be for example

$$\begin{aligned} l^\mu &= \sqrt{\frac{g_{\varphi\varphi}}{2\left(g_{t\varphi}^2 - g_{tt}g_{\varphi\varphi}\right)}}\left(1,0,0,-\frac{g_{t\varphi}+\sqrt{g_{t\varphi}^2 - g_{tt}g_{\varphi\varphi}}}{g_{\varphi\varphi}}\right), \\ n^\mu &= \sqrt{\frac{g_{\varphi\varphi}}{2\left(g_{t\varphi}^2 - g_{tt}g_{\varphi\varphi}\right)}}\left(1,0,0,-\frac{g_{t\varphi}-\sqrt{g_{t\varphi}^2 - g_{tt}g_{\varphi\varphi}}}{g_{\varphi\varphi}}\right), \\ m^\mu &= \frac{1}{\sqrt{2}}\left(0,\frac{i}{\sqrt{g_{rr}}},\frac{1}{\sqrt{g_{\theta\theta}}},0\right). \end{aligned} \tag{6.83}$$

6.2.4.4 Marginal Stable Circular Orbits: Light Rings and ISCO

The study of marginal stable circular orbits is of high relevance. The innermost stable circular orbit (ISCO) of massive particles is the smallest possible radius for a stable circular orbit and is often taken to mark the inner edge of an accretion disk around a black hole. Accelerated charged particles orbiting the black hole emit synchroton radiation whose physical properties are connected with the frequency of geodesics at the ISCO. Therefore, physical properties of an astrophysical black hole can be inferred via measurements of the ISCO through accretion disks.

Light rings are circular null geodesics, typically unstable, allowing light to encircle a black hole before being scattered to infinity or falling into the event horizon. From an observational point of view, they are important for observations made with the Event Horizon Telescope as they are intimately connected with the shadow of the black hole [413].

To compute the ISCO and light rings we follow Ref. [402]. We start by considering the line element of Eq. (6.31) in the form

$$ds^2 = g_{tt}dt^2 + g_{rr}dr^2 + g_{\theta\theta}d\theta^2 + g_{\varphi\varphi}d\varphi^2 + g_{t\varphi}dtd\varphi. \tag{6.84}$$

The two independent killing vectors of the spacetime, $k^\mu = \partial_t$ and $\Phi^\mu = \partial_\varphi$, have the associated conserved reduced energy E and angular momentum L

$$\begin{aligned} E &= -k_\mu \frac{dx^\mu}{d\lambda} = -g_{tt}\dot{t} - g_{t\varphi}\dot{\varphi}, \\ L &= \Phi_\mu \frac{dx^\mu}{d\lambda} = g_{t\varphi}\dot{t} + g_{\varphi\varphi}\dot{\varphi}, \end{aligned} \tag{6.85}$$

where $\dot{=}d/d\lambda$. The above expressions can be rearranged in terms of $\dot{t}$ and $\dot{\varphi}$

$$\begin{aligned}\dot{t} &= \frac{Eg_{\varphi\varphi} + Lg_{t\varphi}}{g_{t\varphi}^2 - g_{tt}g_{\varphi\varphi}},\\ \dot{\varphi} &= -\frac{Eg_{t\varphi} + Lg_{tt}}{g_{t\varphi}^2 - g_{tt}g_{\varphi\varphi}}.\end{aligned} \tag{6.86}$$

Considering orbits restricted to the equatorial plane, $\theta = \pi/2$, the condition associated with the normalization of the four-velocity of the particles becomes

$$-\epsilon = g_{tt}\dot{t}^2 + g_{rr}\dot{r}^2 + g_{\varphi\varphi}\varphi^2 + 2g_{t\varphi}\dot{t}\dot{\varphi}, \tag{6.87}$$

with $\epsilon = \{0, 1, -1\}$ for a massless, massive and tachyon particle, respectively. We disregard $\epsilon = -1$ from now on. Substituting the expressions of Eq. (6.86) in the above condition, and solving for $\dot{r}^2$, we can define the effective potential

$$U_{eff} = \frac{1}{g_{rr}}\left(-\epsilon + \frac{E^2 g_{\varphi\varphi} + 2ELg_{t\varphi} + L^2 g_{tt}}{g_{t\varphi}^2 - g_{tt}g_{\varphi\varphi}}\right), \tag{6.88}$$

such that

$$\dot{r}^2 = U_{eff}. \tag{6.89}$$

The conditions for a circular orbit are $\dot{r} = 0$ and $\ddot{r} = 0$, from which follows that

$$U_{eff} = 0, \qquad \frac{dU_{eff}}{dr} \equiv U'_{eff} = 0, \tag{6.90}$$

at the location of orbit. The dash denotes a derivative with respect to r. These conditions can further be rearranged into algebraic equations that must be satisfied simultaneously

$$\begin{aligned}&E^2 g_{\varphi\varphi} + 2ELg_{t\varphi} + L^2 g_{tt} - \epsilon\left(g_{t\varphi}^2 - g_{tt}g_{\varphi\varphi}\right) = 0,\\ &E^2 g'_{\varphi\varphi} + 2ELg'_{t\varphi} + L^2 g'_{tt} - \epsilon\left(g_{t\varphi}^2 - g_{tt}g_{\varphi\varphi}\right)' = 0.\end{aligned} \tag{6.91}$$

Light Rings

For a light particle, $\epsilon = 0$. In this case, calculations are simpler than in the massive case. Solving the first equation for L in (6.91) and substituting in the second we obtain

$$g'_{\varphi\varphi} + 2g'_{t\varphi}\left(\frac{g_{t\varphi} \pm \sqrt{g_{t\varphi}^2 - g_{tt}g_{\varphi\varphi}}}{g_{tt}}\right) + g'_{tt}\left(\frac{g_{t\varphi} \pm \sqrt{g_{t\varphi}^2 - g_{tt}g_{\varphi\varphi}}}{g_{tt}}\right)^2 = 0, \tag{6.92}$$

which is to be evaluated on a radius r. The smallest root of the above equation is the location of the light ring.

In Boyer-Lindquist coordinates the location of the circular photon orbits of a Kerr black hole are given by [414]

$$r_{BL}^{LR\pm} = 2M\left(1+\cos\left(\frac{2}{3}\arccos\left(\mp\chi\right)\right)\right), \tag{6.93}$$

where the plus sign refers to co-rotating photons, and the minus sign to counter-rotating photons. In quasi-isotropic coordinates the location of the circular photon orbits can be obtained using the inverse transformation in Eq. (6.43).

ISCO

For a massive particle, $\epsilon = 1$. The ISCO is located at a saddle point of the effective potential, such that the condition $U''_{eff} = 0$ should be imposed. This is equivalent to imposing

$$E^2 g''_{\varphi\varphi} + 2ELg''_{t\varphi} + L^2 g''_{tt} - \epsilon\left(g^2_{t\varphi} - g_{tt}g_{\varphi\varphi}\right)'' = 0, \tag{6.94}$$

in addition to Eq. (6.91). To find the location of the ISCO, we first solve Eq. (6.91) for E and L as functions of the metric functions and their first derivatives, and later substitute these onto Eq. (6.94). Similarly to the light-ring case, we obtain a second order equation to be solved for r, the smallest root of which corresponds to the location of the ISCO.

In Boyer-Lindquist coordinates the location of the circular massive particle orbits of a Kerr black hole are given by [414]

$$r_{BL}^{ISCO\pm} = M\left(3+Z_2 \mp \sqrt{(3-Z_1)(3+Z_1+2Z_2)}\right), \tag{6.95}$$

where

$$Z_1 = 1+\left(1-\chi^2\right)^{1/3}\left[(1+\chi)^{1/3}+(1-\chi)^{1/3}\right],$$
$$Z_2 = \sqrt{3\chi^2+Z_1^2},$$

and the plus sign refers to co-rotating particles, and the minus sign to counter-rotating particles. In quasi-isotropic coordinates the location of the circular orbits can be obtained using the inverse transformation in Eq. (6.43).

Orbital frequencies at the ISCO and Light Ring

The orbital angular frequency of particles both at the ISCO and light ring is given by

$$\omega_\pm = \frac{\dot{\varphi}}{\dot{t}} = \frac{-g'_{t\varphi} \pm \sqrt{g'^2_{t\varphi} - g'_{tt}g'_{\varphi\varphi}}}{g'_{\varphi\varphi}}, \tag{6.96}$$

where the above expression is to be evaluated at the location of the ISCO/light ring, ω_+ is the angular frequency of co-rotating particles and ω_- is the angular frequency of counter-rotating particles. In the case of a Kerr black hole we have

$$M\omega_\pm = \pm \frac{1}{\sqrt{48\cos^4\left(\frac{1}{3}\arccos\left(\mp\chi\right)\right)+\chi^2}}, \tag{6.97}$$

at the light ring, and

$$M\omega_\pm = \pm \frac{1}{\left(r_{BL}^{ISCO\pm}/M\right)^{3/2}\pm\chi}, \tag{6.98}$$

at the ISCO. The orbital frequency at the ISCO is associated with the cut-off frequency of the emitted synchrotron radiation generated from accelerated charges in accretion disks, and the angular frequency at the light ring is related to the time-scale of the response of the black hole when it is perturbed (real part of the frequency of the black hole quasi-normal modes) [415].

6.3 Numerical spinning black hole solutions

In this section we validate our numerical infrastructure against well-known results, namely the Kerr black hole, and then proceed to use it to obtain spinning black holes in a modified gravity theory, the Einstein-scalar-Gauss-Bonnet theory.

6.3.1 Validating the code against the Kerr black hole

To validate our numerical infrastructure we will solve the axisymmetric vacuum Einstein equations to numerically obtain the Kerr solution, and compare with analytical results. We choose the following combination of the field equations, $\mathcal{E}^\mu{}_\nu = 0$, which diagonalizes the equations with respect to the operator $\partial_r^2 + r^{-2}\partial_\theta^2$:

$$\begin{aligned}
&-\mathcal{E}^\mu{}_\mu + 2\mathcal{E}^t{}_t + \frac{2Wr_H}{r^2}\mathcal{E}^\varphi{}_t = 0,\\
&\mathcal{E}^\varphi{}_t = 0,\\
&\mathcal{E}^r{}_r + \mathcal{E}^\theta{}_\theta = 0,\\
&\mathcal{E}^\varphi{}_\varphi - \frac{2Wr_H}{r^2}\mathcal{E}^\varphi{}_t - \mathcal{E}^r{}_r - \mathcal{E}^\theta{}_\theta = 0.
\end{aligned} \tag{6.99}$$

In Fig. 6.3.1 we present the results for the comparison of the metric functions obtained numerically with the analytically known ones for a Kerr black hole with $\chi = 0.6$. The initial guess that was used to obtain the results in Fig. 6.3.1 was

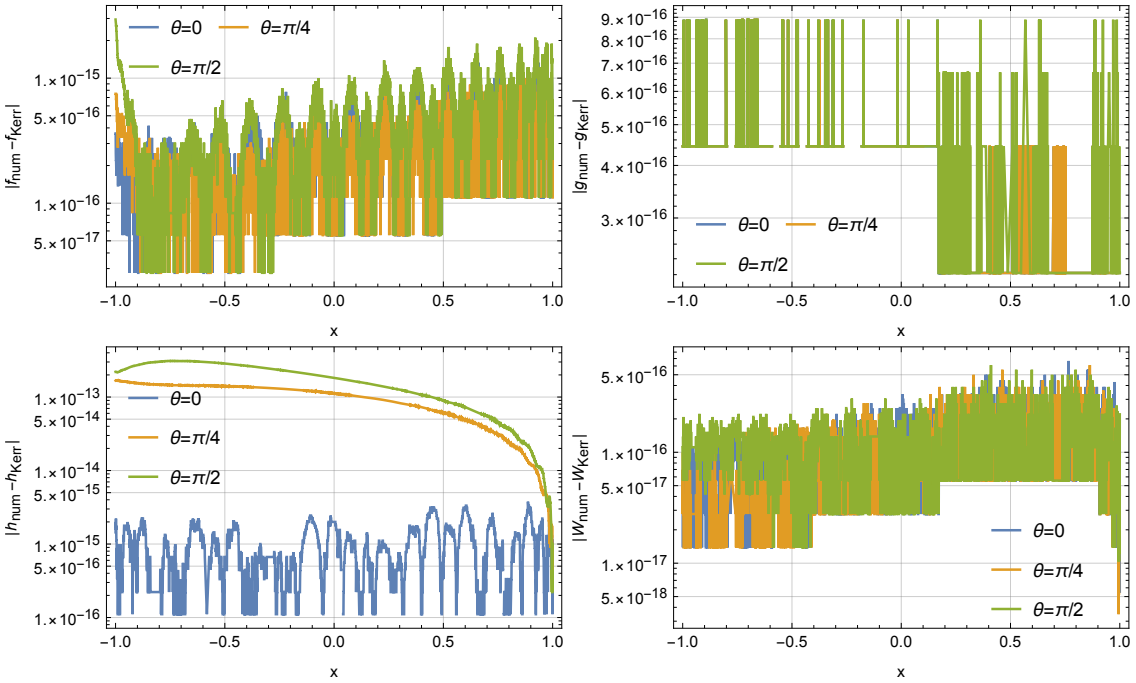

Figure 6.3.1: Comparison between the numerical and analytical results for a Kerr black hole with $\chi = 0.6$, using $N_x = 42$, $N_\theta = 8$. The maximum observed error is of order $\mathcal{O}(10^{-13})$ for the function h, with all other functions being obtained to machine precision. A Schwarzschild black hole was used as an initial guess, and we have used $r_H = 1$.

a Schwarzschild black hole with comparable r_H. The maximum observed error is of order $\mathcal{O}(10^{-13})$ for the metric function h, with all other metric functions being successfully obtained to machine precision. We also explored the whole domain of existence of Kerr black holes, comparing numerically obtained physically relevant quantities with analytical ones, see Fig. 6.3.2 below. These include the mass M, angular momentum J, horizon area A_H and Hawking temperature T_H of the black holes. Furthermore, we computed the (normalized) Smarr relation in Eq. (6.70). Overall, in all quantities we have found remarkable agreement between numerical and analytical results, with the Smarr relation providing accurate error estimates. We also observe that errors are higher when the black holes approach extremality ($\chi \to 1$). This is because in the extremal limit, our metric ansätz is not valid.

6.3.2 Einstein-scalar-Gauss-Bonnet Gravity

Einstein-scalar-Gauss-Bonnet (EsGB) theories of gravity were introduced in the first chapter, and will be discussed in more detail in chapter 7. For convenience, we will reproduce here the action of the theory and its field equations. EsGB theories are

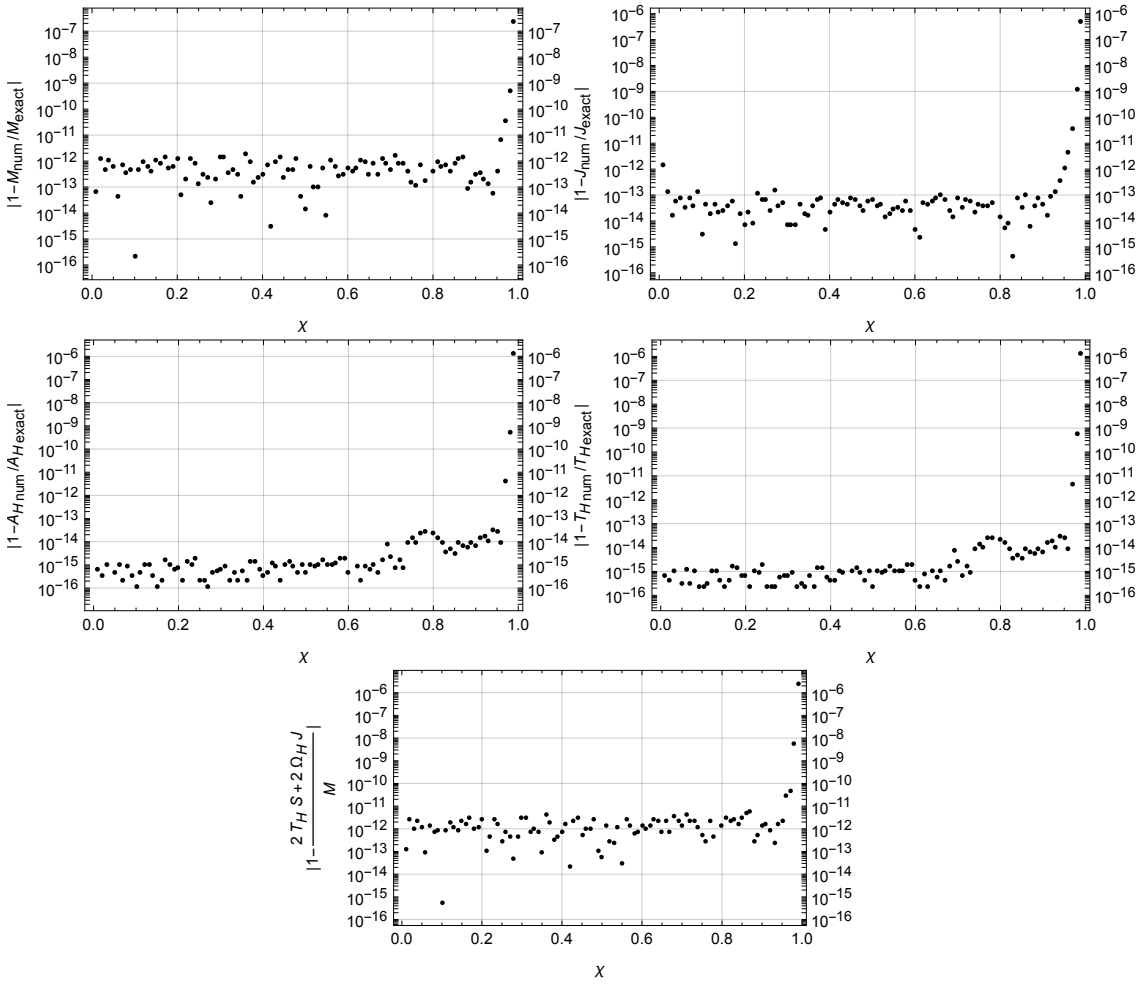

Figure 6.3.2: Comparison of numerical results for M, J, A_H and T_H with analytical ones, throughout the domain of existence of Kerr black holes. Each point represents a different black hole solution. Numerical results were obtained using $N_x = 50$, $N_\theta = 12$. We observe remarkable agreement and small errors overall.

described by the action

$$\mathcal{S} = \frac{1}{16\pi}\int d^4x\sqrt{-g}\left(R - (\nabla\phi)^2 + \frac{\alpha}{4}\xi\left(\phi\right)\mathcal{G}\right), \tag{6.100}$$

which contains a new real scalar field ϕ, which couples non-minimally to the Gauss-Bonnet term via the coupling function $\xi(\phi)$, and α is a coupling constant with dimensions of length squared. No known closed-form black hole solutions are known in these models, even in the static case. One is therefore forced to resort to numerical methods to study black holes in these theories.

The field equations of the action (6.100) are

$$\mathcal{E}_{\mu\nu} \equiv G_{\mu\nu} - T_{\mu\nu} = 0, \tag{6.101}$$

where

$$T_{\mu\nu} = \nabla_\mu\phi\nabla_\nu\phi - \frac{1}{2}g_{\mu\nu}\left(\nabla\phi\right)^2 + \alpha\, P_{\mu\alpha\nu\beta}\nabla^\alpha\nabla^\beta\xi\left(\phi\right),$$

and

$$P_{\alpha\beta\mu\nu} \equiv \frac{1}{4}\epsilon_{\alpha\beta\gamma\delta}R^{\rho\sigma\gamma\delta}\epsilon_{\rho\sigma\mu\nu} = 2\,g_{\alpha[\mu}G_{\nu]\beta} + 2\,g_{\beta[\nu}R_{\mu]\alpha} - R_{\alpha\beta\mu\nu},$$

is the double-dual Riemann tensor (the square brackets denote anti-symmetrization). The scalar field equation is

$$\mathcal{E}_\phi \equiv \Box\phi + \frac{\alpha}{8}\dot{\xi}(\phi)\mathcal{G} = 0, \tag{6.102}$$

where the dot denotes differentiation with respect to the scalar field ϕ. In the stationary and axisymmetric setting we discussed before, we find that the scalar field is subject to the boundary conditions [401, 402]

$$\begin{aligned} &\partial_x\phi = 0, \qquad x = -1, \\ &\phi = 0, \qquad x = 1, \\ &\partial_\theta\phi = 0, \qquad \theta = 0, \pi/2, \end{aligned} \tag{6.103}$$

while the boundary conditions for the metric functions remain the same.

Black holes in the EsGB theory should obey the Smarr formula (6.70), that becomes

$$M + M_s = 2T_H S + 2\Omega_H J, \tag{6.104}$$

where [33]

$$M_s = -\frac{1}{4\pi}\int d^3x\sqrt{-g}\frac{\xi(\phi)}{\xi'(\phi)}\Box\phi, \tag{6.105}$$

and the entropy is given by Eq. (6.69) that in the EsGB case becomes

$$S = \frac{A_H}{4} + \frac{\alpha}{8}\int_H d^2x\sqrt{\mathfrak{h}}\xi(\phi)R^{(2)}, \tag{6.106}$$

where $R^{(2)}$ is the Ricci scalar of the induced metric on the horizon. We will focus on two coupling examples, the linear coupling

$$\xi(\phi) = \phi, \tag{6.107}$$

and the exponential coupling

$$\xi(\phi) = e^{\gamma\phi}. \tag{6.108}$$

We find that for the exponential coupling the Smarr relation takes a rather simple form

$$M + Q_s/\gamma = 2T_H S + 2\Omega_H J, \tag{6.109}$$

where Q_s is the scalar charge of the solution, appearing in the asymptotic expansion of the scalar field

$$\phi \approx \frac{Q_s}{r} + \mathcal{O}\left(r^{-2}\right).$$

It can also be proved that for the linear coupling the following relation holds [416]

$$Q_s = 2\pi\alpha T_H. \tag{6.110}$$

In what follows we use the relations in Eqs. (6.109) and (6.110) to address the accuracy of our numerical solutions for the exponential and linear couplings respectively. This is necessarily as closed-form solutions are unknown. We use the same combination of field equations as in the Kerr case (Eq. (6.99)), along with the scalar field equation (6.102) to solve the system. To solve the system we use a comparable Kerr black hole as an initial guess for the metric functions, and for the scalar field

[33] This relation can also be written as

$$M_s = \frac{1}{4\pi}\int d^3x\sqrt{-g}\,(\nabla\phi)^2\,\frac{\partial}{\partial\phi}\left(\frac{\xi(\phi)}{\xi'(\phi)}\right),$$

provided the coupling does not obey $\xi(\phi) = \xi'(\phi)$ and the scalar field asymptotically vanishes. This is advantageous from a numerical point of view because no second derivatives of the scalar field are required, increasing the accuracy in computing M_s.

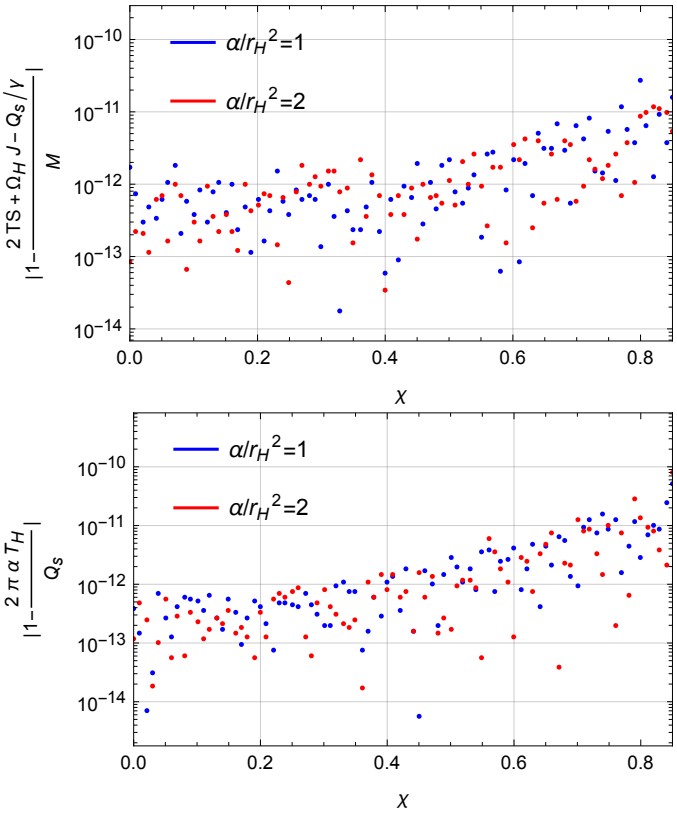

Figure 6.3.3: Smarr relation (top) and relation in Eq. (6.110) (bottom) for numerical solutions in a part of the domain of existence for the theory with the exponential coupling with $\gamma = 1$ and linear coupling, respectively, for different values of α/r_H^2. Each point represents a different black hole solution. Numerical results were obtained using $N_x = 50$, $N_\theta = 12$. We observe small errors, similarly to the Kerr case.

we use the perturbative solution [401, 402]

$$\phi \approx \frac{\alpha}{r_H^2}\frac{415 - 1047x + 942x^2 - 358x^3 + 51x^4 - 3x^5}{12(-3+x)^6}. \tag{6.111}$$

We present the accuracy estimate results (in a part of the domain of existence) using the Smarr relation for the exponential coupling and the relation in Eq. (6.110) for the linear coupling in Fig. 6.3.3. We observe that errors, as measured by the relations (6.109) and (6.110), are small and similar to those presented for the Kerr black hole in Fig. 6.3.2, despite a dramatic increase in the complexity and number of terms in the field equations. Our results also agree remarkably well with perturbative solutions, such as the ones obtained in Ref. [402].

As another test to the code, in Figure 6.3.4 we plot the accuracy as estimated by the Smarr relation (6.109) as a function of both resolutions N_x and N_θ. We

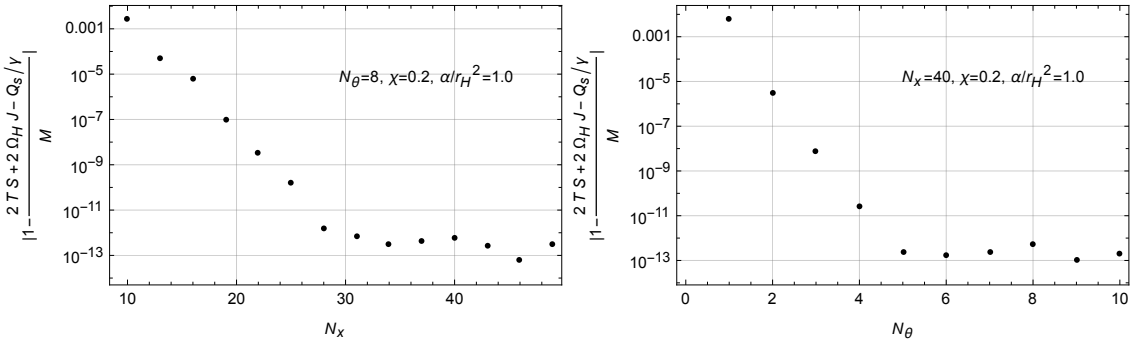

Figure 6.3.4: Smarr relation for numerical solutions with a dilaton coupling ($\gamma = 1$) as a function of the resolution in x (left) and θ (right). We observe exponential convergence to as the resolution is increased.

observe exponential convergence, similarly to the toy model presented in Fig. 6.1.4. Note that the Smarr relation provides only an estimate of maximum error – recall the Kerr case, where most metric functions were actually obtained to a precision of $\sim \mathcal{O}(10^{-16})$ but the Smarr relation attained errors on the order of $\sim \mathcal{O}(10^{-13})$.

To further demonstrate the capabilities of our code, in the following we present some results for the physical properties of EsGB black holes. A plot of the ergoregion for a dilaton black hole with $\gamma = 1$, $\chi = 0.1$ and $\alpha/M^2 = 1.15$ can be found in Fig. 6.3.5. In Fig. 6.3.6 we plot $|1 - S|$ as a function of x and θ, where S is the speciality index defined in Eq. (6.82), for the same EsGB black hole as before, where we can observe that the spacetime is not algebraically special, being Petrov type I. Spinning EsGB black holes were always observed to be Petrov type I.[34]

The perimetral location and angular frequencies at the ISCO and light rings of EsGB dilaton black holes ($\gamma = 1$) are compared with those of a Kerr black hole (with the same χ and M) in Fig. 6.3.7. Note that we have neglected any couplings between the dilaton and matter (see e.g. [84, 417]). We have compared our results in the static and slowly rotating cases with those in Ref. [417], observing remarkable agreement (in the appropriate setup). From Fig. 6.3.7 we observe differences of a few percent in most cases, with the most drastic differences occurring for the location of the co-rotating light ring due to its proximity to the horizon. The qualitative behaviour is as follows: the perimetral radius of both the ISCO and the light ring decreases with α/M^2, and the opposite happens for the angular frequencies[35]. Co-rotating orbits are most affected, and black hole spin enhances the differences of

[34] With our numerical setup, a Kerr black hole typically yields values of $|1 - S|$ on the order of 10^{-15} everywhere, in good agreement with the fact that it is Petrov type D.

[35] We note that, similarly to Refs. [401, 402], positive coordinate shifts in the location of the ISCO/light ring were observed. These are, however, not physically relevant and the perimetral radius should be used, where negative shifts are observed.

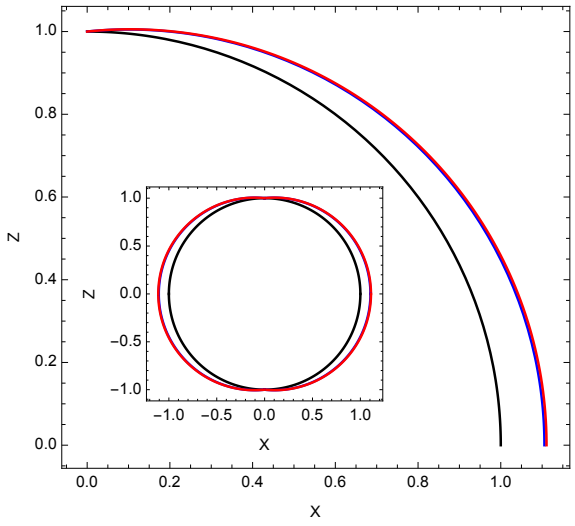

Figure 6.3.5: Ergosphere for a EsGB dilaton black hole with $\gamma = 1$, $\chi = 0.1$ and $\alpha/M^2 = 1.15$ (red), together with the ergosphere of a Kerr black hole with the same χ (blue). The event horizon for both is presented in black.

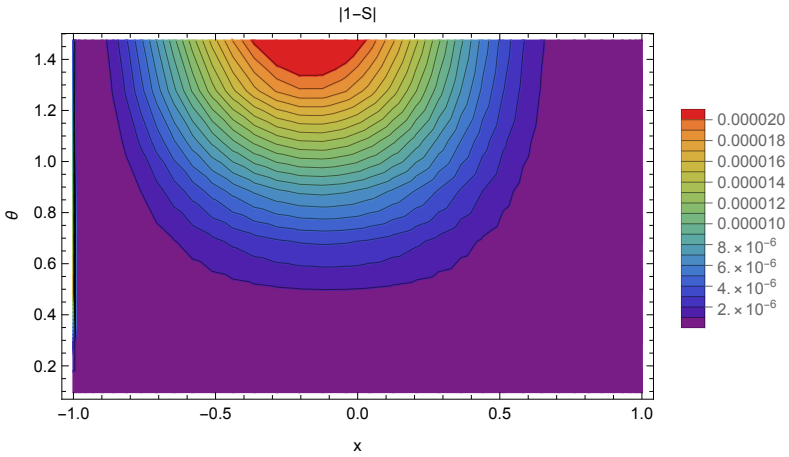

Figure 6.3.6: $|1 - S|$ plotted as a function of x and θ, where S is the speciality index defined in Eq. (6.82), for a EsGB dilaton black hole with $\gamma = 1$, $\chi = 0.1$ and $\alpha/M^2 = 1.15$. The non-vanishing value of $|1 - S|$ demonstrates that the spacetime is Petrov type I.

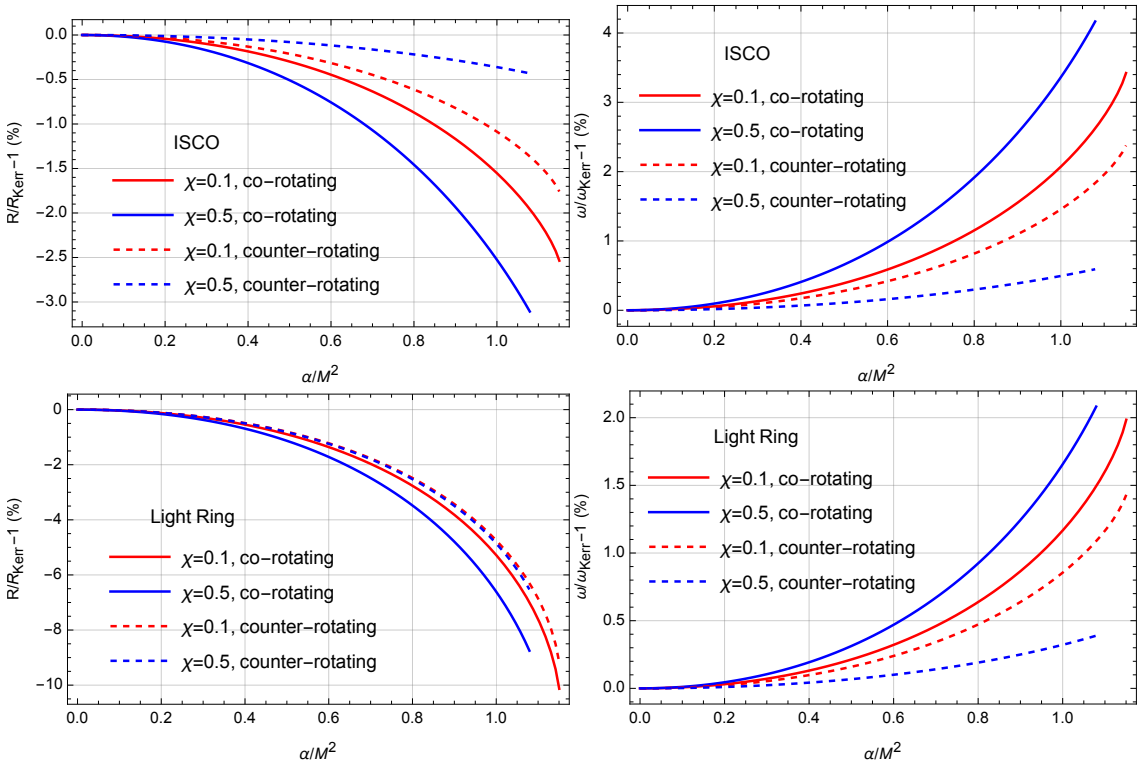

Figure 6.3.7: Comparison between EsGB dilaton ($\gamma = 1$) and Kerr black holes with the same χ (and M) regarding the perimetral radius and angular frequencies at the ISCO (top) and light ring (bottom) as a function of α/M^2, in a part of the domain of existence of solutions.

co-rotating orbits with respect to the Kerr case.

6.4 Comparison with other codes

Similar codes to the one we have developed in this chapter are scarce. Indeed, most of the numerical studies of spinning black holes in modified theories of gravity make use of the non-publicly-available FIDISOL/CADSOL solver [418–420], which implements a finite difference method together with the root finding Newton-Raphson method. The solver is written in Fortran and was first developed in the eighties. Works that use the FIDISOL/CADSOL solver can be found e.g. in Refs. [73, 77, 80, 81, 83, 84, 394–396]. Some of these works have applied the FIDISOL/CADSOL solver in studies of EsGB gravity, much like we did here. However, they report an error of order $\mathcal{O}(10^{-3})$, as estimated by the Smarr relation. In the appendix of Ref. [421], the author gives a comprehensive overview of the FIDISOL/CADSOL solver, benchmarking it against the Kerr solution, with results again showing errors several orders of magnitude higher than those presented in Fig.

6.3.2.

More recently, in Ref. [402] the authors developed the *eXtreme Partial Differential Equations Solver* (XPDES) code which is publicly available, to address similar problems. The code is written in C language, and implements a finite difference method to solve the field equations, similarly to the FIDISOL/CADSOL package. It makes use of the software *Maple* to export the field equations to many large C programming files. Ref. [402] does not discuss errors as estimated by Smarr relations, instead, they (also) benchmark their code against the Kerr solution, and compare their EsGB results to perturbative solutions, finding good agreement. They report typical maximum errors on obtaining the Kerr solution of $\mathcal{O}\left(10^{-6}\right)$, which represents a good improvement when compared with the FIDISOL/CADSOL package, especially given that the XPDES code is open-source and publicly available.

Our code is written in the Julia programming language, which when compared with complied languages such as C code makes it logistically easier to use and adapt, and to implement new models. In our implementation the field equations and boundary conditions are written in a very simple way. For example, the boundary condition

$$f - 2\partial_x f = 0,$$

is written as a residual in code language as

$$f - 2 * dfdx.$$

The code is memory efficient and fast, making use of pseudospectral methods as explained above, with solutions to the field equations being obtained in the order of a few seconds in laptop-class computers. In our (limited) comparisons with the XPDES code, we found that where our code took only a few seconds the XPDES code would take minutes to achieve a lower accuracy.

The results of this chapter, for example in Figs. 6.3.2 and 6.3.3, show that the accuracy of our code is many orders of magnitude better than the accuracy presented by either the FIDISOL/CADSOL package or even the XPDES code.

Once a solution to the field equations has been obtained, our code has built-in functions to compute all the physical properties of the black holes discussed in section 6.2.4, therefore allowing for a simple and comprehensive study of different models. Given that the code has been completed only recently, we have not yet applied it widely. A first application in research work is, however, contained the next chapter. In the future we hope to apply the code to other theories, such as our

regularized 4DEGB theory, and use it to further constrain them using the physical properties described.

Appendix

Appendix 6.A The Kerr-Newman Black Hole

The Kerr-Newman solution solves the Einstein-Maxwell field equations

$$G_{\mu\nu} = 2\left(F_{\mu}{}^{\alpha}F_{\nu\alpha} - \frac{1}{4}g_{\mu\nu}F_{\alpha\beta}F^{\alpha\beta}\right). \tag{6.112}$$

The Einstein-Maxwell field equations can be obtained with the following action principle

$$\mathcal{S} = \frac{1}{16\pi}\int d^4x\sqrt{-g}\left(R - F_{\mu\nu}F^{\mu\nu}\right), \tag{6.113}$$

where $F_{\mu\nu} = \nabla_\mu A_\nu - \nabla_\nu A_\mu$ is the Maxwell tensor. With the ansätz of Eq. (6.31) the Kerr-Newman black hole solution reads (in terms of r_H, M and Q)

$$\begin{aligned} f_{\rm KN} &= \left(1+\frac{r_H}{r}\right)^2\frac{\mathcal{A}}{\mathcal{B}}, \\ g_{\rm KN} &= \left(1+\frac{r_H}{r}\right)^2, \\ h_{\rm KN} &= \frac{\mathcal{A}^2}{\mathcal{B}}, \\ W_{\rm KN} &= \frac{r\left(2M^2-Q^2\right)+2M\left(r^2+r_H^2\right)}{r_H r^3\mathcal{B}}\sqrt{M^2-Q^2-4r_H^2} \end{aligned} \tag{6.114}$$

where

$$\begin{aligned} \mathcal{A} &= \frac{r^2\left(2M^2-Q^2\right)+2Mr\left(r^2+r_H^2\right)+\left(r^2-r_H^2\right)^2}{r^4} - \frac{\left(M^2-Q^2-4r_H^2\right)}{r^2}\sin^2\theta, \\ \mathcal{B} &= \left(\mathcal{A}+\frac{\left(M^2-Q^2-4r_H^2\right)}{r^2}\sin^2\theta\right)^2 - \frac{\left(r^2-r_H^2\right)^2\left(M^2-Q^2-4r_H^2\right)}{r^6}\sin^2\theta, \end{aligned} \tag{6.115}$$

together with the four-potential

$$A_\mu dx^\mu = \left(\tilde{A}_t - \frac{W_{KN}}{r}\left(1-\mathcal{N}\right)\tilde{A}_\varphi\sin^2\theta\right)dt + \tilde{A}_\varphi\sin^2\theta d\varphi, \tag{6.116}$$

where

$$\tilde{A}_\varphi = \frac{Qr\left(1+\frac{M}{r}+\frac{r_H^2}{r^2}\right)\sqrt{M^2-Q^2-4r_H^2}}{r^2\left(1+\frac{M}{r}+\frac{r_H^2}{r^2}\right)^2+(M^2-Q^2-4r_H^2)\cos^2\theta}, \tag{6.117}$$

and

$$\tilde{A}_t = \Phi - \frac{Qr\left(1+\frac{M}{r}+\frac{r_H^2}{r^2}\right)}{r^2\left(1+\frac{M}{r}+\frac{r_H^2}{r^2}\right)^2+(M^2-Q^2-4r_H^2)\cos^2\theta} + \frac{W_{KN}}{r}(1-\mathcal{N})\,\tilde{A}_\varphi \sin^2\theta, \tag{6.118}$$

where Q the electric charge and Φ the electrostatic potential (which can be chosen such that $\tilde{A}_t|_{r_H} = 0$). This particular choice of functions $\tilde{A}_t$ and $\tilde{A}_\varphi$ for the vector potential is such that they are optimised for a numerical setup such as ours.

The total angular momentum (per unit mass), a, of the solution is related to M, Q and r_H via

$$r_H = \frac{\sqrt{M^2-a^2-Q^2}}{2} \equiv \frac{M}{2}\sqrt{1-\chi^2-q^2}, \tag{6.119}$$

where we have defined the dimensionless charge

$$q \equiv Q/M. \tag{6.120}$$

The electric charge can be read off the asymptotic decay of the temporal part of the four potential

$$\tilde{A}_t = \Phi - \frac{Q}{r} + \mathcal{O}\left(r^{-2}\right). \tag{6.121}$$

The Kerr-Newman black hole obeys the well-known Smarr relation

$$M = 2TS + 2\Omega_H J + \Phi Q. \tag{6.122}$$

Note that the Kerr-Newman black hole in the quasi-isotropic coordinate system presented in Eq. (6.31) can be obtained from the standard textbook Boyer-Lindquist coordinates solution with the radial coordinate transformation

$$r_{BL} = r + M + \frac{M^2-a^2-Q^2}{4r} = r\left(1+\frac{M}{r}+\frac{r_H^2}{r^2}\right). \tag{6.123}$$

Details about marginal stable circular orbits in the Kerr-Newman case can be found in Refs. [422, 423].

7 Exploring the Small Mass Limit of Gauss-Bonnet Black Holes

As discussed in chapter 1, prominent examples of alternative theories of gravity to General Relativity (GR) are *Einstein-scalar-Gauss-Bonnet* (EsGB) theories, where a new fundamental scalar is non-minimally coupled to the Gauss-Bonnet term. Such models belong to the Horndeski class of theories [104, 105], and in the simplest case their action takes the form

$$S = \frac{1}{16\pi}\int d^4x\sqrt{-g}\left(R - (\nabla\phi)^2 + \frac{\alpha}{4}\xi(\phi)\,\mathcal{G}\right), \tag{7.1}$$

where ϕ is a real scalar field, $\xi(\phi)$ is the (non-minimal) coupling function, and α the GB coupling constant with dimensions of length squared. Note that even though the scalar-tensor formulations of 4DEGB discussed in the previous chapters also contain scalar-Gauss-Bonnet interactions, we will refer to *EsGB models* as those uniquely described by an action of the form (7.1). Therefore, in our discussions 4DEGB and EsGB refer to two different classes of theories. As discussed in Chapter 1, EsGB models are of wide interest and have been the subject of many works in recent years (see e.g. [70–77, 79–83, 85, 424–434]), and are motivated from both fundamental and phenomenological points of view, that we review next. From a fundamental physics perspective they arise, for example, as the low-energy limit of some string theories [63–66] where the scalar, *the dilaton*, couples exponentially to the GB term, $\xi(\phi) \sim e^{\gamma\phi}$ [82, 83, 85, 435]. From a more phenomenological point of view, they are one of a variety of theories [70–77, 79–83, 85, 424–426, 435–438] that evade the no hair conjecture [439–446] (see [42] for a review), raising the exciting possibility they can be constrained by black hole (BH) physics in the strong-curvature regime. Moreover, in some EsGB theories a dynamical mechanism called *spontaneous scalarization* [74–76, 79–81, 435–438] can occur, such that deviations from GR occur *only* in the strong-curvature regime. Constraints can be theoretical, such as self-consistency, or observational in nature. Indeed, only recently has GR begun to be tested observationally in the strong-field regime [447], with the dawn of gravitational wave

(GW) astronomy [30, 392, 448].

In a striking difference to GR, some EsGB black holes (e.g. with linear and dilatonic couplings) are known to possess a minimum mass solution [71, 82] whose Hawking temperature is finite and non-vanishing, naturally raising the question of what is the fate of black holes in EsGB theories. This conundrum is often overlooked, but was recently explored in Refs. [449, 450], where non-linear numerical simulations of evaporating EsGB dilatonic black holes were performed, supporting the idea that the end-point of Hawking evaporation is likely a naked singularity, violating weak cosmic censorship. This is rather concerning scenario, raising question about the consistency of these EsGB models.

In this chapter our main purpose is to explore further the small mass limit of black holes for several couplings in the simplest EsGB theories, including those allowing for spontaneous scalarization. Our aim is to investigate self-consistency and observational constraints imposed on Gauss-Bonnet theories and their coupling dependence. After providing a novel example of a closed-form solution with a small mass limit, we will complement previous studies on EsGB black hole solutions with a thorough analytical and numerical exploration of the domain of existence of solutions and their inner structure, linking the existence of an inner singularity to the repulsive effects originating from the Gauss-Bonnet term, and the structure of the field equations. Using analytical arguments, this singularity will be shown to overlap with the event horizon in the small mass limit. We will also provide for the first time, in this context, an example of a coupling function where the small mass limit is never reached, showing that a minimum size solution is *not* a generic feature of EsGB theories. Finally, we construct stationary black hole solutions by numerically solving the field equations in axisymmetry, with the aim of exploring the small mass limit once spin is considered, and finish by imposing the tightest constraints on the coupling constant, to date, on the dilatonic and linear theories.

The rest of the chapter is organized as follows. First, in Section 7.1, we introduce a theory which, unlike Eq. (7.1), admits a known analytical example of a static black hole with a small mass limit. This allows us to explore key features with the advantage of an exact solution. In Section 7.2, we discuss the form of coupling functions in standard Gauss-Bonnet theories and their corresponding different phenomenologies. Then in Section 7.3, we explore the small mass limit of static black hole solutions for these theories, and later impose upper bounds on the coupling constant α in Section 7.4. Finally, in Section 7.5, we consider how spin changes the picture.

7.1 Exploring the small mass limit: An analytical example

No analytic closed-form black hole solution is known to EsGB models described by the action (7.1). In the existing literature, therefore, the study of critical solutions in such theories has been performed by resorting to numerical techniques. In this section, we will explore an illustrative example of a related theory with known closed-form black hole solutions.

The theory is the *gravity with a generalized conformal scalar field theory* [4], discussed in Chapter 5. Its action is given by Eq. (5.19), presented again below

$$S = \int \frac{d^4x\sqrt{-g}}{16\pi}\Bigg[R - (\nabla\Phi)^2 - \frac{R}{6}\Phi^2 - 2\lambda\Phi^4 \\ + \alpha\bigg(\log(\Phi)\mathcal{G} - \frac{4G^{\mu\nu}\nabla_\mu\Phi\nabla_\nu\Phi}{\Phi^2} - \frac{4\Box\Phi(\nabla\Phi)^2}{\Phi^3} + \frac{2(\nabla\Phi)^4}{\Phi^4}\bigg)\Bigg], \tag{7.2}$$

which contains the terms present in the EsGB model of Eq. (7.1) with a logarithmic coupling, as well as other non-trivial interactions including a conformal coupling to gravity and a conformally invariant quartic self-coupling. Note that for the purpose of presentation, we have flipped the sign of α relative to the presentation of Ref. [4] and Chapter 5, and that of typical 4D-Einstein-Gauss-Bonnet studies. Also, we set $\beta = 1/6$ such that the scalar possesses a canonical kinetic term like EsGB models do. Among the many interesting features of Eq. (7.2), one that stands out is that a special combination of the field equations decouples from the scalar field, imposing a proportionality condition between the Ricci and GB scalars (see the discussion in chapter 5)

$$R = \frac{\alpha}{2}\mathcal{G}\,. \tag{7.3}$$

This allows for an easy search of closed form solutions. One known closed-form black hole solution to the above theory (with $\lambda^{-1} = 48\alpha$) is given by

$$ds^2 = -f(r)e^{-2\delta(r)}dt^2 + \frac{dr^2}{f(r)} + r^2\left(d\theta^2 + \sin^2\theta d\varphi^2\right), \tag{7.4}$$

with

$$f(r) = 1 - \frac{r^2}{2\alpha}\left(1 - \sqrt{1 - \frac{8M\alpha}{r^3}}\right), \qquad \delta(r) = 0, \\ \Phi(r) = \frac{2\sqrt{3\alpha}}{r}\mathrm{sech}\left(\int^r \frac{dr}{r\sqrt{f}}\right), \tag{7.5}$$

where M is the ADM mass of the black hole, and we take α to be positive. This is the same black hole solution as presented in section 5.2, here reproduced and adapted to the conventions used in this chapter. The scalar field can be seen to be regular on and outside the event horizon located at

$$r_H = M + \sqrt{M^2 + \alpha}. \tag{7.6}$$

Analyzing the Ricci scalar of the solution (7.5) we observe that

$$R \propto r^{-3/2} \left(r^3 - 8M\alpha\right)^{-3/2}, \tag{7.7}$$

revealing the existence of two physical singularities, one located at $r = 0$, and a finite radius singularity located at the point where the quantity inside the square-root in Eq. (7.5) for the function $f(r)$ vanishes

$$r = r_s = 2\left(M\alpha\right)^{1/3} > 0. \tag{7.8}$$

To ensure physical behaviour of the solution we require that i) the singularity located at $r = r_s$ is hidden behind the event horizon ($r_s < r_H$); ii) the metric functions and the scalar field in Eq. (7.5) are real. Under these requirements, it can be shown using Eqs. (7.5), (7.6), and (7.8) that the following condition must hold

$$\frac{M}{\sqrt{\alpha}} > \frac{1}{2\sqrt{2}} \approx 0.353553\,, \tag{7.9}$$

or, in terms of r_H,

$$\frac{r_H}{\sqrt{\alpha}} > \sqrt{2} \approx 1.41421\,. \tag{7.10}$$

In other words there is a minimum mass $M^{min} = \frac{\sqrt{\alpha}}{2\sqrt{2}}$ (or equivalently, a minimum horizon radius $r_H^{min} = \sqrt{2\alpha}$), below which solutions can no longer be described by black holes. For an object with $r_H = r_H^{min}$, r_s and r_H overlap, as can be observed in Fig. 7.1.1. A possible physical interpretation for the minimum mass solution is related to the repulsive effect of the Gauss-Bonnet term on the solutions. Examining the components of the effective stress-energy tensor we get

$$\rho \equiv T^t_{\ t,eff} = -p_r, \qquad p_r \equiv T^r_{\ r,eff} = \frac{3\left(1 - \sqrt{1 - 8\alpha M/r^3}\right)^2}{4\alpha\sqrt{1 - 8\alpha M/r^3}}, \tag{7.11}$$

where ρ and p_r are interpreted as the effective energy density and radial pressure,

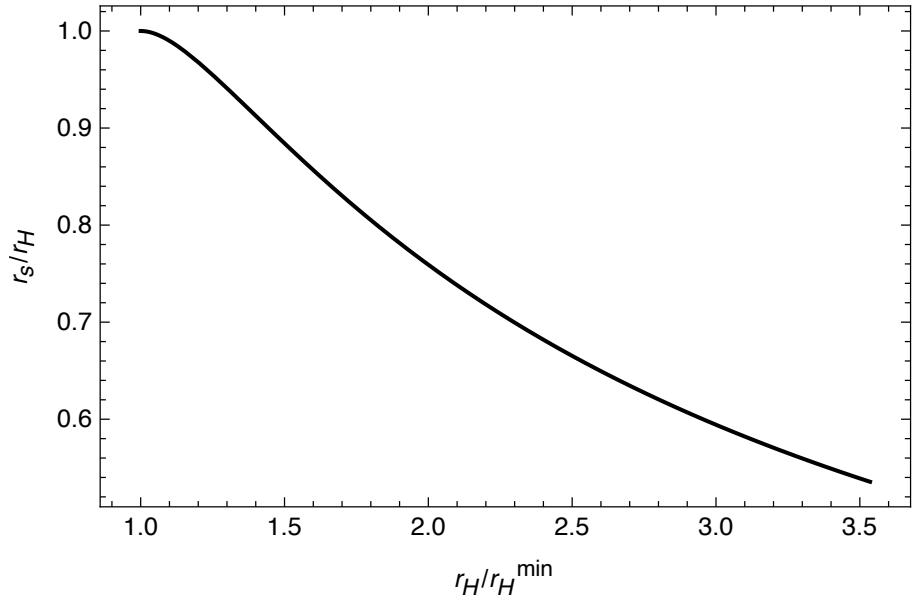

Figure 7.1.1: Location of the finite radius singularity r_s/r_H as a function of r_H/r_H^{min} for the black hole solution of Eq. (7.5). We observe that r_s and r_H overlap as $r_H \to r_H^{min}$.

respectively.[36] The effective radial pressure is positive everywhere (repulsive), and diverges at $r = r_s$. Indeed, for the minimum mass solution, the repulsive effects of the Gauss-Bonnet term dominate over the standard attractive ones, impeding the existence of a regular horizon.

An interesting remark can be made regarding the Hawking temperature of the black hole solution given by

$$T_H = \frac{1}{4\pi} f'(r_H) = \frac{r_H^2 + \alpha}{4\pi r_H \left(r_H^2 - 2\alpha\right)} \,. \tag{7.12}$$

This is that not only is the temperature non-zero as $r_H \to r_H^{min}$, but in fact diverges! Therefore, as the small mass limit is approached, evaporation will not halt and the black hole will continue to lose its mass at a rate [451]

$$\frac{dM}{dt} = -\frac{1}{2\pi} \sum_{\ell,m} \int d\omega \frac{\omega G_{\ell m}(\omega)}{e^{\omega/T_H} \pm 1}, \tag{7.13}$$

where $G_{\ell m}(\omega)$ are the graybody factors for modes with frequency ω, angular dependence (ℓ, m), and the plus/minus sign is related to the emission of fermions/bosons. This intriguing feature casts doubts on the endpoint of Hawking evaporation, with

[36] Note that the dominant energy condition is saturated and e.g. the weak energy condition is violated.

the above calculations suggesting that a naked singularity is a strong endpoint candidate.

To summarize, there are a few lessons to be learned from the example. First, it appears that theories with higher-curvature terms are susceptible to the existence of a finite radius singularity located at $r_s > 0$. The existence of this singularity is, mathematically, intimately tied to terms containing square-roots in the solutions to the field equations, and the requirement that solutions are real. From a more physical point of view, the singularity is related to repulsive effects originating from the Gauss-Bonnet term. Secondly, a minimum mass solution might exist, where the location of the finite radius singularity and of the event horizon overlap. In the above example, this *critical* solution possesses a non-vanishing Hawking temperature, causing the black hole to keep losing its mass. It is unknown what would be the endpoint of evaporation.

7.2 Einstein-scalar-Gauss-Bonnet gravity: Field Equations and the shape of $\xi(\phi)$

We now consider the more standard framework of the action of Eq. (7.1). Varying with respect to the metric tensor we obtain the Einstein equations

$$\mathcal{E}_{\mu\nu} \equiv G_{\mu\nu} - T_{\mu\nu} = 0, \tag{7.14}$$

where

$$T_{\mu\nu} = \nabla_\mu\phi\nabla_\nu\phi - \frac{1}{2}g_{\mu\nu}\left(\nabla\phi\right)^2 + \alpha\, P_{\mu\alpha\nu\beta}\nabla^\alpha\nabla^\beta\xi\left(\phi\right),$$

and

$$P_{\alpha\beta\mu\nu} \equiv \frac{1}{4}\epsilon_{\alpha\beta\gamma\delta}R^{\rho\sigma\gamma\delta}\epsilon_{\rho\sigma\mu\nu} = 2\, g_{\alpha[\mu}G_{\nu]\beta} + 2\, g_{\beta[\nu}R_{\mu]\alpha} - R_{\alpha\beta\mu\nu},$$

is the double-dual Riemann tensor (the square brackets denote anti-symmetrization). The scalar field equation is

$$\mathcal{E}_\phi \equiv \Box\phi + \frac{\alpha}{8}\dot{\xi}(\phi)\mathcal{G} = 0, \tag{7.15}$$

where the dot denotes differentiation with respect to the scalar field ϕ.

Starting with the scalar field equation (7.15), we review how different shapes of the coupling function $\xi(\phi)$ allow different phenomenologies. First we note that classical vacuum GR solutions require that $\phi = 0$, and that these solutions only exists for couplings that obey the condition $\dot{\xi}(0) = 0$. On the other hand solutions of models

whose couplings obey $\dot{\xi}(0) \neq 0$ necessarily differ from those of GR and possess a non-trivial scalar field. Common examples of couplings obeying $\dot{\xi}(0) \neq 0$ are

$$\xi(\phi) = e^{\gamma\phi}, \tag{7.16}$$

and

$$\xi(\phi) = \phi. \tag{7.17}$$

The first, hereby dubbed the *dilatonic* (or exponential) coupling, is motivated from string theory, as it is the coupling that appears in the 4D low-energy limit of heterotic string theory [63–66, 82, 83, 85, 435]. The second – the linear coupling – can be considered as a linearization of the first around $\phi = 0$, and additionally possesses a shift-symmetry in the scalar field [70, 71, 73]. For the dilatonic coupling, we focus on the $\gamma = 1$ case. Note, however, that as discussed in [449, 450] the properties of black hole solutions might differ for other values of γ. In fact, for sufficiently negative values ($\gamma \lesssim -1$), the small mass limit and the small size (radius) limit might not coincide, with small mass limit solutions being regular on and outside the horizon. For all the solutions discussed on this work, however, the minimum size and mass limits coincide, and therefore we will use these terms interchangeably.

As discussed, if the coupling function satisfies $\dot{\xi}(0) = 0$, then $\phi = 0$ solves the field equations and the GR solutions are solutions to the model. If however, $\ddot{\xi}(0) > 0$ then the GR solutions are subject to tachyonic instabilities in the large curvature regime. This can be seen by linearizing the scalar field equation around GR solutions, for example about the Schwarzschild solution. For a perturbation $\delta\phi$ (for which $\dot{\xi}(0 + \delta\phi) \approx \dot{\xi}(0) + \ddot{\xi}(0)\delta\phi$) one finds that

$$\left(\Box_{GR} + \frac{\alpha}{8}\ddot{\xi}(0)\mathcal{G}_{GR}\right)\delta\phi \equiv \left(\Box_{GR} - \mu^2_{eff}\right)\delta\phi = 0, \tag{7.18}$$

where $\mathcal{G}_{GR} = 48M^2/r^6 = 12r_H^2/r^6 > 0$ (with M being the ADM mass of the black hole and r_H the event horizon radius in Schwarzschild-like coordinates). Thus for $\alpha > 0$, if $\ddot{\xi}(0) > 0$ the Schwarzschild black hole may develop an instability (as the effective mass gets negative, $\mu^2_{eff} < 0$) [37]. In this tachyonic regime, it has been shown that another class of solutions with a non-trivial scalar-field profile coexists with the GR solutions and are dynamically preferred, triggering spontaneous scalarization. In order to explore spontaneous scalarization we assume couplings of these type to

[37] See also Ref. [427] for the special case where $\ddot{\xi}(0) = 0$. In this situation, no tachyonic instability exists but GR black holes may become unstable against non-linear scalar perturbations, leading to the formation of scalarized black holes.

obey the conditions

$$\xi(0) = 0, \qquad \dot{\xi}(0) = 0, \qquad \ddot{\xi}(0) = 1, \tag{7.19}$$

The first condition can be imposed as the theory is invariant under $\xi(\phi) \to \xi(\phi)+cte$, the second condition arises by requiring the existence of GR solutions and third condition can be imposed without loss of generality while maintaining a tachyonic instability in the large curvature regime. An example of such a coupling, commonly used in the literature [74, 77, 80, 452–456], and that we shall study here is the "quadratic exponential" coupling

$$\xi(\phi) = \frac{1}{2\beta}\left(1 - e^{-\beta\phi^2}\right), \tag{7.20}$$

where β is a constant (not to be confused with β presented in the context of Chapter 5). Note that this choice is by no means unique, and a simple quadratic coupling $\xi(\phi) = \phi^2/2$ (which is a particular case of Eq. (7.20) in the limit of vanishing β) would suffice to explore spontaneous scalarization *per se*. However, black hole solutions in models with a simple quadratic coupling are unstable, contrarily to those with a quadratic exponential coupling [424], and phenomenologies might differ. We find that for any coupling obeying the conditions (7.19) the instability of a Schwarzschild black hole exists for (see Appendix 7.A for a detailed discussion)

$$r_H/\sqrt{\alpha} \lesssim 0.83. \tag{7.21}$$

Finally, we would like to point that another type of scalarization is possible, being induced by spin. For the Kerr metric, while for dimensionless spins $\chi \leq 0.5$ the Gauss-Bonnet term is positive definite, this is no longer true when higher spins are considered [457, 458]. Therefore, if along with the other conditions in Eq. (7.19) $\ddot{\xi}(0)$ is negative (instead of positive), fast-spinning Kerr black holes might be subject to a tachyonic instability [79–81]. A coupling compatible with this type of scalarization would be the coupling of Eq. (7.20) with a reversed overall sign. We will briefly discuss spin-induced scalarized solutions in Sec. 7.5.

7.3 Static black hole solutions, and their small mass limit

In the existing literature, it has been identified that static EsGB black holes exhibit similar behaviour to that described for the analytic case of Section 7.1. Namely, that

in these situations there is also a minimum mass solution, beyond which solutions can no longer be described by black holes [71,82]. In the shift-symmetric case, it was further noticed that an inner singularity and the horizon overlap in this limit [71]. In this section we explore this small mass limit of EsGB black holes for a generic coupling function, discussing the domains of existence of solutions. To explore the small mass limit of static black holes in EsGB models we employ the static and spherically symmetric line element of Eq. (7.4), for which the field equations are presented in Appendix 7.B. As already noted above no analytic solutions are known, and so numerical methods must be used.

Nonetheless, near the boundaries of our domain, analytic methods can be employed. We assume that a static black hole solution of the model allows the asymptotic expansion near the event horizon (hereby denoted by r_H)

$$f(r)=\sum_{n=1}^{\infty} f_n\,\epsilon^n, \qquad \delta(r)=\sum_{n=0}^{\infty} \delta_n\,\epsilon^n, \qquad \phi(r)=\sum_{n=0}^{\infty} \phi_n\,\epsilon^n, \qquad \epsilon\equiv\frac{r}{r_H}-1 \tag{7.22}$$

then, the near-horizon field equations to zeroth order in ϵ become

$$\begin{aligned}
\mathcal{E}^t{}_t=\mathcal{E}^r{}_r&=\frac{2r_H^2-2f_1r_H^2+\alpha f_1\phi_1\dot{\xi}(\phi_0)}{2r_H^4}=0,\\
\mathcal{E}^\theta{}_\theta=\mathcal{E}^\varphi{}_\varphi&=\frac{(f_1(-2+3\delta_1)-2f_2)\,r_H^2+\alpha f_1^2\phi_1\dot{\xi}(\phi_0)}{2r_H^4}=0,\\
\mathcal{E}_\phi&=\frac{2f_1\phi_1r_H^2+(3\delta_1f_1+f_1^2-2f_2)\,\alpha\dot{\xi}(\phi_0)}{2r_H^4}=0,
\end{aligned} \tag{7.23}$$

which can be solved for f_1 and ϕ_1 in terms of r_H and ϕ_0, implying the following relations

$$f_1=\frac{2r_H^2}{r_H^2+\sqrt{r_H^4-3\alpha^2\dot{\xi}(\phi_0)^2}}, \qquad \phi_1=\frac{-r_H^2+\sqrt{r_H^4-3\alpha^2\dot{\xi}(\phi_0)^2}}{\alpha\dot{\xi}(\phi_0)}. \tag{7.24}$$

From these expressions one immediately finds the remarkable result that the horizon radius has a minimum size beyond which the solution can no longer be described by a black hole[38]. This follows by imposing the reality condition that f_1 and ϕ_1 must be real, leaving us with the condition

$$r_H^4-3\alpha^2\dot{\xi}(\phi_0)^2\geq 0\Leftrightarrow r_H\geq r_H^{min}=\sqrt{\sqrt{3}|\alpha\dot{\xi}(\phi_0)|} \tag{7.25}$$

[38]Hereafter we assume $\alpha>0$.

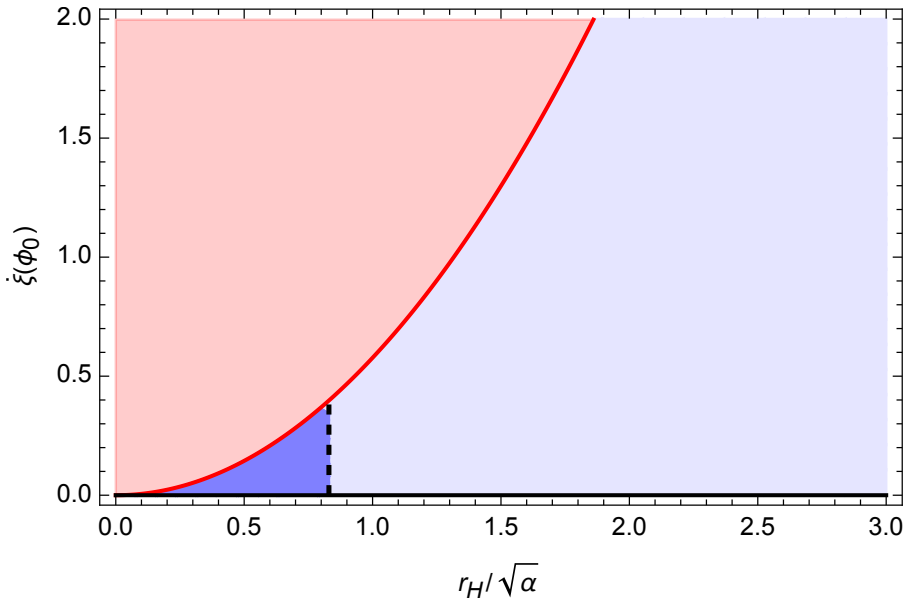

Figure 7.3.1: Domain of existence of black hole solutions with scalar hair (blue region), obtained by plotting the condition of Eq. (7.25) for a general coupling. The darker blue region denotes the region where the Schwarzschild black holes are unstable (*c.f.* Eq. (7.21)), for couplings obeying the conditions of Eq. (7.19). Beyond the red line, solutions can no longer be described by black holes.

or equivalently,

$$\dot{\xi}(\phi_0) \leq \frac{1}{\sqrt{3}} \left(\frac{r_H}{\sqrt{|\alpha|}} \right)^2 . \tag{7.26}$$

The above condition defines a region in the $(r_H/\sqrt{\alpha}, \dot{\xi}(\phi_0))$ plane within which BH solutions with a regular (real) scalar field configuration can exist. This is illustrated in Fig. 7.3.1, where we have also highlighted the spontaneous scalarization condition (7.21). Note, however, that the minimum horizon radius r_H^{min} depends on $\dot{\xi}(\phi_0)$. It is, therefore, conceivable that models where the minimum mass solution as given by Eq. (7.25) is never reached, depending on the behavior of ϕ_0 and of the coupling function.

To further explore the small mass limit of EsGB black holes, consider again the field equations given in Appendix 7.B, where we note that a closed-form expression for $\delta'(r)$ can be obtained by a simple algebraic manipulation of the (r, r) equation. Substituting the value of δ' onto the other field equations we can further rewrite the

whole system of field equations in matrix form[39]

$$\mathcal{M}\mathbf{x}' = \mathbf{b} \tag{7.27}$$

where $\mathcal{M}$ and $\mathbf{b}$ are a 2×2 matrix and a 2×1 column vector respectively, whose components are given in Appendix 7.B, and $\mathbf{x} = [f(r)\ \phi'(r)]^T$. Given the above system of equations, and appropriate initial conditions at some point $r = r_0$, the existence theorem asserts that a solution to the Cauchy problem to extend our solution to a neighboring point r_1 will exist if [459]

$$\det\mathcal{M}|_{r=r0} \neq 0. \tag{7.28}$$

Therefore, if a point $r = r^*$ exists such that the determinant of $\mathcal{M}$ vanishes, the system of field equations will be ill-posed at that point. The existence of such a point would indicate the presence of a coordinate or physical singularity, whose nature would have to be studied by other means. From a numerical point of view, any standard strategy used for numerical integration will stop before r^*. The determinant of $\mathcal{M}$ in Eq. (7.27) is given explicitly by

$$\det\mathcal{M} = \frac{f\left(\alpha^3 f^3 \mathcal{A} + \alpha^2 f^2 \mathcal{B} + \alpha f \mathcal{C} + \mathcal{D}\right)}{2r^4\left(\alpha(1-3f)\phi'\dot{\xi} + 2r\right)^2} \tag{7.29}$$

where the expressions for $\mathcal{A}, \mathcal{B}, \mathcal{C}, \mathcal{D}$ are again given in Appendix 7.B. A simple examination of the determinant (7.29) reveals the existence of two zeros at the locations where $f(r) = 0$, and where

$$\alpha^3 f^3 \mathcal{A} + \alpha^2 f^2 \mathcal{B} + \alpha f \mathcal{C} + \mathcal{D} = 0. \tag{7.30}$$

The first, is related to the location of the event horizon ($r^* = r_H$) and the correspondent singularity is a coordinate one. The second case is more intricate, and is related to a curvature (physical) singularity, as we will see.

As a toy model to help us understand this singularity, consider Eq. (7.30) for a Schwarzschild background. This can be seen as the zeroth order solution in an expansion in α of the dilatonic and linear EsGB models. The solution is

$$r^* = 6^{1/6}\left(M\alpha\right)^{1/3}. \tag{7.31}$$

[39]Here we have used the (t,t) and the scalar field equations.

Similarly to the analytical example in Eq. (7.8), we observe that, at least for very small couplings, there is a singularity obeying (approximately) a proportionality relation $r_s \propto (M\alpha)^{1/3}$.

Let us now explore the behavior of Eq. (7.30) near the event horizon of a EsGB black hole. Using the same near-horizon expansion as before (Eq. (7.22)), we observe that

$$\alpha^3 f^3 \mathcal{A} + \alpha^2 f^2 \mathcal{B} + \alpha f \mathcal{C} + \mathcal{D} = -4 r_H^5 \left(1 - \left(r_H^{min}/r_H\right)^4 + \sqrt{1 - \left(r_H^{min}/r_H\right)^4}\right) + \mathcal{O}(\epsilon)\,, \tag{7.32}$$

where r_H^{min} was defined in Eq. (7.25). Thus, we observe that Eq. (7.30) vanishes at the event horizon if $r_H = r_H^{min}$, indicating the presence of a singularity (other than the typical coordinate one). Therefore, we conclude that in the limit $r_H \to r_H^{min}$, an overlap of the curvature singularity and the event horizon occurs.

In the following sections we will explore the small mass limit of EsGB black holes in more detail, utilizing non-linear numerical solutions, and taking their inner structure into account.

7.3.1 Physical Quantities of Interest

To numerically integrate the field equations in order to obtain the black hole solutions, we match the near-horizon expansion of Eq. (7.22) with the appropriate asymptotic behaviour in far field ($r \to \infty$) limit:

$$f(r) = 1 - \frac{2M}{r} + \mathcal{O}\left(r^{-2}\right)\,, \qquad \delta(r) = \mathcal{O}\left(r^{-2}\right)\,, \qquad \phi(r) = \frac{Q_s}{r} + \mathcal{O}\left(r^{-2}\right)\,. \tag{7.33}$$

where M is the ADM mass and Q_s the scalar charge of the solution.

Horizon quantities of physical interest include the Hawking temperature T_H, the horizon area A_H, and the entropy S. For the line element (7.4) these are given by

$$T_H = \frac{1}{4\pi} f_1 e^{-\delta_0}, \qquad A_H = 4\pi r_H^2, \tag{7.34}$$

$$S = \frac{1}{4} A_H + \frac{\alpha}{8} \int_H d^2x \sqrt{h} \xi(\phi) R^{(2)} = \frac{1}{4} A_H + \pi \alpha \xi(\phi_0) \tag{7.35}$$

where h is the determinant of the induced metric on the horizon, and $R^{(2)}$ its Ricci scalar [407]. The horizon and asymptotic quantities are related by a Smarr-type relation given by [407, 408]

$$M + M_s = 2 T_H S, \tag{7.36}$$

where

$$M_s = -\frac{1}{4\pi}\int d^3x\sqrt{-g}\frac{\xi(\phi)}{\dot{\xi}(\phi)}\Box\phi. \tag{7.37}$$

For the dilatonic coupling (7.16) the above relation simplifies to $M_s = Q_s/\gamma$. Furthermore, it can be shown that for the linear coupling (7.17) the following condition holds [416]

$$Q_s = 2\pi\alpha T_H. \tag{7.38}$$

These conditions can be used to estimate the accuracy of our numerical method.

Once again, an interesting remark can be made about the Hawking temperature, that in the small mass/size limit gives

$$\lim_{r_H\to r_H^{min}} T_H = \frac{e^{-\delta_0}}{2\pi r_H^{min}} > 0 \tag{7.39}$$

and thus, as in the case of section 7.1, evaporation will not halt in the small mass limit and the black hole will continue to lose its mass at a rate given by Eq. (7.13), posing a potential threat to cosmic censorship.

7.3.2 Numerical Method

We now compute numerical solutions to the field equations. We use a Runge-Kutta-45 ordinary differential equation solver and implement a shooting method for the parameter ϕ_0 such that the asymptotic expansions are matched. In more detail, the near horizon expansion of Eq. (7.22) is used to set initial conditions for a numerical integration, with the only free parameter being ϕ_0 (once r_H and α are fixed). The field equations are then integrated from the horizon outwards to large r, the result is compared with the asymptotic expansion at large r, ϕ_0 adjusted, and the procedure repeated until the results of the numerical integration match the asymptotic expansion. Finally, using the results for the shooting parameters, the field equations are integrated from the horizon inwards to probe the internal structure of the black hole. We monitor curvature scalars such as the Ricci and GB scalars throughout the domain of integration, along with the determinant presented in Eq. (7.29). To test the accuracy of the numerical solutions we use the relations (7.36) and (7.38). We remark that errors are on the order of 10^{-8}.

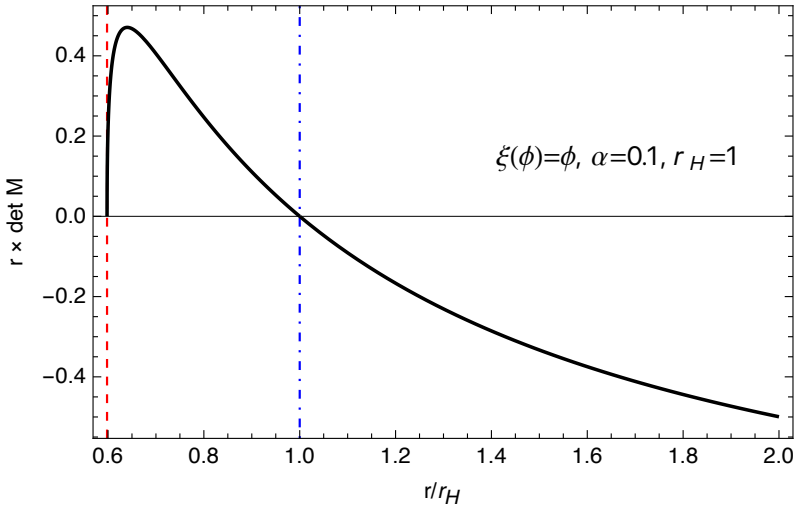

Figure 7.3.2: Determinant presented in Eq. (7.29) for the solution of the plot on the upper left in Fig. 7.3.3. We observe that det$\mathcal{M}$ has two zeros, one at the event horizon (blue dot-dashed line) and another at the singularity r_s (red dashed line).

7.3.3 Numerical Results

Using the numerical algorithm described, we have explored the linear (7.17), dilatonic (7.16) and quadratic exponential (7.20) couplings. For the latter, we explore several values of β.

7.3.3.1 Linear and Dilatonic Couplings

For the linear and dilatonic couplings, by monitoring the Ricci and GB scalars, a finite radius singularity was always found at a radius $r = r_s > 0$ inside the horizon, whose value ultimately depends on the ratio between the horizon radius and the coupling α. The singularity is located where det$\mathcal{M}$ in Eq. (7.29) vanishes inside the event horizon, as observed in Fig. 7.3.2.

In Fig. 7.3.3, we plot the metric functions along with the locations of r_s and r_H for several values of r_H^{min}/r_H. As the horizon radius approaches r_H^{min} (as one would expect to happen dynamically as Hawking evaporation proceeds), the horizon and the singularity overlap, and numerical solutions reveal divergences of the curvature invariants, derivatives of the metric functions and the scalar field. That the location of r_s and r_H overlap when $r_H \to r_H^{min}$ is in agreement with our analytical exploration shown in Eq. (7.32), and is similar to the behaviour observed in the analytical example of Section 7.1 (c.f. Fig. 7.1.1 and Fig. 7.3.4, right).

The domains of existence were constructed for both couplings, and can be observed

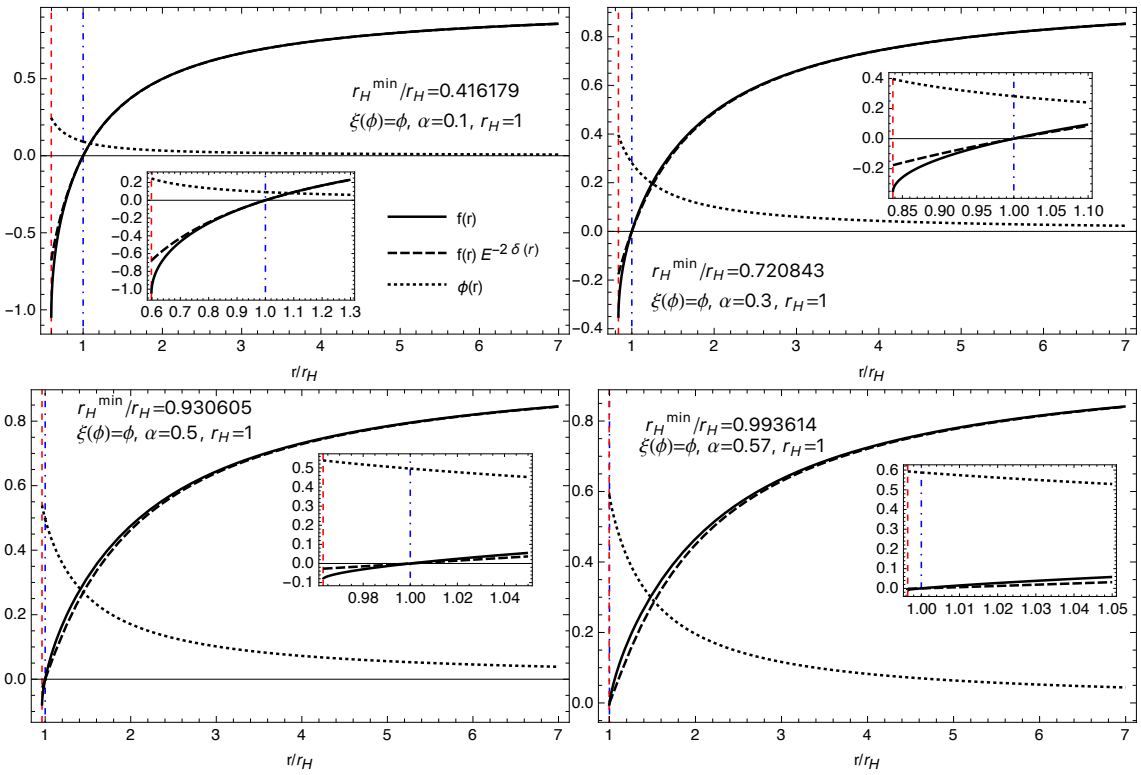

Figure 7.3.3: Metric functions and scalar field for four different values of $r_H/\sqrt{\alpha}$. The blue vertical line denotes the event horizon, while the red one denotes the location of the finite radius singularity r_s.

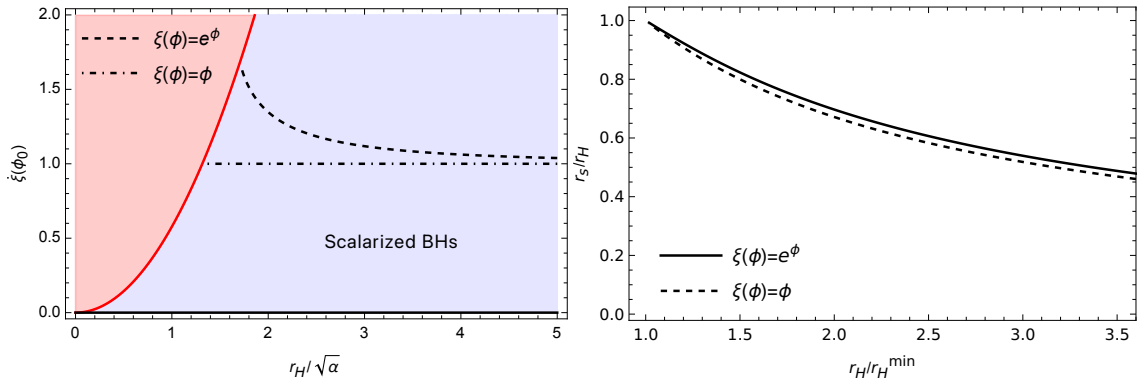

Figure 7.3.4: On the left we observe the domain of existence of black holes for the exponential (dashed line) and linear (dot-dashed line) couplings, delimited by the singular line in red. The intersection of the red line with the black ones denote the point in the domain where the finite radius singularity and the event horizon overlap, as $r_H \to r_H^{min}$, as observed in the figure on the right, for both couplings.

in Fig. 7.3.4 (left), where each point on the dashed and dot-dashed lines represent a numerical black hole solution. Note that the domains of existence end at the red line, where $r_H = r_H^{min}$. Assuming that Hawking radiation gradually reduces the mass of a black hole (and hence r_H) for some fixed α, but that our numerical solutions instantaneously remain an accurate approximation, we see that the fate of all black holes for both these couplings is to follow the lines on Fig. 7.3.4 and to always reach the red line.

7.3.3.2 Quadratic exponential (spontaneous scalarization) coupling

Consider now the coupling of Eq. (7.20). We will perform a similar analysis as before, for several values of β. Note that higher values of β suppress scalarization. The domains of existence for $\beta = 1, 3, 6$ can be observed in Fig. 7.3.5 on the left. We observe that for the $\beta = 1$ case, the domain of existence of solutions is similar to the dilatonic and linear coupling cases, where the location of the horizon and singularity overlap as the black hole shrinks, terminating in a critical solution. However, for $\beta = 3$ and 6, the domain of existence is radically different from the previous cases, as solutions never reach the singular (red) line, allowing the black hole to shrink to $r_H \sim 0$. This is possible due to the dependence of r_H^{min} on the value of the derivative of the coupling function at the horizon (as in Eq. (7.25)), and this behavior was observed for values

$$\beta > \beta_{\text{crit}} \approx 2.33125, \tag{7.40}$$

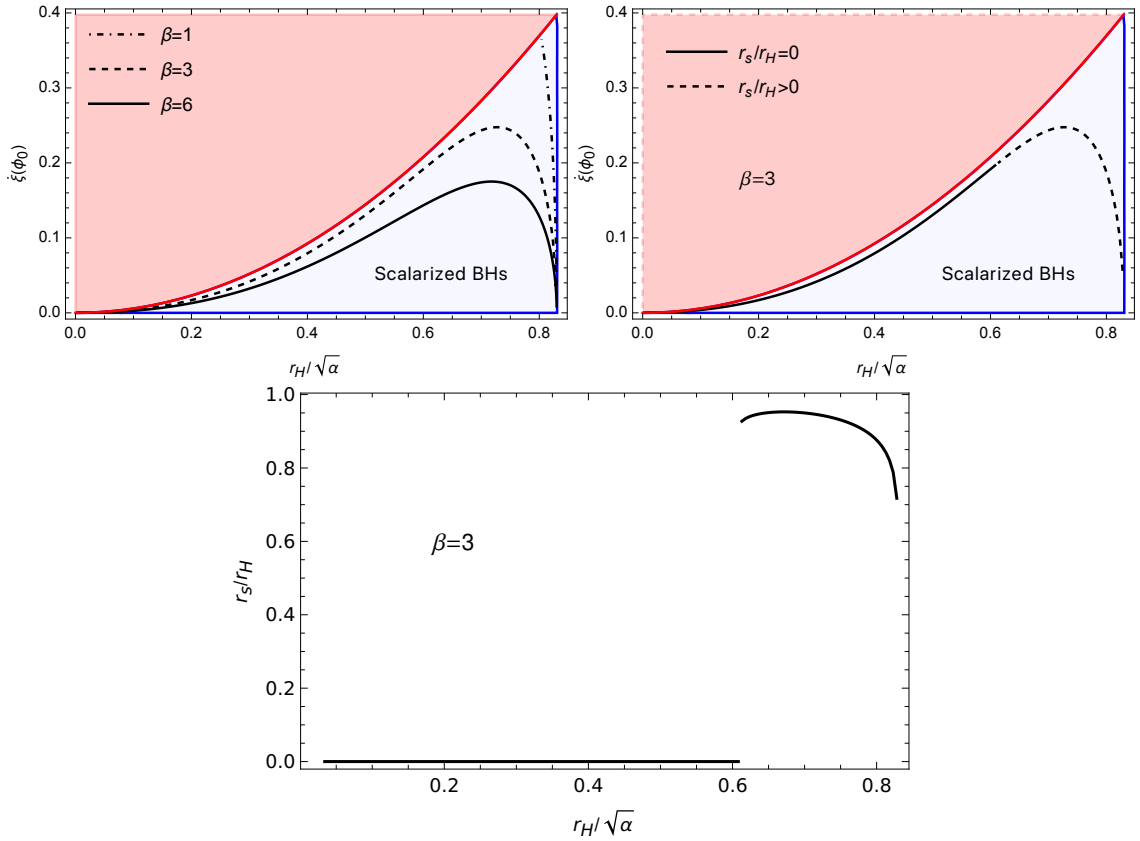

Figure 7.3.5: (Left) Domain of existence of spontaneously scalarized solutions for $\beta = 1, 3, 6$. For values $\beta < \beta_{\rm crit}$, the characteristics of the domain of existence are similar to those of the dilatonic and linear couplings, where the inner singularity and the horizon overlap as the BH shrinks. For larger values of β, solutions never reach $r_H = r_H^{min}$, and can shrink all the way down to $r_H = 0$. (Right) Behavior of the inner finite radius singularity for $\beta = 3$. A finite radius singularity with $r_s > 0$ exists only until the black hole shrinks to a certain $r_H/\sqrt{\alpha}$ value, beyond which there is no singularity other than at the origin. This can be observed at the bottom figure.

while for lower values the black line would intersect the red one, the domain of existence ending in a critical solution.

The behaviour of the inner finite radius singularity is rather curious for $\beta > \beta_{\rm crit}$. We find there exists a finite radius singularity with $r_s > 0$ only until to a certain value of $r_H/\sqrt{\alpha}$, below which there is no singularity other than at the origin. This is shown in Fig. 7.3.5 (right) for $\beta = 3$, where the dashed line show the part of the domain of solutions where $r_s > 0$ and the solid line the part for which $r_s = 0$. The transition is abrupt as shown in Fig. 7.3.5 (bottom), where the location of r_s is plotted as a function of r_H.

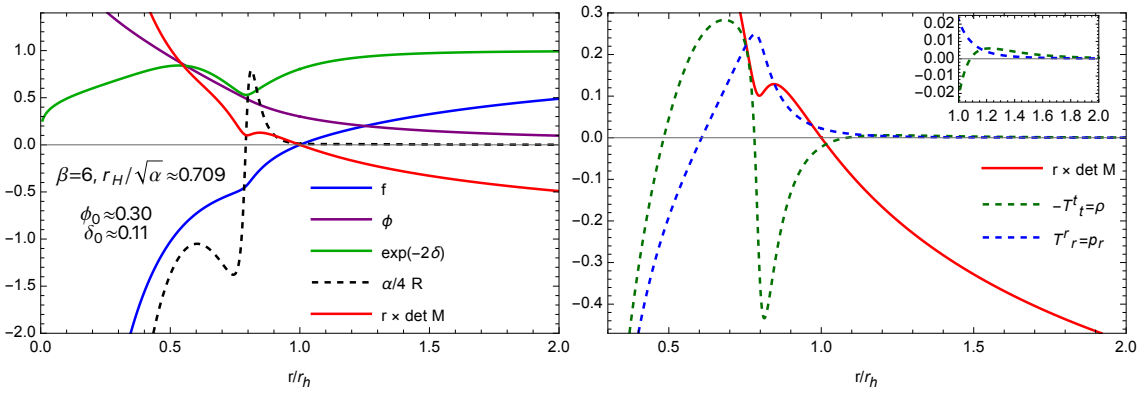

Figure 7.3.6: On the left we observe a fiducial black hole solution with no finite radius singularity (other than at $r = 0$). Note that $\det\mathcal{M}$ never vanishes inside the event horizon and the Ricci scalar is well-behaved all through the domain of integration (except at $r = 0$). On the right we present the components of the stress-energy tensor ρ and p_r (scaled by a factor of 10^{-1} for presentation purposes) for the same solution, where we observe that repulsive effects are maximum near the turning point of the determinant.

On Fig. 7.3.6 we observe a fiducial numerical black hole solution (along with other relevant quantities) for which there is no finite radius singularity. Note that $\det\mathcal{M}$ is strictly positive inside the event horizon. From a physical point of view we note that, as seen by the profile of the radial pressure p_r in Fig. 7.3.6 (right), repulsive effects are maximum near the turning point of $\det\mathcal{M}$. The determinant then gets further away from zero as the repulsive effects get gradually weaker further inside the horizon.

An intuitive view on Hawking evaporation for this coupling would be the following. Starting from a (sufficiently large) Schwarzschild black hole, Hawking radiation will gradually reduce the mass of the black hole (for some fixed α), until the condition of Eq. (7.21) is met. A tachyonic instability would then settle in, leading to dynamical scalarization of the Schwarzschild black hole. The new scalarized solution will itself evaporate, with the endpoint now depending on the value of β. If $\beta < \beta_{\rm crit}$, the picture would be not too different to that of the dilatonic and linear couplings explored in the previous sections and Refs. [449, 450], where the formation of a naked singularity is expected. However, if $\beta > \beta_{\rm crit}$, the evaporation process is expected to be similar to that of a Schwarzschild black hole, going all the way down to scales where quantum effects are expected to be important on general grounds, and our theory breaks down.

Remarkably, the behaviour of the inner singularity for the quadratic-exponential

coupling shows that the critical solution end point of the domain of existence is *not* a generic feature of gravitational theories with higher-order curvature terms.

7.4 Upper bounds on the coupling constant

If evaporation proceeds as expected the behaviour we have been illustrating indicates that the small mass regime of EsGB theories may constrain the *allowed form of couplings* through self-consistency arguments. However, even if evaporation is not taken into account, the minimum allowed size of black holes can place constraints on the strength of the allowed coupling through observational constraints.

To do so it is important to take a different form of the action such that results are consistent across the literature, and thus imposed on equivalent definitions of the coupling constant. When discussing observational constraints, the action for EsGB theories is usually presented in the following form [460–464]

$$\overline{S} = \int d^4x\sqrt{-g}\left(\frac{R}{16\pi} - \frac{1}{2}\left(\nabla\varphi\right)^2 + \overline{\alpha}\, F\left(\varphi\right)\mathcal{G}\right) \tag{7.41}$$

The mapping of the action (7.1) to the above parametrization can be done as

$$\phi = \sqrt{8\pi}\varphi, \qquad \alpha = 64\pi\overline{\alpha}, \tag{7.42}$$

and choosing $\xi(\phi)$ accordingly such that it is compatible with the definition of $F(\varphi)$. To be consistent with the literature, we will constraint the coupling constant $\overline{\alpha}$.

For each of coupling functions, we consider the singular static solution with $r_H = r_H^{min}$. Each of these singular black holes will have an associated minimum mass M_{min}. Assume now that an observation was made, in which a black hole was measured to have mass M_{obs}. To be consistent with the description of a black hole within the EsGB theory we impose that the observed mass is greater than the minimum mass

$$M_{obs}/\sqrt{\overline{\alpha}} > M_{min}/\sqrt{\overline{\alpha}} \equiv m_{min}. \tag{7.43}$$

Note that $M_{min}/\sqrt{\overline{\alpha}} \equiv m_{min}$ is a dimensionless quantity that can be extracted from the numerical solutions. Therefore, reintroducing SI units, we obtain the relation

$$\sqrt{\overline{\alpha}} < \frac{GM_{obs}}{c^2 m_{min}}. \tag{7.44}$$

This last equation allows us to impose an upper bound on the coupling constant for

each coupling function. For the static solutions, we have that

$$\begin{aligned} m_{min} &\approx 4.66717, \qquad \text{for} \qquad F(\varphi) = \varphi, \\ m_{min} &\approx 4.91642, \qquad \text{for} \qquad F(\varphi) = e^{\varphi}. \end{aligned} \tag{7.45}$$

Considering the case of GW190814 [465], where a compact object with a mass of around $M_{obs} = 2.6 M_{\odot}$ was observed, and assuming it is a black hole, our calculations give the upper bound

$$\begin{aligned} \sqrt{\overline{\alpha}} &\lesssim 0.82\,\text{km}, \qquad \text{for} \qquad F(\varphi) = \varphi, \\ \sqrt{\overline{\alpha}} &\lesssim 0.78\,\text{km}, \qquad \text{for} \qquad F(\varphi) = e^{\varphi}. \end{aligned} \tag{7.46}$$

To the best of our knowledge, these constraints are the tightest constraints on $\overline{\alpha}$ so far, with the previous strongest upper bound being $\sqrt{\overline{\alpha}} \lesssim 1.18\,\text{km}$ for the linear coupling [460]. Constraints on the coupling obtained using data from other events can be found in Table 7.4.1.

		Upper bound on $\sqrt{\overline{\alpha}}$ (km)	
Event/Ref.	M_{obs} $(M_{\odot})$	$F(\varphi) = \varphi$	$F(\varphi) = e^{\varphi}$
GW190814 [465]	2.59 ± 0.09	0.82 ± 0.03	0.78 ± 0.03
[466]	3.04 ± 0.06	0.95 ± 0.02	0.91 ± 0.02
[467]	$3.30^{+2.8}_{-0.7}$	$1.04^{+0.89}_{-0.22}$	$0.99^{+0.84}_{-0.21}$
GW200115 [468]	$5.70^{+1.8}_{-2.1}$	$1.80^{+0.57}_{-0.66}$	$1.71^{+0.54}_{-0.63}$

Table 7.4.1: Upper bounds on the coupling $\sqrt{\overline{\alpha}}$ obtained using data from several different events.

7.5 Spinning Black Hole Solutions

So far we have only studied static black hole solutions. In this section we will go one step further and explore spinning black hole solutions in EsGB theories. For this we resort, once again, to numerical integration of the field equations given in Section (7.2). The numerical procedure we adopt follows closely that of chapter 6. Using this numerical method, in order to assess how the existence of a small mass limit changes with spin, we have explored the domain of existence of EsGB black holes for the linear, dilatonic, and quadratic exponential couplings.

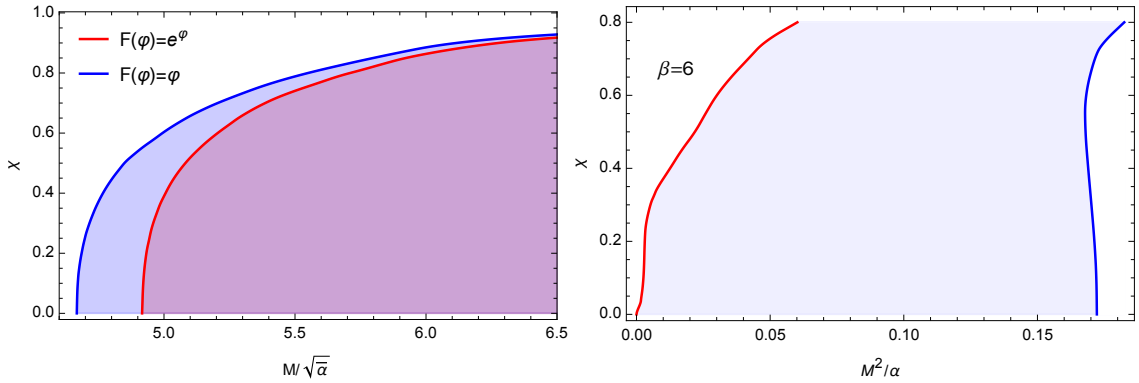

Figure 7.5.1: (Left) Domain of existence of black hole solutions in the $\left(M/\sqrt{\overline{\alpha}}, \chi\right)$ plane (shaded region), with dimensionless spins $\chi \lesssim 0.96$. The blue (red) line denotes the critical line for the linear (exponential) coupling. Note that here we used the convention of Eq. (7.41). (Right) Domain of existence of scalarized BH solutions in the $(M^2/\alpha, \chi)$ plane (shaded region), with dimensionless spins $\chi \lesssim 0.8$, for the coupling of Eq. (7.20) with $\beta = 6$. The blue (red) line denotes the existence (critical) line. For small spins, the absolute values that constitute the critical line should be taken with a pinch of salt because that region of the domain is particularly difficult to explore numerically.

For the dilatonic and linear couplings case ($F(\varphi) = e^{\varphi}$ and $F(\varphi) = \varphi$ in Eq. (7.41)), the domain of existence of solutions with dimensionless spins $\chi \lesssim 0.96$ is displayed in Fig. 7.5.1 (left), where we observe that higher spins result in higher values of the minimum allowed mass (for fixed coupling). This is not unexpected, as spin adds another repulsive effect to the system. In turn, this translates to tighter upper bounds on the allowed value of $\overline{\alpha}$, if spin is considered. Therefore, the constraints of Table 7.4.1 constitute legitimate upper bounds. From the point of view of cosmic censorship and Hawking evaporation, black holes in both the linear and dilatonic theories are expected to give rise to naked singularities as their endpoint, regardless of the initial spin of the solution, again raising questions about the consistency of these theories altogether.

We now consider the spontaneous scalarization coupling of Eq. (7.20) with the particular value $\beta = 6$. In the static case we recall that no minimum mass was observed. We find, however, that when spin is brought into account, the picture changes and critical solutions do appear to exist, as observed in Fig. 7.5.1 (right). It is, however, unclear if the existence of rotating critical solutions changes the self-consistency of the theory from the point of view of cosmic censorship and Hawking evaporation as it is not obvious that these solutions are ever reached. Indeed, a possibility is that during evaporation angular momentum is emitted at a (much)

larger rate than mass, such that a rotating black hole spins down to a non-rotating state (which has no critical configuration) before most of its mass has been given up [469]. The endpoint of evaporation for this coupling is therefore an open question and constitutes an avenue of further research.

Finally, we have obtained preliminary results for spin-induced scalarized black holes, exploring several values of β (for the coupling of Eq. (7.20) with an overall reversed sign). In all cases, critical solutions were reached, in agreement with the results of Refs. [80, 81].

Appendix

Appendix 7.A Onset of instability and spontaneous scalarization of a Schwarzschild black hole

Let us solve the perturbed scalar field equation (7.18) in a Schwarzschild spacetime background given by the line element of Eq. (7.19) with

$$f(r) = 1 - \frac{r_H}{r}, \qquad \delta(r) = 0, \tag{7.47}$$

where $r_H = 2M$. Taking into account that the background geometry is static and spherically symmetric, the scalar field perturbation can be separated in the following way

$$\delta\phi = \frac{u(r)}{r} e^{-i\omega t} Y_{\ell,m}(\theta, \varphi), \tag{7.48}$$

where $Y_{\ell,m}(\theta, \varphi)$ are the spherical harmonics. The resulting equation for the radial part takes a Schrodinger-like form ($\ell = 0$)

$$\frac{du}{dr^*} + \left(\omega^2 - V_{eff}\right) u = 0, \tag{7.49}$$

where $dr^* = dr/f(r)$ and

$$V_{eff} = \left(1 - \frac{r_H}{r}\right)\left(\frac{r_H}{r^3} - \frac{3\alpha r_H^2}{2r^6}\right). \tag{7.50}$$

A sufficient condition for the existence of an unstable mode (bound state as in quantum mechanics) is

$$\int_{-\infty}^{+\infty} V_{eff}(r^*) dr^* = \int_{r_H}^{+\infty} \frac{V_{eff}(r)}{1 - \frac{r_H}{r}} dr < 0. \tag{7.51}$$

The above condition gives $r_H/\sqrt{\alpha} < \sqrt{3/5} \approx 0.774597$ (or equivalently, $M/\sqrt{\alpha} \lesssim 0.387298$). Therefore, Schwarzschild BHs with horizon radius obeying the previous condition, should be unstable in this framework. This, in turn, can be translated into a curvature condition: when the Gauss-Bonnet curvature at the horizon obeys

$$\alpha^2 \mathcal{G}_{GR}|_{r_H} > \frac{100}{3},$$

the Schwarzschild BH should be unstable. This is only a sufficient condition for instability, but bifurcation of solutions actually occurs for slightly smaller curvature. To find the onset of instability we solve numerically the Schrödinger-like equation such that $\omega^2 = 0$ (when $\omega^2 < 0$ the tachyonic instability settles in). We find that the onset of instability occurs approximately at $r_H/\sqrt{\alpha} \approx 0.83$. This condition imposes a boundary on the domain of existence of (spontaneously) scalarized solutions. This result is valid for any coupling obeying the conditions of Eq. (7.19).

Appendix 7.B EsGB Field Equations for a Static and Spherically Symmetric Background

For a static and spherically symmetric background (7.19), the field equations take the form

$$\mathcal{E}^t_{\ t} = \frac{f\left(3\alpha f'\phi'\dot{\xi} - \left(\phi'^2\left(r^2 - 2\alpha(f-1)\ddot{\xi}\right)\right) + 2\alpha(f-1)\phi''\dot{\xi} - 2\right) - f'\left(\alpha\phi'\dot{\xi} + 2r\right) + 2}{2r^2} = 0, \tag{7.52}$$

$$\mathcal{E}^r_{\ r} = \frac{\alpha(3f-1)\phi'\left(f' - 2f\delta'\right)\dot{\xi} - 2rf' + r^2 f\phi'^2 + f\left(4r\delta' - 2\right) + 2}{2r^2} = 0, \tag{7.53}$$

$$\begin{aligned}\mathcal{E}^\theta_{\ \theta} = \mathcal{E}^\varphi_{\ \varphi} = \frac{1}{2r}\Bigg[& f\left(\alpha f''\phi'\dot{\xi} - 2r\delta'^2 + 2\delta' + 2r\delta'' - r\phi'^2\right) \\ & + f'\left(\delta'\left(3r - 5\alpha f\phi'\dot{\xi}\right) + \alpha f\left(\phi'^2\ddot{\xi} + \phi''\dot{\xi}\right) - 2\right) \\ & + \alpha f'^2\phi'\dot{\xi} - rf'' + 2\alpha f^2\left(\phi'\left(\left(\delta'^2 - \delta''\right)\dot{\xi} - \delta'\phi'\ddot{\xi}\right) - \delta'\phi''\dot{\xi}\right)\Bigg] = 0,\end{aligned} \tag{7.54}$$

and the scalar field equation is

$$\mathcal{E}_\phi = \frac{e^\delta}{r^2}\left[\left(r^2 e^{-\delta} f\phi'\right)' + \frac{\alpha}{2}\dot{\xi}\left(\left(f-1\right)e^\delta\left(e^{-2\delta}f\right)'\right)'\right] = 0, \tag{7.55}$$

where the primes denote a derivative with respect to r.

Once a closed-form expression for δ' is obtained by solving $\mathcal{E}^r{}_r$, taking the $\mathcal{E}^t{}_t$ and $\mathcal{E}_\phi$ equations, the above system can also be written in matrix form (Eq. (7.27)) with

$$\begin{aligned}
\mathcal{M}_{11} &= \frac{\alpha(3f-1)\phi'\dot{\xi}-2r}{2r^2}, \qquad \mathcal{M}_{12} = \frac{\alpha(f-1)f\dot{\xi}}{r^2}\\
\mathcal{M}_{21} &= \frac{8r^4 f\phi' + \alpha^2\phi'\left(f\left(r^2(3f(5f-4)+1)\phi'^2 + 6f(f+1) - 14\right)+2\right)\dot{\xi}^2 + 2\alpha r\left(f\left(3r^2(1-3f)\phi'^2 - 6f + 4\right)+2\right)\dot{\xi}}{4r^2 f\left(\alpha(1-3f)\phi'\dot{\xi}+2r\right)^2}\\
\mathcal{M}_{22} &= \frac{f\left(\alpha\dot{\xi}\left(4r^3(1-5f)\phi' + \alpha\left(r^2(f(15f-8)+1)\phi'^2 - 2(f(3f-7)+5)\right)\dot{\xi}\right) + 8r^4\right) + 2\alpha^2\dot{\xi}^2}{2r^2\left(\alpha(1-3f)\phi'\dot{\xi}+2r\right)^2}\\
b_1 &= \frac{f\left(\phi'^2\left(r^2 - 2\alpha(f-1)\ddot{\xi}\right)+2\right)-2}{2r^2}\\
b_2 &= \frac{\alpha\dot{\xi}\left(f\left(-2\alpha(f-1)(3f-1)\phi'^2\left(f\left(r^2\phi'^2-2\right)+2\right)\ddot{\xi} + f\left(r^4(5f-1)\phi'^4 + 4r^2(21f-5)\phi'^2 - 12f + 28\right) - 20\right)+4\right)}{4r^2 f\left(\alpha(1-3f)\phi'\dot{\xi}+2r\right)^2}\\
&+ \frac{-4r^3 f\phi'\left(f\left(r^2\phi'^2+6\right)+2\right) - 4\alpha^2 r f^2(f(15f-8)+1)\phi'^3\dot{\xi}^2}{4r^2 f\left(\alpha(1-3f)\phi'\dot{\xi}+2r\right)^2}
\end{aligned} \tag{7.56}$$

The values appearing in Eq. (7.29) are

$$\begin{aligned}
\mathcal{A} &= 3\phi'\left(5r^2\phi'^2 - 4\right)\dot{\xi}^3,\\
\mathcal{B} &= -6\dot{\xi}^2\left(6r^3\phi'^2 + \alpha\phi'\left(r^2\phi'^2 - 4\right)\dot{\xi} - 2r\right),\\
\mathcal{C} &= \dot{\xi}\left(\alpha\phi'\dot{\xi}+2r\right)\left(14r^3\phi' - \alpha\left(r^2\phi'^2+12\right)\dot{\xi}\right),\\
\mathcal{D} &= -4r\left(2r^4 + \alpha\dot{\xi}\left(r^3\phi' - 3\alpha\dot{\xi}\right)\right).
\end{aligned} \tag{7.57}$$

8 Conclusions

We will conclude with a general discussion of our results and possible future directions.

Chapter 2

In chapter 2 we started by reviewing the Glavan & Lin singular rescaling of the coupling constant and its shortcomings. Later we used the regularization technique developed in Reference [112], and applied it to the novel 4DEGB theory in order to find the regularized action (2.50). This action is free from divergences, and produces well-behaved second-order field equations that can be used for gravitational physics. Our theory reproduces the trace of the field equations of the original theory (which is the only well-defined field equation of the original 4DEGB theory), and complements it with a full set of off-diagonal equations

We have been unable to show that the scalar degree of freedom ϕ decouples from the metric-matter system, except in the lone example of the trace equation, suggesting that the original theory may have a hidden scalar degree of freedom within it. If this is the case, then the 4DEGB theory belongs to the Horndeski of scalar-tensor theories, and therefore does not bypass Lovelock's theorem. This hypothesis is backed-up by a study of the tree-level scattering amplitudes of gravitons in the original 4DEGB theory [226].

We note that the action (2.50) is identical to the one that is obtained by performing a regularized Kaluza-Klein reduction of a $(D+p)$-dimensional Einstein-Gauss-Bonnet theory with a flat p-dimensional internal space [256,257] (presented in section 2.3), as well as being the same action that appears in the context of renormalization group flows for trace anomalies of the effective action of the Nambu-Goldstone boson of broken conformal symmetry [470].

While we believe our theory to be a compelling regularization of the original theory, we note that it is not possible to prove full equivalence of the two theories. This is because the original formulation of the theory does not have a full set of 4-dimensional field equations that can be written in closed form, but also because the dimensional regularization procedure used in [110] does not appear to be unique. That is, there could potentially be arbitrarily many ways in which one could specify

the geometry of the space-time before taking the limit $D \to 4$. There is no guarantee that all possibilities will yield the same solutions, and it is therefore very difficult to establish whether the set of admitted solutions of the two theories will always be the same.

The equivalence of the 2-dimensional theory presented in Reference [112], and outlined in Section 2.2.1 does not suffer from the same difficulty. The $R = T$ theory and the field equations derived from the action (2.38) are demonstrably identical, up to an additional equation that does not affect the metric-matter system. We expect this to be a feature of this procedure which is *only* applicable in 2-dimensions, as in this case there is only a single degree of freedom in the geometry, which means that the trace of the field equations contains all information about the theory. This is not true in dimensions $D > 2$, so the equivalence of the trace equation does not directly imply equivalence of all the field equations.

Chapter 3

In chapter 3 we discussed the phenomenology of the 4D-Einstein-Gauss-Bonnet theories, with a focus on the well-defined theories derived in Chapter 2, in particular the one defined in Eq. (2.50).

We started by generalizing the vacuum BH solution of Glavan & Lin's 4DEGB theory to include electric charge and the effects of a cosmological constant. This BH solution was derived in analytical closed form. Next we studied the asymptotics of the solution as well as its dependence on the parameters of the model. We found that there are two branches of solutions, the positive and negative branch. For the negative branch, the solution resembles the Reissner-Nordström BH in the far field in the absence of a cosmological constant and that the model allows solutions with one, two or no horizons depending on if the mass is equal, above or below a certain critical mass, respectively. Also, in the limit of vanishing coupling constant α it was found that one recovers the GR Reissner-Nordström-AdS solution. We studied briefly the thermodynamics of this new BH, obtaining its Hawking temperature and entropy. Remarkably, for the negative branch, the entropy of the solution obeys the Hawking-Bekenstein area formula plus a logarithmic correction term, having the same form as predicted by some quantum gravity theories such as string theory.

Then, we discussed black holes in the counter-term regularized theory derived in chapter 2. We have shown that the Noether current associated with the scalar field's shift-symmetry can be used to show that the black hole solution in Eq. (3.35) is the unique physical static, spherically-symmetric and asymptotically-flat vacuum solution to this theory. By further relaxing the assumption of staticity, we found that no asymptotically-vanishing time-dependent perturbations to these black hole

solutions are allowed. This establishes a result only slightly less stringent than Birkhoff's theorem from GR, and suggests that the non-rotating black hole solutions of 4DEGB are perturbatively stable.

Motivated by these results, we studied the evaporation properties of black holes in regularized 4DEGB, finding that evaporation halts at a length scale associated with the coupling constant of the theory α, leaving relics of size $r_+ = \sqrt{\alpha}$ that no longer radiate. Assuming that a population of black holes can form, when large perturbations re-enter the horizon during the period of radiation domination after inflation ends, we have estimated the parameter range of the masses of the PBHs at formation that can constitute relic dark matter, as well as constraints on α that allow this. These constraints are given in Fig. 3.5, where the PBH mass at formation can range from $M \approx 0.4$ g to $M \approx 4\times10^5$ g when $\sqrt{\alpha} = \ell_{pl}$, and can reach $M \approx 2\times10^{12}$ g when $\sqrt{\alpha} = 10^{-18}\, m$, which is the maximum value of this coupling for which this scenario is valid.

Afterwards, we explored the cosmologies allowed by the 4DEGB theory in its various formulations. In particular, we have shown that cyclic cosmologies are allowed in 4DEGB gravity, although these are not expected to be physically relevant due to constraints on the coupling constant. The study of a perturbed FLRW Universe was also performed, with the correspondent perturbation equations to first-order being obtained.

Chapter 4

In chapter 4 we have studied the observational constraints that can be imposed on the coupling parameter α of regularized 4DEGB theory in Eq. (2.50). This has included studying the weak field solutions of this theory, and calculating the equations of two body dynamics within it. It has also included the bounds that can be imposed by studying the propagation of electromagnetic and gravitational radiation, as well as black hole shadows, tabletop experiments, primordial nucleosynthesis of the elements, and early universe inflation. Our results are summarized in Table 4.1.

The tightest definite constraint in Table 4.1 comes from observations of the periapsis advance of the LAGEOS II satellite, which gives $|\alpha| \lesssim 10^{10}\,\mathrm{m}^2$. Other observations, which often give tight constraints on alternative theories of gravity are much less constraining, with observations based on gravitational lensing and the Shapiro time delay effect giving no constraints at all. In particular, the recent constraints on the propagational velocity of gravitational waves from GW170817, which are often highly constraining for scalar-tensor theories, are found to be particularly weak in this case.

Being less conservative, we note that early universe inflation appears to rule out

all but the smallest negative values of α, and that binary black hole systems offer the possibility of strong constraints on positive values, leading to the overall range of allowed values being

$$0 \lesssim \alpha \lesssim 10^8\,\mathrm{m}^2\,.$$

These are the strongest constraints that we are aware of, for the regularized 4DEGB theory (4.1).

Taking our conservative constraint of $|\alpha| \lesssim 10^{10}\,\mathrm{m}^2$, it would appear that strong deviations from GR are only possible in the very early universe (at times $t \lesssim 10^{-3}s$) or in the immediate vicinity of stellar-mass black holes ($M \lesssim 100M_\odot$). This is promising in one sense, in that the merger events of such objects are now being recorded by the LIGO/Virgo collaboration with high frequency. It would be particularly interesting to run numerical simulations of such events in 4DEGB, to determine what observational signatures should be expected to result. On the other hand, our results suggest that there is unlikely to be any observable consequences from studying super-massive black holes or the expansion of the late universe. The accelerated expansion of the Universe being driven by this theory, in particular, is ruled out to extremely high significance by these bounds.

We consider the work presented on chapter 4 to be a first study on the observational constraints that can be imposed on 4DEGB, with much remaining work to be done to make these bounds more precise. In particular, effects such as geodetic precession and the Nordvedt effect have not been included here at all, as they will require detailed analyses of spinning and extended bodies in order to be applied. Likewise, strong field calculations have only been estimated, with more work remaining to be done to fully understand rotating and multi-black hole systems. In the end, we expect observations of binary black hole mergers and early universe physics to produce the tightest constraints on the 4DEGB theory, as it is these regimes that the new non-linear gravitational effects of this theory will become most pronounced.

Chapter 5

In chapter 5 we generalized the well-known conformally coupled scalar field theory by computing the most general subset of Horndeski theories whose scalar field equation is conformally invariant. The theory is presented in Eq. (5.19) and is composed of the Einstein-Hilbert term, a cosmological constant, the action of the typical conformally coupled scalar field with a quartic potential, and a scalar-Gauss-Bonnet sector. This Gauss-Bonnet sector is the same we had found previously in chapter 2, when discussing a well-defined regularization of the Gauss-Bonnet term to four dimensions. The theory possesses a purely geometrical field equation that restricts

the possible spacetimes, providing an easy path to find closed-form solutions. Several distinct static black hole solutions and a set of modified cosmological equations, were obtained in closed-form.

The regularized scalar-tensor 4DEGB theories presented in previous chapters had stumbled into a rather simple purely geometric field equation, despite their highly non-trivial structure. This chapter then reveals that the existence of such field equation is intimately connected with (generalized) conformal properties of the scalar field. It is rather intriguing that the dimensional regularization procedures of the Gauss-Bonnet term lead to particular cases of the theory derived in this chapter.

Chapter 6

In chapter 6 we explored how to apply pseudospectral methods to solve stationary and axisymmetric field equations in modified theories of gravity. We started by introducing the reader to spectral methods, along with the necessary mathematics, touching topics such as Chebyshev polynomials, Fourier series and Newton's root finding method, providing a simple example on how to solve a non-linear ODE with these techniques. We then made a connection to black hole physics, introducing our metric ansätz and the Kerr black hole, discussing the boundary conditions of our problem and the spectral expansions to be used. Later, we described our numerical method in detail, and discussed many relevant physical quantities and properties that can be extracted from a stationary and axisymmetric black hole solution. Finally, we benchmarked our code against the Kerr black hole, finding remarkable agreement, and used it to obtain spinning black hole solutions in EsGB gravity for two different couplings, obtaining very small error estimates. We finished by comparing our code and results to other existing codes with the same goal, concluding that our code is able to obtain more accurate solutions by several orders of magnitude.

Chapter 7

In chapter 7 we have explored the small mass limit of stationary (both static and spinning) black holes in theories containing Gauss-Bonnet terms in the action. Starting with an analytical example, we explored the small mass limit of black holes in the generalized conformal scalar field theory of Chapter 5, which contains a Gauss-Bonnet term, and where static closed-form black hole solutions are known. These black holes do possess a minimum mass solution, where an inner singularity and the event horizon overlap. The inner singularity is intimately connected with the reality condition (that solutions must be real), because of the existence of terms containing square-roots on the solution (as is typical in Gauss-Bonnet theories). From a more physical point of view, the singularity is related to repulsive effects originating from

the presence of the Gauss-Bonnet term in the theory.

Later, working with a more standard framework for EsGB theories, using numerical solutions of the field equations, a similar behavior was observed for the dilatonic (7.16) and linear couplings (7.17). A curious case concerns the quadratic-exponential coupling (7.20), where for sufficiently high values of the constant $\beta > \beta_{\rm crit}$ (defined in Eq. (7.40)), no static minimum mass solution was observed, thus showing that the existence of a critical singular black hole is not a generic prediction of theories containing Gauss-Bonnet terms. Then, from the point of view of cosmic censorship, this quadratic-exponential model might be viewed as more realistic option. The singularity structure for these models with $\beta > \beta_{\rm crit}$ is rather different from that of the dilatonic and linear and merits a deeper study. Once spin is considered, critical solutions do exist, but it is unclear if these are ever reached from Hawking evaporation. Also, for the coupling of Eq. (7.20), scalarized black hole solutions exist only for curvatures above a certain threshold, rendering it particularly interesting.

Finally, we used the results concerning the minimum mass solutions into account to impose the tightest upper bounds to date on the coupling constant from observations, for both the dilatonic ($\sqrt{\alpha} \lesssim (0.78 \pm 0.03)$ km) and linear ($\sqrt{\alpha} \lesssim (0.82 \pm 0.03)$ km) theory, with the previous tightest upper bound being $\sqrt{\alpha} \lesssim 1.18$ km [460]. Spin effects were found to only strengthen the previous upper limits.

Future Directions

Looking forward, there is still plenty of work that needs to be done on 4DEGB theories in order to fully understand them. In particular, numerical simulations of the merger of black holes, and the associated gravitational radiation emitted, is currently lacking. It is expected that this would provide the best way to constrain this theory, and so it would be extremely interesting to see such simulations performed. On the mathematical side, the initial value problem of these theories has not yet been proven to be well posed (despite these theories belonging to the Horndeski class, and proofs of well-posedness existing for a sub-set of these [471]). It also appears that the sub-set of regularized theories without a canonical kinetic term for the scalar might exhibit a strong coupling issue, but a more careful analysis is also required on this point. Finally, there are no known exact rotating black hole solutions known to these theories, despite the simplicity of the spherically symmetric vacuum and electrovacuum cases. Using the code described in chapter 6 to study these solutions therefore constitutes an avenue of further research. We also note that new approaches to 4DEGB are also still being developed, such as the intriguing study in Ref. [278], which considers an extra dimension of vanishing proper length [472]. All of these areas, and more, remain to be fully studied in order to have a complete

understanding of this interesting collection of theories. We look forward to such developments, and to seeing where the study of 4D Einstein-Gauss-Bonnet gravity will be taken next.

Concerning the code presented in chapter 6, we plan on complementing it with its own ray-tracing algorithm to compute the black hole shadow and the lensing of light around these objects, given a numerically computed solution. This is rather timely, given current and future observations by the Event Horizon Telescope collaboration. Another avenue we intend to follow is to extend the code to numerically obtain other compact object solutions in generic theories of gravity, such as neutron stars, and bosonic stars. All in all, this project aims at giving the community a free, easy to use and open-source code that computes highly accurate astrophysical solutions, allowing to study, test, and constraint modified gravity and dark matter models. Making use of the code, we further plan on exploring several modified gravity models. In particular, we plan on studying spinning black hole solutions in 4D Einstein-Gauss-Bonnet gravity and the generalized conformally coupled theory.

Bibliography

[1] P. G. S. Fernandes, "Charged black holes in AdS spaces in 4D Einstein Gauss-Bonnet gravity," *Phys. Lett. B*, vol. 805, p. 135468, 2020, 2003.05491. 3, 4, 37, 56

[2] P. G. S. Fernandes, P. Carrilho, T. Clifton, and D. J. Mulryne, "Derivation of Regularized Field Equations for the Einstein-Gauss-Bonnet Theory in Four Dimensions," *Phys. Rev. D*, vol. 102, no. 2, p. 024025, 2020, 2004.08362. 3, 4, 37, 46, 125

[3] T. Clifton, P. Carrilho, P. G. S. Fernandes, and D. J. Mulryne, "Observational Constraints on the Regularized 4D Einstein-Gauss-Bonnet Theory of Gravity," *Phys. Rev. D*, vol. 102, no. 8, p. 084005, 2020, 2006.15017. 3, 4, 37, 38, 78

[4] P. G. S. Fernandes, "Gravity with a generalized conformal scalar field: theory and solutions," *Phys. Rev. D*, vol. 103, no. 10, p. 104065, 2021, 2105.04687. 3, 4, 37, 38, 111, 125, 169

[5] P. G. S. Fernandes, P. Carrilho, T. Clifton, and D. J. Mulryne, "Black holes in the scalar-tensor formulation of 4D Einstein-Gauss-Bonnet gravity: Uniqueness of solutions, and a new candidate for dark matter," *Phys. Rev. D*, vol. 104, no. 4, p. 044029, 2021, 2107.00046. 3, 4, 37, 56, 62, 125

[6] P. G. S. Fernandes, P. Carrilho, T. Clifton, and D. J. Mulryne, "The 4D Einstein-Gauss-Bonnet theory of gravity: a review," *Class. Quant. Grav.*, vol. 39, no. 6, p. 063001, 2022, 2202.13908. 3, 4, 37, 56, 125

[7] P. G. S. Fernandes, D. J. Mulryne, and J. F. M. Delgado, "Exploring the small mass limit of stationary black holes in theories with Gauss–Bonnet terms," *Class. Quant. Grav.*, vol. 39, no. 23, p. 235015, 2022, 2207.10692. 4, 37, 38, 69

[8] P. G. S. Fernandes and D. J. Mulryne, "A new approach and code for spinning black holes in modified gravity," 12 2022, 2212.07293. 4, 37, 38

[9] I. Newton, *Mathematical Principles of Natural Philosophy*. 1687. 19

[10] U. J. Le Verrier 1846. 19

[11] U. J. Le Verrier *Annales de l'Observatoir Impirial de Paris*, vol. 76, 1859. 20

[12] J. Clerk Maxwell, "A Dynamical Theory of the Electromagnetic Field," *Philosophical Transactions of the Royal Society of London Series I*, vol. 155, pp. 459–512, Jan. 1865. 20

[13] A. A. Michelson and E. W. Morley, "On the relative motion of the earth and the luminiferous ether," *American Journal of Science*, vol. s3-34, no. 203, pp. 333–345, 1887, https://www.ajsonline.org/content/s3-34/203/333.full.pdf. 20

[14] A. Einstein, "On the electrodynamics of moving bodies," *Annalen Phys.*, vol. 17, pp. 891–921, 1905. 20

[15] A. Einstein, "Die Feldgleichungen der Gravitation," *Sitzungsberichte der Königlich Preußischen Akademie der Wissenschaften (Berlin*, pp. 844–847, Jan. 1915. 21

[16] D. C. A. Dyson F. W., Eddington A. S., "Determination of the Deflection of Light by the Sun's Gravitational Field from Observations Made at the Total Sclipes of May 29, 1919," *Philosophical Transactions of the Royal Society of London*, 1920. 21

[17] C. M. Will, "The Confrontation between General Relativity and Experiment," *Living Rev. Rel.*, vol. 17, p. 4, 2014, 1403.7377. 21

[18] M. Ishak, "Testing General Relativity in Cosmology," *Living Rev. Rel.*, vol. 22, no. 1, p. 1, 2019, 1806.10122. 21

[19] E. Corbelli and P. Salucci, "The Extended Rotation Curve and the Dark Matter Halo of M33," *Mon. Not. Roy. Astron. Soc.*, vol. 311, pp. 441–447, 2000, astro-ph/9909252. 21

[20] M. Markevitch, A. H. Gonzalez, D. Clowe, A. Vikhlinin, L. David, W. Forman, C. Jones, S. Murray, and W. Tucker, "Direct constraints on the dark matter self-interaction cross-section from the merging galaxy cluster 1E0657-56," *Astrophys. J.*, vol. 606, pp. 819–824, 2004, astro-ph/0309303. 21

[21] N. Aghanim *et al.*, "Planck 2018 results. VI. Cosmological parameters," *Astron. Astrophys.*, vol. 641, p. A6, 2020, 1807.06209. [Erratum: Astron.Astrophys. 652, C4 (2021)]. 21, 108

[22] A. G. Riess *et al.*, "Observational evidence from supernovae for an accelerating universe and a cosmological constant," *Astron. J.*, vol. 116, pp. 1009–1038, 1998, astro-ph/9805201. 21

[23] S. Perlmutter *et al.*, "Measurements of Ω and Λ from 42 high redshift supernovae," *Astrophys. J.*, vol. 517, pp. 565–586, 1999, astro-ph/9812133. 21

[24] S. Weinberg, "The cosmological constant problem," *Rev. Mod. Phys.*, vol. 61, pp. 1–23, Jan 1989. 22

[25] A. Padilla, "Lectures on the Cosmological Constant Problem," 2 2015, 1502.05296. 22

[26] L. Perivolaropoulos and F. Skara, "Challenges for ΛCDM: An update," *New Astron. Rev.*, vol. 95, 2022, 2105.05208. 22

[27] E. Di Valentino, O. Mena, S. Pan, L. Visinelli, W. Yang, A. Melchiorri, D. F. Mota, A. G. Riess, and J. Silk, "In the realm of the Hubble tension—a review of solutions," *Class. Quant. Grav.*, vol. 38, no. 15, p. 153001, 2021, 2103.01183. 22

[28] E. Di Valentino *et al.*, "Cosmology intertwined III: $f\sigma_8$ and S_8," *Astropart. Phys.*, vol. 131, p. 102604, 2021, 2008.11285. 22

[29] S. Carlip, "Quantum gravity: A Progress report," *Rept. Prog. Phys.*, vol. 64, p. 885, 2001, gr-qc/0108040. 22

[30] B. P. Abbott *et al.*, "Observation of Gravitational Waves from a Binary Black Hole Merger," *Phys. Rev. Lett.*, vol. 116, no. 6, p. 061102, 2016, 1602.03837. 22, 124, 168

[31] K. Akiyama *et al.*, "First M87 Event Horizon Telescope Results. I. The Shadow of the Supermassive Black Hole," *Astrophys. J. Lett.*, vol. 875, p. L1, 2019, 1906.11238. 22, 124

[32] K. Akiyama *et al.*, "First Sagittarius A* Event Horizon Telescope Results. I. The Shadow of the Supermassive Black Hole in the Center of the Milky Way," *Astrophys. J. Lett.*, vol. 930, no. 2, p. L12, 2022. 22, 102, 124

[33] R. M. Wald, *General Relativity*. Chicago, USA: Chicago Univ. Pr., 1984. 23

[34] C. W. Misner, K. S. Thorne, and J. A. Wheeler, *Gravitation*. San Francisco: W. H. Freeman, 1973. 23

[35] J. D. Brown, "On variational principles for gravitating perfect fluids," 7 1994, gr-qc/9407008. 24

[36] K. Schwarzschild, "On the gravitational field of a mass point according to Einstein's theory," *Sitzungsber. Preuss. Akad. Wiss. Berlin (Math. Phys.)*, vol. 1916, pp. 189–196, 1916, physics/9905030. 25

[37] G. D. Birkhoff and R. E. Langer, *Relativity and modern physics*. 1923. 25

[38] H. Nariai, "On Some Static Solutions of Einstein's Gravitational Field Equations in a Spherically Symmetric Case," *General Relativity and Gravitation*, vol. 31, p. 945, June 1999. 25

[39] H. Nariai, "On a New Cosmological Solution of Einstein's Field Equations of Gravitation," *General Relativity and Gravitation*, vol. 31, p. 963, June 1999. 25

[40] P. T. Chrusciel, J. Lopes Costa, and M. Heusler, "Stationary Black Holes: Uniqueness and Beyond," *Living Rev. Rel.*, vol. 15, p. 7, 2012, 1205.6112. 26, 124

[41] T. Adamo and E. T. Newman, "The Kerr-Newman metric: A Review," *Scholarpedia*, vol. 9, p. 31791, 2014, 1410.6626. 26

[42] C. A. R. Herdeiro and E. Radu, "Asymptotically flat black holes with scalar hair: a review," *Int. J. Mod. Phys. D*, vol. 24, no. 09, p. 1542014, 2015, 1504.08209. 26, 111, 124, 167

[43] J. M. Bardeen, B. Carter, and S. W. Hawking, "The Four laws of black hole mechanics," *Commun. Math. Phys.*, vol. 31, pp. 161–170, 1973. 27

[44] S. W. Hawking, "Particle Creation by Black Holes," *Commun. Math. Phys.*, vol. 43, pp. 199–220, 1975. [Erratum: Commun.Math.Phys. 46, 206 (1976)]. 27

[45] J. D. Bekenstein, "Black holes and entropy," *Phys. Rev. D*, vol. 7, pp. 2333–2346, Apr 1973. 27

[46] M. Ostrogradsky, "Mémoires sur les équations différentielles, relatives au problème des isopérimètres," *Mem. Acad. St. Petersbourg*, vol. 6, no. 4, pp. 385–517, 1850. 28

[47] H. Weyl *et al.*, "Space–time–matter," *space*, vol. 6, no. r2, p. 64, 1919. 28

[48] E. Cartan, "Sur les équations de la gravitation d'einstein," *Journal de Mathématiques pures et appliquées*, vol. 1, pp. 141–204, 1922. 28

[49] D. Lovelock, "Divergence-free tensorial concomitants," *Aequationes mathematicae*, vol. 4, no. 1-2, pp. 127–138, 1970. 28, 29

[50] D. Lovelock, "The Einstein tensor and its generalizations," *J. Math. Phys.*, vol. 12, pp. 498–501, 1971. 28, 29

[51] T. Padmanabhan and D. Kothawala, "Lanczos-Lovelock models of gravity," *Phys. Rept.*, vol. 531, pp. 115–171, 2013, 1302.2151. 29, 34

[52] J. F. Donoghue, "General relativity as an effective field theory: The leading quantum corrections," *Phys. Rev. D*, vol. 50, pp. 3874–3888, 1994, gr-qc/9405057. 30

[53] K. S. Stelle, "Renormalization of higher-derivative quantum gravity," *Phys. Rev. D*, vol. 16, pp. 953–969, Aug 1977. 30

[54] A. A. Starobinsky, "A New Type of Isotropic Cosmological Models Without Singularity," *Phys. Lett. B*, vol. 91, pp. 99–102, 1980. 31

[55] Y. Akrami *et al.*, "Planck 2018 results. X. Constraints on inflation," *Astron. Astrophys.*, vol. 641, p. A10, 2020, 1807.06211. 31, 74

[56] C. Lanczos, "Elektromagnetismus als natürliche eigenschaft der riemannschen geometrie," *Zeitschrift für Physik*, vol. 73, no. 3-4, pp. 147–168, 1932. 32

[57] C. Lanczos, "A remarkable property of the riemann-christoffel tensor in four dimensions," *Annals of Mathematics*, pp. 842–850, 1938. 32

[58] D. Lovelock, "Dimensionally dependent identities," in *Mathematical Proceedings of the Cambridge Philosophical Society*, vol. 68, pp. 345–350, Cambridge University Press, 1970. 32

[59] S. shen Chern, "On the curvatura integra in a riemannian manifold," *Annals of Mathematics*, vol. 46, no. 4, pp. 674–684, 1945. 32

[60] S. Ferrara, R. R. Khuri, and R. Minasian, "M theory on a Calabi-Yau manifold," *Phys. Lett. B*, vol. 375, pp. 81–88, 1996, hep-th/9602102. 33

[61] I. Antoniadis, S. Ferrara, R. Minasian, and K. S. Narain, "R**4 couplings in M and type II theories on Calabi-Yau spaces," *Nucl. Phys. B*, vol. 507, pp. 571–588, 1997, hep-th/9707013. 33

[62] B. Zwiebach, "Curvature Squared Terms and String Theories," *Phys. Lett. B*, vol. 156, pp. 315–317, 1985. 33

[63] R. I. Nepomechie, "On the Low-energy Limit of Strings," *Phys. Rev. D*, vol. 32, p. 3201, 1985. 33, 167, 173

[64] C. G. Callan, Jr., I. R. Klebanov, and M. J. Perry, "String Theory Effective Actions," *Nucl. Phys. B*, vol. 278, pp. 78–90, 1986. 33, 167, 173

[65] P. Candelas, G. T. Horowitz, A. Strominger, and E. Witten, "Vacuum Configurations for Superstrings," *Nucl. Phys. B*, vol. 258, pp. 46–74, 1985. 33, 167, 173

[66] D. J. Gross and J. H. Sloan, "The Quartic Effective Action for the Heterotic String," *Nucl. Phys. B*, vol. 291, pp. 41–89, 1987. 33, 167, 173

[67] Y. Choquet-Bruhat, "The cauchy problem for stringy gravity," *Journal of mathematical physics*, vol. 29, no. 8, pp. 1891–1895, 1988. 33

[68] C. Teitelboim and J. Zanelli, "Dimensionally continued topological gravitation theory in hamiltonian form," *Classical and Quantum Gravity*, vol. 4, no. 4, p. L125, 1987. 33

[69] N. Deruelle and J. Madore, "On the quasi-linearity of the einstein-" gauss-bonnet" gravity field equations," *arXiv preprint gr-qc/0305004*, 2003. 33

[70] T. P. Sotiriou and S.-Y. Zhou, "Black hole hair in generalized scalar-tensor gravity," *Phys. Rev. Lett.*, vol. 112, p. 251102, 2014, 1312.3622. 34, 125, 167, 173

[71] T. P. Sotiriou and S.-Y. Zhou, "Black hole hair in generalized scalar-tensor gravity: An explicit example," *Phys. Rev. D*, vol. 90, p. 124063, 2014, 1408.1698. 34, 125, 167, 168, 173, 175

[72] M. Saravani and T. P. Sotiriou, "Classification of shift-symmetric Horndeski theories and hairy black holes," *Phys. Rev. D*, vol. 99, no. 12, p. 124004, 2019, 1903.02055. 34, 63, 65, 167

[73] J. F. M. Delgado, C. A. R. Herdeiro, and E. Radu, "Spinning black holes in shift-symmetric Horndeski theory," *JHEP*, vol. 04, p. 180, 2020, 2002.05012. 34, 125, 137, 143, 162, 167, 173

[74] D. D. Doneva and S. S. Yazadjiev, "New Gauss-Bonnet Black Holes with Curvature-Induced Scalarization in Extended Scalar-Tensor Theories," *Phys. Rev. Lett.*, vol. 120, no. 13, p. 131103, 2018, 1711.01187. 34, 35, 125, 167, 174

[75] H. O. Silva, J. Sakstein, L. Gualtieri, T. P. Sotiriou, and E. Berti, "Spontaneous scalarization of black holes and compact stars from a Gauss-Bonnet coupling," *Phys. Rev. Lett.*, vol. 120, no. 13, p. 131104, 2018, 1711.02080. 34, 35, 125, 167

[76] G. Antoniou, A. Bakopoulos, and P. Kanti, "Evasion of No-Hair Theorems and Novel Black-Hole Solutions in Gauss-Bonnet Theories," *Phys. Rev. Lett.*, vol. 120, no. 13, p. 131102, 2018, 1711.03390. 34, 35, 125, 167

[77] P. V. P. Cunha, C. A. R. Herdeiro, and E. Radu, "Spontaneously Scalarized Kerr Black Holes in Extended Scalar-Tensor–Gauss-Bonnet Gravity," *Phys. Rev. Lett.*, vol. 123, no. 1, p. 011101, 2019, 1904.09997. 34, 100, 125, 137, 143, 162, 167, 174

[78] L. G. Collodel, B. Kleihaus, J. Kunz, and E. Berti, "Spinning and excited black holes in Einstein-scalar-Gauss–Bonnet theory," *Class. Quant. Grav.*, vol. 37, no. 7, p. 075018, 2020, 1912.05382. 34

[79] A. Dima, E. Barausse, N. Franchini, and T. P. Sotiriou, "Spin-induced black hole spontaneous scalarization," *Phys. Rev. Lett.*, vol. 125, no. 23, p. 231101, 2020, 2006.03095. 34, 125, 167, 174

[80] C. A. R. Herdeiro, E. Radu, H. O. Silva, T. P. Sotiriou, and N. Yunes, "Spin-induced scalarized black holes," *Phys. Rev. Lett.*, vol. 126, no. 1, p. 011103, 2021, 2009.03904. 34, 125, 137, 143, 162, 167, 174, 188

[81] E. Berti, L. G. Collodel, B. Kleihaus, and J. Kunz, "Spin-induced black-hole scalarization in Einstein-scalar-Gauss-Bonnet theory," *Phys. Rev. Lett.*, vol. 126, no. 1, p. 011104, 2021, 2009.03905. 34, 125, 137, 143, 162, 167, 174, 188

[82] P. Kanti, N. E. Mavromatos, J. Rizos, K. Tamvakis, and E. Winstanley, "Dilatonic black holes in higher curvature string gravity," *Phys. Rev. D*, vol. 54, pp. 5049–5058, 1996, hep-th/9511071. 34, 125, 167, 168, 173, 175

[83] B. Kleihaus, J. Kunz, and E. Radu, "Rotating Black Holes in Dilatonic Einstein-Gauss-Bonnet Theory," *Phys. Rev. Lett.*, vol. 106, p. 151104, 2011, 1101.2868. 34, 125, 137, 143, 162, 167, 173

[84] B. Kleihaus, J. Kunz, S. Mojica, and E. Radu, "Spinning black holes in Einstein–Gauss-Bonnet–dilaton theory: Nonperturbative solutions," *Phys. Rev. D*, vol. 93, no. 4, p. 044047, 2016, 1511.05513. 34, 137, 143, 160, 162

[85] P. V. P. Cunha, C. A. R. Herdeiro, B. Kleihaus, J. Kunz, and E. Radu, "Shadows of Einstein–dilaton–Gauss–Bonnet black holes," *Phys. Lett. B*, vol. 768, pp. 373–379, 2017, 1701.00079. 34, 125, 167, 173

[86] J. L. Blázquez-Salcedo, F. S. Khoo, and J. Kunz, "Quasinormal modes of Einstein-Gauss-Bonnet-dilaton black holes," *Phys. Rev. D*, vol. 96, no. 6, p. 064008, 2017, 1706.03262. 34

[87] S. Nojiri, S. D. Odintsov, and M. Sasaki, "Gauss-Bonnet dark energy," *Phys. Rev. D*, vol. 71, p. 123509, 2005, hep-th/0504052. 34

[88] P.-X. Jiang, J.-W. Hu, and Z.-K. Guo, "Inflation coupled to a Gauss-Bonnet term," *Phys. Rev. D*, vol. 88, p. 123508, 2013, 1310.5579. 34

[89] P. Kanti, R. Gannouji, and N. Dadhich, "Gauss-Bonnet Inflation," *Phys. Rev. D*, vol. 92, no. 4, p. 041302, 2015, 1503.01579. 34

[90] S. Chakraborty, T. Paul, and S. SenGupta, "Inflation driven by Einstein-Gauss-Bonnet gravity," *Phys. Rev. D*, vol. 98, no. 8, p. 083539, 2018, 1804.03004. 34

[91] S. D. Odintsov and V. K. Oikonomou, "Viable Inflation in Scalar-Gauss-Bonnet Gravity and Reconstruction from Observational Indices," *Phys. Rev. D*, vol. 98, no. 4, p. 044039, 2018, 1808.05045. 34

[92] S. D. Odintsov and V. K. Oikonomou, "Inflationary Phenomenology of Einstein Gauss-Bonnet Gravity Compatible with GW170817," *Phys. Lett. B*, vol. 797, p. 134874, 2019, 1908.07555. 34

[93] S. D. Odintsov and V. K. Oikonomou, "Swampland Implications of GW170817-compatible Einstein-Gauss-Bonnet Gravity," *Phys. Lett. B*, vol. 805, p. 135437, 2020, 2004.00479. 34

[94] P. Kanti, J. Rizos, and K. Tamvakis, "Singularity free cosmological solutions in quadratic gravity," *Phys. Rev. D*, vol. 59, p. 083512, 1999, gr-qc/9806085. 34

[95] J. Madore, *An Introduction to Noncommutative Geometry*. 11 2008. 34

[96] Y. Fujii and K. Maeda, *The scalar-tensor theory of gravitation*. Cambridge Monographs on Mathematical Physics, Cambridge University Press, 7 2007. 34

[97] R. D. Peccei and H. R. Quinn, "CP Conservation in the Presence of Instantons," *Phys. Rev. Lett.*, vol. 38, pp. 1440–1443, 1977. 34

[98] N. Chow and J. Khoury, "Galileon Cosmology," *Phys. Rev. D*, vol. 80, p. 024037, 2009, 0905.1325. 34

[99] P. Brax, C. Burrage, and A.-C. Davis, "Laboratory Tests of the Galileon," *JCAP*, vol. 09, p. 020, 2011, 1106.1573. 34

[100] A. Barreira, B. Li, W. A. Hellwing, L. Lombriser, C. M. Baugh, and S. Pascoli, "Halo model and halo properties in Galileon gravity cosmologies," *JCAP*, vol. 04, p. 029, 2014, 1401.1497. 34

[101] J. Khoury and A. Weltman, "Chameleon fields: Awaiting surprises for tests of gravity in space," *Phys. Rev. Lett.*, vol. 93, p. 171104, 2004, astro-ph/0309300. 34

[102] J. Khoury and A. Weltman, "Chameleon cosmology," *Phys. Rev. D*, vol. 69, p. 044026, 2004, astro-ph/0309411. 34

[103] T. Damour and G. Esposito-Farese, "Nonperturbative strong field effects in tensor - scalar theories of gravitation," *Phys. Rev. Lett.*, vol. 70, pp. 2220–2223, 1993. 35, 97

[104] G. W. Horndeski, "Second-order scalar-tensor field equations in a four-dimensional space," *Int. J. Theor. Phys.*, vol. 10, pp. 363–384, 1974. 35, 51, 115, 167

[105] T. Kobayashi, "Horndeski theory and beyond: a review," *Rept. Prog. Phys.*, vol. 82, no. 8, p. 086901, 2019, 1901.07183. 35, 51, 99, 115, 123, 167

[106] T. Kobayashi, M. Yamaguchi, and J. Yokoyama, "Generalized G-inflation: Inflation with the most general second-order field equations," *Prog. Theor. Phys.*, vol. 126, pp. 511–529, 2011, 1105.5723. 35

[107] K. Van Acoleyen and J. Van Doorsselaere, "Galileons from Lovelock actions," *Phys. Rev. D*, vol. 83, p. 084025, 2011, 1102.0487. 35

[108] C. Charmousis and M. Tsoukalas, "Lovelock Galileons and black holes," *Phys. Rev. D*, vol. 92, no. 10, p. 104050, 2015, 1506.05014. 35

[109] C. Charmousis, B. Gouteraux, and E. Kiritsis, "Higher-derivative scalar-vector-tensor theories: black holes, Galileons, singularity cloaking and holography," *JHEP*, vol. 09, p. 011, 2012, 1206.1499. 35

[110] D. Glavan and C. Lin, "Einstein-Gauss-Bonnet Gravity in Four-Dimensional Spacetime," *Phys. Rev. Lett.*, vol. 124, no. 8, p. 081301, 2020, 1905.03601. 36, 39, 40, 46, 53, 55, 56, 59, 80, 124, 125, 192

[111] M. J. Duff, "Twenty years of the weyl anomaly," *Classical and Quantum Gravity*, vol. 11, no. 6, p. 1387, 1994. 36

[112] R. B. Mann and S. F. Ross, "The D —> 2 limit of general relativity," *Class. Quant. Grav.*, vol. 10, pp. 1405–1408, 1993, gr-qc/9208004. 36, 37, 46, 47, 48, 49, 192, 193

[113] R. A. Konoplya and A. F. Zinhailo, "Quasinormal modes, stability and shadows of a black hole in the 4D Einstein–Gauss–Bonnet gravity," *Eur. Phys. J. C*, vol. 80, no. 11, p. 1049, 2020, 2003.01188. 37, 60, 100

[114] M. Guo and P.-C. Li, "Innermost stable circular orbit and shadow of the $4D$ Einstein–Gauss–Bonnet black hole," *Eur. Phys. J. C*, vol. 80, no. 6, p. 588, 2020, 2003.02523. 37, 60, 100

[115] S.-W. Wei and Y.-X. Liu, "Testing the nature of Gauss-Bonnet gravity by four-dimensional rotating black hole shadow," 3 2020, 2003.07769. 37, 100

[116] R. A. Konoplya and A. Zhidenko, "Black holes in the four-dimensional Einstein-Lovelock gravity," *Phys. Rev. D*, vol. 101, no. 8, p. 084038, 2020, 2003.07788. 37

[117] K. Hegde, A. Naveena Kumara, C. L. A. Rizwan, A. K. M., and M. S. Ali, "Thermodynamics, Phase Transition and Joule Thomson Expansion of novel 4-D Gauss Bonnet AdS Black Hole," 3 2020, 2003.08778. 37

[118] A. Casalino, A. Colleaux, M. Rinaldi, and S. Vicentini, "Regularized Lovelock gravity," *Phys. Dark Univ.*, vol. 31, p. 100770, 2021, 2003.07068. 37

[119] S. G. Ghosh and S. D. Maharaj, "Radiating black holes in the novel 4D Einstein–Gauss–Bonnet gravity," *Phys. Dark Univ.*, vol. 30, p. 100687, 2020, 2003.09841. 37

[120] D. D. Doneva and S. S. Yazadjiev, "Relativistic stars in 4D Einstein-Gauss-Bonnet gravity," 3 2020, 2003.10284. 37

[121] Y.-P. Zhang, S.-W. Wei, and Y.-X. Liu, "Spinning Test Particle in Four-Dimensional Einstein–Gauss–Bonnet Black Holes," *Universe*, vol. 6, no. 8, p. 103, 2020, 2003.10960. 37

[122] S. G. Ghosh and R. Kumar, "Generating black holes in $4D$ Einstein-Gauss-Bonnet gravity," *Class. Quant. Grav.*, vol. 37, no. 24, p. 245008, 2020, 2003.12291. 37

[123] R. A. Konoplya and A. Zhidenko, "BTZ black holes with higher curvature corrections in the 3D Einstein-Lovelock gravity," *Phys. Rev. D*, vol. 102, no. 6, p. 064004, 2020, 2003.12171. 37

[124] R. A. Konoplya and A. Zhidenko, "(In)stability of black holes in the $4D$ Einstein–Gauss–Bonnet and Einstein–Lovelock gravities," *Phys. Dark Univ.*, vol. 30, p. 100697, 2020, 2003.12492. 37

[125] R. Kumar and S. G. Ghosh, "Rotating black holes in 4D Einstein-Gauss-Bonnet gravity and its shadow," *JCAP*, vol. 07, no. 07, p. 053, 2020, 2003.08927. 37

[126] A. Kumar and R. Kumar, "Bardeen black holes in the novel 4D Einstein-Gauss-Bonnet gravity," 3 2020, 2003.13104. 37

[127] C.-Y. Zhang, P.-C. Li, and M. Guo, "Greybody factor and power spectra of the Hawking radiation in the 4D Einstein–Gauss–Bonnet de-Sitter gravity," *Eur. Phys. J. C*, vol. 80, no. 9, p. 874, 2020, 2003.13068. 37

[128] S. A. Hosseini Mansoori, "Thermodynamic geometry of the novel 4-D Gauss–Bonnet AdS black hole," *Phys. Dark Univ.*, vol. 31, p. 100776, 2021, 2003.13382. 37

[129] S.-W. Wei and Y.-X. Liu, "Extended thermodynamics and microstructures of four-dimensional charged Gauss-Bonnet black hole in AdS space," *Phys. Rev. D*, vol. 101, no. 10, p. 104018, 2020, 2003.14275. 37

[130] D. V. Singh, S. G. Ghosh, and S. D. Maharaj, "Clouds of strings in 4D Einstein–Gauss–Bonnet black holes," *Phys. Dark Univ.*, vol. 30, p. 100730, 2020, 2003.14136. 37

[131] M. S. Churilova, "Quasinormal modes of the Dirac field in the consistent 4D Einstein–Gauss–Bonnet gravity," *Phys. Dark Univ.*, vol. 31, p. 100748, 2021, 2004.00513. 37

[132] S. U. Islam, R. Kumar, and S. G. Ghosh, "Gravitational lensing by black holes in the 4D Einstein-Gauss-Bonnet gravity," *JCAP*, vol. 09, p. 030, 2020, 2004.01038. 37

[133] A. K. Mishra, "Quasinormal modes and strong cosmic censorship in the regularised 4D Einstein–Gauss–Bonnet gravity," *Gen. Rel. Grav.*, vol. 52, no. 11, p. 106, 2020, 2004.01243. 37

[134] A. Kumar and S. G. Ghosh, "Hayward black holes in the novel 4D Einstein-Gauss-Bonnet gravity," 4 2020, 2004.01131. 37

[135] S. Nojiri and S. D. Odintsov, "Novel cosmological and black hole solutions in Einstein and higher-derivative gravity in two dimensions," *EPL*, vol. 130, no. 1, p. 10004, 2020, 2004.01404. 37, 49

[136] D. V. Singh and S. Siwach, "Thermodynamics and P-v criticality of Bardeen-AdS Black Hole in 4D Einstein-Gauss-Bonnet Gravity," *Phys. Lett. B*, vol. 808, p. 135658, 2020, 2003.11754. 37

[137] S.-L. Li, P. Wu, and H. Yu, "Stability of the Einstein Static Universe in 4D Gauss-Bonnet Gravity," 4 2020, 2004.02080. 37

[138] M. Heydari-Fard, M. Heydari-Fard, and H. R. Sepangi, "Bending of light in novel $4D$ Gauss-Bonnet-de Sitter black holes by Rindler-Ishak method," 4 2020, 2004.02140. 37

[139] R. A. Konoplya and A. F. Zinhailo, "Grey-body factors and Hawking radiation of black holes in $4D$ Einstein-Gauss-Bonnet gravity," *Phys. Lett. B*, vol. 810, p. 135793, 2020, 2004.02248. 37

[140] X.-H. Jin, Y.-X. Gao, and D.-J. Liu, "Strong gravitational lensing of a 4-dimensional Einstein–Gauss–Bonnet black hole in homogeneous plasma," *Int. J. Mod. Phys. D*, vol. 29, no. 09, p. 2050065, 2020, 2004.02261. 37, 100

[141] C. Liu, T. Zhu, and Q. Wu, "Thin Accretion Disk around a four-dimensional Einstein-Gauss-Bonnet Black Hole," *Chin. Phys. C*, vol. 45, no. 1, p. 015105, 2021, 2004.01662. 37

[142] C.-Y. Zhang, S.-J. Zhang, P.-C. Li, and M. Guo, "Superradiance and stability of the regularized 4D charged Einstein-Gauss-Bonnet black hole," *JHEP*, vol. 08, p. 105, 2020, 2004.03141. 37

[143] B. Eslam Panah, K. Jafarzade, and S. H. Hendi, "Charged 4D Einstein-Gauss-Bonnet-AdS black holes: Shadow, energy emission, deflection angle and heat engine," *Nucl. Phys. B*, vol. 961, p. 115269, 2020, 2004.04058. 37

[144] A. Naveena Kumara, C. L. A. Rizwan, K. Hegde, M. S. Ali, and A. K. M, "Rotating 4D Gauss-Bonnet black hole as particle accelerator," 4 2020, 2004.04521. 37

[145] A. Aragón, R. Bécar, P. A. González, and Y. Vásquez, "Perturbative and non-perturbative quasinormal modes of 4D Einstein–Gauss–Bonnet black holes," *Eur. Phys. J. C*, vol. 80, no. 8, p. 773, 2020, 2004.05632. 37

[146] D. Malafarina, B. Toshmatov, and N. Dadhich, "Dust collapse in 4D Einstein–Gauss–Bonnet gravity," *Phys. Dark Univ.*, vol. 30, p. 100598, 2020, 2004.07089. 37

[147] S.-J. Yang, J.-J. Wan, J. Chen, J. Yang, and Y.-Q. Wang, "Weak cosmic censorship conjecture for the novel $4D$ charged Einstein-Gauss-Bonnet black hole with test scalar field and particle," *Eur. Phys. J. C*, vol. 80, no. 10, p. 937, 2020, 2004.07934. 37

[148] M. A. Cuyubamba, "Stability of asymptotically de Sitter and anti-de Sitter black holes in $4D$ regularized Einstein–Gauss–Bonnet theory," *Phys. Dark Univ.*, vol. 31, p. 100789, 2021, 2004.09025. 37

[149] S. Ying, "Thermodynamics and Weak Cosmic Censorship Conjecture of 4D Gauss-Bonnet-Maxwell Black Holes via Charged Particle Absorption," *Chin. Phys. C*, vol. 44, no. 12, p. 125101, 2020, 2004.09480. 37

[150] F.-W. Shu, "Vacua in novel 4D Einstein-Gauss-Bonnet Gravity: pathology and instability?," *Phys. Lett. B*, vol. 811, p. 135907, 2020, 2004.09339. 37

[151] A. Casalino and L. Sebastiani, "Perturbations in Regularized Lovelock Gravity," *Phys. Dark Univ.*, vol. 31, p. 100771, 2021, 2004.10229. 37, 107

[152] J. Rayimbaev, A. Abdujabbarov, B. Turimov, and F. Atamurotov, "Magnetized particle motion around 4-D Einstein-Gauss-Bonnet Black Hole," 4 2020, 2004.10031. 37

[153] P. Liu, C. Niu, and C.-Y. Zhang, "Instability of the novel 4D charged Einstein-Gauss-Bonnet de-Sitter black hole," 4 2020, 2004.10620. 37

[154] X.-X. Zeng, H.-Q. Zhang, and H. Zhang, "Shadows and photon spheres with spherical accretions in the four-dimensional Gauss–Bonnet black hole," *Eur. Phys. J. C*, vol. 80, no. 9, p. 872, 2020, 2004.12074. 37

[155] X.-H. Ge and S.-J. Sin, "Causality of black holes in 4-dimensional Einstein–Gauss–Bonnet–Maxwell theory," *Eur. Phys. J. C*, vol. 80, no. 8, p. 695, 2020, 2004.12191. 37

[156] K. Jusufi, A. Banerjee, and S. G. Ghosh, "Wormholes in 4D Einstein–Gauss–Bonnet gravity," *Eur. Phys. J. C*, vol. 80, no. 8, p. 698, 2020, 2004.10750. 37

[157] M. S. Churilova, "Quasinormal modes of the test fields in the consistent 4D Einstein–Gauss-Bonnet–(anti)de Sitter gravity," *Annals Phys.*, vol. 427, p. 168425, 2021, 2004.14172. 37

[158] R. Kumar, S. U. Islam, and S. G. Ghosh, "Gravitational lensing by charged black hole in regularized 4D Einstein–Gauss–Bonnet gravity," *Eur. Phys. J. C*, vol. 80, no. 12, p. 1128, 2020, 2004.12970. 37

[159] G. Alkaç and D. O. Devecioğlu, "Three dimensional modified gravities as holographic limits of Lancsoz-Lovelock theories," *Phys. Lett. B*, vol. 807, p. 135597, 2020, 2004.12839. 37

[160] S. G. Ghosh and S. D. Maharaj, "Noncommutative inspired black holes in regularized 4D Einstein–Gauss–Bonnet theory," *Phys. Dark Univ.*, vol. 31, p. 100793, 2021, 2004.13519. 37

[161] K. Yang, B.-M. Gu, S.-W. Wei, and Y.-X. Liu, "Born–Infeld black holes in 4D Einstein–Gauss–Bonnet gravity," *Eur. Phys. J. C*, vol. 80, no. 7, p. 662, 2020, 2004.14468. 37

[162] P. Liu, C. Niu, X. Wang, and C.-Y. Zhang, "Traversable Thin-shell Wormhole in the Novel 4D Einstein-Gauss-Bonnet Theory," 4 2020, 2004.14267. 37

[163] S. Devi, R. Roy, and S. Chakrabarti, "Quasinormal modes and greybody factors of the novel four dimensional Gauss–Bonnet black holes in asymptotically de Sitter space time: scalar, electromagnetic and Dirac perturbations," *Eur. Phys. J. C*, vol. 80, no. 8, p. 760, 2020, 2004.14935. 37

[164] K. Jusufi, "Nonlinear magnetically charged black holes in 4D Einstein-Gauss-Bonnet gravity," *Annals Phys.*, vol. 421, p. 168285, 2020, 2005.00360. 37

[165] R. A. Konoplya and A. Zhidenko, "4*D* Einstein-Lovelock black holes: Hierarchy of orders in curvature," *Phys. Lett. B*, vol. 807, p. 135607, 2020, 2005.02225. 37

[166] X. Qiao, L. OuYang, D. Wang, Q. Pan, and J. Jing, "Holographic superconductors in 4D Einstein-Gauss-Bonnet gravity," *JHEP*, vol. 12, p. 192, 2020, 2005.01007. 37

[167] P. Liu, C. Niu, and C.-Y. Zhang, "Instability of the Novel 4D Charged Einstein-Gauss-Bonnet Anti de-Sitter Black Hole," 5 2020, 2005.01507. 37

[168] D. Samart and P. Channuie, "Generalized gravitational phase transition in novel 4D Einstein-Gauss-Bonnet gravity," 5 2020, 2005.02826. 37

[169] A. Banerjee and K. N. Singh, "Color flavor locked strange stars in 4D Einstein-Gauss-Bonnet gravity," *Phys. Dark Univ.*, vol. 31, p. 100792, 2021, 2005.04028. 37

[170] G. Narain and H.-Q. Zhang, "Cosmic evolution in novel-Gauss Bonnet Gravity," 5 2020, 2005.05183. 37

[171] N. Dadhich, "On causal structure of 4*D*-Einstein–Gauss–Bonnet black hole," *Eur. Phys. J. C*, vol. 80, no. 9, p. 832, 2020, 2005.05757. 37

[172] S. Chakraborty and N. Dadhich, "Limits on stellar structures in Lovelock theories of gravity," *Phys. Dark Univ.*, vol. 30, p. 100658, 2020, 2005.07504. 37

[173] S. G. Ghosh, D. V. Singh, R. Kumar, and S. D. Maharaj, "Phase transition of AdS black holes in 4D EGB gravity coupled to nonlinear electrodynamics," *Annals Phys.*, vol. 424, p. 168347, 2021, 2006.00594. 37

[174] A. Banerjee, T. Tangphati, and P. Channuie, "Strange Quark Stars in 4D Einstein-Gauss-Bonnet Gravity," *Astrophys. J.*, vol. 909, no. 1, p. 14, 2021, 2006.00479. 37

[175] G. Narain and H.-Q. Zhang, "Lorentzian quantum cosmology in novel Gauss-Bonnet gravity from Picard-Lefschetz methods," 6 2020, 2006.02298. 37

[176] Z. Haghani, "Growth of matter density perturbations in 4D Einstein–Gauss–Bonnet gravity," *Phys. Dark Univ.*, vol. 30, p. 100720, 2020, 2005.01636. 37, 80, 105

[177] Z.-C. Lin, K. Yang, S.-W. Wei, Y.-Q. Wang, and Y.-X. Liu, "Equivalence of solutions between the four-dimensional novel and regularized EGB theories in a cylindrically symmetric spacetime," *Eur. Phys. J. C*, vol. 80, no. 11, p. 1033, 2020, 2006.07913. 37

[178] S. Shaymatov, J. Vrba, D. Malafarina, B. Ahmedov, and Z. Stuchlík, "Charged particle and epicyclic motions around $4D$ Einstein–Gauss–Bonnet black hole immersed in an external magnetic field," *Phys. Dark Univ.*, vol. 30, p. 100648, 2020, 2005.12410. 37

[179] H. Mohseni Sadjadi, "On cosmic acceleration in four dimensional Einstein-Gauss-Bonnet gravity," 7 2020, 2005.10024. 37

[180] A. Banerjee, T. Tangphati, D. Samart, and P. Channuie, "Quark Stars in 4D Einstein–Gauss–Bonnet Gravity with an Interacting Quark Equation of State," *Astrophys. J.*, vol. 906, no. 2, p. 114, 2021, 2007.04121. 37

[181] R. Svarc, J. Podolsky, and O. Hruska, "Kundt spacetimes in the Einstein-Gauss-Bonnet theory," *Phys. Rev. D*, vol. 102, no. 8, p. 084012, 2020, 2007.06648. 37

[182] K. Hegde, A. Naveena Kumara, C. L. A. Rizwan, M. S. Ali, and A. K. M, "Null Geodesics and Thermodynamic Phase Transition of Four-Dimensional Gauss-Bonnet AdS Black Hole," 7 2020, 2007.10259. 37

[183] H.-L. Li, X.-X. Zeng, and R. Lin, "Holographic phase transition from novel Gauss–Bonnet AdS black holes," *Eur. Phys. J. C*, vol. 80, no. 7, p. 652, 2020. 37

[184] Y.-Y. Wang, B.-Y. Su, and N. Li, "Hawking–Page phase transitions in four-dimensional Einstein–Gauss–Bonnet gravity," *Phys. Dark Univ.*, vol. 31, p. 100769, 2021, 2008.01985. 37

[185] C. Gao, S. Yu, and J. Qiu, "Nonsingular black holes and nonsingular universes in the regularized Lovelock gravity," *Phys. Dark Univ.*, vol. 31, p. 100754, 2021, 2008.12594. 37

[186] M. Zhang, C.-M. Zhang, D.-C. Zou, and R.-H. Yue, "Phase transition and Quasinormal modes for Charged black holes in 4D Einstein-Gauss-Bonnet gravity," *Chin. Phys. C*, vol. 45, no. 4, p. 045105, 2021, 2009.03096. 37

[187] K. Jafarzade, M. Kord Zangeneh, and F. S. N. Lobo, "Optical features of AdS black holes in the novel 4D Einstein-Gauss-Bonnet gravity coupled to nonlinear electrodynamics," 9 2020, 2009.12988. 37

[188] H. Ghaffarnejad, E. Yaraie, and M. Farsam, "Quantum State Dependence of Thermodynamic Phase Transition in 4D AdS Gauss-Bonnet Quantum Black Holes Surrounded With Cloud of Strings," 10 2020, 2010.07108. 37

[189] K. Jafarzade, M. Kord Zangeneh, and F. S. N. Lobo, "Shadow, deflection angle and quasinormal modes of Born-Infeld charged black holes," *JCAP*, vol. 04, p. 008, 2021, 2010.05755. 37

[190] M. Farsam, E. Yaraie, H. Ghaffarnejad, and E. Ghasami, "Cooling-heating phase transition for 4D AdS Bardeen Gauss-Bonnet Black Hole," 10 2020, 2010.05697. 37

[191] A. Colléaux, "Dimensional aspects of Lovelock-Lanczos gravity," 10 2020, 2010.14174. 37

[192] B. Mu, J. Liang, and X. Guo, "Thermodynamics with pressure and volume of 4D Gauss-Bonnet AdS Black Holes under the scalar field," 10 2020, 2011.00273. 37

[193] O. Donmez, "Bondi-Hoyle Accretion around the Non-rotating Black Hole in 4D Einstein-Gauss-Bonnet Gravity," *Eur. Phys. J. C*, vol. 81, no. 2, p. 113, 2021, 2011.04399. 37

[194] S. Hansraj, A. Banerjee, L. Moodly, and M. K. Jasim, "Isotropic compact stars in 4D Einstein-Gauss-Bonnet gravity," *Class. Quant. Grav.*, vol. 38, no. 3, p. 035002, 2021, 2011.08701. 37

[195] H. C. D. Lima, C. L. Benone, and L. C. B. Crispino, "4D Einstein-Gauss-Bonnet gravity: Massless particles and absorption of planar spin-0 waves," *Phys. Lett. B*, vol. 811, p. 135921, 2020, 2011.13446. 37

[196] A. Abdujabbarov, J. Rayimbaev, B. Turimov, and F. Atamurotov, "Dynamics of magnetized particles around 4-D Einstein Gauss–Bonnet black hole," *Phys. Dark Univ.*, vol. 30, p. 100715, 2020. 37

[197] H. Mohseni Sadjadi, "On cosmic acceleration in four-dimensional Einstein–Gauss–Bonnet gravity," *Phys. Dark Univ.*, vol. 30, p. 100728, 2020. 37

[198] R. Li and J. Wang, "Energy and entropy compensation, phase transition and kinetics of four dimensional charged Gauss-Bonnet Anti-de Sitter black holes on the underlying free energy landscape," 12 2020, 2012.05424. 37

[199] C.-M. Zhang, D.-C. Zou, and M. Zhang, "Triple points and phase diagrams of Born-Infeld AdS black holes in 4D Einstein-Gauss-Bonnet gravity," *Phys. Lett. B*, vol. 811, p. 135955, 2020, 2012.06162. 37

[200] Z. Li, Y. Duan, and J. Jia, "The deflection of charged massive particles by a 4-Dimensional charged Einstein-Gauss-Bonnet black hole," 12 2020, 2012.14226. 37

[201] H.-Y. Lin and X.-M. Deng, "Rational orbits around 4 D Einstein–Lovelock black holes," *Phys. Dark Univ.*, vol. 31, p. 100745, 2021. 37

[202] M. Zahid, S. U. Khan, and J. Ren, "Shadow cast and center of mass energy in a charged Gauss-Bonnet-AdS black hole," 1 2021, 2101.07673. 37

[203] S. I. Kruglov, "4D Einstein–Gauss–Bonnet Gravity Coupled with Nonlinear Electrodynamics," *Symmetry*, vol. 13, no. 2, p. 204, 2021. 37

[204] P. Liu, C. Niu, and C.-Y. Zhang, "Instability of regularized 4D charged Einstein-Gauss-Bonnet de-Sitter black holes," *Chin. Phys. C*, vol. 45, no. 2, p. 025104, 2021. 37

[205] P. Liu, C. Niu, and C.-Y. Zhang, "Linear instability of charged massless scalar perturbation in regularized 4D charged Einstein-Gauss-Bonnet anti de-Sitter black holes," *Chin. Phys. C*, vol. 45, no. 2, p. 025111, 2021. 37

[206] M. Zhang, C.-M. Zhang, D.-C. Zou, and R.-H. Yue, "$P - V$ criticality and Joule-Thomson Expansion of Hayward-AdS black holes in 4D Einstein-Gauss-Bonnet gravity," 2 2021, 2102.04308. 37

[207] K. Meng, L. Cao, J. Zhao, F. Qin, T. Zhou, and M. Deng, "Dyonic Born-Infeld black hole in 4D Einstein-Gauss-Bonnet gravity," 2 2021, 2102.05112. 37

[208] C. Ding, X. Chen, and X. Fu, "Einstein-Gauss-Bonnet gravity coupled to bumblebee field in four dimensional spacetime," 2 2021, 2102.13335. 37

[209] G. Z. Babar, F. Atamurotov, and A. Z. Babar, "Gravitational lensing in 4-D Einstein–Gauss–Bonnet gravity in the presence of plasma," *Phys. Dark Univ.*, vol. 32, p. 100798, 2021, 2103.00316. 37

[210] C.-H. Wu, Y.-P. Hu, and H. Xu, "Hawking Evaporation of Einstein-Gauss-Bonnet AdS Black Holes in $D \geqslant 4$ dimensions," 2 2021, 2103.00257. 37

[211] O. Donmez, "Dynamical Evolution of the Shock Cone around $4D$ Einstein-Gauss Bonnet Rotating Black Hole," 3 2021, 2103.03160. 37

[212] D. Chen, C. Gao, X. Liu, and C. Yu, "The correspondence between shadows and test fields in four-dimensional charged Einstein-Gauss-Bonnet black holes," 3 2021, 2103.03624. 37

[213] J.-X. Feng, B.-M. Gu, and F.-W. Shu, "Theoretical and observational constraints on regularized $4D$ Einstein-Gauss-Bonnet gravity," *Phys. Rev. D*, vol. 103, p. 064002, 2021, 2006.16751. 37, 80

[214] M. A. García-Aspeitia and A. Hernández-Almada, "Einstein–Gauss–Bonnet gravity: Is it compatible with modern cosmology?," *Phys. Dark Univ.*, vol. 32, p. 100799, 2021, 2007.06730. 37

[215] D. Wang and D. Mota, "4D Gauss-Bonnet gravity: cosmological constraints, H_0 tension and large scale structure," 3 2021, 2103.12358. 37, 80

[216] V. Motta, M. A. García-Aspeitia, A. Hernández-Almada, J. Magaña, and T. Verdugo, "Taxonomy of Dark Energy Models," 4 2021, 2104.04642. 37

[217] S. I. Kruglov, "Einstein − Gauss − Bonnet gravity with nonlinear electrodynamics," *Annals Phys.*, vol. 428, p. 168449, 2021. 37

[218] J. Li, S. Chen, and J. Jing, "Tidal effects in 4D Einstein-Gauss-Bonnet Black Hole Spacetime," 5 2021, 2105.01267. 37

[219] F. Atamurotov, S. Shaymatov, P. Sheoran, and S. Siwach, "Charged black hole in $4D$ Einstein-Gauss-Bonnet gravity: Particle motion, plasma effect on weak gravitational lensing and centre-of-mass energy," 5 2021, 2105.02214. 37

[220] M. Bousder and M. Bennai, "Particle-antiparticle in 4D charged Einstein-Gauss-Bonnet black hole," *Phys. Lett. B C*, vol. 817, p. 136343, 2021, 2105.05038. 37

[221] A. Övgün and E. I. Guendelman, "Black hole with Confining Electric Potential in $4D$ novel Einstein-Gauss-Bonnet gravity," 5 2021, 2105.05035. 37

[222] M. Gürses, T. c. Şişman, and B. Tekin, "Is there a novel Einstein–Gauss–Bonnet theory in four dimensions?," *Eur. Phys. J. C*, vol. 80, no. 7, p. 647, 2020, 2004.03390. 37, 44, 45

[223] M. Gurses, T. c. Şişman, and B. Tekin, "Comment on "Einstein-Gauss-Bonnet Gravity in 4-Dimensional Space-Time"," *Phys. Rev. Lett.*, vol. 125, no. 14, p. 149001, 2020, 2009.13508. 37, 44, 45

[224] J. Arrechea, A. Delhom, and A. Jiménez-Cano, "Inconsistencies in four-dimensional Einstein-Gauss-Bonnet gravity," *Chin. Phys. C*, vol. 45, no. 1, p. 013107, 2021, 2004.12998. 37, 44, 45

[225] J. Arrechea, A. Delhom, and A. Jiménez-Cano, "Comment on "Einstein-Gauss-Bonnet Gravity in Four-Dimensional Spacetime"," *Phys. Rev. Lett.*, vol. 125, no. 14, p. 149002, 2020, 2009.10715. 37, 44, 45

[226] J. Bonifacio, K. Hinterbichler, and L. A. Johnson, "Amplitudes and 4D Gauss-Bonnet Theory," *Phys. Rev. D*, vol. 102, no. 2, p. 024029, 2020, 2004.10716. 37, 44, 46, 192

[227] W.-Y. Ai, "A note on the novel 4D Einstein–Gauss–Bonnet gravity," *Commun. Theor. Phys.*, vol. 72, no. 9, p. 095402, 2020, 2004.02858. 37, 44, 49

[228] S. Mahapatra, "A note on the total action of 4D Gauss–Bonnet theory," *Eur. Phys. J. C*, vol. 80, no. 10, p. 992, 2020, 2004.09214. 37, 44, 46

[229] M. Hohmann, C. Pfeifer, and N. Voicu, "Canonical variational completion and 4D Gauss-Bonnet gravity," *Eur. Phys. J. Plus*, vol. 136, no. 2, p. 180, 2021, 2009.05459. 37, 44, 46

[230] L.-M. Cao and L.-B. Wu, "On the "Einstein-Gauss-Bonnet Gravity in Four Dimension"," 3 2021, 2103.09612. 37, 44

[231] M. Heydari-Fard, M. Heydari-Fard, and H. R. Sepangi, "Thin accretion disks around rotating black holes in $4D$ Einstein-Gauss-Bonnet gravity," 5 2021, 2105.09192. 37

[232] S. I. Kruglov, "Einstein-Gauss-Bonnet gravity with rational nonlinear electrodynamics," *EPL*, vol. 133, no. 6, p. 69001, 2021. 37

[233] D. Ghorai and S. Gangopadhyay, "Analytical study of holographic superconductor with backreaction in $4d$ Gauss-Bonnet gravity," 5 2021, 2105.09423. 37

[234] H. Ghaffarnejad, "4D AdS Gauss-Bonnet Black Holes in presence of cloud of strings with harmonic horizons countless," 5 2021, 2105.12729. 37

[235] C.-M. Zhang, M. Zhang, and D.-C. Zou, "Joule-Thomson Expansion of Born-Infeld AdS Black Holes in 4D Einstein-Gauss-Bonnet gravity," 5 2021, 2106.00183. 37

[236] A. K. Mishra, Shweta, and U. K. Sharma, "Non-exotic wormholes in 4-D Einstein-Gauss-Bonnet gravity," 6 2021, 2106.04369. 37

[237] H. Shah, Z. Ahmad, and H. H. Shah, "Quintessence background for $4D$ Einstein-Gauss-Bonnet black holes," *Phys. Lett. B*, vol. 818, p. 136383, 2021. 37

[238] S. Eslamzadeh, J. T. Firouzjaee, and K. Nozari, "Radiation from Einstein-Gauss-Bonnet de Sitter Black Hole via Tunneling Process," 7 2021, 2107.07947. 37

[239] G. A. Marks, F. Simovic, and R. B. Mann, "Phase Transitions in 4D Gauss-Bonnet-de Sitter Black Holes," 7 2021, 2107.11352. 37

[240] M. Bousder and M. Bennai, "Charged 4D Einstein-Gauss-Bonnet-AdS black hole in isobaric process: Thermal conduction, compressibility and Bose Einstein distribution," *Nucl. Phys. B*, vol. 969, p. 115476, 2021. 37

[241] S. I. Kruglov, "New model of 4D Einstein–Gauss–Bonnet gravity coupled with nonlinear electrodynamics," 8 2021, 2108.07695. 37

[242] J. M. Z. Pretel, A. Pradhan, and A. Banerjee, "Electrically Charged Quark Stars in $4D$ Einstein-Gauss-Bonnet Gravity," 8 2021, 2108.07454. 37

[243] S.-B. Kong, H. Abdusattar, Y. Yin, and Y.-P. Hu, "P-V Criticality of the FRW Universe in the Novel 4D Gauss-Bonnet Gravity," 8 2021, 2108.09411. 37

[244] M. G. Y., A. Behnamfard, S. Fakhry, and J. T. Firouzjaee, "The Integrated Sachs-Wolfe Effect in 4D Einstein-Gauss-Bonnet Gravity," 7 2021, 2107.00562. 37

[245] H. S. Vieira, "Quasibound states, stability and wave functions of the test fields in 4D Einstein–Gauss–Bonnet gravity," 7 2021, 2107.02065. 37

[246] G. Gyulchev, P. Nedkova, T. Vetsov, and S. Yazadjiev, "Image of the thin accretion disk around compact objects in the Einstein-Gauss-Bonnet gravity," 6 2021, 2106.14697. 37

[247] J. Badía and E. F. Eiroa, "Shadow of axisymmetric, stationary and asymptotically flat black holes in the presence of plasma," 6 2021, 2106.07601. 37

[248] T. Tangphati, A. Pradhan, A. Banerjee, and G. Panotopoulos, "Anisotropic Stars in 4D Einstein-Gauss-Bonnet Gravity," 9 2021, 2109.00195. 37

[249] Y.-M. Huang, Y. Tian, and X.-N. Wu, "Collapsing dust thin shell in Einstein-Gauss-Bonnet gravity," 9 2021, 2109.08921. 37

[250] K. N. Singh, S. K. Maurya, A. Dutta, F. Rahaman, and S. Aktar, "Quark stars in 4-dimensional Einstein–Gauss–Bonnet gravity," *Eur. Phys. J. C*, vol. 81, no. 10, p. 909, 2021, 2110.03182. 37

[251] H. Dimov, M. Radomirov, I. N. Iliev, R. C. Rashkov, and T. Vetsov, "Global and Local Thermodynamics of the Rotating Gauss-Bonnet BTZ Black Hole," 10 2021, 2110.05166. 37

[252] G.-Q. Li, "Quantum gravity effect on the entropy of a novel four-dimensional Gauss-Bonnet black hole," *EPL*, vol. 135, no. 3, p. 30002, 2021. 37

[253] G.-Q. Li, J.-X. Mo, and Y.-W. Zhuang, "Corrections to Hawking radiation and Bekenstein-Hawking entropy of novel four-dimensional black holes in Gauss-Bonnet gravity," *Gen. Rel. Grav.*, vol. 53, no. 10, p. 97, 2021. 37

[254] B. Chatterjee, "Black holes in Einstein-Gauss-Bonnet gravity: dynamical and 4-dimensional novel stationary black hole," 10 2021, 2110.13850. 37

[255] D. V. Singh, B. K. Singh, and S. Upadhyay, "4D AdS Einstein-Gauss-Bonnet black hole with Yang-Mills field and its thermodynamics," *Annals Phys.*, vol. 434, p. 168642, 2021. 37

[256] H. Lu and Y. Pang, "Horndeski gravity as $D \to 4$ limit of Gauss-Bonnet," *Phys. Lett. B*, vol. 809, p. 135717, 2020, 2003.11552. 37, 46, 53, 125, 192

[257] T. Kobayashi, "Effective scalar-tensor description of regularized Lovelock gravity in four dimensions," *JCAP*, vol. 07, p. 013, 2020, 2003.12771. 37, 46, 53, 125, 192

[258] R. A. Hennigar, D. Kubizňák, R. B. Mann, and C. Pollack, "On taking the D $\to$ 4 limit of Gauss-Bonnet gravity: theory and solutions," *JHEP*, vol. 07, p. 027, 2020, 2004.09472. 37, 46, 125

[259] K. Aoki, M. A. Gorji, and S. Mukohyama, "A consistent theory of $D \to$ 4 Einstein-Gauss-Bonnet gravity," *Phys. Lett. B*, vol. 810, p. 135843, 2020, 2005.03859. 37, 46, 55, 82, 125

[260] S. Shahidi and N. Khosravi, "Constrained 4D Gauss-Bonnet gravity and its cosmological implications," 5 2021, 2105.02372. 37

[261] C. Charmousis, A. Lehébel, E. Smyrniotis, and N. Stergioulas, "Astrophysical constraints on compact objects in 4D Einstein-Gauss-Bonnet gravity," *JCAP*, vol. 02, no. 02, p. 033, 2022, 2109.01149. 37

[262] S. X. Tian and Z.-H. Zhu, "Non-full equivalence of the four-dimensional Einstein-Gauss-Bonnet gravity and Horndeksi gravity for Bianchi type I metric," 4 2020, 2004.09954. 37

[263] R. A. Hennigar, D. Kubiznak, R. B. Mann, and C. Pollack, "Lower-dimensional Gauss–Bonnet gravity and BTZ black holes," *Phys. Lett. B*, vol. 808, p. 135657, 2020, 2004.12995. 37

[264] H. Lu and P. Mao, "Asymptotic structure of Einstein-Gauss-Bonnet theory in lower dimensions," *Chin. Phys. C*, vol. 45, no. 1, p. 013110, 2021, 2004.14400. 37

[265] L. Ma and H. Lu, "Vacua and Exact Solutions in Lower-D Limits of EGB," *Eur. Phys. J. C*, vol. 80, no. 12, p. 1209, 2020, 2004.14738. 37

[266] G. Gabadadze and G. Tukhashvili, "Conformal/Poincaré Coset, cosmology, and descendants of Lovelock terms," *Phys. Rev. D*, vol. 102, no. 2, p. 024054, 2020, 2005.01729. 37

[267] D. A. Easson, T. Manton, and A. Svesko, "$D \to$ 4 Einstein-Gauss-Bonnet gravity and beyond," *JCAP*, vol. 10, p. 026, 2020, 2005.12292. 37

[268] R. A. Hennigar, D. Kubiznak, and R. B. Mann, "Rotating Gauss-Bonnet BTZ Black Holes," *Class. Quant. Grav.*, vol. 38, no. 3, p. 03LT01, 2021, 2005.13732. 37

[269] Y.-L. Wang and X.-H. Ge, "Black holes in 4D Einstein-Maxwell-Gauss-Bonnet gravity coupled with scalar fields," 11 2020, 2011.08604. 37

[270] D. Easson, T. Manton, M. Parikh, and A. Svesko, "The Stringy Origins of Galileons and their Novel Limit," 12 2020, 2012.12277. 37

[271] K. Aoki, M. A. Gorji, and S. Mukohyama, "Cosmology and gravitational waves in consistent $D \to$ 4 Einstein-Gauss-Bonnet gravity," *JCAP*, vol. 09, p. 014, 2020, 2005.08428. 37, 55, 82, 83, 100

[272] K. Aoki, M. A. Gorji, S. Mizuno, and S. Mukohyama, "Inflationary gravitational waves in consistent $D \to 4$ Einstein-Gauss-Bonnet gravity," *JCAP*, vol. 01, p. 054, 2021, 2010.03973. 37, 55, 83

[273] Z.-B. Yao, M. Oliosi, X. Gao, and S. Mukohyama, "Minimally modified gravity with an auxiliary constraint: A Hamiltonian construction," *Phys. Rev. D*, vol. 103, no. 2, p. 024032, 2021, 2011.00805. 37

[274] J. Pan, X. Qiao, D. Wang, Q. Pan, Z.-Y. Nie, and J. Jing, "Holographic superconductors in 4D Einstein-Gauss-Bonnet gravity with backreactions," 9 2021, 2109.02207. 37

[275] M. Heydari-Fard and M. Heydari-Fard, "Null geodesics and shadow of $4D$ Einstein-Gauss-Bonnet black holes surrounded by quintessence," 9 2021, 2109.02059. 37

[276] A. Banerjee, S. Hansraj, and L. Moodly, "Charged stars in $4D$ Einstein–Gauss–Bonnet gravity," *Eur. Phys. J. C*, vol. 81, no. 9, p. 790, 2021. 37

[277] B. Narzilloev, S. Shaymatov, I. Hussain, A. Abdujabbarov, B. Ahmedov, and C. Bambi, "Motion of Particles and Gravitational Lensing Around (2+1)-dimensional BTZ black holes in Gauss-Bonnet Gravity," 9 2021, 2109.02816. 37

[278] S. Sengupta, "4D Einstein-Gauss-Bonnet Gravity Generated By Invisible Extra Dimensions," 9 2021, 2109.10388. 37, 197

[279] G. Alkac, G. D. Ozen, and G. Suer, "Cubic Lovelock Gravity in Lower Dimensions," 3 2022, 2203.01811. 37

[280] D. G. Boulware and S. Deser, "String-generated gravity models," *Phys. Rev. Lett.*, vol. 55, pp. 2656–2660, Dec 1985. 41, 43

[281] Z.-Y. Fan, B. Chen, and H. Lu, "Criticality in Einstein–Gauss–Bonnet gravity: gravity without graviton," *Eur. Phys. J. C*, vol. 76, no. 10, p. 542, 2016, 1606.02728. 42

[282] P. S. Apostolopoulos, G. Siopsis, and N. Tetradis, "Cosmology from an AdS Schwarzschild black hole via holography," *Phys. Rev. Lett.*, vol. 102, p. 151301, 2009, 0809.3505. 42

[283] N. Bilic, "Randall-Sundrum versus holographic cosmology," *Phys. Rev. D*, vol. 93, no. 6, p. 066010, 2016, 1511.07323. 42

[284] J. E. Lidsey, "Holographic Cosmology from the First Law of Thermodynamics and the Generalized Uncertainty Principle," *Phys. Rev. D*, vol. 88, p. 103519, 2013, 0911.3286. 42

[285] R.-G. Cai, L.-M. Cao, and Y.-P. Hu, "Corrected Entropy-Area Relation and Modified Friedmann Equations," *JHEP*, vol. 08, p. 090, 2008, 0807.1232. 42

[286] J. E. Lidsey, "Thermodynamics of Anomaly-Driven Cosmology," *Class. Quant. Grav.*, vol. 26, p. 147001, 2009, 0812.2791. 42

[287] V. L. Ginzburg, D. A. Kirzhnits, and A. A. Lyubushin, "The role of quantum fluctuations of the gravitational field in General Relativity theory and Cosmology," *Sov. Phys. JETP*, vol. 33, pp. 242–246, 1971. 42

[288] P. O. Mazur and E. Mottola, "Weyl cohomology and the effective action for conformal anomalies," *Phys. Rev. D*, vol. 64, p. 104022, 2001, hep-th/0106151. 42

[289] N. Birrell and P. Davies, *Quantum Fields in Curved Space*. Cambridge Monographs on Mathematical Physics, Cambridge University Press, 1984. 42

[290] R.-G. Cai, L.-M. Cao, and N. Ohta, "Black Holes in Gravity with Conformal Anomaly and Logarithmic Term in Black Hole Entropy," *JHEP*, vol. 04, p. 082, 2010, 0911.4379. 43, 62

[291] R.-G. Cai, "Thermodynamics of Conformal Anomaly Corrected Black Holes in AdS Space," *Phys. Lett. B*, vol. 733, pp. 183–189, 2014, 1405.1246. 43, 62

[292] G. Cognola, R. Myrzakulov, L. Sebastiani, and S. Zerbini, "Einstein gravity with Gauss-Bonnet entropic corrections," *Phys. Rev. D*, vol. 88, no. 2, p. 024006, 2013, 1304.1878. 43, 62

[293] P. Horava, "Quantum Gravity at a Lifshitz Point," *Phys. Rev. D*, vol. 79, p. 084008, 2009, 0901.3775. 43

[294] A. Kehagias and K. Sfetsos, "The Black hole and FRW geometries of non-relativistic gravity," *Phys. Lett. B*, vol. 678, pp. 123–126, 2009, 0905.0477. 43

[295] A. M. Polyakov, "Quantum Gravity in Two Dimensions," *Modern Physics Letters A*, vol. 2, pp. 893–898, Jan. 1987. 47

[296] T. Strobl, *Gravity in two space-time dimensions*. PhD thesis, Aachen, Tech. Hochsch., 1999, hep-th/0011240. 47

[297] D. F. Carneiro, E. A. Freiras, B. Goncalves, A. G. de Lima, and I. L. Shapiro, "On useful conformal tranformations in general relativity," *Grav. Cosmol.*, vol. 10, pp. 305–312, 2004, gr-qc/0412113. 48, 50, 115, 116

[298] M. P. Dabrowski, J. Garecki, and D. B. Blaschke, "Conformal transformations and conformal invariance in gravitation," *Annalen Phys.*, vol. 18, pp. 13–32, 2009, 0806.2683. 48, 50, 115, 116

[299] A. E. Sikkema and R. B. Mann, "Gravitation and Cosmology in Two-dimensions," *Class. Quant. Grav.*, vol. 8, pp. 219–236, 1991. 49

[300] R. B. Mann, A. Shiekh, and L. Tarasov, "Classical and Quantum Properties of Two-dimensional Black Holes," *Nucl. Phys. B*, vol. 341, pp. 134–154, 1990. 49

[301] R. B. Mann, S. Morsink, A. Sikkema, and T. Steele, "Semiclassical gravity in (1+1)-dimensions," *Phys. Rev. D*, vol. 43, pp. 3948–3957, 1991. 49

[302] S. M. Morsink and R. B. Mann, "Black hole radiation of Dirac particles in (1+1)-dimensions," *Class. Quant. Grav.*, vol. 8, pp. 2257–2268, 1991. 49

[303] R. Mann, "Two dimensional quantum gravity coupled to matter," *Physics Letters B*, vol. 294, p. 310–316, Nov 1992. 49

[304] R. B. Mann, A. Shiekh, and L. Tarasov, "Classical and Quantum Properties of Two-dimensional Black Holes," *Nucl. Phys. B*, vol. 341, pp. 134–154, 1990. 49

[305] C. G. Torre, "Symmetric Criticality in Classical Field Theory," *AIP Conf. Proc.*, vol. 1360, no. 1, pp. 63–74, 2011, 1011.3429. 57

[306] M. Cvetic, S. Nojiri, and S. D. Odintsov, "Black hole thermodynamics and negative entropy in de Sitter and anti-de Sitter Einstein-Gauss-Bonnet gravity," *Nucl. Phys.*, vol. B628, pp. 295–330, 2002, hep-th/0112045. 61

[307] R.-G. Cai, "Gauss-Bonnet black holes in AdS spaces," *Phys. Rev. D*, vol. 65, p. 084014, 2002, hep-th/0109133. 61

[308] P. Nicolini, A. Smailagic, and E. Spallucci, "Noncommutative geometry inspired Schwarzschild black hole," *Phys. Lett. B*, vol. 632, pp. 547–551, 2006, gr-qc/0510112. 70

[309] S. Kováčik, "R^3_λ inspired black holes," 4 2015, 1504.04460. 70

[310] I. Dymnikova, "Vacuum nonsingular black hole," *Gen. Rel. Grav.*, vol. 24, pp. 235–242, 1992. 70

[311] S. Kováčik, "Hawking-Radiation Recoil of Microscopic Black Holes," 2 2021, 2102.06517. 70, 72

[312] S. Di Gennaro and Y. C. Ong, "Feasibility of Primordial Black Hole Remnants as Dark Matter in View of Hawking Radiation Recoil," 4 2021, 2104.08919. 70, 72

[313] A. Bonanno and M. Reuter, "Spacetime structure of an evaporating black hole in quantum gravity," *Phys. Rev. D*, vol. 73, p. 083005, 2006, hep-th/0602159. 70

[314] B. Koch and F. Saueressig, "Black holes within Asymptotic Safety," *Int. J. Mod. Phys. A*, vol. 29, no. 8, p. 1430011, 2014, 1401.4452. 70

[315] B. Carr, K. Kohri, Y. Sendouda, and J. Yokoyama, "Constraints on Primordial Black Holes," 2 2020, 2002.12778. 72

[316] B. Carr and F. Kuhnel, "Primordial Black Holes as Dark Matter: Recent Developments," *Ann. Rev. Nucl. Part. Sci.*, vol. 70, pp. 355–394, 2020, 2006.02838. 72

[317] J. H. MacGibbon, "Can Planck-mass relics of evaporating black holes close the universe?," *Nature*, vol. 329, pp. 308–309, 1987. 72

[318] S. Rasanen and E. Tomberg, "Planck scale black hole dark matter from Higgs inflation," *JCAP*, vol. 01, p. 038, 2019, 1810.12608. 72

[319] J. D. Barrow, E. J. Copeland, and A. R. Liddle, "The cosmology of black hole relics," *Phys. Rev. D*, vol. 46, pp. 645–657, Jul 1992. 72

[320] A. M. Green and A. R. Liddle, "Constraints on the density perturbation spectrum from primordial black holes," *Phys. Rev. D*, vol. 56, pp. 6166–6174, 1997, astro-ph/9704251. 72

[321] S. Alexeyev, A. Barrau, G. Boudoul, O. Khovanskaya, and M. Sazhin, "Black hole relics in string gravity: Last stages of Hawking evaporation," *Class. Quant. Grav.*, vol. 19, pp. 4431–4444, 2002, gr-qc/0201069. 72

[322] P. Chen and R. J. Adler, "Black hole remnants and dark matter," *Nucl. Phys. B Proc. Suppl.*, vol. 124, pp. 103–106, 2003, gr-qc/0205106. 72

[323] P. Chen, "Inflation induced Planck-size black hole remnants as dark matter," *New Astron. Rev.*, vol. 49, pp. 233–239, 2005, astro-ph/0406514. 72

[324] K. Nozari and S. H. Mehdipour, "Gravitational uncertainty and black hole remnants," *Mod. Phys. Lett. A*, vol. 20, pp. 2937–2948, 2005, 0809.3144. 72

[325] A. Barrau, D. Blais, G. Boudoul, and D. Polarski, "Peculiar relics from primordial black holes in the inflationary paradigm," *Annalen Phys.*, vol. 13, pp. 115–123, 2004, astro-ph/0303330. 72

[326] B. J. Carr, J. H. Gilbert, and J. E. Lidsey, "Black hole relics and inflation: Limits on blue perturbation spectra," *Phys. Rev. D*, vol. 50, pp. 4853–4867, 1994, astro-ph/9405027. 72

[327] B. V. Lehmann, C. Johnson, S. Profumo, and T. Schwemberger, "Direct detection of primordial black hole relics as dark matter," *JCAP*, vol. 10, p. 046, 2019, 1906.06348. 72

[328] J. A. de Freitas Pacheco and J. Silk, "Primordial Rotating Black Holes," *Phys. Rev. D*, vol. 101, no. 8, p. 083022, 2020, 2003.12072. 72

[329] Y. Bai and N. Orlofsky, "Primordial Extremal Black Holes as Dark Matter," *Phys. Rev. D*, vol. 101, no. 5, p. 055006, 2020, 1906.04858. 72

[330] B. V. Lehmann and S. Profumo, "Black hole remnants are not too fast to be dark matter," 5 2021, 2105.01627. 72

[331] P. Chen, Y. C. Ong, and D.-h. Yeom, "Black Hole Remnants and the Information Loss Paradox," *Phys. Rept.*, vol. 603, pp. 1–45, 2015, 1412.8366. 72

[332] P. Villanueva-Domingo, O. Mena, and S. Palomares-Ruiz, "A brief review on primordial black holes as dark matter," *Front. Astron. Space Sci.*, vol. 8, p. 87, 2021, 2103.12087. 73

[333] N. Aghanim *et al.*, "Planck 2018 results. VI. Cosmological parameters," *Astron. Astrophys.*, vol. 641, p. A6, 2020, 1807.06209. 74

[334] K. A. Malik and D. Wands, "Cosmological perturbations," *Phys. Rept.*, vol. 475, pp. 1–51, 2009, 0809.4944. 79

[335] C. M. Will, *Theory and experiment in gravitational physics*. Cambridge university press, 2018. 84, 89, 98

[336] E. Poisson and C. M. Will, *Gravity: Newtonian, post-newtonian, relativistic*. Cambridge University Press, 2014. 86

[337] L. Landau and E. Lifschitz, *The Classical Theory of Fields: Volume 2*. Course of theoretical physics, Elsevier Science, 1975. 91, 94

[338] E. Pitjeva and N. Pitjev, "Relativistic effects and dark matter in the solar system from observations of planets and spacecraft," *Monthly Notices of the Royal Astronomical Society*, vol. 432, no. 4, pp. 3431–3437, 2013. 94, 109

[339] A. Fienga, J. Laskar, P. Kuchynka, H. Manche, G. Desvignes, M. Gastineau, I. Cognard, and G. Theureau, "The inpop10a planetary ephemeris and its applications in fundamental physics," *Celestial Mechanics and Dynamical Astronomy*, vol. 111, no. 3, p. 363, 2011. 94

[340] D. M. Lucchesi and R. Peron, "Accurate Measurement in the Field of the Earth of the General-Relativistic Precession of the LAGEOS II Pericenter and New Constraints on Non-Newtonian Gravity," *Phys. Rev. Lett.*, vol. 105, p. 231103, 2010, 1106.2905. 95, 109

[341] R. Abuter *et al.*, "Detection of the Schwarzschild precession in the orbit of the star S2 near the Galactic centre massive black hole," *Astron. Astrophys.*, vol. 636, p. L5, 2020, 2004.07187. 95, 96, 109

[342] S. Hawking, "Black holes in the brans-dicke," *Communications in Mathematical Physics*, vol. 25, no. 2, pp. 167–171, 1972. 96

[343] R. A. Hulse and J. H. Taylor, "Discovery of a pulsar in a binary system," *The Astrophysical Journal*, vol. 195, pp. L51–L53, 1975. 96

[344] A. G. Lyne, M. Burgay, M. Kramer, A. Possenti, R. Manchester, F. Camilo, M. McLaughlin, D. Lorimer, N. D'Amico, B. Joshi, *et al.*, "A double-pulsar system: A rare laboratory for relativistic gravity and plasma physics," *Science*, vol. 303, no. 5661, pp. 1153–1157, 2004. 96

[345] M. Kramer *et al.*, "Tests of general relativity from timing the double pulsar," *Science*, vol. 314, pp. 97–102, 2006, astro-ph/0609417. 97, 109

[346] S. S. Shapiro, J. L. Davis, D. E. Lebach, and J. Gregory, "Measurement of the solar gravitational deflection of radio waves using geodetic very-long-baseline interferometry data, 1979–1999," *Physical Review Letters*, vol. 92, no. 12, p. 121101, 2004. 98

[347] B. Bertotti, L. Iess, and P. Tortora, "A test of general relativity using radio links with the cassini spacecraft," *Nature*, vol. 425, no. 6956, pp. 374–376, 2003. 98

[348] B. Abbott *et al.*, "GW170817: Observation of Gravitational Waves from a Binary Neutron Star Inspiral," *Phys. Rev. Lett.*, vol. 119, no. 16, p. 161101, 2017, 1710.05832. 99, 109, 122

[349] A. Goldstein *et al.*, "An Ordinary Short Gamma-Ray Burst with Extraordinary Implications: Fermi-GBM Detection of GRB 170817A," *Astrophys. J. Lett.*, vol. 848, no. 2, p. L14, 2017, 1710.05446. 99

[350] V. Savchenko *et al.*, "INTEGRAL Detection of the First Prompt Gamma-Ray Signal Coincident with the Gravitational-wave Event GW170817," *Astrophys. J. Lett.*, vol. 848, no. 2, p. L15, 2017, 1710.05449. 99

[351] T. Baker, E. Bellini, P. Ferreira, M. Lagos, J. Noller, and I. Sawicki, "Strong constraints on cosmological gravity from GW170817 and GRB 170817A," *Phys. Rev. Lett.*, vol. 119, no. 25, p. 251301, 2017, 1710.06394. 99, 100, 123

[352] P. Creminelli and F. Vernizzi, "Dark Energy after GW170817 and GRB170817A," *Phys. Rev. Lett.*, vol. 119, no. 25, p. 251302, 2017, 1710.05877. 99, 100

[353] J. M. Ezquiaga and M. Zumalacárregui, "Dark Energy After GW170817: Dead Ends and the Road Ahead," *Phys. Rev. Lett.*, vol. 119, no. 25, p. 251304, 2017, 1710.05901. 99, 100

[354] K. Akiyama *et al.*, "First M87 Event Horizon Telescope Results. I. The Shadow of the Supermassive Black Hole," *Astrophys. J.*, vol. 875, no. 1, p. L1, 2019, 1906.11238. 100

[355] K. Akiyama *et al.*, "First M87 Event Horizon Telescope Results. VI. The Shadow and Mass of the Central Black Hole," *Astrophys. J. Lett.*, vol. 875, no. 1, p. L6, 2019, 1906.11243. 100, 101

[356] S. Vagnozzi and L. Visinelli, "Hunting for extra dimensions in the shadow of M87*," *Phys. Rev. D*, vol. 100, no. 2, p. 024020, 2019, 1905.12421. 100

[357] A. Held, R. Gold, and A. Eichhorn, "Asymptotic safety casts its shadow," *JCAP*, vol. 06, p. 029, 2019, 1904.07133. 100

[358] T. Zhu, Q. Wu, M. Jamil, and K. Jusufi, "Shadows and deflection angle of charged and slowly rotating black holes in Einstein-Æther theory," *Phys. Rev. D*, vol. 100, no. 4, p. 044055, 2019, 1906.05673. 100

[359] K. Gebhardt, J. Adams, D. Richstone, T. R. Lauer, S. M. Faber, K. Gültekin, J. Murphy, and S. Tremaine, "The Black Hole Mass in M87 from Gemini/NIFS Adaptive Optics Observations," *ApJ*, vol. 729, p. 119, Mar. 2011, 1101.1954. 101

[360] J. L. Walsh, A. J. Barth, L. C. Ho, and M. Sarzi, "The M87 Black Hole Mass from Gas-dynamical Models of Space Telescope Imaging Spectrograph Observations," *ApJ*, vol. 770, p. 86, June 2013, 1304.7273. 101

[361] B. Abbott *et al.*, "Observation of Gravitational Waves from a Binary Black Hole Merger," *Phys. Rev. Lett.*, vol. 116, no. 6, p. 061102, 2016, 1602.03837. 102

[362] B. Abbott *et al.*, "Properties of the Binary Black Hole Merger GW150914," *Phys. Rev. Lett.*, vol. 116, no. 24, p. 241102, 2016, 1602.03840. 102, 109

[363] B. Abbott *et al.*, "Tests of general relativity with GW150914," *Phys. Rev. Lett.*, vol. 116, no. 22, p. 221101, 2016, 1602.03841. [Erratum: Phys.Rev.Lett. 121, 129902 (2018)]. 102

[364] B. P. Abbott *et al.*, "The basic physics of the binary black hole merger GW150914," *Annalen Phys.*, vol. 529, no. 1-2, p. 1600209, 2017, 1608.01940. 102

[365] B. P. Abbott *et al.*, "GW170608: Observation of a 19-solar-mass Binary Black Hole Coalescence," *Astrophys. J.*, vol. 851, no. 2, p. L35, 2017, 1711.05578. 103

[366] B. Abbott *et al.*, "GW190814: Gravitational waves from the coalescence of a 23 solar mass black hole with a 2.6 solar mass compact object," *The Astrophysical Journal*, vol. 896, p. L44, jun 2020. 103

[367] E. Fischbach and D. E. Krause, "Constraints on light pseudoscalars implied by tests of the gravitational inverse square law," *Phys. Rev. Lett.*, vol. 83, pp. 3593–3596, 1999, hep-ph/9906240. 104

[368] E. Adelberger, B. R. Heckel, S. A. Hoedl, C. Hoyle, D. Kapner, and A. Upadhye, "Particle Physics Implications of a Recent Test of the Gravitational Inverse Sqaure Law," *Phys. Rev. Lett.*, vol. 98, p. 131104, 2007, hep-ph/0611223. 104, 105, 109

[369] W.-H. Tan, S.-Q. Yang, C.-G. Shao, J. Li, A.-B. Du, B.-F. Zhan, Q.-L. Wang, P.-S. Luo, L.-C. Tu, and J. Luo, "New test of the gravitational inverse-square law at the submillimeter range with dual modulation and compensation," *Phys. Rev. Lett.*, vol. 116, p. 131101, Mar 2016. 104, 105

[370] S. M. Carroll and M. Kaplinghat, "Testing the Friedmann equation: The Expansion of the universe during big bang nucleosynthesis," *Phys. Rev. D*, vol. 65, p. 063507, 2002, astro-ph/0108002. 105

[371] A. Arbey, "AlterBBN: A program for calculating the BBN abundances of the elements in alternative cosmologies," *Comput. Phys. Commun.*, vol. 183, pp. 1822–1831, 2012, 1106.1363. 105

[372] C. Pitrou, A. Coc, J.-P. Uzan, and E. Vangioni, "Precision big bang nucleosynthesis with improved Helium-4 predictions," *Phys. Rept.*, vol. 754, pp. 1–66, 2018, 1801.08023. 106

[373] E. Aver, K. A. Olive, and E. D. Skillman, "The effects of He I λ10830 on helium abundance determinations," *JCAP*, vol. 07, p. 011, 2015, 1503.08146. 106, 109

[374] N. Bocharova, K. Bronnikov, and V. Melnikov, "," *Vestn. Mosk. Univ. Ser. III Fiz. Astron.*, no. 6, pp. 706–709, 1970. 112

[375] J. Bekenstein, "Black Holes with Scalar Charge," *Annals Phys.*, vol. 91, pp. 75–82, 1975. 112

[376] J. Bekenstein, "Exact solutions of Einstein conformal scalar equations," *Annals Phys.*, vol. 82, pp. 535–547, 1974. 112

[377] C. Martinez, R. Troncoso, and J. Zanelli, "De Sitter black hole with a conformally coupled scalar field in four-dimensions," *Phys. Rev. D*, vol. 67, p. 024008, 2003, hep-th/0205319. 112

[378] C. Martinez, J. P. Staforelli, and R. Troncoso, "Topological black holes dressed with a conformally coupled scalar field and electric charge," *Phys. Rev. D*, vol. 74, p. 044028, 2006, hep-th/0512022. 112

[379] A. Anabalon and H. Maeda, "New Charged Black Holes with Conformal Scalar Hair," *Phys. Rev. D*, vol. 81, p. 041501, 2010, 0907.0219. 112

[380] A. Padilla, D. Stefanyszyn, and M. Tsoukalas, "Generalised Scale Invariant Theories," *Phys. Rev. D*, vol. 89, no. 6, p. 065009, 2014, 1312.0975. 112, 114

[381] S. de Haro, I. Papadimitriou, and A. C. Petkou, "Conformally Coupled Scalars, Instantons and Vacuum Instability in AdS(4)," *Phys. Rev. Lett.*, vol. 98, p. 231601, 2007, hep-th/0611315. 112

[382] G. Dotti, R. J. Gleiser, and C. Martinez, "Static black hole solutions with a self interacting conformally coupled scalar field," *Phys. Rev. D*, vol. 77, p. 104035, 2008, 0710.1735. 112

[383] E. Gunzig, V. Faraoni, A. Figueiredo, T. Rocha, and L. Brenig, "What can we learn from nonminimally coupled scalar field cosmology?," *Int. J. Theor. Phys.*, vol. 39, pp. 1901–1932, 2000. 112

[384] J. Oliva and S. Ray, "Conformal couplings of a scalar field to higher curvature terms," *Class. Quant. Grav.*, vol. 29, p. 205008, 2012, 1112.4112. 112

[385] A. Cisterna, A. Neira-Gallegos, J. Oliva, and S. C. Rebolledo-Caceres, "Plebański-Demiański solutions in quadratic gravity with conformally coupled scalar fields," *Phys. Rev. D*, vol. 103, no. 6, p. 064050, 2021, 2101.03628. 112

[386] N. Caceres, J. Figueroa, J. Oliva, M. Oyarzo, and R. Stuardo, "Quadratic gravity and conformally coupled scalar fields," *JHEP*, vol. 04, p. 157, 2020, 2001.01478. 112

[387] D. Soper, *Classical Field Theory*. Dover Books on Physics, Dover Publications, 2008. 114

[388] B. P. Abbott *et al.*, "GW151226: Observation of Gravitational Waves from a 22-Solar-Mass Binary Black Hole Coalescence," *Phys. Rev. Lett.*, vol. 116, no. 24, p. 241103, 2016, 1606.04855. 124

[389] B. P. Abbott *et al.*, "GW170104: Observation of a 50-Solar-Mass Binary Black Hole Coalescence at Redshift 0.2," *Phys. Rev. Lett.*, vol. 118, no. 22, p. 221101, 2017, 1706.01812. [Erratum: Phys.Rev.Lett. 121, 129901 (2018)]. 124

[390] B. . P. . Abbott *et al.*, "GW170608: Observation of a 19-solar-mass Binary Black Hole Coalescence," *Astrophys. J. Lett.*, vol. 851, p. L35, 2017, 1711.05578. 124

[391] B. P. Abbott *et al.*, "GW170814: A Three-Detector Observation of Gravitational Waves from a Binary Black Hole Coalescence," *Phys. Rev. Lett.*, vol. 119, no. 14, p. 141101, 2017, 1709.09660. 124

[392] B. P. Abbott *et al.*, "GW170817: Observation of Gravitational Waves from a Binary Neutron Star Inspiral," *Phys. Rev. Lett.*, vol. 119, no. 16, p. 161101, 2017, 1710.05832. 124, 168

[393] K. Akiyama *et al.*, "First Sagittarius A* Event Horizon Telescope Results. VI. Testing the Black Hole Metric," *Astrophys. J. Lett.*, vol. 930, no. 2, p. L17, 2022. 124

[394] C. A. R. Herdeiro and E. Radu, "Kerr black holes with scalar hair," *Phys. Rev. Lett.*, vol. 112, p. 221101, 2014, 1403.2757. 125, 137, 143, 162

[395] C. Herdeiro and E. Radu, "Construction and physical properties of Kerr black holes with scalar hair," *Class. Quant. Grav.*, vol. 32, no. 14, p. 144001, 2015, 1501.04319. 125, 137, 143, 162

[396] C. Herdeiro, E. Radu, and H. Rúnarsson, "Kerr black holes with Proca hair," *Class. Quant. Grav.*, vol. 33, no. 15, p. 154001, 2016, 1603.02687. 125, 137, 143, 162

[397] S. Alexander and N. Yunes, "Chern-Simons Modified General Relativity," *Phys. Rept.*, vol. 480, pp. 1–55, 2009, 0907.2562. 125

[398] R. Jackiw and S. Y. Pi, "Chern-Simons modification of general relativity," *Phys. Rev. D*, vol. 68, p. 104012, 2003, gr-qc/0308071. 125

[399] K. Yagi, N. Yunes, and T. Tanaka, "Slowly Rotating Black Holes in Dynamical Chern-Simons Gravity: Deformation Quadratic in the Spin," *Phys. Rev. D*, vol. 86, p. 044037, 2012, 1206.6130. [Erratum: Phys.Rev.D 89, 049902 (2014)]. 125

[400] P. A. Cano and A. Ruipérez, "String gravity in D=4," *Phys. Rev. D*, vol. 105, no. 4, p. 044022, 2022, 2111.04750. 125

[401] A. Sullivan, N. Yunes, and T. P. Sotiriou, "Numerical black hole solutions in modified gravity theories: Spherical symmetry case," *Phys. Rev. D*, vol. 101, no. 4, p. 044024, 2020, 1903.02624. 125, 157, 159, 160

[402] A. Sullivan, N. Yunes, and T. P. Sotiriou, "Numerical black hole solutions in modified gravity theories: Axial symmetry case," *Phys. Rev. D*, vol. 103, no. 12, p. 124058, 2021, 2009.10614. 125, 151, 157, 159, 160, 163

[403] P. G. S. Fernandes, "https://github.com/pgsfernandes/SpinningBlackHoles.jl." 125

[404] J. Boyd, *Chebyshev and Fourier Spectral Methods: Second Revised Edition*. Dover Books on Mathematics, Dover Publications, 2001. 126, 129

[405] Y. Xie, J. Zhang, H. O. Silva, C. de Rham, H. Witek, and N. Yunes, "Square Peg in a Circular Hole: Choosing the Right Ansatz for Isolated Black Holes in Generic Gravitational Theories," *Phys. Rev. Lett.*, vol. 126, no. 24, p. 241104, 2021, 2103.03925. 137

[406] B. Shoshany, "OGRe: An Object-Oriented General Relativity Package for Mathematica," *J. Open Source Softw.*, vol. 6, p. 3416, 2021, 2109.04193. 145

[407] V. Iyer and R. M. Wald, "Some properties of Noether charge and a proposal for dynamical black hole entropy," *Phys. Rev. D*, vol. 50, pp. 846–864, 1994, gr-qc/9403028. 147, 178

[408] S. Liberati and C. Pacilio, "Smarr Formula for Lovelock Black Holes: a Lagrangian approach," *Phys. Rev. D*, vol. 93, no. 8, p. 084044, 2016, 1511.05446. 147, 178

[409] R. Brito, V. Cardoso, and P. Pani, "Superradiance: New Frontiers in Black Hole Physics," *Lect. Notes Phys.*, vol. 906, pp. pp.1–237, 2015, 1501.06570. 148

[410] B. Carter, "Global structure of the kerr family of gravitational fields," *Phys. Rev.*, vol. 174, pp. 1559–1571, Oct 1968. 149

[411] J. B. Achour, A. De Felice, M. A. Gorji, S. Mukohyama, and M. C. Pookkillath, "Disformal map and Petrov classification in modified gravity," *JCAP*, vol. 10, p. 067, 2021, 2107.02386. 150

[412] E. Berti, F. White, A. Maniopoulou, and M. Bruni, "Rotating neutron stars: An Invariant comparison of approximate and numerical spacetime models," *Mon. Not. Roy. Astron. Soc.*, vol. 358, pp. 923–938, 2005, gr-qc/0405146. 150

[413] P. V. P. Cunha and C. A. R. Herdeiro, "Shadows and strong gravitational lensing: a brief review," *Gen. Rel. Grav.*, vol. 50, no. 4, p. 42, 2018, 1801.00860. 151

[414] L. Rezzolla, "An Introduction to Astrophysical Black Holes and Their Dynamical Production," in *Lecture Notes in Physics, Berlin Springer Verlag* (F. Haardt, V. Gorini, U. Moschella, A. Treves, and M. Colpi, eds.), vol. 905, p. 1, 2016. 153

[415] V. Cardoso, A. S. Miranda, E. Berti, H. Witek, and V. T. Zanchin, "Geodesic stability, Lyapunov exponents and quasinormal modes," *Phys. Rev. D*, vol. 79, no. 6, p. 064016, 2009, 0812.1806. 154

[416] K. Prabhu and L. C. Stein, "Black hole scalar charge from a topological horizon integral in Einstein-dilaton-Gauss-Bonnet gravity," *Phys. Rev. D*, vol. 98, no. 2, p. 021503, 2018, 1805.02668. 158, 179

[417] P. Pani and V. Cardoso, "Are black holes in alternative theories serious astrophysical candidates? The Case for Einstein-Dilaton-Gauss-Bonnet black holes," *Phys. Rev. D*, vol. 79, p. 084031, 2009, 0902.1569. 160

[418] W. Schönauer and E. Schnepf, "Software considerations for the "black box"; solver fidisol for partial differential equations," *ACM Trans. Math. Softw.*, vol. 13, pp. 333–349, 12 1987. 162

[419] W. Schönauer and R. Wei, "Special issue on parallel algorithms for numerical linear algebra efficient vectorizable pde solvers," *Journal of Computational and Applied Mathematics*, vol. 27, no. 1, pp. 279 – 297, 1989. 162

[420] W. Schönauer and T. Adolph, "How we solve pdes," *Journal of Computational and Applied Mathematics*, vol. 131, no. 1–2, pp. 473 – 492, 2001. 162

[421] J. F. M. Delgado, *Spinning Black Holes with Scalar Hair and Horizonless Compact Objects within and beyond General Relativity*. PhD thesis, Aveiro U., 2022, 2204.02419. 162

[422] N. Dadhich and P. P. Kale, "Equatorial circular geodesics in the kerr–newman geometry," *Journal of Mathematical Physics*, vol. 18, no. 9, pp. 1727–1728, 1977. 166

[423] C.-Y. Wang, D.-S. Lee, and C.-Y. Lin, "Null and timelike geodesics in the Kerr-Newman black hole exterior," *Phys. Rev. D*, vol. 106, no. 8, p. 084048, 2022, 2208.11906. 166

[424] C. F. B. Macedo, J. Sakstein, E. Berti, L. Gualtieri, H. O. Silva, and T. P. Sotiriou, "Self-interactions and Spontaneous Black Hole Scalarization," *Phys. Rev. D*, vol. 99, no. 10, p. 104041, 2019, 1903.06784. 167, 174

[425] D. D. Doneva, L. G. Collodel, C. J. Krüger, and S. S. Yazadjiev, "Black hole scalarization induced by the spin: 2+1 time evolution," *Phys. Rev. D*, vol. 102, no. 10, p. 104027, 2020, 2008.07391. 167

[426] C. A. R. Herdeiro, A. M. Pombo, and E. Radu, "Aspects of Gauss-Bonnet Scalarisation of Charged Black Holes," *Universe*, vol. 7, no. 12, p. 483, 2021, 2111.06442. 167

[427] D. D. Doneva and S. S. Yazadjiev, "Beyond the spontaneous scalarization: New fully nonlinear dynamical mechanism for formation of scalarized black holes," 7 2021, 2107.01738. 167, 173

[428] N. Andreou, N. Franchini, G. Ventagli, and T. P. Sotiriou, "Spontaneous scalarization in generalised scalar-tensor theory," *Phys. Rev. D*, vol. 99, no. 12, p. 124022, 2019, 1904.06365. [Erratum: Phys.Rev.D 101, 109903 (2020)]. 167

[429] N. Franchini, M. Bezares, E. Barausse, and L. Lehner, "Fixing the dynamical evolution in scalar-Gauss-Bonnet gravity," 5 2022, 2206.00014. 167

[430] J. L. Ripley and F. Pretorius, "Hyperbolicity in Spherical Gravitational Collapse in a Horndeski Theory," *Phys. Rev. D*, vol. 99, no. 8, p. 084014, 2019, 1902.01468. 167

[431] J. L. Ripley and F. Pretorius, "Gravitational collapse in Einstein dilaton-Gauss–Bonnet gravity," *Class. Quant. Grav.*, vol. 36, no. 13, p. 134001, 2019, 1903.07543. 167

[432] V. K. Oikonomou, "A refined Einstein–Gauss–Bonnet inflationary theoretical framework," *Class. Quant. Grav.*, vol. 38, no. 19, p. 195025, 2021, 2108.10460. 167

[433] V. K. Oikonomou and F. P. Fronimos, "Reviving non-minimal Horndeski-like theories after GW170817: kinetic coupling corrected Einstein–Gauss–Bonnet

inflation," *Class. Quant. Grav.*, vol. 38, no. 3, p. 035013, 2021, 2006.05512. 167

[434] S. D. Odintsov, V. K. Oikonomou, and F. P. Fronimos, "Rectifying Einstein-Gauss-Bonnet Inflation in View of GW170817," *Nucl. Phys. B*, vol. 958, p. 115135, 2020, 2003.13724. 167

[435] C. A. R. Herdeiro, E. Radu, N. Sanchis-Gual, and J. A. Font, "Spontaneous Scalarization of Charged Black Holes," *Phys. Rev. Lett.*, vol. 121, no. 10, p. 101102, 2018, 1806.05190. 167, 173

[436] P. G. S. Fernandes, C. A. R. Herdeiro, A. M. Pombo, E. Radu, and N. Sanchis-Gual, "Spontaneous Scalarisation of Charged Black Holes: Coupling Dependence and Dynamical Features," *Class. Quant. Grav.*, vol. 36, no. 13, p. 134002, 2019, 1902.05079. [Erratum: Class.Quant.Grav. 37, 049501 (2020)]. 167

[437] P. G. S. Fernandes, C. A. R. Herdeiro, A. M. Pombo, E. Radu, and N. Sanchis-Gual, "Charged black holes with axionic-type couplings: Classes of solutions and dynamical scalarization," *Phys. Rev. D*, vol. 100, no. 8, p. 084045, 2019, 1908.00037. 167

[438] P. G. S. Fernandes, "Einstein–Maxwell-scalar black holes with massive and self-interacting scalar hair," *Phys. Dark Univ.*, vol. 30, p. 100716, 2020, 2003.01045. 167

[439] R. Ruffini and J. A. Wheeler, "Introducing the black hole," *Physics Today*, vol. 24, pp. 30–41, 1 1971. 167

[440] J. D. Bekenstein, "Black hole hair: 25 - years after," in *2nd International Sakharov Conference on Physics*, pp. 216–219, 5 1996, gr-qc/9605059. 167

[441] J. D. Bekenstein, "Nonexistence of baryon number for static black holes," *Phys. Rev. D*, vol. 5, pp. 1239–1246, Mar 1972. 167

[442] T. P. Sotiriou, "Black Holes and Scalar Fields," *Class. Quant. Grav.*, vol. 32, no. 21, p. 214002, 2015, 1505.00248. 167

[443] L. Hui and A. Nicolis, "No-Hair Theorem for the Galileon," *Phys. Rev. Lett.*, vol. 110, p. 241104, 2013, 1202.1296. 167

[444] J. D. Bekenstein, "Novel ''no-scalar-hair'' theorem for black holes," *Phys. Rev. D*, vol. 51, no. 12, p. R6608, 1995. 167

[445] S. W. Hawking, "Black holes in the Brans-Dicke theory of gravitation," *Commun. Math. Phys.*, vol. 25, pp. 167–171, 1972. 167

[446] T. P. Sotiriou and V. Faraoni, "Black holes in scalar-tensor gravity," *Phys. Rev. Lett.*, vol. 108, p. 081103, 2012, 1109.6324. 167

[447] E. Berti *et al.*, "Testing General Relativity with Present and Future Astrophysical Observations," *Class. Quant. Grav.*, vol. 32, p. 243001, 2015, 1501.07274. 167

[448] R. Abbott *et al.*, "GWTC-2: Compact Binary Coalescences Observed by LIGO and Virgo During the First Half of the Third Observing Run," *Phys. Rev. X*, vol. 11, p. 021053, 2021, 2010.14527. 168

[449] F. Corelli, M. De Amicis, T. Ikeda, and P. Pani, "What is the fate of Hawking evaporation in gravity theories with higher curvature terms?," 5 2022, 2205.13006. 168, 173, 184

[450] F. Corelli, M. De Amicis, T. Ikeda, and P. Pani, "Nonperturbative gedanken experiments in Einstein-dilaton-Gauss-Bonnet gravity: nonlinear transitions and tests of the cosmic censorship beyond General Relativity," 5 2022, 2205.13007. 168, 173, 184

[451] G. W. Gibbons and S. W. Hawking, *Euclidean Quantum Gravity*. WORLD SCIENTIFIC, 1993, https://www.worldscientific.com/doi/pdf/10.1142/1301. 171

[452] D. D. Doneva and S. S. Yazadjiev, "Dynamics of the nonrotating and rotating black hole scalarization," *Phys. Rev. D*, vol. 103, no. 6, p. 064024, 2021, 2101.03514. 174

[453] K. V. Staykov, J. L. Blázquez-Salcedo, D. D. Doneva, J. Kunz, P. Nedkova, and S. S. Yazadjiev, "Axial perturbations of hairy Gauss-Bonnet black holes with massive self-interacting scalar field," 12 2021, 2112.00703. 174

[454] V. I. Danchev, D. D. Doneva, and S. S. Yazadjiev, "Constraining scalarization in scalar-Gauss-Bonnet gravity through binary pulsars," 12 2021, 2112.03869. 174

[455] J. L. Blázquez-Salcedo, D. D. Doneva, S. Kahlen, J. Kunz, P. Nedkova, and S. S. Yazadjiev, "Axial perturbations of the scalarized Einstein-Gauss-Bonnet black holes," *Phys. Rev. D*, vol. 101, no. 10, p. 104006, 2020, 2003.02862. 174

[456] J. L. Blázquez-Salcedo, D. D. Doneva, J. Kunz, and S. S. Yazadjiev, "Radial perturbations of the scalarized Einstein-Gauss-Bonnet black holes," *Phys. Rev. D*, vol. 98, no. 8, p. 084011, 2018, 1805.05755. 174

[457] S. Hod, "Onset of spontaneous scalarization in spinning Gauss-Bonnet black holes," *Phys. Rev. D*, vol. 102, no. 8, p. 084060, 2020, 2006.09399. 174

[458] S. Hod, "Nontrivial spatial behavior of the Gauss-Bonnet curvature invariant of rapidly-rotating Kerr black holes," *Phys. Rev. D*, vol. 105, no. 8, p. 084013, 2022, 2204.13122. 174

[459] S. O. Alexeev and M. V. Pomazanov, "Black hole solutions with dilatonic hair in higher curvature gravity," *Phys. Rev. D*, vol. 55, pp. 2110–2118, 1997, hep-th/9605106. 177

[460] Z. Lyu, N. Jiang, and K. Yagi, "Constraints on Einstein-dilation-Gauss-Bonnet gravity from Black Hole-Neutron Star Gravitational Wave Events," 1 2022, 2201.02543. 185, 186, 197

[461] N. Yunes, K. Yagi, and F. Pretorius, "Theoretical Physics Implications of the Binary Black-Hole Mergers GW150914 and GW151226," *Phys. Rev. D*, vol. 94, no. 8, p. 084002, 2016, 1603.08955. 185

[462] S. E. Perkins, R. Nair, H. O. Silva, and N. Yunes, "Improved gravitational-wave constraints on higher-order curvature theories of gravity," *Phys. Rev. D*, vol. 104, no. 2, p. 024060, 2021, 2104.11189. 185

[463] R. Nair, S. Perkins, H. O. Silva, and N. Yunes, "Fundamental Physics Implications for Higher-Curvature Theories from Binary Black Hole Signals in the LIGO-Virgo Catalog GWTC-1," *Phys. Rev. Lett.*, vol. 123, no. 19, p. 191101, 2019, 1905.00870. 185

[464] K. Yagi, L. C. Stein, N. Yunes, and T. Tanaka, "Post-Newtonian, Quasi-Circular Binary Inspirals in Quadratic Modified Gravity," *Phys. Rev. D*, vol. 85, p. 064022, 2012, 1110.5950. [Erratum: Phys.Rev.D 93, 029902 (2016)]. 185

[465] R. Abbott *et al.*, "GW190814: Gravitational Waves from the Coalescence of a 23 Solar Mass Black Hole with a 2.6 Solar Mass Compact Object," *Astrophys. J. Lett.*, vol. 896, no. 2, p. L44, 2020, 2006.12611. 186

[466] T. Jayasinghe *et al.*, "A unicorn in monoceros: the 3 M$\odot$ dark companion to the bright, nearby red giant V723 Mon is a non-interacting, mass-gap black hole candidate," *Mon. Not. Roy. Astron. Soc.*, vol. 504, no. 2, pp. 2577–2602, 2021, 2101.02212. 186

[467] T. A. Thompson *et al.*, "A noninteracting low-mass black hole-giant star binary system," *Science*, vol. 366, pp. 637–640, Nov. 2019, 1806.02751. 186

[468] R. Abbott *et al.*, "Observation of Gravitational Waves from Two Neutron Star–Black Hole Coalescences," *Astrophys. J. Lett.*, vol. 915, no. 1, p. L5, 2021, 2106.15163. 186

[469] D. N. Page, "Particle Emission Rates from a Black Hole. 2. Massless Particles from a Rotating Hole," *Phys. Rev. D*, vol. 14, pp. 3260–3273, 1976. 188

[470] Z. Komargodski and A. Schwimmer, "On Renormalization Group Flows in Four Dimensions," *JHEP*, vol. 12, p. 099, 2011, 1107.3987. 192

[471] G. Papallo and H. S. Reall, "On the local well-posedness of Lovelock and Horndeski theories," *Phys. Rev. D*, vol. 96, no. 4, p. 044019, 2017, 1705.04370. 197

[472] S. Sengupta, "Gravity theory with a dark extra dimension," *Phys. Rev. D*, vol. 101, no. 10, p. 104040, 2020, 1908.04830. 197